THE COPOLYMERIZATION OF α-METHYL STYRENE AND METHYL METHACRYLATE AT HIGH PRESSURES

A Thesis Submitted for the Degree of
Doctor of Philosophy
in the Engineering Faculty
of University of London
and
Diploma of Imperial College

by

I. A. ANTONAS

M.Sc. in Advanced Chemical Engineering
Istanbul Technical University

M.Sc. in Polymer Chemistry
University of Lancaster

July, 1976

Department of Chemical Engineering
and Chemical Technology,
IMPERIAL COLLEGE,
LONDON S.W.7

ABSTRACT

This research was undertaken to investigate the effect of high pressure on a copolymerization system in which one of the monomers is close to its ceiling temperature, and shows a strong tendency to depropagation. The initial aim was to determine the copolymerization reactivity ratios and their dependence on pressure; and to relate the behaviour of the system to these effects, together with the pressure-dependence of the monomer-polymer equilibrium constant. Further conclusions concerning the component reactions can also be obtained from such data. The system investigated is α-methyl styrene - methyl methacrylate, which has been studied by previous research workers at normal pressure over a range of temperatures, but has not previously been studied at high pressure. The characteristics of the homopolymerization of the two monomers are well established; and the monomer - polymer equilibrium of α-methyl styrene (normal ceiling temperature 60°C) has been previously investigated at 1 bar and at high pressures.

Copolymerization reactions were carried out at 60°C over a wide range of compositions; and at ten different pressures in the range from 1 bar to 5000 bars. The copolymers were analysed by micro-elemental analysis and also by nuclear magnetic resonance. The normal pressure results agreed satisfactorily with the results of other researchers.

The nuclear magnetic resonance analysis of the copolymers also yielded information about their microstructure, which provides some evidence of the possible sequence of reactions during the copolymerization.

The average molecular weights of the copolymers were measured. The experimental data also provide some information on the rates of copolymerization as a function of pressure. These results are recorded but not discussed in detail as they are incidental to the main purpose of the research.

The copolymer composition data of this research are considered together with data obtained by other researchers at normal pressure and varying temperature. The results were analysed by various theoretical equations and the reactivity ratios were obtained. The fitting of the

composition data to the predominantly nonlinear equations was accomplished by nonlinear regression methods, using a CDC 6400 computer and the results for the Mayo-Lewis equation were compared with the results of current solution methods.

The goodness of fit of the various equations was found to depend on the number of parameters they contain. The two parameter equations of the 'terminal' model and also those developed by Wittmer show quite satisfactory goodness of fit. The three parameter 'penultimate unit' equation and one four parameter equation of 'penpenultimate unit' model showed poor goodness of fit but acceptably small sum of squares. Equations with more parameters could not be fitted because although on occasions the sum of squares was reasonably low the convergence was slow and the results failed to give smooth curves in r vs. P plots.

None of the equations produced r vs. P curves of the type expected, i.e. $\ln r \propto P$. This may indicate the need of a more elaborate equation with a higher number of parameters but a limit is imposed by the accuracy of the experimental points. It is nevertheless possible to draw some conclusions from the r vs. P curves obtained.

CONTENTS

ACKNOWLEDGEMENTS

It is a duty and a pleasure for me to express my gratitude to all members of my family, who have supplied the major part of the conditioning which created in me a deep-seated affection for the learning process.

My main thanks in this project are due to Dr.K.E. Weale who is, inasfar as I understand doctorate research and studentship, a perfect supervisor. All through my research, he has been most helpful, understanding and flexible in his attitude to my work.

I should like to thank the glass workshop team:- Mr.K. Grose, Mr.A. Jones, and Mr.C. Smith; the stores team:- Mr.T. Agus, Mr.B. Francis, Mr.T. Richards and Mrs.A. Woollard; the librarians:- Miss S. Bell and Miss V. Milne (all in alphabetical order); and all the staff and technicians of the Chemical Engineering Department for their ready help and their friendship.

Since I believe that the doctorate is not simply specific research but is also a complete training, I would take this opportunity to thank also Prof.R.W. Sargent for his valuable enlightment in various aspects of this training.

I. INTRODUCTION

1.1 Importance of Copolymers and High Pressure Copolymers

The copolymerization process became important after the understanding of basic polymer structure and reaction mechanisms, and during the search for a perfect substitute for natural rubber. The search for a synthetic material to substitude natural rubber was carried on during and between the two world wars, and, since little or nothing was known about stereoregular polymerization of isoprene to cispolyisoprene until the 1950's, effort was directed to producing copolymers such as styrene-butadiene and butadiene-acrylonitrile. Copolymers were found to be superior to their parent homopolymers in the sense that they cover a wide and continuous spectrum of property combination which includes the properties of the parent homopolymers and also some additional properties attributed to the particular copolymer. These properties are attainable by varying the microstructure of the copolymer as well as the fraction of the comonomers in the chain. The microstructure of the copolymer can be varied from completely random sequences to block sequences of each monomer following the other.

The outcome of copolymerization studies in terms of polymer chemistry was the study of physical chemistry of the polymerization process. For example the relative reactivities of the growing chains towards the various monomers can be obtained from copolymerization studies. Also the polymerization behaviour of monomers which do not homopolymerize can be studied from their copolymerization reactions.

The effect and importance of pressure on copolymerization can be viewed in two aspects: (i) the effect of pressure on copolymerization as a polymerization reaction, (ii) the effect of pressure particular to polymerization reaction. In the first it is the effect of pressure on a chemical reaction, operating through the individual chemical reactions of the polymerization process. This may result in considerable acceleration of the overall reaction, alteration of the polymer-monomer equilibrium, and an increase in molecular weight.

In the second it is because pressure is one of the parameters that has an effect on the nature of the end product of the copolymerization reaction. By varying this parameter it is possible to obtain copolymers with a desired microstructure; and also in chemical terms it is possible to obtain more understanding of the exact mechanism of the copolymerization reactions.

1.2 Free Radical Polymerization

1.2.1 Production of Free Radicals

For a molecule to produce free radicals by thermal dissociation at moderate temperatures it must contain weak valence bonds such as peroxide bonds. It is important to know the rate of dissociation which may depend on solvent and concentration as well as temperature. Sometimes the dissociation may go through more than one step in which case not all the steps may produce active radicals or radicals may attack other initiator molecules to give inductive dissociation. The dissociation mechanism depends on the radical itself but most of the thermal initiators have an activation energy for dissociation of about 30kcal/mole. Although the rate of dissociation thus depends strongly upon temperature, each initiator has a useful temperature range of 20 to 30^{o}C. Apart from thermal process some radicals may undergo a dissociation process activated by light energy. The rate of production of radicals by photo-dissociation may not be as fast as thermal-dissociation but initiation can be achieved at very low temperatures. Another way of activating dissociation is by high frequency radiation such as γ-rays. In this case the radiation energy is so high that it may split a C=C double bond to produce radicals and thus the presence of a catalyst is not needed.

The two main sources of radicals are the peroxides and the azo compounds which involve the decomposition of a weak valence bond between two oxygen or two nitrogen atoms respectively. Peroxide initiators include many types of substances that contain the peroxide group, e.g.,

a. Persulphates

$$S_2O_8^{--} \longrightarrow 2SO_4^{\cdot -}$$

b. Hydroperoxides

$$R.O.O.H \longrightarrow R.O^{\cdot} + {}^{\cdot}O.H$$

c. Di-alkyl peroxides

$$R.O.O.R \longrightarrow 2R.O^{\cdot}$$

d. Di-acyl(di-aroyl) peroxides

$$R.CO.O.O.CO.R \longrightarrow 2R.CO.O^{\cdot} \longrightarrow 2R^{\cdot} + 2CO_2$$

e. Peresters

$$R.CO.O.O.R' \longrightarrow R.CO.O^{\cdot} + R'O^{\cdot}$$

On the other hand azo compounds are group of compounds with the general structure,

$$R.N{:}N.R \longrightarrow 2R^{\cdot} + N_2$$

The most common peroxide initiator in polymerization is dibenzoyl peroxide which is a diaroyl peroxide. It has an activation energy, according to various researchers, between 29 and 31 kcal/mole, and A factors between $3*10^{13}$ and $6*10^{14}$ sec^{-1}. These small variations may be due to different reaction conditions employed during the actual experiments. Dibenzoyl peroxide is best used as a polymerization initiator between 60° and $80^{\circ}C$. Dibenzoyl peroxide is susceptible to induced decomposition and to transfer reactions, and the complicated reaction mechanism may give a fractional order of reaction.

The most common azo initiator is azo-bis-isobutyronitrile, (AZBN)

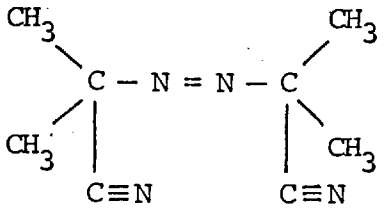

As a thermal initiator it is nearly in the same temperature range as benzoyl peroxide but it also dissociates to free radicals by the influence of near u.v. light and can be used as a photo-initiator. Unlike benzoyl peroxide its decomposition is accurately first order. The decomposition rate shows very small differences in various solvents,

and as it is not susceptible to radical attacks gives no induced decomposition or transfer reactions. Although the decomposition of AZBN for the production of free radicals can be represented as

$$(CH_3)_2C(CN)\cdot N{:}N\cdot C(CH_3)_2\cdot CN \longrightarrow 2(CH_3)_2C(CN)\cdot + N_2$$

the actual decomposition mechanism in a solvent involves more than two steps[1,2,3]. AZBN was first prepared by Thiele and Heuser[4] and tetramethylsuccinodinitrile was found to be the product of its thermal decomposition. A more thorough study by Bickel and Waters[5] showed that the terminal products of the thermal decomposition consist of

(I) Tetramethylsuccinodinitrile (84%)

(II) Isobutyronitrile (3.5%)

(III) Tricyanohexane (9%)

They postulated that during the decomposition reaction, after the elimination of N_2, the radicals dimerize to give (I), and disproportionate to give (II), and methacrylonitrile. Later methacrylonitrile reacts further with radicals to give (III). IR spectophotometric studies during the course of the reaction shows the existence of an unstable intermediate product[1]. This is methyl ketene-cyanisopropylimine and is formed by the combination of $(CH_3)_2C(CN)\cdot$ and $(CH_3)_2C{:}C{:}N\cdot$ radicals. The keteneimine is not stable and rearranges to (I) at 60°C. It is only during the photolysis of AZBN at 25°C that an appreciable amount of keteneimine is formed as end product. The formation of a second type of a radical is attributed to the resonance-stabilized states of the cyano radical

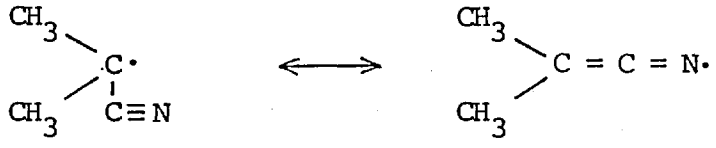

and the keteneimine radical can initiate polymerization with approximately the efficiency of the cyano radical[3].

One difficulty with 2-cyano-2-propyl radicals is that they react with oxygen

$$(CH_3)_2C(CN)\cdot + O_2 \longrightarrow (CH_3)_2C(CN)\cdot O\cdot O\cdot$$

and the resulting radical may have a differrent reactivity from the cyano radical. Combination of the peroxy radical with the cyano radicals gives a peroxide which in turn dissociate to a radical. Talat-Erben and Önol[6] showed that the reactions with oxygen can involve even more complicated stages.

The rate constant for the decomposition of AZBN was determined by van Hook and Tobolsky[7] in experiments conducted over the range 37° to 100°C and is given by:

$$k = 1.58 * 10^{15} \exp(-30.8 \text{ kcal mole}^{-1}/RT) \text{ sec}^{-1} \qquad (1.2.1)$$

The most effective temperature range for initiation by AZBN is from 45° to 65°C.

Arnett[50] showed that the solvent is essentially without effect on the decomposition of AZBN and the dependence of k upon temperature is given by

$$\log_{10} k = -(7019/T) + 17.807 \qquad (1.2.1a)$$

which is in agreement with Overberger et al[54] and Lewis and Matheson[55] as seen below:

Table I a

Rate constants for the decomposition of AZBN

	k, min^{-1}			
°C	Arnett	Overberger, et al	Lewis and Matheson	van Hook and Tobolsky(*)
50	$1.2*10^{-4}$	$1.1*10^{-4}$	$1.5*10^{-4}$	$1.15*10^{-4}$
77	$5.7*10^{-3}$	$6.5*10^{-3}$	$6.3*10^{-3}$	$4.73*10^{-3}$

(*) Calculated from eq.(1.2.1)

1.2.2 Free Radical Polymerization Kinetics

The general mechanism of free radical polymerization can be given as follows, where $R_I\cdot$ is a free radical produced from the decomposition of a initiator molecule, $R_r\cdot$ is polymer radical with r units of monomer, M is a monomer and S is a solvent molecule

Initiation:

$$\text{Initiator} \longrightarrow 2R^{\bullet}_{I} \qquad \text{rate constant} = k_I$$

$$(\text{Rate of formation of } R^{\bullet}_{I} = I = 2fk_I[\text{Initiator}])$$

$$R^{\bullet}_{I} + M \longrightarrow R^{\bullet}_{1} \qquad \text{rate constant} = k_{pI}$$

Propagation:

$$R^{\bullet}_{1} + M \longrightarrow R^{\bullet}_{2} \qquad " \quad " \qquad k_{p1}$$

$$R^{\bullet}_{2} + M \longrightarrow R^{\bullet}_{3} \qquad " \quad " \qquad k_{p2}$$

$$R^{\bullet}_{r} + M \longrightarrow R^{\bullet}_{r+1} \qquad " \quad " \qquad k_{pr}$$

Transfer:

$$R^{\bullet}_{r} + M \longrightarrow P_r + M^{\bullet} \qquad " \quad " \qquad k_{fr}$$

$$M^{\bullet} + M \longrightarrow R^{\bullet}_{2} \qquad " \quad " \qquad k_{pM}$$

Termination by combination:

$$R^{\bullet}_{r} + R^{\bullet}_{q} \longrightarrow P_{r+q} \qquad " \quad " \qquad k_{trq}$$

Termination by disproportionation:

$$R^{\bullet}_{r} + R^{\bullet}_{q} \longrightarrow P_r + P_q \qquad " \quad " \qquad k'_{trq}$$

(1.2.2)

In order to derive kinetic equations from the reaction scheme above one has to make some assumptions. These are as follows:

(i) The reactivities of chain radicals are independent of their chain length. In this case $k_{p1}=k_{p2}=....=k_{pr}=k_p$ and also k_{fr}, k_{trq} and k'_{trq} are independent of r and q. The validity of this assumption has been tested experimentally by various researchers[8,9,10].

(ii) The chain length is sufficiently long, so that it can be said that the total consumption rate of the monomer is equal only to the rate of propagation; and the consumption of the monomer during the initiation and transfer steps can be ignored. Therfore

$$-d[M]/dt = k_p[R^{\bullet}_{n}][M] \qquad (1.2.3)$$

(iii) There exists a stationary state where during polymerization the concentration of the intermediate radical products stay constant. In actual fact the rate of change of radical concentration is much

smaller than the rate of change of monomer concentration

$$\frac{d[R\cdot]}{dt} \ll \frac{d[M]}{dt} \tag{1.2.4}$$

On the assumption that

$$\frac{d[R\cdot]}{dt} = 0$$

or more specifically

$$\begin{aligned} d[R\cdot_1]/dt &= 0, \quad d[R\cdot_r]/dt = 0 \\ d[R\cdot_I]/dt &= 0, \quad d[M\cdot]/dt = 0 \end{aligned} \tag{1.2.5}$$

Then the full expressions for the stationary state condition are given as

$$\frac{d[R\cdot_I]}{dt} = I - k_{pI}[R\cdot_I][M] = 0 \tag{1.2.6}$$

$$\frac{d[R\cdot_1]}{dt} = k_{pI}[R\cdot_I][M] - (k_p+k_f)[R\cdot_1][M] - (k_t+k_t')[R\cdot_1]\sum_n [R\cdot_n] = 0$$

$$\frac{d[R\cdot_2]}{dt} = k_p[R\cdot_1][M] + k_{pM}[M\cdot][M] - (k_p+k_f)[R\cdot_2][M] - (k_t+k_t')[R\cdot_2]\sum_n [R\cdot_n] = 0$$

$$\frac{d[R\cdot_r]}{dt} = k_p[R\cdot_{r-1}][M] - (k_p+k_f)[R\cdot_r][M] - (k_t+k_t')[R\cdot_r]\sum_n [R\cdot_n] = 0$$

$$\frac{d[M\cdot]}{dt} = k_f[M]\sum_n [R\cdot_n] - k_{pM}[M\cdot][M] = 0 \tag{1.2.7}$$

When these equations are summed they yield

$$I = (k_t+k_t')[R\cdot]^2 \tag{1.2.8}$$

where

$$[R\cdot] = \sum_n [R\cdot_n]$$

When added the only term which does not cancel but is omitted is $k_p[R\cdot_r][M]$. This is because when r is too large $[R\cdot_r]$ becomes too small. The reaction rate becomes

$$-\frac{d[M]}{dt} = \sum_n k_p[R\cdot_n][M] = k_p[M]\left(\frac{I}{k_t+k_t'}\right)^{1/2} \tag{1.2.9}$$

and the average kinetic chain length, ν, i.e., the average number of

molecules consumed for each chain initiation, is

$$\nu = -\frac{1}{I}\frac{d[M]}{dt} = k_p[M]\left\{I(k_t+k_t')\right\}^{1/2} \qquad (1.2.10)$$

and the average chain length or degree of polymerization (DP), i.e., the average number of molecules consumed for each inactive polymer molecule, is

$$\overline{DP} = \frac{k_p[R\cdot][M]}{k_f[R\cdot][M] + (k_t/2+k_t')[R\cdot]^2}$$

$$= \frac{k_p[M]}{k_f[M] + (k_t/2+k_t')\left\{I/(k_t+k_t')\right\}^{1/2}} \qquad (1.2.11)$$

The average life-time of a kinetic chain, τ, (in other words the time during which each radical consumes ν monomer molecules), is given by

$$\frac{\tau}{[R\cdot]}\frac{d[M]}{dt} = \nu \qquad (1.2.12)$$

$$\tau = [R\cdot]/I = \left\{I(k_t+k_t')\right\}^{-1/2} \qquad (1.2.13)$$

In general it is adequate to treat the polymerization processes by means of these assumptions but the equations were developed without simplifying assumptions by Gee and Melville, and others[11].

If equation (1.2.11) is put in the form

$$\frac{1}{\overline{DP}} = \frac{k_f}{k_p} + \frac{(k_t/2+k_t')\left\{I/(k_t+k_t')\right\}^{1/2}}{k_p[M]} \qquad (1.2.14)$$

and by assuming that the termination is exclusively by disproportionation one gets

$$\frac{1}{\overline{DP}} = \frac{k_f}{k_p} + \frac{(Ik_t')^{1/2}}{k_p[M]} \qquad (1.2.15)$$

Substituting $I=2k_I f[In]$, where k_I is the initiation rate constant, f is the efficiency and $[In]$ is the concentration of the initiator

$$\frac{1}{\overline{DP}} = \frac{k_f}{k_p} + \frac{(2k_I f[In]k_t')^{1/2}}{k_p[M]} \qquad (1.2.16)$$

The rate constant for the reactions can be axpressed in an Arrhenius form

$$k = A \exp(-E/RT)$$

Therefore

$$\frac{1}{P_n} = a \exp\left(\frac{-E_f+E_p}{RT}\right) + b \exp\left(\frac{-E_t/2-E_i/2+E_p}{RT}\right) \qquad (1.2.17)$$

where

$$a = Af/A_p \quad , \quad b = (2f[In]A_iA_t)^{1/2}/([M]A_p)$$

By differentiating this with respect to temperature one obtains

$$\frac{d(1/\overline{DP})}{dT} = \frac{-a(-E_f+E_p)}{RT^2} \exp\left(\frac{-E_f+E_p}{RT}\right) - \frac{b(-E_t/2-E_i/2+E_p)}{RT^2} \exp\left(\frac{-E_t/2-E_i/2+E_p}{RT}\right) \qquad (1.2.18)$$

at $d(1/DP)/dT=0$ where DP is a maximum

$$T_M = \frac{E_f-E_t/2-E_i/2}{R \ln\left(\frac{a(E_f-E_p)}{b(E_p-E_t/2-E_i/2)}\right)} \qquad (1.2.19)$$

and since $T_M>0$ equation (1.2.19) yields

$$E_f > E_p > \frac{E_t+E_i}{2} \qquad (1.2.20)$$

This is the condition for the existance of maximum in DP along the temperature coordinate and was demonstrated for the polymerization of vinyl acetate and methyl methacrylate[12,13].

If the transfer reaction is negligible it can be seen that DP will decrease continuously with increasing temperature without going through a maximum.

1.2.3 Chemical Initiation of Radical Polymerization

The decomposition of an initiator molecule in a liquid phase was treated according to two theories developed by two groups of researchers. Schulz and Huseman[70] approached the phenomenon of initiator decomposition reaction as one that goes through an activated complex and this complex is in equilibrium with the monomer and the initiator

$$K_I = \frac{[C]}{[M]([In]-[C])} \qquad (1.2.21)$$

where [C], [M] and [In] are the concentrations of the complex, the monomer and the initiator respectively. Then

$$[C] = K_I[In][M]/(1+K_I[M]) \qquad (1.2.22)$$

and from equation (1.2.9)

$$-\frac{d[M]}{dt} = k_p\left(\frac{k_I K_I[In]}{k_t+k'_t}\right)^{1/2}[M]^{3/2}(1+K_I[M])^{-1/2} \qquad (1.2.23)$$

so the order of the reaction will be between unity and 3/2 depending on the magnitude of [M].

The other theory is the "cage effect" developed by Matheson[71]. According to this theory the free radicals rejoin after decomposition unless they can escape a hypothetical cage surrounding the initiator. So, if $k_I[In]$ is the rate of initiator decomposition

$$I = \frac{rk_I[In][M]}{1+r[M]} \qquad (1.2.24)$$

where r is the reactivity ratio of a radical towards a monomer and to its own kind. Then from equations (1.2.9) and (1.2.24)

$$-\frac{d[M]}{dt} = k_p\left(\frac{rk_I[In]}{k_t+k'_t}\right)^{1/2}[M]^{3/2}(1+r[M])^{-1/2} \qquad (1.2.25)$$

1.2.4 Molecular Weight Distribution in Polymers and Copolymers

The distribution of chain lengths in a polymerization can be derived statistically. This problem was first investigated by Bursian and Sorokin[14] for linear chain reactions and applied to polymerization by Schulz[15] (see also Gee and Melville[11] and Herington and Robertson[16]). If τ_p shows an average time each propagation step takes and τ_f, τ_{fs} and τ_t show the average time taken by each chain from the time it starts as a single radical till the time it terminates by transfer to monomer or solvent and by a termination reaction, respectively, then

$$\frac{1}{\tau} = \frac{1}{\tau_p} + \frac{1}{\tau_f} + \frac{1}{\tau_{fs}} + \frac{1}{\tau_t} \qquad (1.2.26)$$

Here it will be generalised that there is transfer to monomer and solvent and termination can be by both combination and disproportionation. It can easily be seen that the probability of any radical undergoing a propagation reaction instead of any other reaction is

$$\zeta = \frac{1}{\tau_p} \Big/ \frac{1}{\tau} = \frac{1}{\tau_p} \Big/ \left(\frac{1}{\tau_p} + \frac{1}{\tau_f} + \frac{1}{\tau_t}\right) \qquad (1.2.27)$$

Substituting for the τ's from

$$1/\tau_p = k_p M \quad ; \quad 1/\tau_f = k_f M \quad , \quad 1/\tau_t = k_t R^{\cdot} = \left\{I(k_t + k_t')\right\}$$

one obtains

$$\zeta = k_p M \Big/ \left(k_p M + k_{fs} S + k_f M + \left\{I(k_t + k_t')^{1/2}\right\}\right) \qquad (1.2.28)$$

With the assumptions of stationary state condition and constancy of monomer and initiator concentrations similar equations as section (1.2.3) can be derived for the concentrations of intermediate radical products. This time transfer to solvent is also taken into account

$$R_r^{\cdot} + S \xrightarrow{k_{fs}} P_r + S^{\cdot} \qquad (1.2.29)$$

and I denotes rate of formation for $R_1^{\cdot}$. Therefore

$$\frac{dR_1^{\cdot}}{dt} = I - k_p M R_1^{\cdot} + (k_{fs} S + k_f M) R^{\cdot} - (k_{fs} S + k_f M) R_1^{\cdot} - (k_t + k_t') R_r^{\cdot} R^{\cdot} = 0 \qquad (1.2.30)$$

$$\frac{dR_r\cdot}{dt} = k_p M R_{r-1}\cdot - k_p M R_r\cdot - (k_{fs}S+k_f M)R_r\cdot - (k_t+k_t')R_r\cdot R\cdot = 0 \tag{1.2.31}$$

The square brackets are omitted for simplicity. On the other hand, for long chains,

$$-\frac{dM}{dt} = I + k_p M R\cdot + k_f M R\cdot = k_p M R\cdot \tag{1.2.32}$$

In the above equation $R\cdot$ denotes the total radical concentration as $\sum_n [R_n\cdot]$ in the previous section, which is

$$R\cdot = \left\{I/(k_t+k_t')\right\}^{1/2}$$

Substituting this into equations (1.2.30), (1.2.31) and (1.2.32)

$$R_1\cdot = \left(\frac{I}{k_t+k_t'}\right)^{1/2} \frac{k_{fs}S+k_f M+\left\{I(k_t+k_t')\right\}^{1/2}}{k_p M+k_{fs}S+k_f M+\left\{I(k_t+k_t')\right\}^{1/2}} \tag{1.2.33}$$

$$R_r\cdot = R_{r-1}\cdot \frac{k_p M}{k_p M+k_{fs}S+k_f M+\left\{I(k_t+k_t')\right\}^{1/2}} \quad , r\geqslant 2 \tag{1.2.34}$$

$$\frac{dM}{dt} = k_p M \left\{I/(k_t+k_t')\right\}^{1/2} \tag{1.2.35}$$

Then for the formation rate of a polymer with chain length r,

$$\frac{dP_r}{dt} = (k_{fs}S+k_f M)R_r\cdot + \frac{1}{2}k_t \sum_{n=1}^{r-1} R_n\cdot R_{r-n}\cdot + k_t' R_r\cdot R\cdot \tag{1.2.36}$$

If the above assumptions are considered equations (1.2.33) and (1.2.34) become

$$R_1\cdot = \left(\frac{I}{k_t+k_t'}\right)^{1/2}(1-\zeta) \tag{1.2.37}$$

$$R_r\cdot = \zeta R_{r-1}\cdot = \left(\frac{I}{k_t+k_t'}\right)^{1/2}(1-\zeta)\,\zeta^{r-1} \quad , r\geqslant 2 \tag{1.2.38}$$

where ζ is already defined and $(1-\zeta)\,\zeta^{r-1}$ is the probability of formation of a chain with length r. After proper mathematical manipulations equation (1.2.36) becomes

$$-\frac{dP_r}{dt} = \left(\frac{I}{k_t+k_t'}\right)^{1/2} (1-\zeta)\ \zeta^{r-1}\left[k_{fs}S+k_fM+\left(\frac{I}{k_t+k_t'}\right)^{1/2}\left(\frac{(r-1)k_t(k_{fs}S+k_fM+\{I(k_t+k_t')\}^{1/2})}{2k_pM}+k_t'\right)\right] \tag{1.2.39}$$

For a conversion ΔM monomers at time t where

$$P_r = \frac{dP_r}{dt}\,t \quad , \qquad \Delta M = \frac{dM}{dt}\,t = k_pMt\left(\frac{I}{k_t+k_t'}\right)^{1/2}$$

Equations (1.2.39) gives the general distribution function

$$P_r = \frac{\Delta M}{k_pM}(1-\zeta)\ \zeta^{r-1}\left[k_{fs}S+k_fM+\left(\frac{I}{k_t+k_t'}\right)^{1/2}\left(\frac{(r-1)k_t(k_{fs}S+k_fM+\{I(k_t+k_t')\}^{1/2})}{2k_pM}+k_t'\right)\right] \tag{1.2.40}$$

For special cases where termination is exclusively (i) by disproportionation, (ii) by combination equation (1.2.40) gives

$$\text{(i)}\quad P_r = \Delta M(1-\zeta)^2\,\zeta^{r-1} \tag{1.2.41}$$

$$\text{(ii)}\quad P_r = \frac{\Delta M}{k_pM}(1-\zeta)\ \zeta^{r-1}\left[k_{fs}S+k_fM+(r-1)(Ik_t)^{1/2}\left(\frac{k_{fs}S+k_fM+(Ik_t)^{1/2}}{2k_pM}\right)\right] \tag{1.2.42}$$

Here ζ in each case is one having the appropriate termination constants zero.

In order to calculate the various molecular weights it is necessary to calculate the appropriate moments from the above equations and this is done by the long chain assumption as

$$\sum_{r=1} P_r = \frac{\Delta M}{k_pM}\left\{k_{fs}S + k_fM + \left(\frac{I}{k_t+k_t'}\right)^{1/2}\left(\frac{k_t}{2}+k_t'\right)\right\} \tag{1.2.43}$$

$$\sum_{r=1} rP_r = \Delta M$$

$$\sum_{r=1} r^2P_r = \frac{2k_pM\,\Delta M}{\left[k_{fs}S+k_fM+\{I(k_t+k_t')\}^{1/2}\right]^2}\left[k_{fs}S + k_fM + \left(\frac{I}{k_t+k_t'}\right)^{1/2}(3/2k_t+k_t')\right] \tag{1.2.45}$$

In turn the average degrees of polymerization are obtained from

$$\bar{r} = \frac{\sum_{r=1} rP_r}{\sum_{r=1} P_r} \qquad (1.2.46)$$

$$\bar{r}_w = \frac{\sum_{r=1} r^2P_r}{\sum_{r=1} rP_r} \qquad (1.2.47)$$

where $\bar{r}$ is the number average degree of polymerization and $\bar{r}_w$ is the weight average degree of polymerization. Likewise for corresponding molecular weights

$$\bar{M}_n = \frac{\sum MP_r}{\sum P_r} \qquad (1.2.48)$$

$$\bar{M}_w = \frac{\sum M^2P_r}{\sum MP_r} \qquad (1.2.49)$$

The ratio $\bar{r}_w/\bar{r}$ is an indication of polydispersity of the polymer. In the general case it can be seen that

$$\bar{r}_w/\bar{r} = 3/2 \qquad (1.2.50)$$

but if the termination is solely by disproportionation

$$\bar{r}_w/\bar{r} = 2 \qquad (1.2.51)$$

and this ratio also gives an indication of the type of termination that accompanies the particular polymerization.

A simlified form of equation (1.2.40) is found in the case where $r \gg 1$ so $\zeta^{r-1} = \zeta^r$ and $\zeta = 1$,

$$P_r = \frac{4\,\Delta M}{\bar{r}^3}\, re^{-2r/\bar{r}} \qquad (1.2.52)$$

Studies of copolymers were carried out by Simha and Bronson[17], Stockmayer[18] and Melville, Noble and Watson[19]. The method of calculation is the same and the distribution equation derived is

$$W_{r,y} = \frac{re^{-r/\bar{r}}}{\bar{r}^2}\left(\frac{r}{2\pi n_o m_o \kappa}\right)^{1/2} e^{-ry^2/2n_o m_o \kappa} \qquad (1.2.53)$$

Here y is the deviation in composition as n_o-n or m_o-m where n and m denote the mole fractions of A and B in the copolymer respectively. κ is given by

$$\kappa = \frac{r_A A^2+2r_A r_B AB+r_B B^2}{r_A A^2+2AB+r_B B^2} \qquad (1.2.54)$$

For individual distributions of length and composition

$$W_r = \frac{r}{\bar{r}^2} e^{-r/\bar{r}} \qquad (1.2.55)$$

$$W_y = \frac{3}{4} \left(\frac{\bar{r}}{2n_o m_o \kappa}\right)^{1/2} \left(1+\frac{\bar{r}y^2}{2n_o m_o \kappa}\right)^{-5/2} \qquad (1.2.56)$$

If a fraction f of the termination is assumed to be by combination (unlike the exclusive disproportionation discussed above) then

$$W_{r,y} = (1-f+\frac{fr}{2\bar{r}}) \frac{re^{-r/\bar{r}}}{\bar{r}^2} \left(\frac{r}{2\pi n_o m_o \kappa}\right)^{1/2} e^{-ry^2/2n_o m_o \kappa} \qquad (1.2.57)$$

As for the distribution of sequences in a single copolymer chain one obtains the function

$$A_n = \frac{\alpha^{n-1}}{(\alpha+1)^n} \qquad (1.2.58)$$

$$B_n = \frac{\beta^{n-1}}{(\beta+1)^n} \qquad (1.2.59)$$

where $\alpha=r_A f_A/(1-f_A)$ and $\beta=r_B(1-f_A)/f_A$ with r's the reactivity ratios and f_A the feed mole fraction of component A. The average sequence lengths can be determined from the mean of the distribution A_n and B_n.

$$\bar{N}_A = \sum_{n=1} nA_n = \frac{1}{(\alpha+1)} \sum_{n=0} (n+1) \left(\frac{\alpha}{\alpha+1}\right)^n = 1+\alpha \qquad (1.2.60)$$

$$\bar{N}_B = \sum_{n=1} nB_n = \frac{1}{(\beta+1)} \sum_{n=0} (n+1) \left(\frac{\beta}{\beta+1}\right)^n = 1+\beta \qquad (1.2.61)$$

The derivation of the sequence distributions are from statistic considerations and are delt with in more detail in section (4.2).

1.3 General Aspects of Copolymerization

1.3.1 The Copolymerization Equation

The first attempt to describe the copolymerization process kinetically was made by Dostal [20] in 1936. In this treatment Dostal assumed that the kinetic behaviour of the growing copolymer chain depended solely on the terminal active monomer unit and was independent of the overall composition of the chain itself. Therefore the copolymerization process was defined in four reaction steps:

$$\begin{aligned} M_1\cdot + M_1 &\longrightarrow M_1\cdot \quad \text{rate: } k_{11}[M_1\cdot][M_1] \\ M_1\cdot + M_2 &\longrightarrow M_2\cdot \quad k_{12}[M_1\cdot][M_2] \\ M_2\cdot + M_1 &\longrightarrow M_1\cdot \quad k_{21}[M_2\cdot][M_1] \\ M_2\cdot + M_1 &\longrightarrow M_1\cdot \quad k_{22}[M_2\cdot][M_1] \end{aligned} \qquad (1.3.1)$$

where M_1 and M_2 are the two monomers and $M_1\cdot$ and $M_2\cdot$ are the polymer chains ending with respective radical units. From these considerations Dostal derived, in his original notation, the composition equation in the following way: the consumption rates of the individual monomers were

$$q_A = (\alpha a + \beta b_A)A \qquad (1.3.2)$$

$$q_B = (\alpha a_B + \beta b)B \qquad (1.3.3)$$

where α and β were the probabilities of finding units A and B in the copolymer, A and B are the concentrations of monomers A and B in the feed and $a=k_{aa}$, $a_B=k_{ab}$, $b_A=k_{ba}$ and $b=k_{bb}$. Having

$$\alpha : \beta = q_A : q_B \qquad (1.3.4)$$

one arrives at

$$\frac{\beta}{\alpha} = \frac{\alpha a_B + \beta b}{\alpha a + \beta b_A} \cdot \frac{B}{A} \qquad (1.3.5)$$

with

$$\alpha + \beta = 1 \qquad (1.3.6)$$

But although Dostal obtained correct rate and composition expressions he never produced experimental results to support his theory. This was probably due to the large number of rate coefficients to be estimated. The first reliable experimental data came from the work done on the copolymerization of styrene and methyl methacrylate by Norrish and Brookman[21] in 1939. These data were still not precise enough to test the theory for its assumptions. The best development on the calculation of the composition came from Wall[22] in 1941 who first claim that the composition of the copolymer depended on the relative reactivities of the two monomers towards the two radicals and so he put forward the concept of reactivity ratios

$$k_{11}/k_{12} = r_1 \ , \ k_{22}/k_{21} = r_2 \qquad (1.3.7)$$

He went further to make an additional assumption that

$$r_1 = 1/r_2 \qquad (1.3.8)$$

to produce the simple copolymer composition equation

$$X = rx \qquad (1.3.9)$$

where X and x were the ratio of the two monomers in the feed and in the copolymer respectively as a/b and r was the relative addition rate k_a/k_b of A and B units to the growing chain. This equation, although valid for a few cases, is far from being general.

The first precise and systematic study of copolymerization was made by Mayo et al. which gave the data necessary to check on the theories. In 1944 Mayo and Lewis[23] and Alfrey and Goldfinger[24] separately developed the first general copolymerization equation. In their treatment they did not only consider the reactivity of the monomer, like Wall, but also of the radical end of the growing chain and the effect of the concentrations of the respective monomers and radical ends. Thus the mole fraction of A units in the copolymer is

$$-\frac{d[A]}{dt} = k_{aa}[A\cdot][A] + k_{ba}[B\cdot][A] \qquad (1.3.10)$$

and for B

$$-\frac{d[B]}{dt} = k_{bb}[B\cdot][B] + k_{ab}[A\cdot][B] \qquad (1.3.11)$$

where k_{aa} is the rate constant for the addition of a radical ending in unit A to monomer A, and so on. Dividing the rate of consumption of A by that of B one gets

$$\frac{d[A]}{d[B]} = \frac{k_{aa}[A\cdot][A] + k_{ba}[B\cdot][A]}{k_{ab}[A\cdot][B] + k_{bb}[B\cdot][B]} \qquad (1.3.12)$$

By assuming the steady-state condition where

$$[B\cdot] = \frac{k_{ab}}{k_{ba}} \frac{[B]}{[A]} [A\cdot] \qquad (1.3.13)$$

and defining $r_1 = k_{aa}/k_{ab}$ and $r_2 = k_{bb}/k_{ba}$ one gets

$$\frac{d[A]}{d[B]} = \frac{[A]}{[B]} \frac{r_1[A] + [B]}{r_2[B] + [A]} \qquad (1.3.14)$$

The ratio on the left hand side is also the ratio of the monomer units in the copolymer chain. Therefore, using small letters to show the concentrations of the monomer units in the copolymer mixture and capital letters to show the same in the copolymer chain, (which is the notation used for the rest of the thesis) one obtains for the general copolymerization equation

$$\frac{A}{B} = \left(\frac{a}{b}\right) \frac{r_1 a + b}{r_2 b + a} \qquad (1.3.15)$$

This, of course, is the equation for the composition of the initial copolymer or, since the composition of the feed will change during the course of copolymerization process due to the inequality of the feed and copolymer compositions, the differential form is the instantaneous copolymer composition. The equation, when plotted as a/(a+b) vs. A/(A+B) gives a family of curves which are analogous to the curves of solution vs. vapour compositions in binary distillation. In fact the copolymerization process may even show an 'azeotrope' if the curve cuts the A=a diagonal.

1.3.2 The Relation between Monomer Structure and Reactivity

The structure of the monomer can be considered to affect the reactivity of free radicals in three ways; these are resonance, polar and steric factors. Steric effects can not be put on a quantitative basis but the resonance stabilization and the polarity were treated by Alfrey and Price[25] in the so-called Q-e scheme, in a semi-quantitative way.

The idea of the Q-e scheme was "...to find a simple pattern of copolymerization behaviour which would allow each individual monomer to be described by characteristis constants. This would simplify the experimental task of estimating the reactivity ratios of various monomer pairs. Instead of estimating the reactivity ratios for all the pair combinations possible for all monomers it would have been enough to estimate the reactivity ratios of one monomer with a few others in order to calculate the characteristic constants, then to use these constants to calculate the reactivity ratios of the particular monomer with the rest of the monomers. The usefulness of such a concept becomes even more obvious when one considers multi-component copolymerization."

The Q-e scheme combines the effects of resonance stabilization and polarity in the sense that Q defines the former and e the latter. The resonance stabilization of the radical has much to do with the conjugation of the double bond with the double bonds, if any, present in the substituent groups. Thus the resonance stabilization is high in the case of styrene radical where the double bonds in the phenyl group are conjugated with the ethylene double bond. Therefore although styrene monomer is not stable or unreactive the growing chain radical is quite and relatively unreactive. The reverse is true in the case of vinyl acetate. To show this on the potential energy diagram one takes the case of attacking radical and produced radical separately. Since in the reaction the governing factors are the potential energies of attacked monomer and the product radical, in the four possible reactions:

$$A\cdot + A \longrightarrow A\cdot \qquad (1)$$

$$A\cdot + B \longrightarrow B\cdot \qquad (2)$$

$$B\cdot + A \longrightarrow A\cdot \qquad (3)$$
$$B\cdot + B \longrightarrow B\cdot \qquad (4) \qquad (1.3.16)$$

(1) and (2) are respectively similar to (3) and (4) so we only need to treat the competition between reaction (1) and (2) and (1) and (3). In the potential energy diagram the potential energy of the system is plotted against the separation of the reactants. Curve I shows the increase of the potential energy in the approaching monomer and curve II shows the increase of the potential energy in the product radical due to the streching of the bond joining the terminal monomer to the rest of the radical (see fig.(1)). In the case of reactions (1) and (2) one has two kinds of monomers being attacked and two kinds of radicals being produced. Supposing the radical B· has a resonance stabilization its curve IIb (fig.(1)) will be lower than that of A·, IIa. Similarly the same substituent on the monomer B will produce, although much less, some resonance stabilization and place the curve Ib accordingly. Then one can write

$$\Delta H_{ab} = \Delta H_{aa} - x_m + x_r \qquad (1.3.17)$$

where $x_m = E_{pA} - E_{pB}$ and $x_r = E_{pA\cdot} - E_{pB\cdot}$. With a good approximation one can also write(26,27)

$$E_{aa} - E_{ab} = \alpha(x_r - x_m) \quad 0 < \alpha < 1 \qquad (1.3.18)$$

By assuming that the pre-exponential factors are approximately equal

$$\frac{k_{aa}}{k_{ab}} = \frac{\exp(-E_{aa}/RT)}{\exp(-E_{ab}/RT)} = \exp(-\alpha(x_r - x_m)/RT \qquad (1.3.19)$$

which is proposed to be equal to Q [27] in the Q-e scheme.

In the case of reactions (1) and (3) (fig.(2)) there will be only curve II with Ia and Ib. Therefore

$$E_{ba} - E_{aa} = x_r - x_t = \gamma x_r \quad 0 < \gamma < 1 \qquad (1.3.20)$$

$$k_{aa}/k_{ba} = \exp(\gamma x_r/RT) \qquad (1.3.21)$$

The polarity is the distribution of the electric charges in the monomer and the radical. If an electron-withdrawing group is present

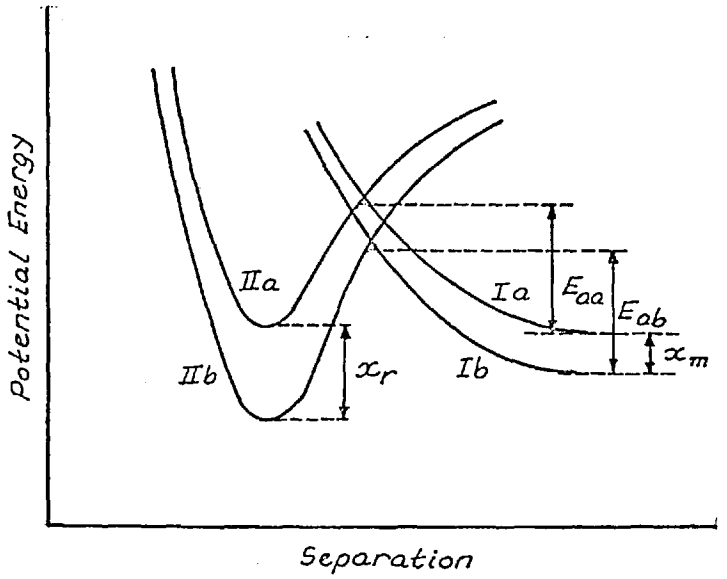

Fig.1 Potential energy diagram for reactions (1) and (2) of equation (1.3.16).

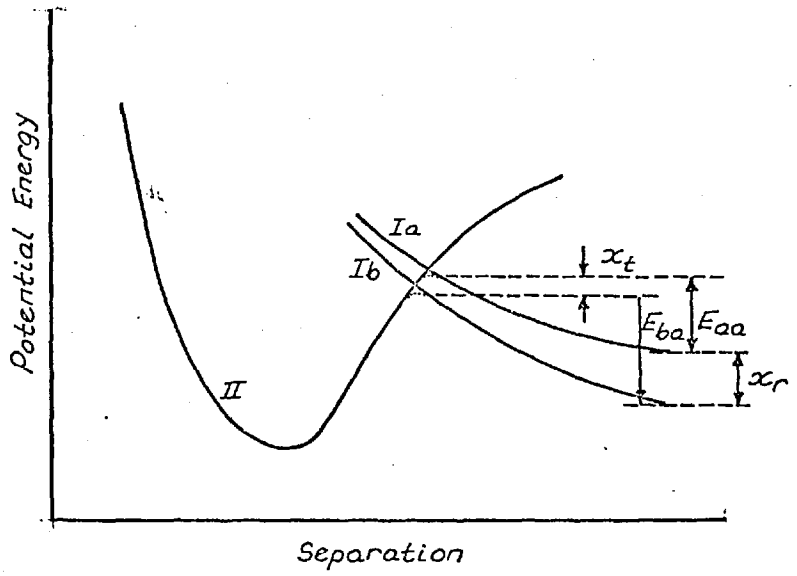

Fig.2 Potential energy diagram for reactions (1) and (3) of equation (1.3.16).

on the substituent this will be expected to withdraw electrons from the polarizable double bond or radical to give it a positive character. On the other hand a negative character will be gained by a substituent group which is electron-donating. A free radical with a positive character will show a tendency to react with a monomer with a negative group.

With these generalizations one can write the rate constant of any radical i adding the monomer j as

$$k_{ij} = P_i Q_j \exp(-e_i e_j) \qquad (1.3.22)$$

where P_i is the characteristic of radical i, Q_j is the mean reactivity of monomer j and e_i and e_j are the corresponding polarities. When one wants to find the relative reactivity of radical i towards all radicals present, where in the binary case it is only j and its own monomer i, one has

$$k_{ii} = P_i Q_i \exp(-e_i^2) \qquad (1.3.23)$$

and as P_i cancels out, for reactivity ratio

$$\frac{k_{ii}}{k_{ij}} = Q_i/Q_j \exp(-e_i(e_i-e_j)) \qquad (1.3.24)$$

or for monomers A and B,

$$\frac{k_{aa}}{k_{ba}} = Q_a/Q_b \exp(-e_a(e_a-e_b)) \qquad (1.3.25)$$

Where there is severe steric hindrance the Q-e scheme is no longer applicable. There are mainly two kinds of steric hindrance in vinyl polymerization, namely of 1,2-Disubstituted ethylenes and 1,1-Disubstituted ethylenes. In the former, due to the bulky substituents on the end carbon atom of the attacking radical and on the carbon atom being attacked, the monomer is reluctant to homopolymerize (fig.(3a)). Although it may copolymerize with other active radicals its reactivity ratio tends to be zero or near zero. In the latter the steric hindrance is somewhat different. When the monomer is carrying the carbon atoms 1 and 2 (fig.(3b)) joins the radical at 3, that carbon atom has

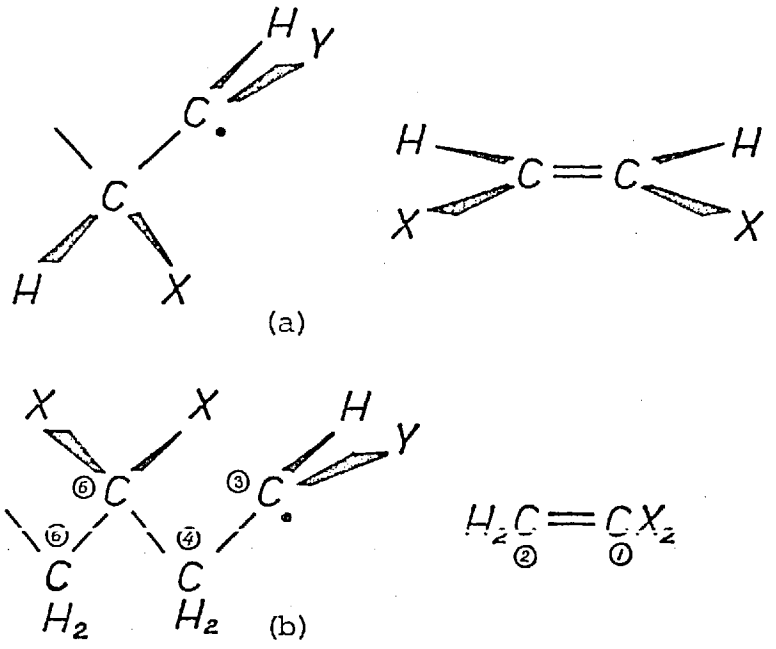

Fig.3 Configurational formulation of radical addition reaction for (a) 1,2 and (b) 1,1 disubstituted ethylenes.

to comply with the tetrahedral arrangements of carbon-carbon σ bonds thus pushing the bulky substituents towards those on carbon atom 5. The effect of this is more pronounced in the product than in the transition state giving rise to a tendency to depolymerization and a low heat of polymerization. The size of the substituents affect the overall reaction not only by slowing down the forward reaction but to a greater extent by speeding up the reverse reaction. If the ceiling temperature for the polymerization is high enough the Q-e scheme may still be applicable as in the case of methyl methacrylate; but with monomers having rather low ceiling temperatures, like α-methyl styrene, it is not possible to apply the Q-e scheme. One way of applying the Q-e scheme to the systems involving a monomer M, and, say, α-methyl styrene would be to use the scheme in the calculation of r_1 only but not r_2.

1.3.3 Effect of Temperature on Reactivity Ratios

The effect of temperature on the reactivity ratios is due to its effect on the individual rate constants. So if one writes the Arrhenius equation

$$k = Ae^{-E/RT}$$

or in terms of transition state theory

$$k = (\kappa T/h)\, e^{\Delta S^{\neq}/R - \Delta H^{\neq}/RT} \qquad (1.3.26)$$

where $\Delta S^{\neq}$ is the entropy and $\Delta H^{\neq}$ is the heat of activation. For the reactivity ratio

$$r_1 = \frac{k_{11}}{k_{12}} = \exp((\Delta S^{\neq}_{11} - \Delta S^{\neq}_{12})/R - (\Delta H^{\neq}_{11} - \Delta H^{\neq}_{12})/RT) \qquad (1.3.27)$$

One can assume that $\Delta S^{\neq}$ is very nearly the same for both reactions, then

$$r_1 = e^{-(\Delta H^{\neq}_{11} - \Delta H^{\neq}_{12})/RT} \qquad (1.3.28)$$

This shows that a plot of log r_1 vs. $1/T$ would give a straight line with slope $(\Delta H^{\neq}_{12} - \Delta H^{\neq}_{11})/2.303R$ and zero intercept. Since the heat

of activation for the propagation reaction is small and the difference even smaller the dependence on the temperature will not be very marked. Also reactivity ratios close to unity will give the least change with temperature.

1.3.4 Probability Considerations

The first to use probability considerations in order to derive the copolymer composition equation were Godfinger and Kane[28]. Since the copolymerization reaction is a competitive reaction we may allocate probabilities to each competitive step. Supposing at a certain instant the terminal active unit of a growing polymer chain is A, then, with the assumption that any unit preceding the active terminal unit has no effect on the reaction, one has two competetive reactions

$$\begin{aligned} A\cdot + A &\xrightarrow{k_{aa}} AA\cdot \\ A\cdot + B &\xrightarrow{k_{ab}} AB\cdot \end{aligned} \qquad (1.3.29)$$

the rates of reactions being

$$-\frac{d[A]}{dt} = k_{aa}[A\cdot][A] \qquad (1.3.30)$$

$$-\frac{d[B]}{dt} = k_{ab}[A\cdot][B] \qquad (1.3.31)$$

For the probability of A adding A one gets

$$P_{aa} = \frac{k_{aa}[A\cdot][A]}{k_{aa}[A\cdot][A] + k_{ab}[A\cdot][B]} \qquad (1.3.32)$$

or by dividing by $k_{ab}[A\cdot][B]$

$$P_{aa} = \frac{r_A x}{r_A x + 1} \qquad (1.3.33)$$

where $r_A = k_{aa}/k_{ab}$ and $x = [A]/[B]$. Similarly

$$P_{ab} = \frac{1}{r_A x + 1} = 1 - P_{aa} \qquad (1.3.34)$$

For the case of B as terminal active unit where B adds either B or A

$$P_{ba} = \frac{1}{1 + r_B/x} = 1 - P_{bb} \qquad (1.3.35)$$

where $r_B = k_{bb}/k_{ba}$.

For the derivation of the composition equation Goldfinger and Kane developed a treatment which does not involve the stationary state assumption. The abundance of n sequential A units in the copolymer chain is given by

$$N_n = P_{aa}^{n-1} P_{ab} \qquad (1.3.36)$$

The number average sequence length of a is the sum of sequence probabilities weighted by the number of a's in each sequence

$$W_a = P_{ab} + 2P_{aa}P_{ab} + \cdots + nP_{aa}^{n-1}P_{ab} \qquad (1.3.37)$$

$$W_a = \frac{P_{ab}}{P_{aa}} \sum_{n=1} nP_{aa}^n \qquad (1.3.38)$$

which, since $P_{ab} = 1-P_{aa}$, is an equation of the form

$$S_n = \frac{1-x}{x} \sum_{n=1} nx^n \qquad (1.3.39)$$

and corresponds to the series

$$S_n = 1 + x + x^2 + x^3 + \cdots + x^n \qquad (1.3.40)$$

which is the summation

$$S_n = \frac{1}{x} \sum_{n=1} x^n \qquad (1.3.41)$$

and

$$S_n = \frac{1-x^n}{1-x} \qquad n \longrightarrow \infty \qquad (1.3.42)$$

$$S_n = \frac{1}{1-x} \qquad \text{for } x < 1 \qquad (1.3.43)$$

From this we get

$$W_a = \frac{1}{1-P_{aa}} = \frac{1}{P_{ab}} \qquad (1.3.44)$$

Similarly

$$W_b = \frac{1}{P_{ba}} \qquad (1.3.45)$$

The composition of the copolymer chain would be

$$W_a/W_b$$

so

$$X = \frac{A}{B} = \frac{W_a}{W_b} = \frac{P_{ba}}{P_{ab}} \qquad (1.3.46)$$

From equations (1.3.20) and (1.3.21)

$$X = \frac{1 + r_A x}{1 + r_B/x} \qquad (1.3.47)$$

The copolymerization composition equation derived in this section considered only the terminal unit model which assumes that only the terminal active unit on a growing radical chain has influence on the copolymerization reaction and also that all four copolymerization reactions are practically irreversible. The derivation of the composition equations for higher models like the penultimate unit influence or the depropagation of reaction steps will be given later in chapter IV.

1.3.5 Composition Distribution Equation

The instantaneous composition of the copolymer, apart from the azeotrope point, is in general not equal to that of the comonomer feed. Thus the comonomer mixture is bound to change during the course of the reaction, with a consequent change in the composition of the instantaneous copolymer being formed. The composition of the copolymer at a particular conversion is the average composition which is somewhere

between the first instantaneous composition and the last. The equation (1.3.15) is only applicable to very low conversions, and to the azeotropic feed composition. Its actual form is the differential form and it is only truly applicable to the instantaneous copolymerization.

$$\frac{dm_1}{dm_2} = \frac{M_1}{M_2}\frac{r_1M_1 + M_2}{r_2M_2 + M_1} \qquad (1.3.48)$$

Here m_1 and m_2 are mole fractions of the monomers in the copolymer and M_1 and M_2 in the feed. The subscripts show the first and the second monomer and $r_2=k_{22}/k_{21}$ (the nomenclature used here is slightly different, in order to correspond better with the references). Equation (1.3.46) may be combined with Rayleigh's distillation equation

$$\frac{dM}{M} = \frac{dM_1}{m_1-M_1} \qquad (1.3.49)$$

for a type of system which is analogous to copolymerization. From the combination of these equations one derives a differential composition distribution function[72]

$$\frac{dM}{Mdm_1} = -\frac{\left[M_1^2(r_1+r_2-2)-2M_1(r_2-1)+r_2\right]^3}{\left[M_1^2(r_1-2r_1r_2+r_2)+2M_1(r_1-1)r_2+r_2\right](r_2-1)-(r_1+r_2-2)M_1]M_1(1-M_1)} \qquad (1.3.50)$$

where $M=M_1+M_2$. From this equation it is possible to evaluate composition distribution curves provided the initial and final monomer composition and the degree of conversion is known. By integrating equation (1.3.50) one obtains an integral composition distribution equation

$$\log\frac{M^o}{M} = \frac{r_2}{1-r_2}\log\frac{M_1^o}{M_1} + \frac{r_1}{1-r_1}\log\frac{M_2^o}{M_2} - \frac{1-r_1r_2}{(1-r_1)(1-r_2)}\log\left\{\frac{[2-r_1-r_2]M_1^o+r_1-1}{[2-r_1-r_2]M_1+r_1-1}\right\} \qquad (1.3.51)$$

where M is the remaining monomer moles after certain conversion. From the above equation it is possible to obtain the degree of conversion if the monomer composition is known by analysis. Combining equations (1.3.50) and (1.3.51) one obtains

$$\frac{dM}{M^{o}dm_1} = \left(\frac{M_1^{o}}{M_1}\right)^{\frac{r_2}{(r_2-1)}} \left(\frac{1-M_1^{o}}{1-M_1}\right)^{r_1(r_1-1)} \left(\frac{\frac{r_2-1}{r_1+r_2-2} - M_1^{o}}{\frac{r_2-1}{r_1+r_2-2} - M_1}\right)^{\frac{1-r_1r_2}{(1-r_1)(1-r_2)}}$$

$$\frac{\left[M_1^2(r_1+r_2-2)-2M_1(r_2-1)+r_2\right]^3}{\left[M_1^2(r_1-2r_1r_2+r_2)+2M_1(r_1-1)r_2+r_2\right](r_2-1)+(r_1+r_2-2)M_1\,M_1(1-M_1)} \qquad (1.3.52)$$

To evaluate copolymer composition distribution (or drift) curves a simpler method is Skeist's[29] graphical integration method. The function to be graphically integrated is the distillation equation of Rayleigh (eq. (1.3.49))

$$\ln \frac{M}{M_1} = \int_{M_1^{o}}^{M_1} \frac{dM_1}{m_1-M_1} \qquad (1.3.53)$$

For the graphical integration $1/(m_1-M_1)$ is to be plotted against differential conversion, $c=dM/M$. The values obtained by graphical integration are plotted against conversion, $c=M/M_o$, i.e., c vs. m_1. The curve gives the instantaneous copolymer compositions at every degree of conversion. The average composition of the copolymer can be obtained by the integral average of the curve from zero conversion.

1.3.6 Molecular Weight and Overall Rate of Reaction in Copolymerization

It is possible to obtain the overall rate and molecular weight relationship from the complicated copolymerization mechanism by making certain assumptions. In addition to the usual radical polymerization assumptions three more are needed:

(i) The rate of initiation is independent of the composition of the feed.

(ii) Any transfer reaction is not accompanied by retardation.

(iii) There are only four propagation and three termination reactions.

Therefore, apart from the four propagation reactions, there is one radical production (assuming a homolytic cleavage of the initiator),

$$\text{Initiator} \xrightarrow{k_I} 2R\cdot$$

and three termination reactions (assuming only combination),

$$2\ \sim\!\sim A\cdot \xrightarrow{k_{taa}} \sim\!\sim A\text{-}A\sim\!\sim$$

$$\sim\!\sim A\cdot + \sim\!\sim B\cdot \xrightarrow{k_{tab}} \sim\!\sim A\text{-}B\sim\!\sim$$

$$2\ \sim\!\sim B\cdot \xrightarrow{k_{tbb}} \sim\!\sim B\text{-}B\sim\!\sim$$

In the steady state, since the rate of radical production will be equal to that of radical disappearance,

$$2k_I[In] = 2(k_{taa}[A\cdot]^2 + k_{tab}[A\cdot][B\cdot] + k_{tbb}[B\cdot]^2) \quad (1.3.54)$$

where [In] is the initiator concentration, and the square brackets show the corresponding radical concentrations. It is assumed that during propagation

$$k_{ab}[A\cdot][B] = k_{ba}[B\cdot][A] \quad (1.3.55)$$

so

$$[B\cdot] = (k_{ab}/k_{ba})([B]/[A])[A\cdot] = \beta[A\cdot] \quad (1.3.56)$$

$$= (k_{ab}/k_{ba})([B]/[A])$$

from equations (1.3.54) and (1.3.56)

$$k_I[In] = [A\cdot]^2(k_{taa}+k_{tab}\beta+k_{tbb}\beta^2) \quad (1.3.57)$$

$$[A\cdot] = (k_I[In]/(k_{taa}+k_{tab}\beta+k_{tbb}\beta^2))^{1/2} \quad (1.3.58)$$

$$[B\cdot] = (k_I[In]\beta^2/(k_{taa}+k_{tab}\beta+k_{tbb}\beta^2))^{1/2} \quad (1.3.59)$$

By using the equations (1.3.56), (1.3.58) and (1.3.59) the rates of consumption of individual monomers are found directly

$$-\frac{dA}{dt} = (k_{aa}[A]+k_{ba}\beta[A])(k_I[In]/(k_{taa}+k_{tab}\beta+k_{tbb}\beta^2))^{1/2} \quad (1.3.60)$$

$$-\frac{dB}{dt} = (k_{ab}[B]+k_{bb}\beta\,[B])\,(k_I[In]/(k_{taa}+k_{tab}\beta+k_{tbb}\beta^2))^{1/2} \qquad (1.3.61)$$

For overall rate of consumption of monomers

$$R = -\frac{d(A+B)}{dt} = (k_{aa}[A]+k_{ba}\beta\,[A]+k_{ab}[B]+k_{bb}\beta\,[B])\,(k_I[In]/(k_{taa}+k_{tab}\beta+k_{tbb}\beta^2))^{1/2} \qquad (1.3.62)$$

Since the degree of polymerization for radical polymerization is

$$DP = \frac{\text{rate of propagation}}{\text{rate of initiation}} = \frac{k_p[R\cdot]\,[M]}{k_I[In]} \qquad (1.3.63)$$

in the steady state

$$DP = \frac{k_p[R\cdot]\,[M]}{k_t[R\cdot]^2} \qquad (1.3.64)$$

and for the polymerization

$$DP = \frac{k_{aa}[A]+k_{ba}\beta\,[A]+k_{ab}[B]+k_{bb}\beta\,[B]}{(k_I[In])^{1/2}(k_{taa}+k_{tab}\beta+k_{tbb}\beta^2)^{1/2}} \qquad (1.3.65)$$

From the equations for overall rate and degree of polymerization it can be seen that for a fixed monomer ratio the overall rate is directly proportional to the monomer and to the square root of the initiator concentrations, but the degree of polymerization is directly proportional to the monomer and inversly proportional to the square root of the initiator concentrations

$$R \propto [M][In]^{1/2} \qquad (1.3.66)$$

$$DP \propto [M][In]^{-1/2} \qquad (1.3.67)$$

From these two proportionalities it is possible to obtain a third one

$$DP \propto R \qquad (1.3.68)$$

which means for a constant initiator concentration the DP is directly proportional to the rate, and as rate changes with varying monomer composition so does the DP.

According to Walling[30] equation (1.3.68) can be written in a

more analytical way by some suitable parametric notation, i.e.,

$$R = -\frac{(r_A[A]^2+2[A][B]+r_B[B]^2)\,(I^{1/2}/\delta_A)}{r_A^2[A]+2\phi\, r_A r_B[A][B]\,\delta_B/\delta_A+r_B^2[B]^2(\delta_B/\delta_A)^{2\,1/2}} \qquad (1.3.69)$$

$$r_a=\frac{k_{aa}}{k_{ab}} \quad , \quad r_B=\frac{k_{bb}}{k_{ba}} \quad , \quad \delta_A^2=\frac{k_{taa}}{k_{aa}^2} \quad , \quad \delta_B^2=\frac{k_{tbb}}{k_{bb}^2}$$

$$\phi=\frac{k_{tba}^2}{k_{taa}k_{tbb}} \qquad I=k_i[In]$$

The δ 's are ratios of termination and propagation rate constants for individual monomers and can be obtained from the kinetic study of their homopolymerizations. The r's are the reactivity ratios and can be obtained from composition studies of the copolymer. The determination of ϕ, provided the other parameters are established, can be done by estimating the overall rate of the copolymerization reaction at various feed compositions.

1.4 Effect of Pressure on Chemical Reactions

Of the two theories of reaction rates the collision theory has not been very succesfully used to interpret the pressure effect on the rate of liquid-phase reactions, in terms of the collision number, Z, or the frequency factor, A. On the other hand it has proved possible to explain and predict the pressure effect on the rate by means of the transition state theory, (both qualitatively and semi-quantitatively). In the collision theory, besides the collision number, Z, and the frequency, A, it is necessary to use an empirical probability factor, P, to explain the 'slow' reactions. Transition state theory on the other hand was developed not empirically but on the basis of fundamental physical properties such as dimensions, vibration frequencies, masses, etc., of the reacting molecules and has therefore been termed the theory of absolute reaction rates. It is possible to explain the P factor

by the transition state theory using the partition function concept, hence

$$P = (q_v/q_r)^3 \qquad (1.4.1)$$

where q_v and q_r are the vibrational and transitional partition functions.

The transition state theory assumes the existence of a transition complex which is in equilibrium with the reactants[31,32,33].

$$A + B + \cdots \rightleftharpoons X^{\neq} \longrightarrow \text{products} \qquad (1.4.2)$$

The transition complex posesses a potential energy surface similar to that an ordinary molecule and it can be treated by statistical methods in the same way. But in addition to having three translational degrees of freedom it has a fourth one along the reaction coordinate. By statistical considerations it can be found that[3]

$$\text{Rate of reaction} = [X^{\neq}](\kappa T/h) \qquad (1.4.3)$$

where κ is the Boltzmann constant and h is the Planck constant. Therefore the effective rate of crossing the energy barrier for the complex in the reaction coordinate is the universal frequency of $\kappa T/h$, which depends only on temperature. A reaction rate can be expressed as

$$\text{Rate of reaction} = k[A][B]\cdots \qquad (1.4.4)$$

and hence from (1.4.3) and (1.4.4)

$$k = \frac{\kappa T}{h} \cdot \frac{[X^{\neq}]}{[A][B]\cdots} = \frac{\kappa T}{h} K^{\neq} \qquad (1.4.5)$$

where $K^{\neq}$ is the equilibrium constant for

$$A + B + \cdots \rightleftharpoons X^{\neq} \qquad (1.4.6)$$

The system is assumed to be ideal to allow the use of concentrations instead of activities.

The dependence of k on pressure can be obtained directly from equation (1.4.5), thus

$$\left(\frac{\partial \ln k}{\partial P}\right)_T = \left(\frac{\partial \ln K^{\neq}}{\partial P}\right)_T \qquad (1.4.7)$$

and if mole fraction on molality is used as concentration unit

$$-RT\left(\frac{\partial \ln k}{\partial P}\right)_T = -RT\left(\frac{\partial \ln K^{\neq}}{\partial P}\right)_T = \left(\frac{\partial\, \Delta G^{\neq}}{\partial P}\right)_T = \Delta V^{\neq} \qquad (1.4.8)$$

$\Delta G^{\neq}$ is the standard change of free energy during the formation of the complex and $\Delta V^{\neq}$, the corresponding molar volume change, is called the 'activation volume'.

If the actual reaction is a reversible reaction

$$A + B + \cdots \rightleftharpoons M + N + \cdots \qquad (1.4.9)$$

then the pressure effect on the equilibrium constant is related to the partial molar volume change which accompanies the formation of the products from the reactants, ΔV^{o}

$$RT\left(\frac{\partial \ln K}{\partial P}\right)_T = -\Delta V^{o} \qquad (1.4.10)$$

The equation of the theory of absolute reaction rates can be used to express the temperature dependence of the rate constant. Since

$$-RT \ln K^{\neq} = \Delta G^{\neq} \qquad (1.4.11)$$

and

$$\Delta G^{\neq} = \Delta H^{\neq} - T\,\Delta S^{\neq} \qquad (1.4.12)$$

therefore

$$K^{\neq} = e^{\Delta S^{\neq}/R}\, e^{-\Delta H^{\neq}/RT} \qquad (1.4.13)$$

where $\Delta S^{\neq}$ and $\Delta H^{\neq}$ are the differences in entropy and enthalpy between the complex and the reactants. Then

$$k = (\kappa T/h)\, e^{\Delta S^{\neq}/R}\, e^{-\Delta H^{\neq}/RT} \qquad (1.4.14)$$

Since, (from eq.(1.4.8)), $\Delta V^{\neq}$ is the property of a reaction that determines the behaviour of reaction rate with pressure it is important to define its sign, magnitude and behaviour. If $\Delta V^{\neq}$ is negative, i.e., if the reaction goes through a transition complex with a molar volume less than the reactants the rate of the reaction increases with increasing pressure. A positive $\Delta V^{\neq}$ gives a decrease in rate with increasing pressure. The magnitude of $\Delta V^{\neq}$ determines the amount of increase of k per unit of ΔP.

For relatively low pressures $\Delta V^{\neq}$ can be assumed to be constant

but at higher pressures the curve of ln k tends to be concave to the pressure axis. This indicates that there is a decrease in $\Delta V^{\neq}$; which in turn means that the compressibility of the reactants is higher than that of the transition complex. If the curvature is not great the ln k vs. P curve can fit to the equation

$$\ln k = a + bP + cP^2 \qquad (1.4.15)$$

In general, if the suggested reason for the decrease of $\Delta V^{\neq}$ is true, it must be possible to fit this decrease to a more physically meaningful equation. On this respect Benson and Berson[34] made an attempt by assuming that the Tait equation is applicable to the transition state as well as the reaction medium.

$$V_p^{\neq} = V_1^{\neq}\left[1 - C^{\neq}\log_{10}\left(\frac{B^{\neq}+P}{B^{\neq}+1}\right)\right] \qquad (1.4.16)$$

Although this theory of Benson and Berson seems logical, lack of accurate kinetic data for non-polar reactions makes the application of an adequate test impossible thus the attempt to fit a 'Tait-like curve' to the experimental points of k vs. P has been strongly criticised by Hamann[35]. Until there is accurate kinetic data it is doubtful that this theory will get any confirmation and therefore be applied.

1.5 Effect of Pressure on Radical Polymerization

1.5.1 General

The effect of pressure on the rates of polymerization reaction is an overall effect which contains the effects on the individual reactions of the radical polymerization mechanism given in section (1.2.2). But nevertheless the effect of pressure on propagation usually predominates in the overall effect.

The propagation reaction is an addition process which is accompanied by contraction. This contraction in molar volumes favours the process thermodynamically. The transition state complex is an intermediate between reactants and products so the activation volume $\Delta V^{\neq}$ is negative and so the reaction rate increases with increased pressure.

In obtaining an expression for the overall effect of pressure one must consider the activation volumes of the various individual reactions which contribute to the overall rate, thus for an overall activation volume one gets (from eqs. (1.2.24) and (1.4.8))

$$\Delta V^{\neq}_{pol} = \Delta V^{\neq}_{p} + \Delta V^{\neq}_{I}/2 - \Delta V^{\neq}_{t}/2 \qquad (1.5.1)$$

and the overall change in reaction rate can be shown as

$$\left(\frac{\partial \ln k}{\partial P}\right)_T = - \frac{\Delta V^{\neq}_{pol}}{RT} \qquad (1.5.2)$$

In equation (1.5.1) $\Delta V^{\neq}_{I}$ and $\Delta V^{\neq}_{t}$ are the activation volumes of initiator decomposition and termination. $\Delta V^{\neq}_{I}$ for radical initiators is positive so the rate of dissociation is reduced by an increase in applied pressure. This is because at least one valency bond is lenghtened in the activated complex, so giving rise to a positive activation volume. For $\Delta V^{\neq}_{t}$ one expects a negative value since the transition state is more compact and an increase in pressure should increase the termination reaction. But it is found[40] that as the pressure increases k_t for styrene decreases. The reason is that the viscosity of the reaction medium increases with pressure and since the termination reaction of long chain radicals is diffusion-controlled this increase in viscosity slows down the rate of termination.

It can be seen that, since decreases in k_I and k_t and an increase in k_p all favour the growth of the chain, the effect of pressure on the degree of polymerization will clearly be a positive one, i.e., an increase in pressure will produce higher degree of polymerization. But the effect of pressure on the degree of polymerization will entirely depend on the sign of $\Delta V^{\neq}_{pol}$ which is in turn dictated by the relative magnitudes of the individual activation volumes with different signs. Generally $\Delta V^{\neq}_{pol}$ is negative and in the case of styrene ($\Delta V^{\neq}_{p}$ = -13.5 cm^3/mole[43] and $\Delta V^{\neq}_{t}$ = 11 cm^3/mole = $2\Delta V^{\neq}_{I}$) it appears to be around -16 cm^3/mole.

It is possible to calculate the degree of polymerization, approximately, for high pressure polymerization from equation (1.5.1) or equation (1.5.2) and experimental data for the rate constants. Even if there is transfer the change of transfer rates by pressure

is very close to that of k_p so their ratios do not change and hence do not affect DP.

1.5.2 Dissociation of Thermal Initiators under Pressure

The pressure-dependence of the dissociation of benzoyl peroxide is complicated by the existance of both homolytic and induced decompositions[37].

$$(PhCOO)_2 \xrightarrow{k_1} 2PhCOO\cdot$$

$$2PhCOO\cdot \xrightarrow{k_2} CO_2 + PhCOOPh \qquad (1.5.3)$$

$$PhCOO\cdot + (PhCOO)_2 \xrightarrow{k_3} PhCOOh + CO_2 + PhCOO\cdot$$

Nicholson and Norrish[41] derive the consumption rate from the above mechanism as

$$-d\phi/dt = k_1\phi + k_3(k_1/k_2)^{1/2}\phi^{3/2} \qquad (1.5.4)$$

where ϕ is the concentration of Bz_2O_2. k_1, being the rate constant of a unimolecular reaction of which activation volume is positive, is expected to decrease with increasing pressure. On the other hand k_2 and k_3 should increase with increasing pressure since[38] the activated complex of a bimolecular reaction has a smaller molar volume than the reactants. Nicholson and Norrish found k_1, the homolytic decomposition rate constant, to be increasing with pressure and $k_3(k_1/k_2)$, the induced rate constant combination, as a whole to decrease with pressure –showing the effect of k_3 to be more pronounced than $(k_1/k_2)^{1/2}$.

AZBN, as described in section (1.2.1), dissociates via several reaction steps before it produces final radicals, but these do not involve induced decomposition, and the reaction is, as a whole, unimolecular. Ewald[39] studied the effect of pressure on this rate constant and, as shown in fig.(4), found it to decrease with increased pressure. Some of the results of these findings are also given in Table (I). The ratio k-scavenger to k-direct decreases with increased pressure to show that wasted radicals are less at high pressures.

1.5.3 Radical Polymerization at High Pressures -Polymerization of Styrene

The effects of pressure on radical polymerization have been sudied for various monomers and especially for styrene. Merrett and Norrish[42] studied the high pressure styrene polymerization in relation to overall rate of polymerization and molecular weight (fig.(6)). According to these researches the rate of polymerization increases exponentially up to 2000 atm. and then still increases exponentially but with a lesser slope. They pointed out that in reality the data may show a continuous decrease in slope. As for the mode of reaction and molecular weight they claimed that these parameters depend mainly on the rate of mutual termination. If one assumes that transfer and termination by reaction with initiator are negligible and termination is mainly by mutual interaction then the rate of polymerization is of the 0.5 order to the initiator concentration

$$R = k_p\left(\frac{k_I}{k_t} I\right)^{1/2} \qquad (1.5.5)$$

But in the limiting case of $k_t = 0$ termination is mainly by reaction with initiator and the reaction is to the zeroth order of initiator concentration

$$R = k_p \frac{k_I}{k_{ti}} \qquad (1.5.6)$$

Their results show that this might be true since the order of the reaction drops from 0.5 to 0.4 until 3000 atm. which then stays constant. The increase of molecular weight until 3000 atm. and its leveling off at higher pressures was explained in the same manner by the same researchers: when the mutual termination reaction rate constants that have similar increases with pressure

$$DP = \frac{k_p}{k_{fm}+k_{ti}C+k_{fi}C} \qquad (1.5.7)$$

But Guarise[74] has shown that more probably this drop in reaction order is due to an increase in the proportion of thermally initiated

polymerization.

On the other hand Nicholson and Norrish[40] went on to calculate the individual rate constants from their rate and molecular weight date. Their results of rate constants are shown in fig.(5). They attributed the lessening of the decrease of ln (k_t/k_{to}) to the dependence of this constant to the viscosity of the medium, since they showed that k_t is inversely proportional to the viscosity of the medium under pressure.

For the various rate constants of transfer reactions studies were made on solution polymerizations. Walling and Pellon[43], Salahuddin[44] and Maulik[45] showed that C_s $(=k_{fs}/k_p)$ was practically insensitive to pressure, indicating that rate constant of transfer reaction to solvent was affected by pressure in the same order as k_p. But C_s results of Toohey and Weale[118] are in contrast with the above in the sense that these researches show a decrease in C_s with increased pressure. Nicholson and Norrish were unable to measure the other transfer constants from their experiments because even the magnitude of these constants were beyond the experimental error.

Nicholson and Norrish k_p results give a $\Delta V_p^{\neq}$ of -13.4 and it is not possible to calculate $\Delta V_I^{\neq}$ and $\Delta V_t^{\neq}$ with accuracy from their results for k_I and k_t but they seem to be of similar magnitude and sign. Walling and Pellon who used a different technique obtained the value of -11.5 cm^3/mole for $\Delta V_p^{\neq}$. The calculation of ΔV by Kobeko[46] from his high pressure polymerization data of styrene shows a decrease in this parameter indicating that $\Delta V^{\neq}$ also should decrease at higher pressures.

In the case of polymerization reactions with a substantial reverse reaction (depropagation) the effect of pressure on this reaction must also be considered. This, namely the effect of pressure on equilibrium polymerization, is discussed in section (2.4).

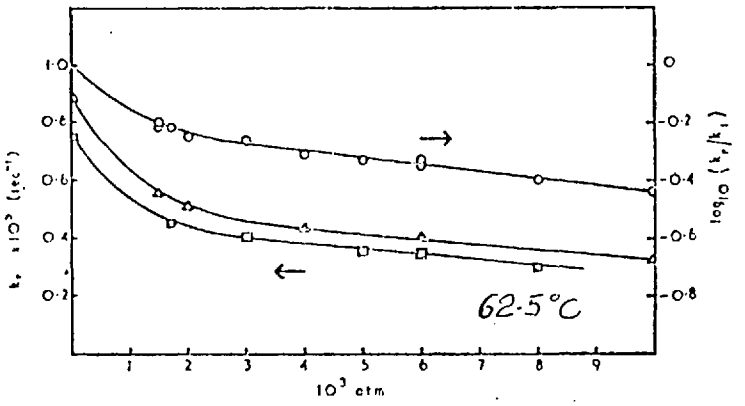

Fig.4 Pressure dependence of the dissociation rate constants of AZBN.

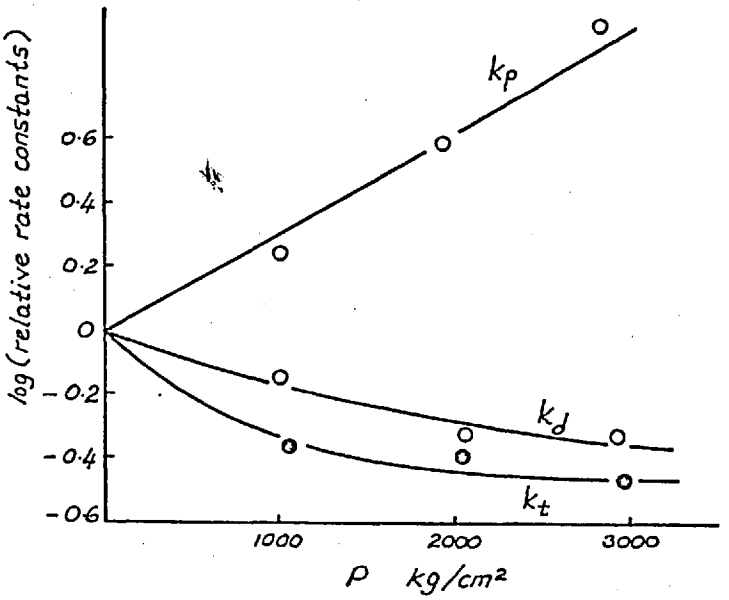

Fig.5 Pressure dependence of the individual rate constants of styrene polymerization.

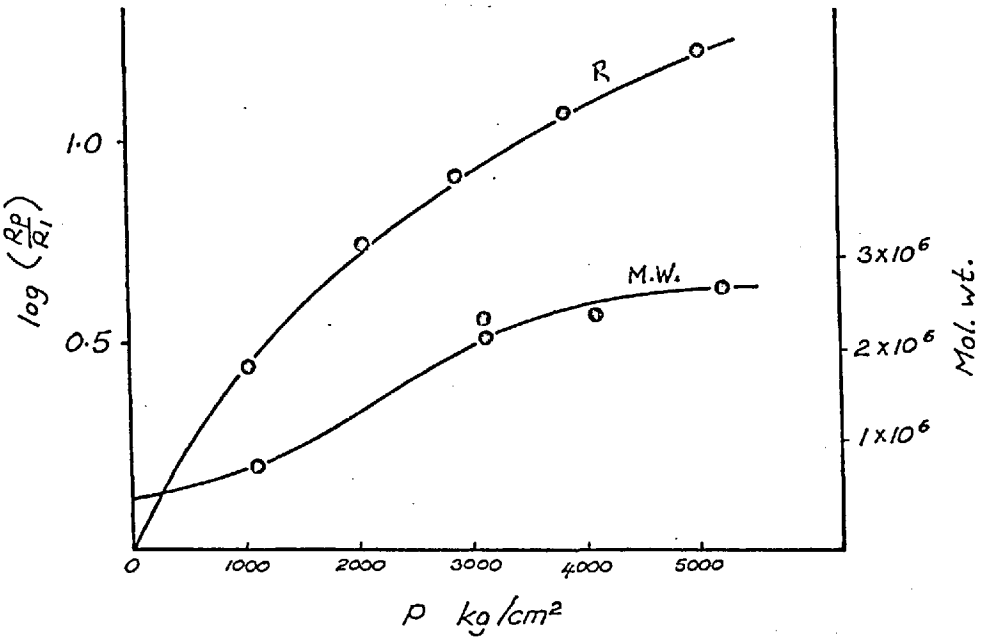

Fig.6 Pressure dependence of overall rate of polymerization and molecular weight of styrene polymerization.

TABLE 1.—DISSOCIATION OF 2:2'-AZO-*bis*-*iso*BUTYRONITRILE IN TOLUENE

pressure atm	$\bar{k} \times 10^5$ (sec^{-1}) 70° C direct	$k \times 10^5$ (sec^{-1}) 62·5° C direct	$k \times 10^5$ (sec^{-1}) 62·5° C scavenger	$\frac{k\text{ (scavenger)}}{k\text{ (direct)}}$
1	5·50	1·87	0·892	0·447
1500	4·47	1·52	0·552	0·363

1.6 Brief Review of Previous Work on the Effect of Pressure on Copolymerization Reactions

The effects of pressure on copolymerization reactions are again a combination of the effects of pressure on the individual component reactions which are somewhat greater in number than those in homopolymerization reactions. Lamb and Weale[47] have studied the copolymerization of three systems under pressures up to 4000 bars. These systems were:

styrene - methyl methacrylate
styrene - diethyl fumarate
methyl methacrylate - maleic anhydride

The pressure copolymerizations showed rate and molecular weight increases similar to those observed in homopolymerizations (Tables (II) to (IV)). The rate increase with pressure was exponential and the molecular weight increased up to 3000 atm. but then leveled off. There was no apparent change in monomer reactivity ratios and this was attributed to the equal effect of pressure on individual propagation steps. The $\Delta V^{\neq}_{pol}$ was in the range of -18 to -25 cm^3/mole. The termination factor ϕ was also calculated and this exhibited, in the case of styrene-methyl methacrylate, a higher positive change initially, especially for high styrene feeds, followed by a leveling off (Table (V)).

Ogo and Imoto[48] studied the effect of pressure on some less ideal systems, i.e., systems that are not explicable by the terminal unit model of copolymerization. They studied styrene-maleic anhydride with a penultimate model and showed that there is a tendency towards the terminal unit model under pressure (Table (VI), fig.(7) and (8)). They calculated $\Delta V^{\neq}$ for this system, and also reactivity ratios and $\Delta V^{\neq}$'s for the styrene-fumaronitrile system according to a penpenultimate unit model (Table (VII), fig.(9)). The other systems they studied under pressure include: fumaronitrile with 1,1 - diphenyl ethylene, methyl acrylate, vinylphenyl ether, α-methyl styrene, methyl methacrylate and trans-stilbene. The results obtained from these systems were interpreted as showing that high pressure tends to eliminate the penultimate effect in the copolymerization.

Table II

Polymerization of styrene and of methyl methacrylate at high pressures

Styrene t=60°C, I =0.1			MMA t=40°C, I =0.1			MMA t=45°C, I =0.04	
P,atm	Rate,%/h	MW*10^6	P,atm	Rate,%/h	η_{CHCl_3}	P,atm	Rate,%/h
1	1.55	0.22	1	0.55	6.85	1	0.69
1000	2.88	0.47	1000	0.99	12.2	2000	3.17
2000	5.20	0.72	2000	2.70	16.6		
3000	9.98	0.85	3000	7.90	21.1		
			4000	28.0	22.9		

Table III

Rates of copolymerization and properties of copolymers (t=60°C; I =0.1 in systems A and B, and 0.05 in C; in toluene; P=atm; Rate=%/h; F_A=A in pol.)

A. St + MMA				B. St + DEF				C. MMA+Mal.An.in 50%mole benzene		
P	Rate	F_A	η	P	Rate	F_A	η	P	Rate	η_{sp}
Initial %A = 19.0				Initial %A = 26.2				Initial %A = 15.0		
1	2.66	-	1.11	1	1.14	49.8	0.57	1	4.34	1.10
1000	6.29	26.3	2.19	1000	2.43	-	0.78	1000	9.90	2.04
1500	8.24	26.4	2.86	1500	3.24	52.9	0.88	1500	16.9	2.67
2500	17.2	28.0	4.01	2000	4.56	-	0.93	2000	30.4	3.38
3000	23.2	24.6	4.05	2500	7.64	52.4	0.98	2500	47.4	4.06
3500	60.1	26.0	-	3000	12.2	-	1.03	3000	97.1	4.59
3800	80.0	-	4.10	3340	13.6	51.6	1.03	3500	194.	4.33
				4000	27.7	-	1.03	4000	79.5	5.27
Initial %A = 48.0				Initial %A = 58.6				Initial %A = 25.1		
1	1.68	-	1.12	1	1.65	59.6	0.67	1	4.80	1.18
1000	3.27	48.7	2.03	1000	4.06	-	1.10	1040	12.6	2.42
1500	4.66	49.0	2.47	1500	5.63	57.9	1.32	1500	18.0	3.16
2000	7.08	49.5	2.85	2000	8.71	-	1.48	2000	33.1	3.87
2500	9.28	50.0	3.23	2500	15.1	58.9	1.59	2500	58.2	4.64
3000	13.1	48.3	3.55	3000	25.6	-	1.74	3000	108.0	5.08
3500	21.9	50.1	-	3500	41.0	59.7	1.79	3500	201.0	5.27
4000	29.4	-	3.60	4000	61.3	-	1.78	4000	88.0	-

Table II (cont'd)

P	Rate	F_A	η	P	Rate	F_A	η	P	Rate	η_{sp}
Initial %A = 78.6				Initial %A = 84.7				Initial %A = 34.6		
1	1.37	-	1.01	1	1.79	72.4	0.71	1	3.75	1.15
1070	2.89	-	1.78	1000	4.24	-	1.14	1000	10.1	2.69
1500	3.64	-	2.01	1500	6.13	72.1	1.49	1500	20.9	3.54
2000	5.00	73.2	2.43	2000	9.71	-	1.62	2000	33.7	4.35
2500	6.48	72.7	2.72	2500	16.3	70.1	1.81	2500	55.8	4.89
3000	9.01	73.4	2.82	3000	24.1	-	2.06	3000	107.0	5.37
3500	12.6	73.7	2.87	3500	42.3	70.0	2.14	3500	166.0	5.60
4000	20.0	-	2.90	4000	71.1	-	2.13	4000	106.0	-

Table IV

Monomer reactivity ratios at high pressures

P,atm	St(A)-MMA(B)		St(A) DEF(B)		MMA(A)-Mal.Anhyd.(B)	
	r_a	r_b	r_a	r_b	r_a	r_b
1	-	-	0.35	0.03	2.10	0.00
1000	0.53	0.47	-	-	-	-
1500	0.50	0.48	0.26	0.01	-	-
2000	0.53	0.45	-	-	2.40	0.00
2500	0.53	0.48	0.27	0.02		
3000	0.57	0.54	-	-		
3500	0.59	0.50	0.30	0.02		

Table V

Monomer reactivity ratios calculated from penultimate unit model. Styrene(1)-Mal.Anhyd.(2)

	P,atm					
	1	1000	1500	2000	2500	3000
St.mole%			ϕ			
79	46	80	106	100	105	112
48	29	39	48	41	42	40
19	14	12	15	13	15	16

Table VI

Monomer reactivity ratios calculated from penultimate unit model

Styrene(1)-Mal.Anhyd.(2)

P(kg/cm^2)	r_1	r_1'	r_1'/r_1
1	0.023	0.065	2.8
2000	0.022	0.055	2.5
4000	0.023	0.042	1.7

$r_1 = k_{111}/k_{112}$

$r_1' = k_{111}/k_{212}$

Table VII

Monomer reactivity ratios r_1, r_1', r_1'' and the effect of pressure.

Styrene(1)-Fum.Nit.(2)

P(kg/cm^2)	r_1	r_1'	r_1''
1	0.06	1.0	2.0
2000	0.057	0.94	1.7
3000	0.053	0.87	1.3
4000	0.05	0.8	1.0

$r_1 = k_{111}/k_{1112}$

$r_1' = k_{211211}/k_{211212}$

$r_1'' = k_{21211}/k_{21212}$

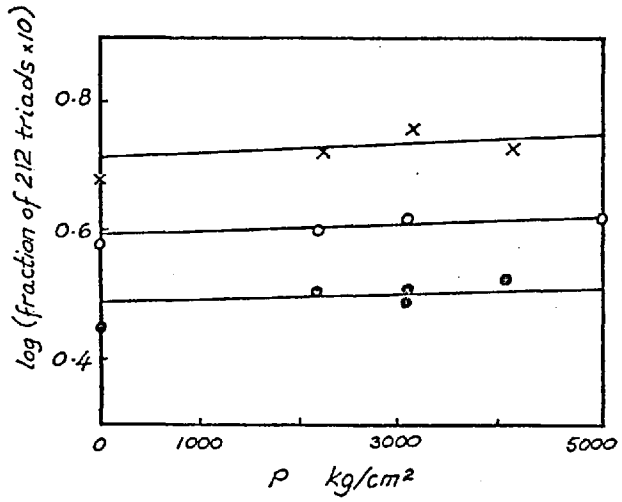

Fig.7 Pressure dependence of the formation of triad fraction in St.-Mal.Anhyd. system.

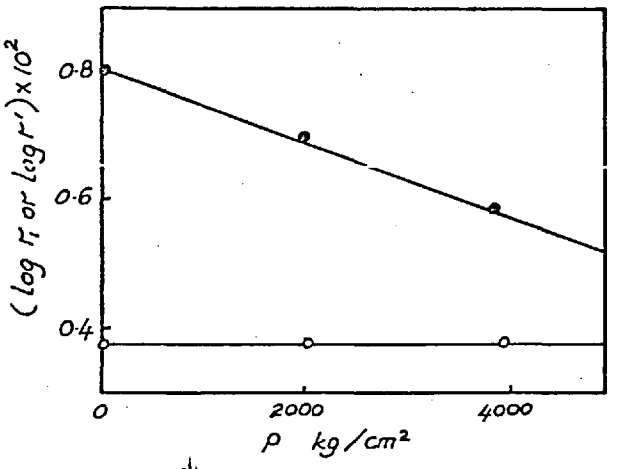

Fig.8 Pressure dependence of penultimate unit model reactivity ratios of St.-Mal.Anhyd. system.

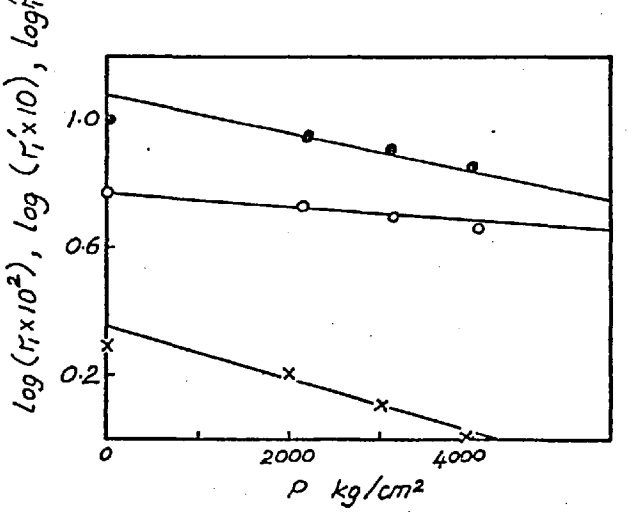

Fig.9 Pressure dependence of penpenultimate unit model reactivity ratios of St.-Fum.Nit. system.

1.7 Aims of the Present Study

The general aim of the present sudy was to investigate the effect of pressure on a copolymerization system which does not abide by the rules of classical copolymerization models due to either depropagation or penultimate unit effects.

Aspects of interest in such a system include:-

(1) Pressure effects on the copolymer composition curves, hence the reactivity ratios.

(2) Possible effects on microstructure of the copolymer, hence the choice of correct copolymerization mechanism.

(3) Pressure dependence of rate of copolymerization.

(4) Pressure dependence of molecular weight.

It is also of considerable interest to investigate whether the theoretical treatments developed for such systems at ordinary pressure can be extended to give a satisfactory description of the pressure effects; and to relate these to existing data on the high pressure homopolymerization of the monomers. On the other hand it always more enlighting to study a system which does not conform with the special cases of a general picture of this phenomenon. In the present case to study a copolymerization system which does not fit to the special classical theory would reveal more information about the general mechanism of copolymerization reaction.

II. RELEVANT ASPECTS OF THE EXPERIMENTAL SYSTEM

2.1 Reason for Choice of the MMA - αMS System

For this research the system αMS - MMA was chosen because one of the monomers shows depropagation in its homopolymerization at relatively low temperatures and the system does not fit the simple 'terminal-unit' theory. There is also a number of experimental studies of the system at 1 atm. (section (6.1)) and theoretical work based on them (section (4.1)) which make the system well defined. Each of the monomers has also been studied in copolymerization with other monomers and in homopolymerization; there are also data on the polymer – monomer equilibrium for αMS at high pressures. The system also exhibits a convenient rate of reaction and solution properties which are useful during the reaction and separation of polymers. Finally the αMS - MMA copolymers are very suitable for composition and microstructure analysis by NMR.

2.2 Relevant Data on the Polymerization of MMA

Baysal and Tobolsky[49] give the polymerization data on initiator concentration, R_p, $[\eta]$, and P_n for various initiators as shown in Table (VIII). From the same data R_p vs. $[In]^{1/2}$ is shown for the four initiators in fig.(10). The experimental straight lines give

$$R_p^2 = a + B_I[In] = B_I[In] \qquad (2.2.1)$$

a is a constant and is the rate of thermal polymerization. In the range of initiator concentrations used a is negligible compared to $B_I[In]$. B_I is an experimentally determined quantity for each initiator and is obtained from the squares of the slopes of the straight lines. B_I values for the initiators used are given in Table (IX).

For the monoradical initiated bulk polymerization with no chain transfer one has[49]

$$\frac{1}{P_n} = C_m + AR_p \qquad (2.2.2)$$

$$A = (2k_{td}+k_{tc})/k_p^2[M]^2 \ , \ C_m = k_{tr,m}/k_p$$

(similar to section (1.2.3)) which means in this case one should have a straight line for $1/P_n$ vs. R_p which is called the monoradical line. The initiators which exihibit chain transfer should approach the monoradical line asymptotically at low concentrations of the initiator. From the same data of Baysal and Tobolsky $1/P_n$ vs. R_p is shown for the four initiators in fig.(11). AZBN and Bz_2O_2 give straight lines which show that they are monoradicals. The slope of this line gives $A = 0.826$ (R_p in moles lt^{-1} sec^{-1}) and the intercept gives $C_m = 1*10^{-5}$.

In fig.(12) the data from Table (VIII) are plotted as $1/P_n$ vs. $[In]_o$ and $[In]_o$ vs. %conversion $hour^{-1}$ for AZBN.

Arnett(50) shows by the constancy of $R/c^{1/2}$ for the polymerization of MMA at 50°C with AZBN concentrations ranging from $0.47*10^{-2}$ to $21.06*10^{-2}$ mole/lt that the initial rate of polymerization is proportional to the square root of initiator concentration. That would indicate that the termination reaction is second order with respect to growing chains and the initiation is first order with respect to the initiator concentration.

O'Brien and coworkers[51] determined R_p from polymerizations carried out at 60°C with AZBN at various concentrations -from $4.28*10^{-4}$ to $61.5*10^{-4}$ mole/lt- as given in Table (X). They used the equation

$$R_p = 2.49*10^{-5} \ (d\alpha/dt) \qquad (2.2.3)$$

to evaluate R_p in lt^{-1} sec^{-1} and $d\alpha/dt$ is the gravimetric rate conversion of %conv./hour.

A plot of R_p vs. $(AZBN)^{1/2}$ gave a straight line passing through the origin. The slope of this line was $3.04*10^{-3}$ corresponding to

$$R_p = 3.04*10^{-3} \ (AZBN)^{1/2} \qquad (2.2.4)$$

The data of Baysal which gave the relation

$$R_p = 2.93*10^{-3} \ (AZBN)^{1/2} \qquad (2.2.5)$$

and of Bonsal et al.[52] which gave the relation

$$R_p = 3.11*10^{-3} \ (AZBN)^{1/2} \qquad (2.2.6)$$

are in good agreement with the results of O'Brien and coworkers.

O'Brien and coworkers determined the average degree of polymerization of poly-MMA samples using the equation

$$\bar{P}_n = 2.22*10^3 [\ ]^{1/0.76}_{C_6H_6} \qquad (2.2.7)$$

of Schuele, Kinsinger and Fox[53]. Although this equation gave somewhat lower $\bar{P}_n$ values than those of Baysal and Tobolsky and Baxendale et al., this equation, as accepted by many researchers, is the most accurate relationship available.

O'Brien's results gave a straight line for the plot of $1/P_n$ vs. $(AZBN)^{1/2}$ with a positive intercept

$$1/P_n = 2.97*10^{-3}\ (AZBN)^{1/2} + 0.7*10^{-5} \qquad (2.2.8)$$

This is in good agreement with Baysal and Tobolsky's relationship. Bonsall and coworkers' relationship

$$1/P_n = 1.77*10^{-3}\ (AZBN)^{1/2} + 5.5*10^{-5} \qquad (2.2.9)$$

may be due to limited investigation and insufficient results. But Arnett used Baxendale and coworkers' equation

$$P_n = 2.81*10^3 [\eta]^{1.32}_{C_6H_6} \quad (20^oC) \qquad (2.2.10)$$

to evaluate his data and obtained the equation

$$1/P_n = 0.854*10^{-3}\ (AZBN)^{1/2} + 3.8*10^{-5} \qquad (2.2.11)$$

2.3 Equilibrium Polymerization

Like all chemical reactions polymerization reactions are in theory reversible, although the reverse reaction is not detectable in most of them since the reverse reaction is negligibly slow. In the case of 1,1-disubstituted ethylenes the depolymerization reaction becomes apparent because of the steric effect mentioned in section (1.3.1) and enters into an appreciable competition with the forward reaction. Steric hindrance in the polymer markedly affects the enthalpy change of the reaction. Since the change in entropy remains approximately

Table VIII

Polymerization of MMA at 60°C

Initiator	In mole/lt	yield wt%	time min	$R_p * 10^5$ mole/lt sec	η	$1/P_n * 10^5$
Bz_2O_2	0.16	15.0	29.0	81.2	0.874	6.49
	0.09	11.4	30.0	59.6	1.10	4.86
	0.04	14.4	57.0	39.6	1.47	3.38
	0.0083	3.5	30.0	18.0	3.04	1.36
	0.002	3.46	56.0	9.7	5.02	0.72
	0.0004	3.41	125.0	4.27	7.20	0.46
AZBN	0.1427	7.13	10.0	111.8	0.651	9.39
	0.057	5.33	12.0	69.5	0.95	5.85
	0.0285	4.98	16.0	48.8	1.28	3.99
	0.0114	4.84	24.0	31.6	1.86	2.51
	0.0057	4.40	30.0	23.0	2.50	1.73
	0.00114	2.74	40.0	10.6	4.27	0.89
Photo	-	2.25	25.0	14.1	3.75	1.04
	-	2.91	45.0	10.2	4.25	0.89
	-	2.40	45.0	8.29	3.97	0.97
	-	1.69	45.0	5.95	5.38	0.68
t-BHP	0.0955	1.56	23.0	5.25	0.292	15.3
	0.0764	1.92	26.0	5.79	0.54	7.62
	0.0573	1.00	60.0	5.04	0.60	6.80
	0.0382	7.05	260.0	4.20	2.50	1.35
	0.0191	1.10	104.0	3.13	3.98	0.79
CHP	0.1395	2.78	28.0	15.36	0.99	5.55
	0.0558	3.43	42.0	11.31	1.57	3.11
	0.0279	5.64	77.0	11.36	2.22	2.01
	0.0112	4.56	108.0	6.55	3.90	0.99
	0.0056	3.99	170.0	3.64	5.20	0.69

Table X

Rate of polymerization of MMA with AZBN at 60°C

AZBN $*10^4$ mole lt^{-1}	da/dt %/hr	R_p*10^5 mole/lt sec	$R_p / AZBN^{1/2} *10^3$
4.28	2.45	6.10	2.95
4.28	2.48	6.18	2.98
9.12	3.73	9.29	3.08
9.12	3.73	9.29	3.08
16.3	4.97	12.4	3.07
16.3	5.08	12.6	3.12
24.2	6.24	15.5	3.15
25.7	6.32	15.7	3.10
31.8	6.67	16.6	2.94
31.8	6.89	17.2	3.05
32.7	7.13	17.8	3.10
33.9	6.91	17.2	2.96
33.9	6.98	17.4	2.99
46.6	8.08	20.1	2.95
61.5	9.83	24.5	3.12

Table IX

Kinetic constant B_I for the bulk polymerization of MMA at 60°C

Catalyst	B_I
Bz_2O_2	$4.00*10^{-6}$
AZBN	$8.59*10^{-6}$
CHP	$2.49*10^{-8}$
t-BHP	$4.06*10^{-9}$

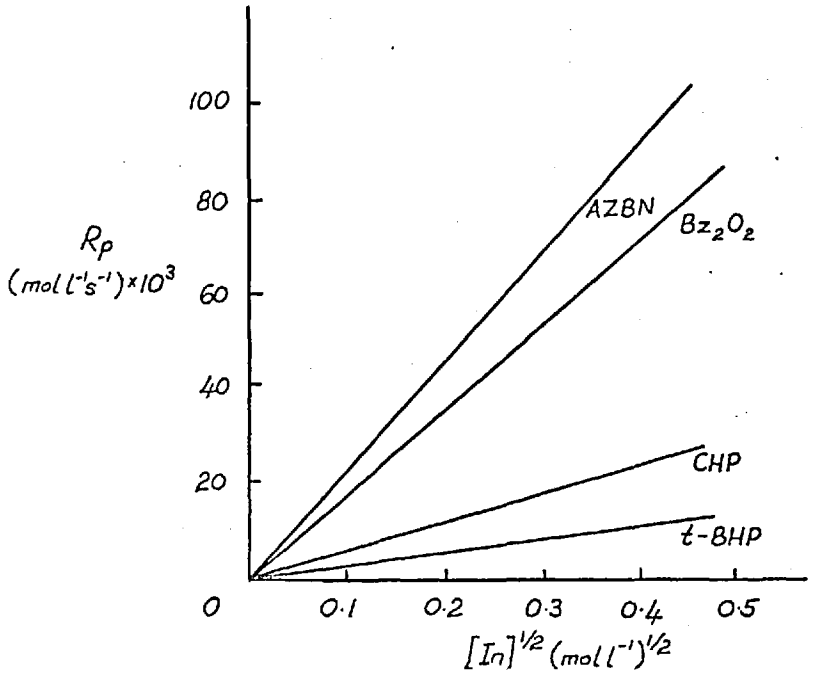

Fig.10 Dependence of polymerization rate on various initiators' concentrations.

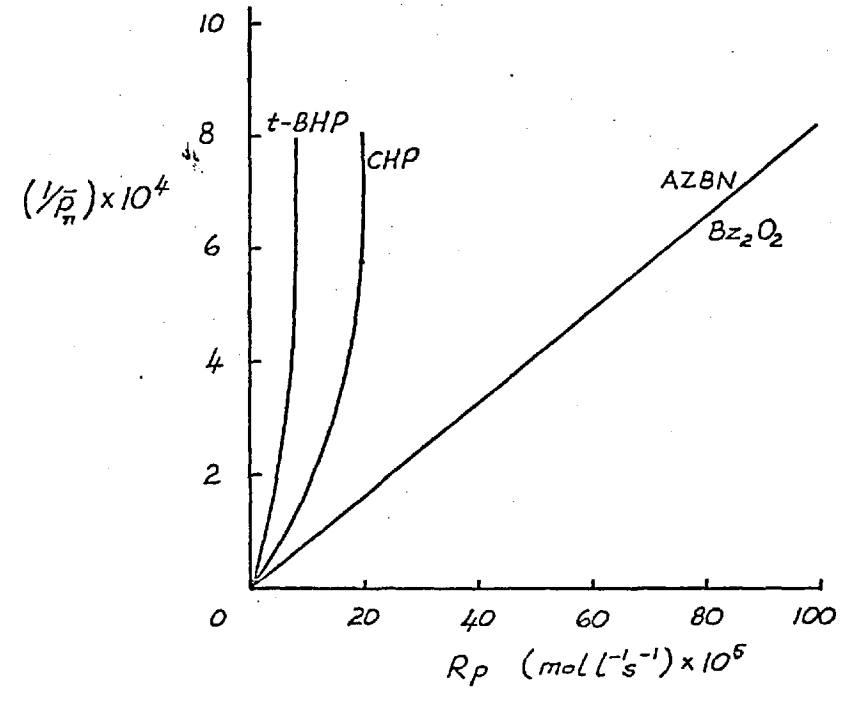

Fig.11 Dependence of molecular weight on rate of polymerizations obtained by various initiators.

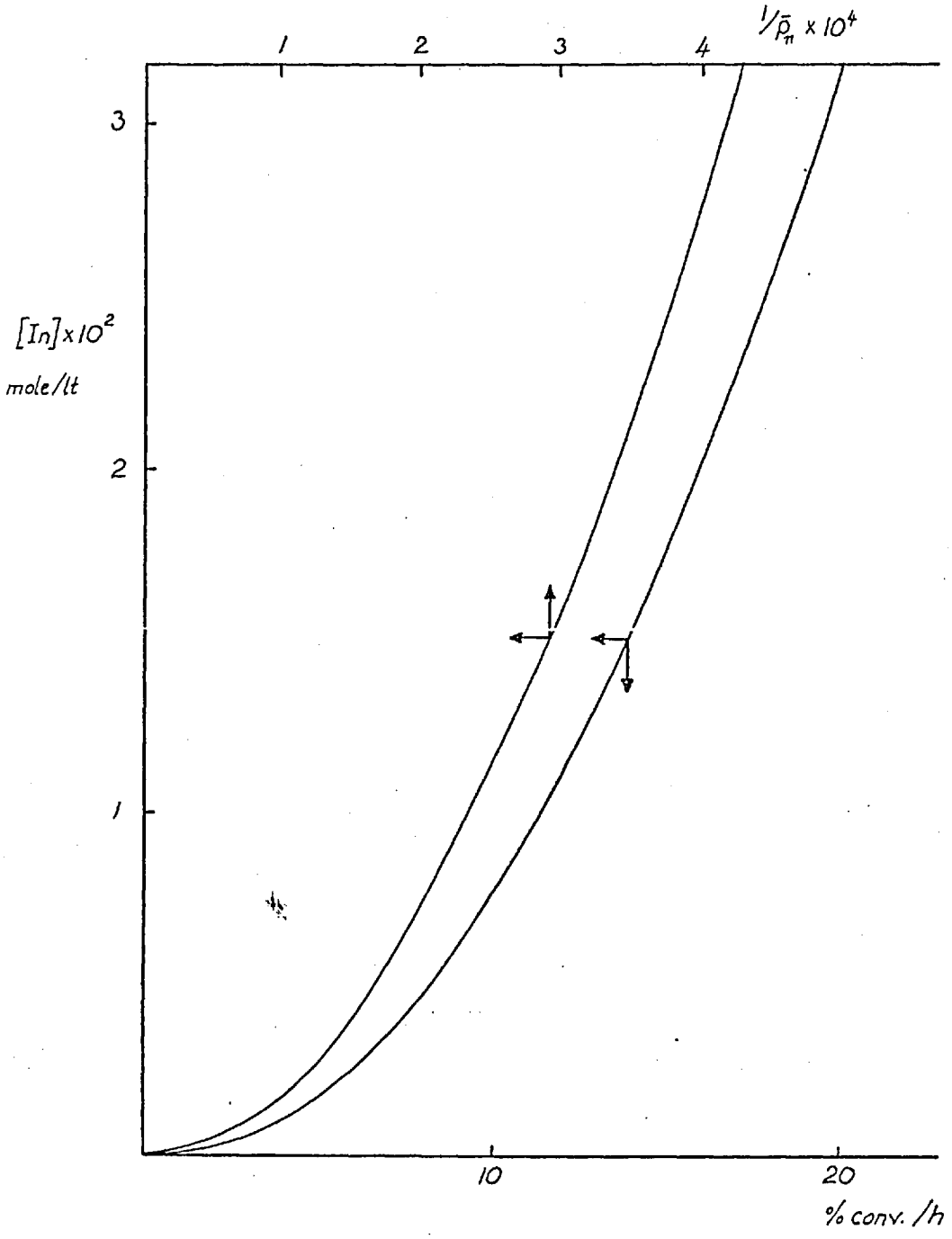

Fig.12 Dependence of molecular weight and conversion on the initial AZBN concentrations.

the same the change in ΔH_p gives rise to the activation energy of depropagation as seen from the equation

$$E_p - E_d = \Delta H_p \qquad (2.3.1)$$

for long chains. ΔH_p is usually negative and E_d is much larger than E_p so although k_d (rate constant for reverse reaction) is much smaller than k_p, when the temperature is increased k_d will increase faster than k_p and eventually reach the same value. At the point where $k_d \geqslant k_p$ there is no polymer formation since it is decomposed as soon as it is formed. At all conditions the monomer is in a state of equilibrium with the polymer and hence the process is called equilibrium polymerization. The temperature (at constant pressure), where there is no polymer formation in a bulk polymerization; or where $[M]_e$, the equilibrium concentration of the monomer in a solvent, is unity, is called the ceiling temperature. Many polymers formed below their ceiling temperatures can exit even above their ceiling temperatures but this is only a metastable state and once the degradative centres are initiated on the polymer it decomposes back to its monomer.

From the above concept it seems obvious that if the activation energies for the forward and the reverse reactions are appropriate it is also possible for the floor temperature to exist. In practice this is the case for at least one monomer, namely sulphur, which does not form its eightmer at temperatures below the floor temperature.

The concept of ceiling temperature can be analysed both thermodynamically and kinetically. Thermodynamically every chemical reaction is accompanied by a change in Gibbs free energy. The effect of this change on the reaction can be summarized like below[82]:

K	ΔG^o/J mole^{-1}	Inference
10^4	-23000	reaction almost complete
10	-5700	" 'favourable'
1	0	" 'central'
10^{-1}	5700	" 'just feasible'
10^{-4}	23000	" very 'unfavourable'

Exactly the same generalization can be made for the polymerization reaction.

The Gibbs free energy of a system is defined by

$$G = H - TS \tag{2.3.2}$$

and hence its change can be given as

$$\Delta G = \Delta H - T\Delta S \tag{2.3.3}$$

where ΔH and ΔS are the differences in enthalpy and entropy between the polymer and monomer as

$$\Delta H = H_{polymer} - H_{monomer} \tag{2.3.4}$$

The ceiling temperature has already been defined as an equilibrium temperature so

$$T_c = \Delta H_p / \Delta S_p \tag{2.3.5}$$

The enthalpy and entropy changes considered here are of each monomer unit and if the degree of polymerization is large enough they are identical with the heat and entropy changes of the polymerization reaction. As is shown later in this section, at equilibrium

$$\Delta S_p = R \ln(A_p/A_d) + R \ln[M] = \Delta S_p^o + R \ln[M] \tag{2.3.6}$$

where ΔS_p^o is the entropy change of the reaction at standard state, i.e., when concentration (activity) is unity. Therefore

$$T_c = \frac{\Delta H_p}{\Delta S_p^o + R \ln[M]_e} \tag{2.3.7}$$

From the above concept the generalization made in the beginning of the section can be understood more clearly and a better picture can be formed of the thermodynamic possibility of polymerization. If polymerization can be thought of as a process rather than successive reactions, the formation of polymer, since it is an associative process, is always accompanied by a decrease in entropy. This makes it necessary for ΔH to be negative and of a greater magnitude than the entropy term at temperatures up to the ceiling temperature. As mentioned before, a steric hindrance decreases ΔH and so the T_c. In the case of sulphur ΔH is positive but since in its monomeric state sulphur is crystalline, i.e., more ordered, polymerization is accompanied by a positive ΔS and the concept is reversed giving rise to a floor temperature instead of a ceiling temperature.

From statistical considerations the number average degree of polymerization for any equilibrium polymerization is given by[56,57,58]

$$DP = \frac{1}{1 - K[M]_e} \qquad (2.3.8)$$

where K is the equilibrium constant and $[M]_e$ is the equilibrium monomer concentration. In the case of $DP \gg 1$ the above equation gives

$$K = 1/[M]_e \qquad (2.3.9)$$

The relation between initial and equilibrium monomer concentration is given by

$$[M_o] = [M]_e + \frac{K'[M]_e^2}{(1 - K[M]_e)^2} \qquad (2.3.10)$$

where K' is the equilibrium constant for the initiation and to accept this to be equal to K is a possible assumption. The degree of polymerization in relation to initial concentration (also $DP \gg 1$) is given by

$$DP = \left[\frac{[M_o]}{K'} K^2 - \frac{K}{K'}\right]^{1/2} \qquad (2.3.11)$$

If K' is assumed to be equal to K then

$$DP = ([M_o]K)^{1/2} \qquad (2.3.12)$$

Equilibrium in vinyl polymerization has been treated by various researchers successfully with or without the above assumption. In the case of polymerization of methyl methacrylate Dainton and Ivin[56] and Bywater[57] treated the problem with the above assumption whereas Tobolsky[58] treated the problem as a two-constant case and from the measured DP of polymethyl methacrylate and equation (2.3.11) derived $K' = 3*10^{-5}$ and $K \cong 3$.

By the differentiation of the equation of DP with T after substituting $K = \exp(\Delta S^o/R)\exp(-\Delta H^o/RT)$ and then setting $dDP/dT = 0$ one can obtain a maximum for DP[61], as long as $K \gg K'$. A maximum for the polymerization of α-methyl styrene can be seen from the results of Kilroe[59] and Mitani et al.[60]. In the case of Mitani et al., although this is not mentioned in their paper, it can be seen by plotting their results on a T vs. P plot (see section (2.4)). It is also mentioned[61] that

if $\Delta H^{o'} \gg \Delta H^{o}$ the temperature where the maximum occurs and the ceiling temperature will be very close together.

The kinetic approach to the ceiling temperature concept is made by taking the forward and the reverse reactions to be equal in rate at the equilibrium,

$$k_d[R\cdot]\,[M] = k_d[R\cdot] \tag{2.3.13}$$

or in the Arrhenius form,

$$A_p \exp(-E_p/RT_c)\,[M] = A_d \exp(-E_d/RT_c) \tag{2.3.14}$$

and then solving for T_c

$$T_c = \frac{E_p - E_d}{R \ln(A_p[M]/A_d)} = \frac{\Delta H_p}{R \ln(A_p[M]/A_d)} \tag{2.3.15}$$

since

$$A = (kT/h) \exp(S^{\neq}/R) \tag{2.3.16}$$

$$\Delta S^{o} = \Delta S_p^{\neq} - \Delta S_d^{\neq} = -R \ln(A_d/A_p) \tag{2.3.17}$$

Therefore

$$T_c = \frac{\Delta H_p}{\Delta S^{o} + R \ln[M]} \tag{2.3.18}$$

For the molecular weight distribution of polymers formed in equilibrium polymerization Eisenberg and Tobolsky[62] and Schulz and Flory[63] obtained similar results

$$N_x/N = n_x = (K[M]_e)^{n-1}(1-K[M]_e) \tag{2.3.19}$$

where n_x is the ratio of number of polymer molecules with x units to total number of polymer molecules. Also

$$DP_n = 1/(1-K[M]_e) \tag{2.3.20}$$

$$DP_w = (1+ K[M]_e)/(1-K[M]_e) \tag{2.3.21}$$

and the polydispersity

$$DP_w/DP_n = 1+ K[M]_e = 2 - 1/P_n \cong 2 \tag{2.3.22}$$

2.4 Previous Studies on the Polymerization of αMS at Normal and High Pressures

α-methyl styrene has been investigated by a number of research workers in the studies of the equilibrium polymerization of vinyl polymers. Thus many researchers studied its polymerization at normal pressure with various initiators and by a variety of mechanisms. McCormick[64] and Worsfold and Bywater[65] studied the system of α-methyl styrene – poly-α-methyl styrene in tetrahydrofuran (THF) and successfully applied equation (2.3.9) to their results. These researchers used naphtalene sodium as an anionic initiator; as did Tobolsky, Rembaum and Eisenberg[76] who also used diphenylacetylenesodium at 0°C. The latter researchers carried out the polymerization in THF and found that with both initiators the equilibrium monomer concentration at 0°C is equal to 0.89 mole/kg. The calculated values of ΔH and ΔS from the experimental results of various researchers are given below

$-\Delta H_{ss}$ (kcal/mole)	$-\Delta S_{ss}$ (eu)	Ref.
6.96	24.8	(64)
8.02	28.75	(65)
7.47	26.5	(76)
8.50	30.6	(83)

From the experimental data McCormick established the ceiling temperature for α-methyl styrene to be 61°C.

Other researchers to study the polymerization ofα-methyl styrene at normal pressures were Okamura et al.[119] using the borontrifluoride – diethyl ether complex at -78°C; Brown and Mathieson[86] using trichloroacetic acid in ethylene dichloride at 20°C; and Lowry[87], the first researcher to claim the homopolymerization of α-methyl styrene by radical mechanism at normal pressure, who polymerized the monomer with a radical initiator at 15°C for five days.

The study of polymerization of α-methyl styrene at high pressures was mainly done with radical and ionic initiators by Sapiro et al.[84], Kilroe and Weale[59], Elroy and Weale[85], Mitani et al.[60], and Stein

et al.[66].

Kilroe and Weale show that although the depolymerization reaction is favoured more by temperature causing the conversion to reach zero after passing a maximum, it is less favoured by pressure compared with propagation reaction, thus leading to an increase in the ceiling temperature. They found a linear increase in the ceiling temperature with pressure having a zero pressure intercept of 60°C. By the application of the Clausius-Clapeyron equation

$$\frac{dT_c}{dP} = \frac{T_c \Delta V}{\Delta H}$$

and using the value of $\Delta H = -8.4$ kcal/mole as given by Dainton and Ivin[56], the molar volume difference between products and reactants which is related to the equilibrium constant by the equation

$$\frac{\ln K}{P} = - \frac{\Delta V}{RT}$$

was found to be

$$V = - 14.7 \text{ cm}^3/\text{mole}$$

These researchers also show that although the conversion to solid polymer is decreased after the observed maximum there is a considerable and increasing amount of dimer formed even after the maximum. The formation of this dimer, with uncertain structure was explained to be via an allyl transfer between two monomers. This did not cast doubt on the retardation effect of the depropagation reaction or on the ceiling temperature concept. Kilroe and Weale found that the dependence of this reaction rate on the initiator concentration is similar to styrene polymerization[59].

Mitani and his coworkers, in their high pressure polymerization studies of α-methyl styrene in THF at temperatures of 50°, 60°, 70° and 80°C, obtained polymerization heats and entropies at various pressures but their extrapolated normal pressure values are quite different from those of other researchers.

Pressure (kg/cm^2)	ΔH (kcal/mole)	ΔS (cal/mole deg)
1	-4.0	-16.4
2000	-7.09	-23.4
3000	-9.20	-28.7
4000	-9.98	-30.1
5000	-11.58	-33.8

From their van t'Hoff plots they calculate that the activation volume ($V^{\neq}$) increases with increasing temperature, but is independent of pressure up to 5000 atm.. Mitani and his coworkers, apart from the dubious correction of their 50°C values by making allowance for partial freezing of the monomer, also interpreted their own results erroneously. They show an increase in the degree of polymerization (intrinsic viscosity) with pressure but contrary to their statement it is apparent that the degree of polymerization falls with increasing temperature. Although Mitani and coworkers' results cover a range of initial monomer concentrations the present research is concerned only with bulk copolymerizations. Mitani and coworkers' results are therefore considered here only with respect to constant monomer concentration. The concentration chosen was 6 mole/lt.

If the intrinsic viscosity values of Mitani and coworkers are taken at one initial monomer concentration (6 mole/lt) and plotted against temperature a better view of the decrease of DP on temperature can be obtained (fig.(13)). Although these values do not produce a maximum like the one obtained by Kilroe and Weale at 4860 atm. for bulk polymerization, the pattern of curves may suggest the possibility of a maximum somewhere at a lower pressure.

Tobolsky and Eisenberg[62] applied equation (2.3.8) and an equation for the change of degree of polymerization with temperature

$$\frac{dP}{dT} = \frac{\Delta H^{o}/RT^{2}}{K[In]\{2 - (K[In])^{1/2}\}} \qquad (2.4.1)$$

to α-methyl styrene polymerization. In their study they used the data of Worsfold and Bywater[65] and also of McCormick[64]. Their plots of DP vs. T do not yield a maximum and this could be due to the different initiation mechanism, and equation (2.4.1) does not apply to

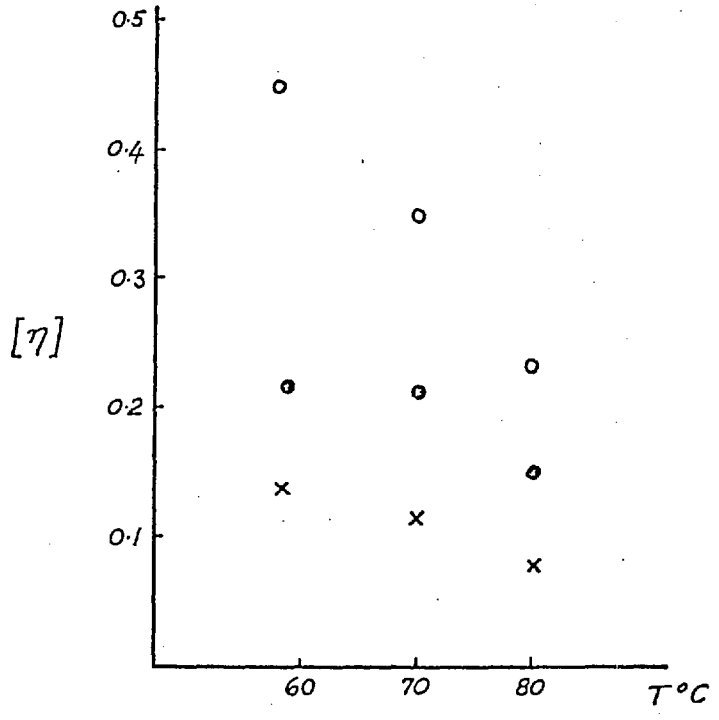

Fig.13 Dependence of equilibrium polymer intrinsic viscosity on temperature (from Mitani et al.).

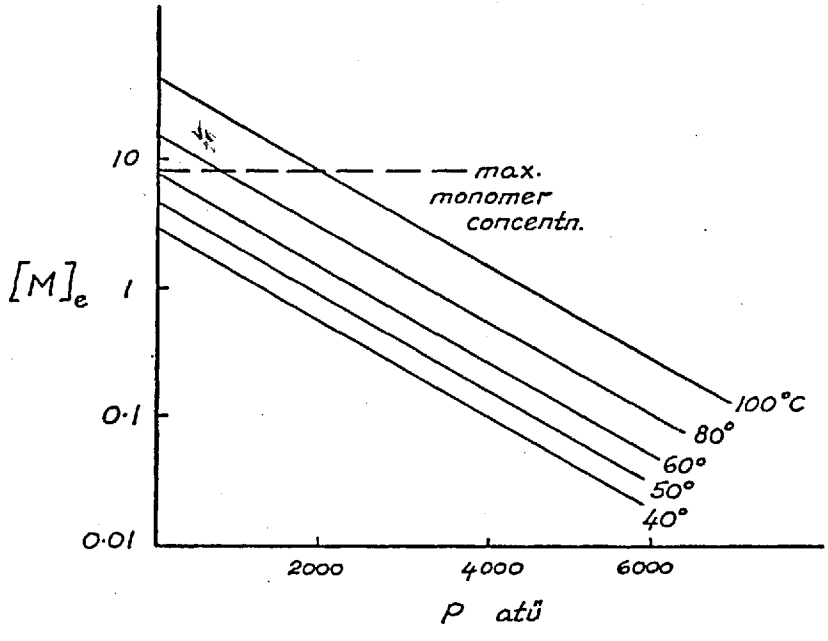

Fig.14 Equilibrium monomer concentration at various pressures and temperatures.

radical initiated polymerization of Kilroe and Weale (Bz_2O_2) and Mitani et al. (AZBN).

Stein and his coworkers extended the study of equilibrium monomer concentration from 1 atm. to 5000 atu measuring it at 500 atm. intervals. Using ΔH and ΔS values of McCormick as well they determined ceiling temperatures for polymerizations at 0 to 5000 atu, with initial concentrations varying from 0.01 to 7 mole/lt. Their results are given in fig. (14).

2.5 Copolymerization of αMS with Acrylic Monomers

The Q and e values of α-methyl styrene are given as

$$Q = 0.98 \quad , \quad e = -1.27$$

in the literature[77]. These values, when combined with the Q and e values of methyl methacrylate in equation (1.3.24) give (1=MMA, 2=αMS)

$$r_1 = 0.41$$
$$r_2 = 0.16$$

Walling and coworkers give values of r_1 and r_2 for α-methyl styrene and methyl methacrylate copolymerization at 60°C (for the terminal unit model) as:

$$r_1 = 0.50 \pm 0.03$$
$$r_2 = 0.14 \pm 0.01$$

By the same researchers the relative reactivity of α-methyl styrene with methacrylate radical compared with styrene was given as 0.97 ± 0.06. The monomer reactivity ratio product is

$$r_1 r_2 = 0.07 \pm 0.007$$

Ham[80] studied the copolymerization of α-methyl styrene and applied his expanded copolymerization theory and equation (see section (4.1)) to find a set of reactivity ratios which take account of the penultimate effect. This was suggested by the fact that α-methyl styrene copolymers with more than 75 mole % α-methyl styrene units cannot be obtained, which would arise from the inability of a chain ending in two

α-methyl styrene units to add a third unit in sequence. The reactivity ratios of α-methyl styrene and acrylonitrile obtained by Ham from the classical terminal unit model are (1=αMS)

$$r_1 = 0.1 \pm 0.02$$
$$r_2 = 0.06 \pm 0.02$$

but from the penultimate unit model he obtained

$$r_1 = 0.0$$
$$r_1' = 0.04$$
$$r_1'' = 0.13$$

These show the considerable difference between the values r_1' and r_1'' the mean of which should give r_1 of the terminal model.

Wittmer[98] obtained classical reactivity ratio values for α-methyl styrene and methyl methacrylate copolymerization as (1=αMS)

$$r_1 = 0.30$$
$$r_2 = 0.55$$

at 60°C. From more complex models of copolymerization at 60°C Wittmer obtains

model (1) $r_1 = 0.60$, $r_2 = 0.55$

model (2) $r_1 = 0.35$, $r_2 = 0.55$

which he calls the actual reactivity ratios (see section (4.1))

Ito et al.[88] in their attempt to obtain the microstructure parameters of the system MMA-αMS obtained values of the reactivity ratios as (2=αMS)

$$r_1 = 0.45 \pm 0.08$$
$$r_2 = 0.16 \pm 0.05$$

Finally O'Driscoll[81] obtained the values of (2=αMS)

$$r_1 = 0.40$$
$$r_2 = 0.15$$

for the MMA-αMS copolymerization at 60°C, by the Finemann-Ross plot (terminal unit model).

The complete set of previous data for α-methyl styrene - methyl methacrylate copolymerization including the microstructure data as well as copolymer composition is given in section (6.1). Some of the above researchers have also obtained reactivity ratio values for α-methyl styrene copolymers at other temperatures than 60°C which are also given in the same section. O'Driscoll et al. do not give r values at 114° and 147°C but mention that they are negative, which demonstrates the inapplicability of the terminal model at these temperatures.

The only available reactivity ratio results for high pressure copolymerization of αMS is by Asai[36] . He produced three sets of reactivity ratios for the system MMA-αMS at different pressures and 60°C, which are given below (2=αMS).

P(kg/cm^2)	r_1	r_2
1	0.50	0.14
100	0.57	0.16
1000	0.73	0.20

III. EXPERIMENTAL PROCEDURES

3.1 Apparatus and Equipment

3.1.1 Vacuum Line

The vacuum line used was a standard type, and built for this purpose. As seen in fig. (15) it consisted of eight openings with taps attached to a main line made of glass tube 20 mm diameter. The main line was made as two sections with a tap as separator. This separated the two halves and allowed one section to be used and kept under vacuum while the rest of the line was not, and also had a vent of its own. The two openings of this section were one B19 socket and one B19 cone. The main section had three openings of B10 socket and one opening of B19 cone. The B10 sockets were mainly to attach the B10 cone openings of the reaction ampoules and the B19 cone to attach a flask. A tap separated the main line from the rest of the vacuum line. Between this tap and the system of pumps there were attached, in order, one rotary McLeod pressure gauge which allowed accurate pressure readings down to 10^{-5} torr and one cold tap contained in a dewar flask topped up with liquid nitrogen. One accesory to the vacuum line was, as seen in fig. (16), a separate attachment which could be joined to opening no. (7) and allowed for an extention of the vacuum line without lengthening the main line itself. This consisted of eight openings with B10 sockets and individual taps attached in a circular arrangement on to a glass chamber with a B19 cone on top. For a batch of not more than three ampoules the B10 socket on the larger section of the line would be used but for a batch of more than three ampoules, (in fact up to eleven), the accesory would be used. Without this a larger line would be required which in turn would mean more space and less efficiency of molecular distillation.

The taps in the vacuum line were entirely of Quickfit PTFE taps which needed no greasing. On the other hand all the cone-socket joints were Quickfit joints and were greased with Edwards Speedivac high grade silicon vacuum grease regularly. If necessary the line was tested for

leaks through the glass by a 'Tesla' high voltage tester.

The system of pumps consisted of one rotary and one mercury diffusion pump. The rotary pump was an Edward ES-50 single stage pump and the mercury pump was an Edward EM1 water cooled, electrically heated mercury diffusion pump. The rotary pump would evacuate the line down to 10^{-2} torrs by itself, and then the mercury diffusion pump, working with the rotary pump would decrease the pressure down to 10^{-5} torrs.

3.1.2 Reaction Vessel

The reaction vessels were simply glass ampoules of capacity 8 to 20 cm^3 for normal pressure work and 5 cm^3 for high pressure work. The ones for normal pressure were made of glass tubes of diameter 15 to 21 cm (outside) and in general there were no strict measurements for their dimensions. Those used for high pressure work had very specific dimensions because of the restricting length and diameter of the high pressure vessel. The general shape for the normal pressure ampoules, and the specific shape and dimensions of the high pressure ampoules are given in fig. (17). For the mouths of the both kinds of ampoules B10 cones were used. At the joint of the ampoule to its shank no constriction was made. This necessitated more caution during sealing but also eased the cleaning of the ampoules. The ampoules were cleaned by leaving 24 hours in 10% solution of DECON® in distilled water and then washing at least five times with mains water and three times with distilled water. Apart from the dimensions the main difference between high pressure and normal pressure ampoules was that the high pressure ampoules contained a break-seal at the bottom which allowed, (after sealing the top) when broken in mercury, to flush mercury into the evacuated ampoule. The specific dimensions permitted three ampoules to be placed in the container inside high pressure vessel (fig. (18)), at a time.

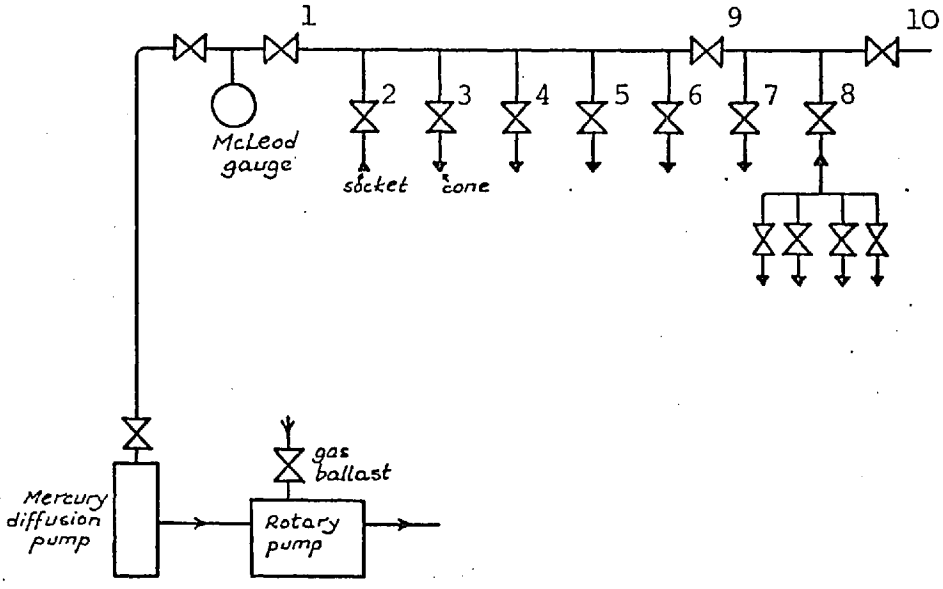

Fig.15 The vacuum line.

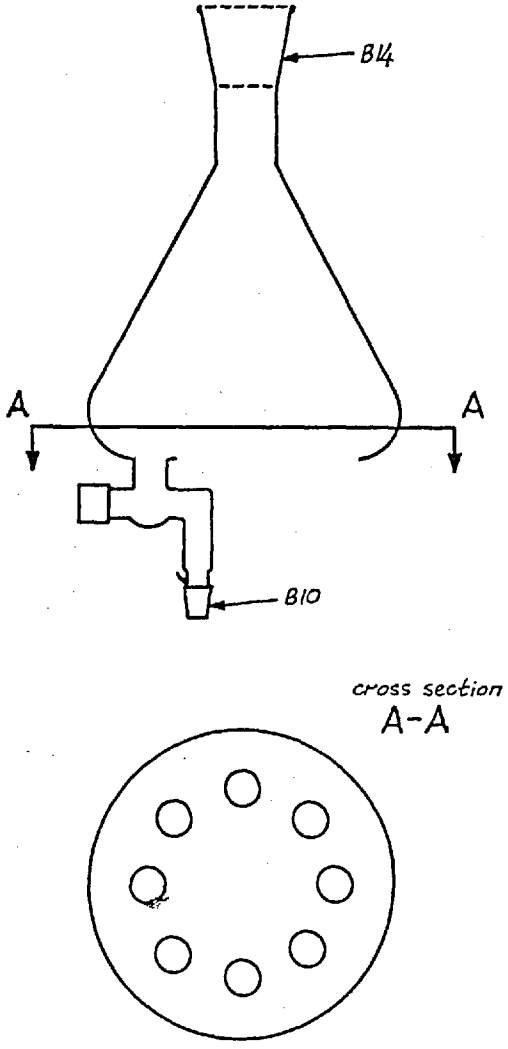

Fig.16 Accessory for multiple ampoule attachments.

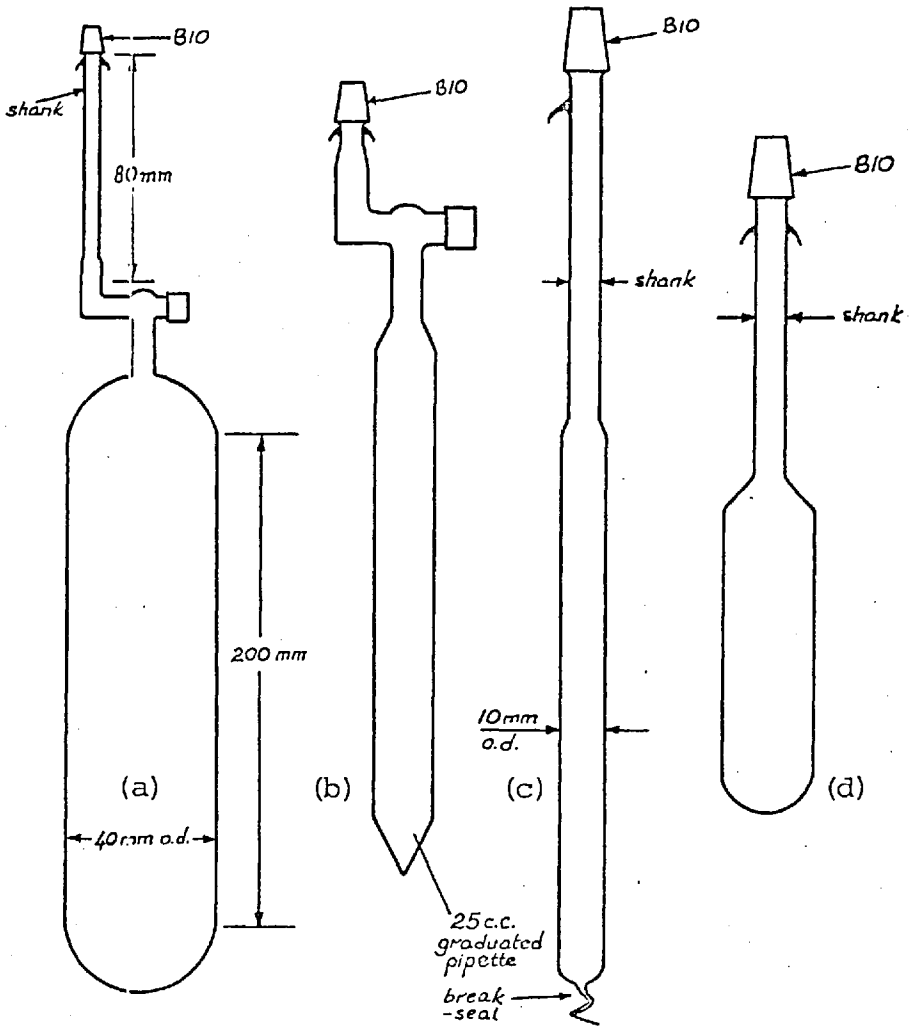

Fig.17 Glassware for the polymerization experiments: a) purified monomer container, b) measuring cylinder for molecular distillation, c) high pressure ampoules, d) normal pressure ampoules.

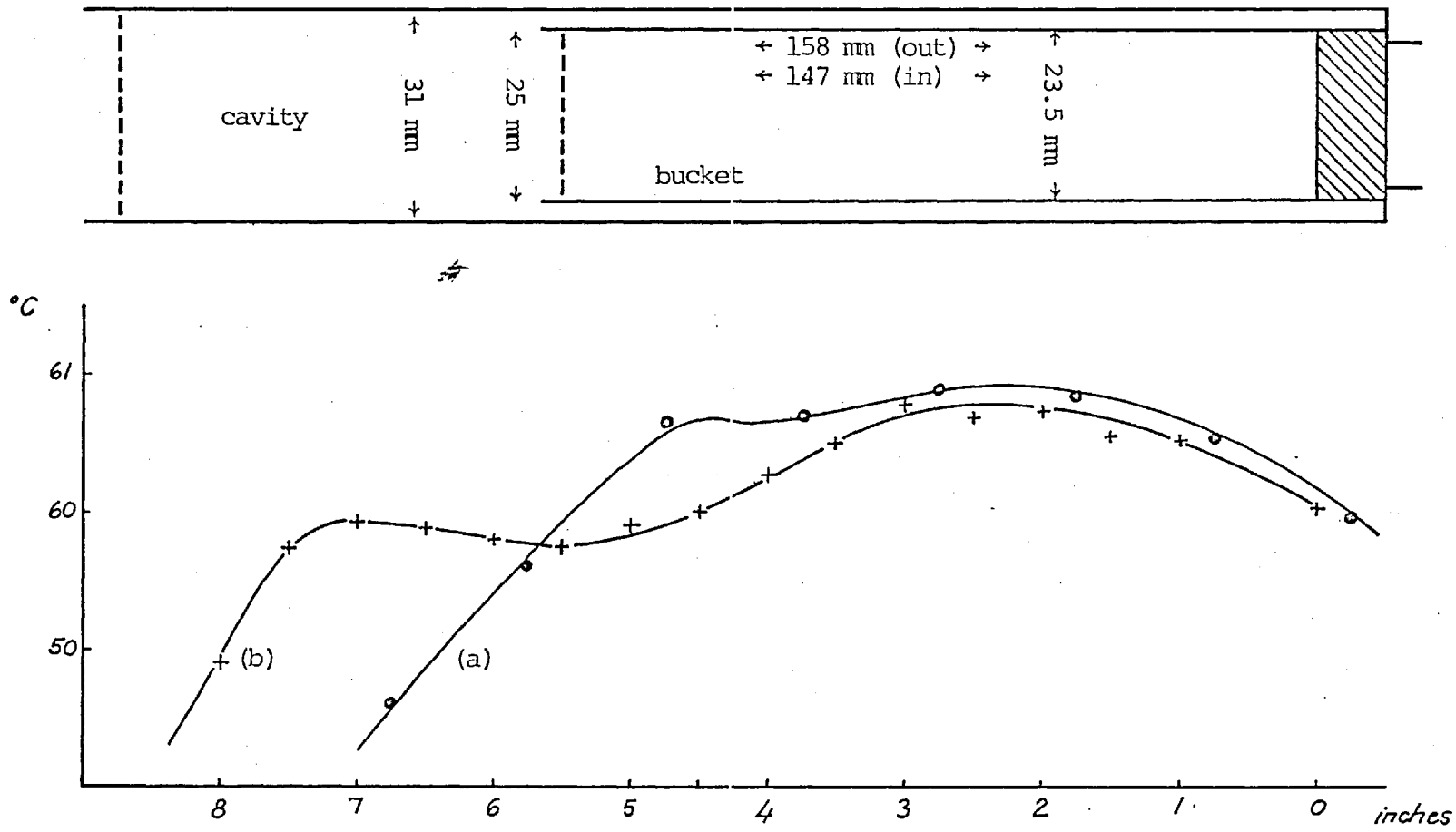

Fig.18 High pressure vessel reaction cavity with the container bucket for ampoules and its axial temperature variation with the top a) open, b) closed.

3.1.3 Pressure Vessel

The pressure vessel and ancillary equipment used for this research is shown diagramatically in figs. (19a) and (19b). The vessel itself was a compound-cylinder high pressure vessel made from Vibrac steele. Its dimensions were:

overall length: 400 mm
external diameter: 153 mm
bore: 31 mm
length of reaction space: 210 mm

The reaction space was further diminished by the need to use a mercury bucket made of stainless steel which held some mercury on which the reaction ampoules floated and which acted as a pressure transmitting seal. The dimensions of the bucket were as shown in fig. (18). Below the mouth of the bucket 147mm by 23.5mm Ø reaction space was available.

The vessel formed the upper part of a differential-piston intensifier. Paraffin was pumped into the bottom of the intensifier and pressure was transmitted to the lower piston of 36 mm diameter, which was obturated with a Bridgeman unsupported-area packing. The thrust on this piston was transmitted, via a thrust block, to the upper piston of 16 mm diameter, obturated with a hard rubber Poulter packing, which moved in the lower part of the pressure vessel. This arrangement gave a pressure intensification of approximately 5:1 ratio. The pressure calibration of the system, in the pressure range of 1 - 5000 bars is given in fig. (20). This graph was obtained by reading the high and low pressure gauges directly while increasing and decreasing the pressure in the line. The pressure difference between two lines is due to the frictional resistance of the rubber seal. The graph was used to determine the reaction pressure during the runs carried out without a gauge at the high pressure side. The top of the vessel was sealed with a steel screw plug and and O-ring. The screw plug and the piston were greased with

The pressure vessel was surrounded by a heater element block which was controlled by a Gallenkamp Thermoregulator and an electronic relay. The heater element was rated at 1000 watts and this much heat input was found to be too high to be controlled with minimum temperatur

fluctuations and overshoots. The heat input was therefore controlled by a power controller and the optimum heat input was found to be approximately 100 watts. The temperature control of the vessel was one of an equilibrium between a localised heat input and heat loss through overall surface of the metal vessel. To improve the stability the exposed parts of the vessel were covered with a 20 mm thick jute heat insulator wherever possible. When the temperature outside the vessel, at the thermoregulator, was $67^{\circ}C \pm 0.75$ the interior temperature, as checked with a thermocouple, was $60^{\circ}C \pm 0.05$ (at single point). The difference of approximately $7^{\circ}C$ arises because the reaction space is in the temperature gradient between the heat input and the heat sink; and the decrease of fluctuation is due to the smoothing effect of the massive metal block. This kind of arrangement produces a small temperature gradient along the length of the reaction vessel bore and is shown in fig.(18) constructed from axial temperature measurements with the thermocouple. The temperature gradient was within acceptable limits.

The pressurization of the vessel was done as follows: first it was ensured that there was enough paraffin in the paraffin container. Then, after closing the valves (F) and (K) paraffin was pumped by a manual pump into the high pressure section through a 9 mm o.d., 3 mm i.d. stainless steel tube, as a pre-pressurization. Since it was possible to pump easily up to 700 bars of pressure (as indicated by the low pressure gauge), this pre-pressurization could be used as actual pressurization for reaction pressures below 500 bars without the use of the intensifier. Otherwise, after the pre-pressurization, valve (K) was opened to let pressure into the lower intensifier cylinder. At this moment, to equalize the thrust, the two pistons would move upward. It was important to ensure that the pistons were initially slightly above their lowest position, to avoid a jerky movement which could strain the gauge. Once the pressures in the two sections were equal valve (J) was closed and by further pumping the reaction vessel was brought up to the desired pressure level.

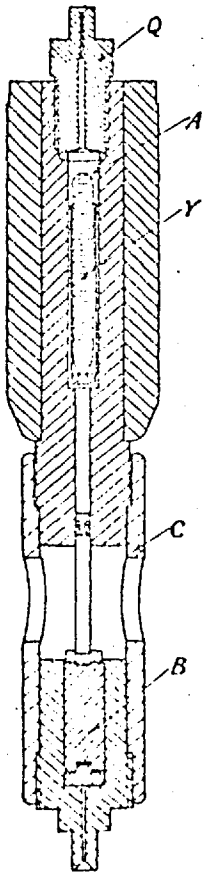

Fig.19a The pressure vessel

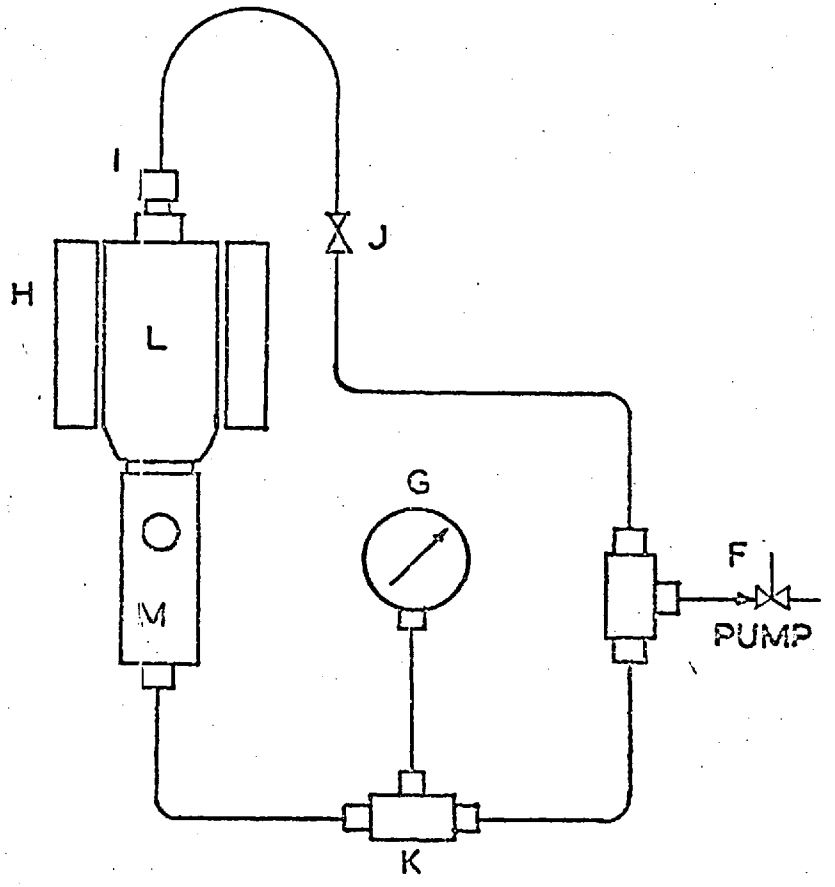

Fig.19b Pressure vessel and ancillary equipment, G) pressure gauge, M) intensifier, L) pressure vessel, H) thermostat heater, I) plug screw.

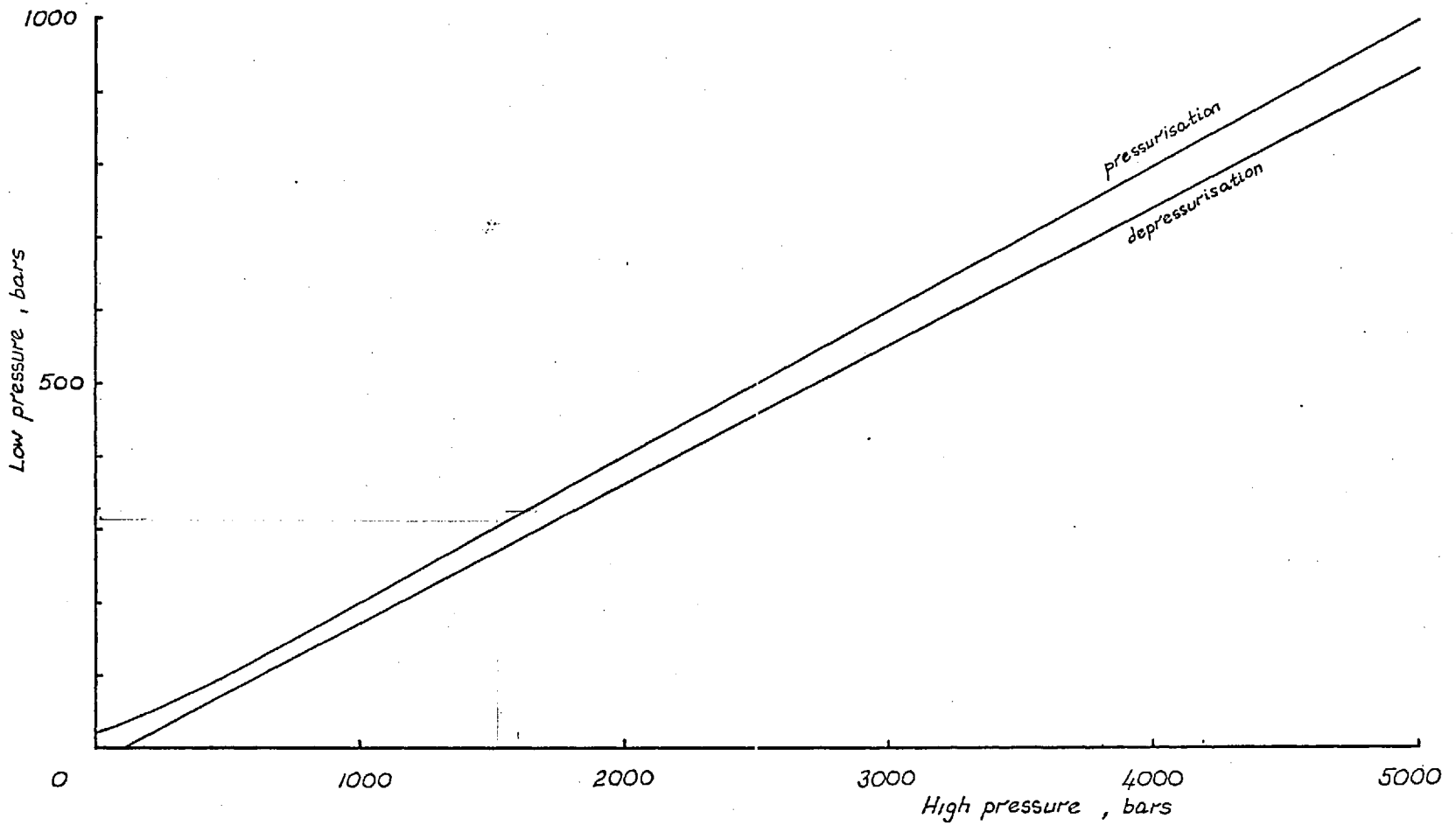

Fig.20 Pressure calibration curve for the low and high pressure sides of the high pressure vessel.

3.2 Purification of Materials

a) AZBN : Azo-bis-isobutyronitrile was obtained from Kodak Chemicals ltd. and purified[89] by dissolving in chloroform at room temperature and filtering into 40-60°C petroleum ether for precipitation. This process was repeated twice. The final precipitate was recovered on a Buchner funnel and washed with petroleum ether. Purified AZBN was dried at room temperature overnight and kept in the dark. Its purity was checked by a melting point at 103°C.

b) MMA : Methyl methacrylate monomer, obtained from BDH, contained 100 ppm quiniline as polymerization inhibitor. The monomer was freed from its inhibitor by fractionation through a 50 cm Vigreaux column at slightly reduced pressure. The boiling point of MMA is 100°C (NP). The middle 70% fraction boiling at 78°C at reduced pressure was taken as pure monomer. Since water has the same boiling point as that of MMA it cannot be removed by distillation, so the monomer, before distillation, was left overnight over CaH_2. Distilled MMA was kept over diphenylpicrylhydrazyl (DPPH) at -30°C in the dark until needed. Further purification of MMA was obtained by molecular distillation into the ampoules.

c) αMS : α-methyl styrene, obtained from Kodak Chemicals Ltd. contained 100 ppm quinoline as polymerization inhibitor. Owing to its high boiling point of 164°C it was necessary to use reduced-pressure fractionation. For the fractionation a 50 cm Vigreaux column was used with asbestos rope wound around the still and the column for thermal insulation. The middle 70% fraction boiling at 94°C under 60 mm Hg pressure was taken as pure monomer. Prior to distillation the monomer was kept over CaH_2 overnight to remove water. The distilled monomer was kept at -30°C, in the dark. The monomer was used shortly after distillation, or otherwise redistilled, since it tends to oxidise slowly to acetophenone and formaldehyde even at low temperatures.

For both distillations, to prevent contamination, PTFE sleeves were used for the glass joints, instead of grease.

3.3 Vacuum Manipulation

The copolymers in this research were prepared by bulk polymerization in sealed ampoules. The monomers were distilled into the ampoules (whenever their boiling points permitted), to ensure their high purity. The ampoules were degassed before sealing in order to prevent oxygen inhibition or peroxide formation.

To prepare the vacuum line for degassing the ampoules, the rotary pump was first put into operation for a preliminary evacuation, followed by (after few minutes) by the mercury diffusion pump. The usual precaution taken against vapours of any kind, including the monomers, was to fill the cold trap with liquid nitrogen and top up as required. When the pressure reached app. 10^{-5} torr, which was usually after 15 to 30 minutes, the line was assumed to be ready for the degassing operations.

AZBN and αMS were placed into the ampoules by a pipette prior to the vacuum manipulation because the high boiling point of αMS did not allow molecular distillation.

For the molecular distillation of MMA into the ampoule a special measuring cylinder was used to measure the monomer into the ampoule. This attachment was made by sealing the bottom of a 25 ml graduated pyrex pipette and connecting a B10 cone and a quickfit PTFE tap to its mouth-piece (fig.(17b)).

The molecular distillation proceeded as follows: the flask containing MMA, which had been purufied and kept in the cold with DPPH in, was connected to the line. The monomer was crudely degassed in order to in order to increase the efficiency of the distillation. This was done by the cycle of (i) freezing in liquid nitrogen, (ii) evacuation by opening the tap and (iii) thawing after closing the tap; the cycle was carried out twice. Next, a container of the type shown in fig.(17a) was attached to (2) and evacuated. Reaching again the maximum vacuum, the system of flask and container was disconnected from the line by closing (1). With this arrangement by keeping the flask at room temperature and the container immersed in liquid nitrogen a steady flow of monomer from the flask into the container was accomplished. When the container was filled it would be degassed once more, thawed and

stored in the deep freeze (with DPPH in). All through the vacuum manipulation all the thawing operations were done by submerging the frozen glassware in methanol because of the property of the frozen MMA to crack the glass unless fast and homogeneous warming was ensured.

MMA was transfered into the measuring cylinder and then into the ampoules in the same manner, but without any need for pre-degassing of MMA. The AZBN-αMS solution, though, which was inserted into the ampoules by a pipette, was degassed prior to the MMA transfer. Care was taken, while thawing the ampoules, not to increase the temperature much above the melting point as the solution contained the initiator. The molecular distillation of MMA into the individual ampoules was effected in the same manner and by the use of the appropriate taps.

Finally the ampoules were degassed by 3 to 5 cycles of evacuation and sealed off, while frozen, with an oxy-propane blow-pipe at an appropriate point on the shank to allow them to fit the pressure vessel.

3.4 Copolymerization and Copolymer Isolation

Copolymers for this research were prepared by bulk polymerization initiated with AZBN. This initiator has been shown (section (1.2.1)) to be safe to handle and dissociate according to a well-defined mechanism. Unlike bezoyl peroxide the reaction does not involve induced decomposition, and its overall kinetics are of first order.

The initiator concentration used in the experiments was calculated to give the most convenient polymerization time in the conditions employed. Assuming that the introduction of αMS as a comonomer into the AZBN-MMA system would reduce the rate of polymerization and the degree of polymerization substantially the Author estimated, also from fig.(12), that a concentration of 0.02 mg/lt of AZBN would give a satisfactory rate of polymerization and molecular weight. Since it was best, for the comparison of the copolymers, to use the same initiator concentration for all the various reactions the initiator concentration had to be chosen so as not to give extreme values at the extremes of the pressure and composition ranges. For example, a choice of initiator concentration which would give the best rate and molecular weight

at one extreme, say, at normal pressure and with 90 mole % αMS in the feed, may not give a satisfactory rate and molecular weight at the other, i.e., at 5000 bar pressure and with 10 mole % αMS in the feed. The chosen concentration gave quite reasonable all round rates, i.e., from 3 to 100 hours for a 5% weight conversion.

If 250 mg of copolymer is considered to be enough for various analytical procedures and also 5% conversion is considered to be the optimum conversion for copolymerization (due to composition drift), 5 ml of comonomer bulk mixture is needed for each experiment. From this point of view it was possible to construct high pressure ampoules to take 5 ml of feed mixture leaving ample extra volume for sealing-off clearence and mercury pressure seal and still fit in the pressure vessel in threes. This was the basis for the strict dimensions of the high pressure ampoules (fig.(17)) and it reduced the time and the manual work on the high pressure by a factor of three.

At the selected concentration and volume the amount of the initiator per ampoule is too little to be weighed accurately on the balance. The procedure was to introduce the initiator into the ampoule in solution with αMS. The AZBN-αMS solution was prepared just before the vacuum manipulations with freshly distilled αMS at a concentration of 0.2 mg/lt so that 0.5 ml of the solution would suffice to carry the initiator into the ampoules. Enough solution was made each time for the batch and not more than 15 minutes were allowed to pass from the start of the making of the solution to the first freezing of the ampoules on the vacuum line.

The ampoules were first weighed, then 0.5 ml of the initiator solution was inserted into each (apart from the cases where less αMS was needed and more concentrated solution was prepared). Then enough MS was added into each ampoule to bring the total αMS content to the desired approximate αMS mole fraction. The ampoules were then weighed again to obtain the exact weight of αMS and attached to the vacuum line for the following MMA distillation, degassing and sealing-off. The sealed ampoules were again weighed with their parts to obtain the exact amount of MMA introduced.

The ampoules were kept in the deep freeze at -30°C until they were used for the experiments. The safety of this was proved with a

blank experiment. No polymerization observed after 8 weeks in the deep freeze -much less than the usual storage time. The rate of decomposition of AZBN (as mentioned in section (1.2.1)) at -30°C is negligible and at 20°C is very small. For the copolymerization the break seals of the ampoules were broken in mercury under a nitrogen atmosphere to let mercury fill the empty space in the ampoule without any oxygen contamination. The ampoules were then placed into the bucket which was then inserted into the high pressure vessel. The vessel was sealed and the pressure was increased to the desired value.

When the reaction was over the ampoules were taken out and after washing off the paraffin and removing the mercury the polymer solution was washed out with a solvent mixture of toluene-acetone. The mixture was brought up to a volume of 100 ml with the solvent mixture and added dropwise into 400 ml of petroleum ether for precipitation. The precipitate was filtered on a constant weight sintered glass filter (grade 4) and dried overnight in vacuo. When necessary the precipitates were redissolved in chloroform and reprecipitated in petroleum ether for higher purity.

3.5 Analysis of Copolymers

3.5.1 Nuclear Magnetic Resonance

Isotopes of certain nuclei, apart from having properties of charge and mass, also exhibit a nuclear spin. Since a spinning charge generates a magnetic field the angular momentum is associated with a magnetic moment, μ. This kind of nucleus, especially if its size is small (e.g. a proton), can be likened to a very small magnet. The only difference between these nuclei and and small magnets is that when placed in a magnetic field they do not flip over towards the direction of the magnetic field but instead, being spinning bodies, like a gyroscope in a gravitational field. Their spin axes undergo a precession movement along the magnetic field direction. The frequency of this so-called Lamor precession is ν_o and given by

$$h\nu_o = \frac{\mu H_o}{I} \qquad (3.5.1)$$

where H_o is the applied magnetic field, h is the Planck constant and I is the spin quantum number which is 1/2 for protons. If the applied magnetic field is increased to very high values the precession frequency increases but the spin axis never aligns itself with the direction of the magnetic field. But if another magnetic field, perpendicular to H_o, is applied and rotated with the same frequency ν_o, the spin axis can be made to flip over. This second magnetic field, H_1, though not indicated in fig.(21a), can be much smaller than H_o.

If H_1 is rotated at exactly the same frequency as the precession of μ, then ν_o, the magnetic moment, will experience large oscillations between its previous angle with H_o and the direction of H_o in a resonating fashion.

In practice the equipment used to detect and measure the frequency ν_o and the sign of μ the so-called NMR spectrometer consists of a large magnet of 10 to 50 kilogauss of strength, with the sample tube placed in its magnetic field. The present day spectrometers use magnets of the srength 14,000, 23,500 and 47,000 kilogauss which correspond to Larmor precession frequencies for protons of 60, 100 and 200 Mc/sec ; as can be found from equation (3.5.1).

The radio-frequency transmitter develops an oscillating magnetic field (through the coil (a) of fig.(22)) perpendicular to the field H_o and the sample tube. This oscillating magnetic field serves as a rotating magnetic field because it may be thought of as two rotating magnetic fields which are in phase but opposite in direction. When one of the components serves as H_1 the complementary one will be too far from having any significant effect. The detection of the resonance can in practice be done in two ways. One is to have a NMR spectrometer set-up as shown in fig.(22) and change the strength of H_o by increasing slowly the magnetic field of the smaller coils m by a sweeping action while keeping ν_o constant. When, c.f. equation (3.5.1), H_o comes to the resonance value μ flips over onto H_o and this action induces a voltage through the coil (b) which has its axis on the axis of the sample tube. This voltage is detected on the recorder as a Lorentzian peak. The second

way of detection is to combine coils (a) and (b) into one and sweep ν_o while keeping H_o constant. At the resonance value of ν_o there is an energy absorption by resonance which again is detected as a peak.

Although all nuclei of the same kind, like protons, under the same magnetic field would resonate with the same frequency, for protons in molecules of various structures this is not so. The difference is very small but still is of measurable magnitude, and is of very much use to the analytical chemist. This difference arises from the various degrees of abundance of electrons around a particular proton due to the various bonds and atoms in its vicinity. When electron clouds are placed in a magnetic field orbital currents are formed which give rise to slight magnetic fields parallel to H_o. Although weak, these fields, being in the opposite direction, form a screen between the proton and the magnetic field which is called shielding and makes it necessary to have a stronger magnetic field, H_o, in order to achieve resonance with post -screen local magnetic field,

$$H_{loc} = H_o\ (1 - \sigma) \qquad (3.5.2)$$

where σ is the screening constant: the thickness of the electron cloud which screens the proton. Then equation (3.5.1) becomes

$$h\nu_o = \mu H_o\ (1 - \sigma)/\ I \qquad (3.5.3)$$

The analysis of the electron cloud around the proton is the basis of the NMR method. This shielding is not much, only about 800 cps. variation of ν_o in a 14,100 Gauss field, but is enough to give valuable information to the analytical chemist. The variations in local electron density can be due to two reasons.

a. Electronegative groups or atoms in the vicinity of the protons in question may attack the electrons and thus de-shield the proton. Protons of this kind appear to be resonating at lower values of H_o. Protons far away from such groups give their peaks at higher H_o values.

b. Certain molecular structures allow electrons to flow in certain preffered directions thus exhibiting a diamagnetic anisotropy. Certain protons around this structure may show shielding and others de-shielding. An example of this is the benzene ring and the de-shielded protons attached to it. This kind of effect may be less than the induced effect but nevertheless gives valuable information. Shielding of this

kind may also have long distance effects and, for example, the benzene ring apart from de-shielding its own protons, may shield, to a lesser extent, other distant protons which may fall into the shielding field of the ring. The shielding region of the benzene ring can be shown diagramatically in fig.(21b).

Another effect found in nuclear resonance is the direct coupling of certain nuclei with each other through the intervening chemical bonds. This causes the polarization of the orbital motions of the valence bonds and thus a splitting of the peaks of the protons in question into doublets. If more than two protons are involved the resulting splitting will be much more complicated and the intensities and the number of the peaks will give a Pascal triangle.

In the analysis of NMR spectra various conventions are used at the present day. One of them is to show the peaks on a scale of parts per million relative change in H_o or less commonly in ν_o. Another is to use a referance substance dissolved in the sample and refer all shifts to this internal referance. A standard internal referance is tetramethylsilane and to its peak position a value of 10.00 τ is assigned. The rest of the peaks are expressed in τ units. Sometimes a δ scale may be used which simply is $\delta=10-\tau$. The advantage of this dimensionless scale is that it is independent of the field strength H_o.

Application of NMR to copolymers is discussed in section (4.3).

3.5.2 Copolymer Composition from NMR Spectra

The spectra of methyl methacrylate and α-methyl styrene monomers are shown in figures (24a) and (24b) respectively. The main difference between the spectra of the monomers and their polymers is that the polymer spectra possess a broader set of peaks which is due to the direct coupling of the protons with their consecutive neighbours. The spectrum of methyl methacrylate consists of one singlet peak for the methoxy protons at 6.3 τ and two multiplet peaks for the ethylene protons at 3.95 and 4.45 τ. When polymerized the ethylene protons become methyne protons and resonate at a field strength corresponding to the region from 7.7 to 8.5 τ. In the spectrum of α-methyl styrene the main

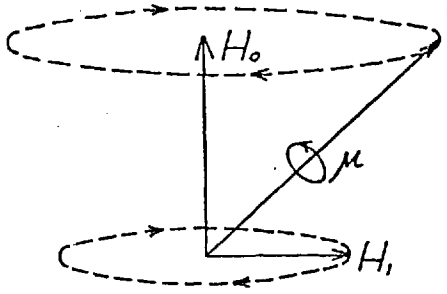

Fig.21a Magnetic field components of NMR spectometer.

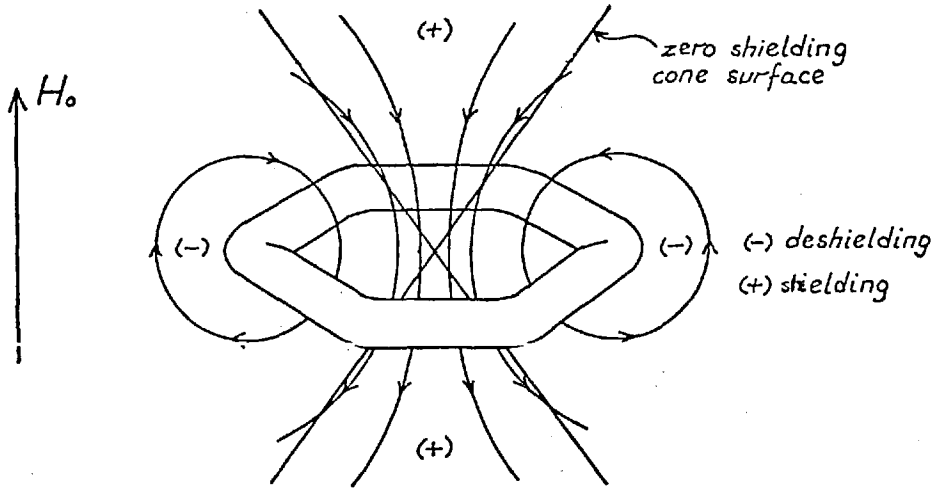

Fig.21b The shielding region of the benzene ring.

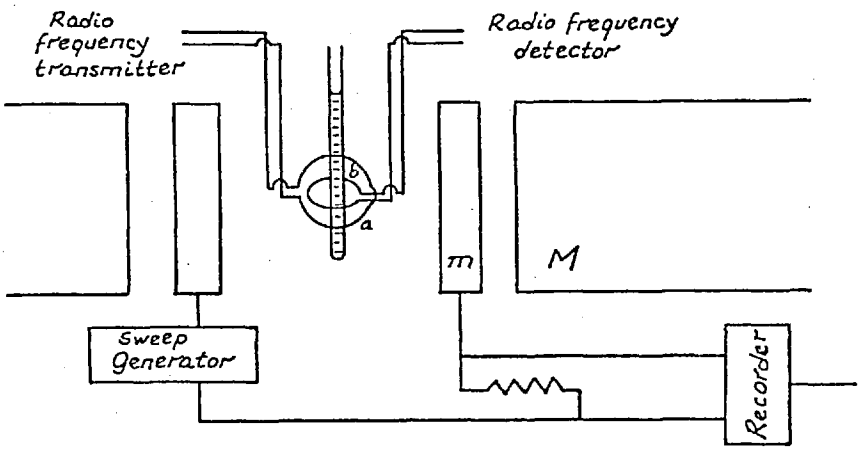

Fig.22 Schematic diagram of a standard NMR spectometer.

NUCLEAR MAGNETIC RESONANCE SPECTRAL DATA

Agricultural and Mechanical College of Texas — American Petroleum Institute Research Project 44 — College Station, Texas

Contributed by the Humble Oil and Refining Company, Baytown, Texas

Isopropenylbenzene (α-Methylstyrene) (liquid) — Serial No. 256 — October 31, 1962

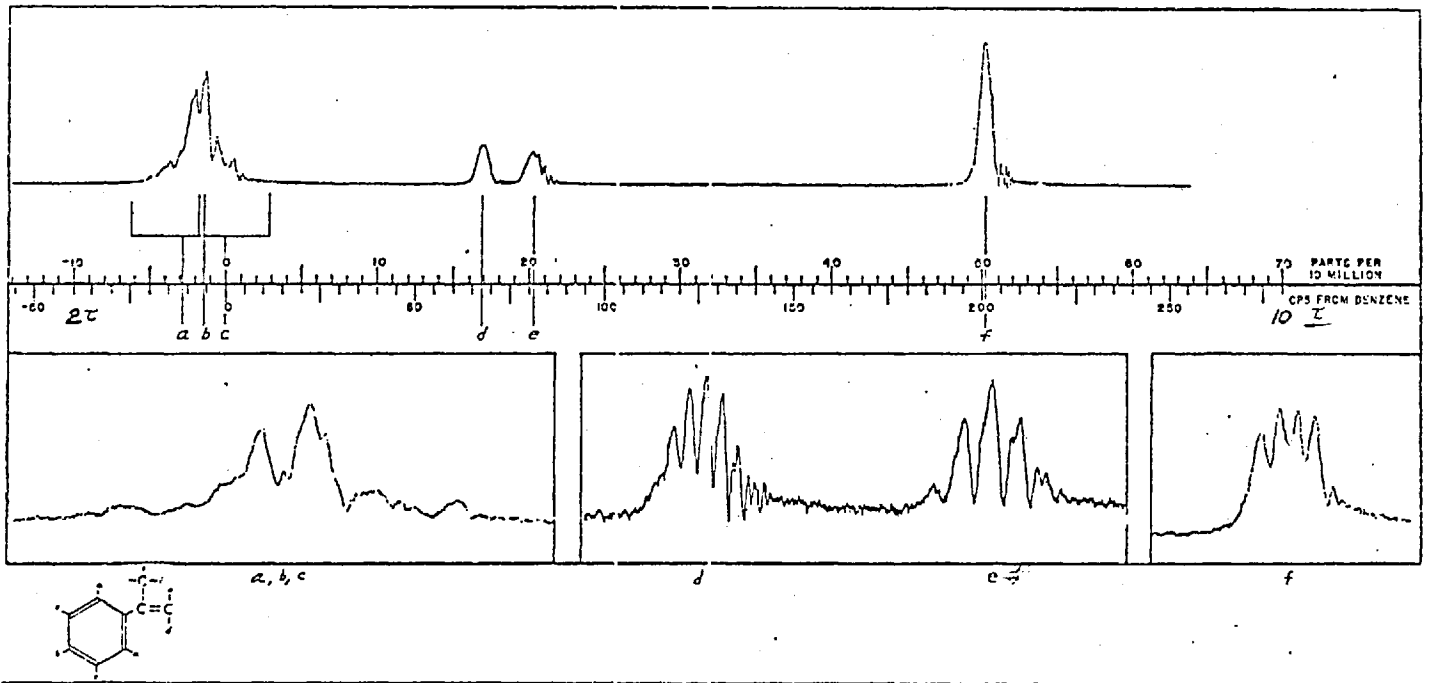

COMPOUND		INSTRUMENT AND CONDITIONS
Name: Isopropenylbenzene (α-Methyl-styrene) C_9H_{10}	State: Liquid	Instrument: Varian Associates Spectrometer, Model V-4310C Frequency: 40 Mcps — RF Field Intensity (H_1): 9400 gauss Scanning Rates: Standard (Spectrum A): 4.85 cps/second Other (Expanded): 0.92 cps/second
Source: Eastman Kodak Company	Temperature:	External Reference: Internal Reference: Cyclohexane (peak not shown)
Purity:	Cell: Glass tube, 5 mm OD	Concentration: Precision of Measurement: Resonance Position: Internal Benzene as 0.0 cps

LABORATORY: Humble Oil and Refining Company, Research and Development Division, Baytown, Texas

Serial No. 256

Fig. 24a NMR spectrum of α-methyl styrene.

NUCLEAR MAGNETIC RESONANCE SPECTRAL DATA

Agricultural and Mechanical College of Texas — Manufacturing Chemists Association Research Project — College Station, Texas

Contributed by the Union Carbide Chemicals Company, South Charleston, West Virginia

Methyl 2-methylpropenoate (Methyl methacrylate)(liquid) — Serial No. 144 — June 30, 1962

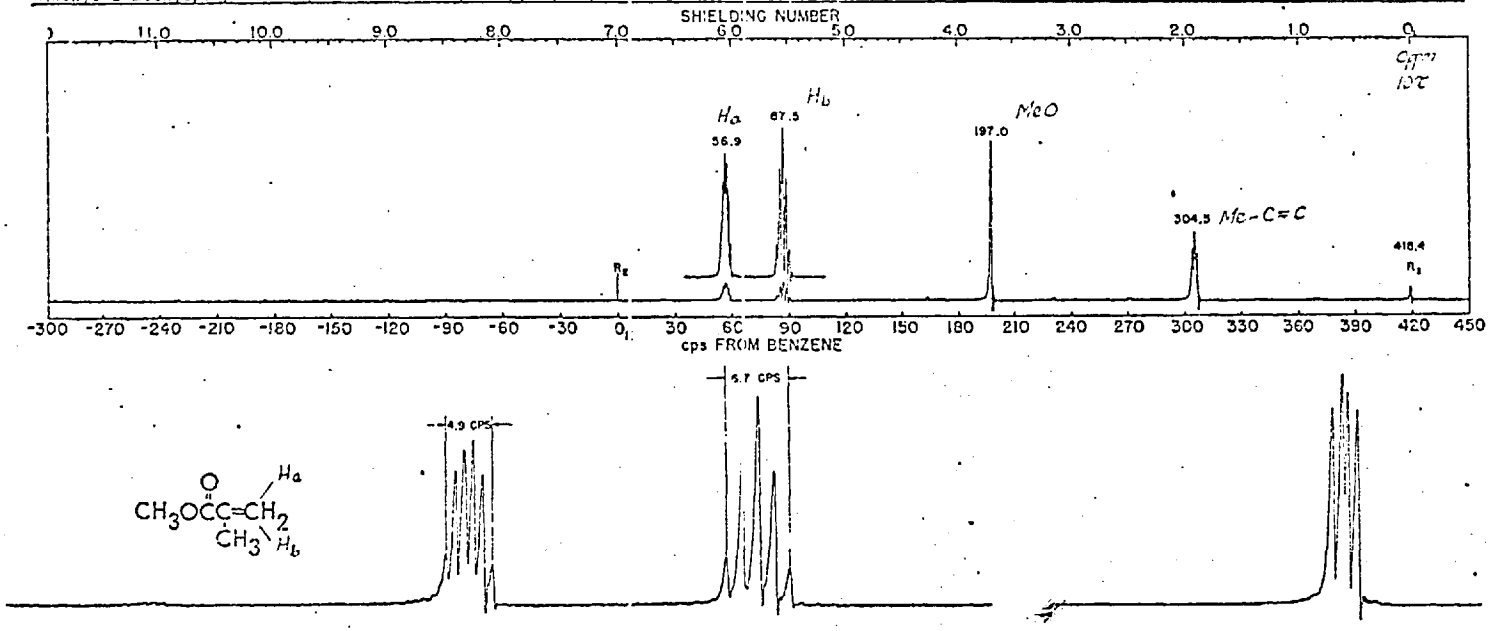

COMPOUND		INSTRUMENT AND CONDITIONS
Name: Methyl methacrylate $C_5H_8O_2$	State: Liquid, degassed	Instrument: Varian Associates Model A-60 Frequency: 60 Mcps — RF Field Intensity (H_1): Scanning Rates: Standard (Spectrum A): 1.00 cps/sec Other (Spectrum B): 0.20 cps/sec
Source: Rohm and Haas Purity:	Temperature: Ambient Cell: Varian Associates precision tube	External Reference: Benzene in capillary tube Internal Reference: $(CH_3)_4Si$ Concentration: About one per cent Resonance Position: 418.4 cps from benzene Precision of Measurement:

LABORATORY: Union Carbide Chemicals Company, Research and Development Department, South Charleston, West Virginia

MCA Serial No. 144

Fig.24b NMR spectrum of methyl methacrylate.

difference is the benzene peak at ~2.8 τ instead of the methoxy peak. The other two peaks again belong to the ethylene protons but at a sligtly lower field, 4.7 and 5.05 τ respectively, and α-methyl protons at 8.0 τ (methyl protons of MMA give their peak at 8.1 τ).

The spectra of copolymers of αMS and MMA with varying composition are shown in figures (25a) to (25i). The basic difference of these spectra from a hypothetical spectra of mixtures of homopolymers would be (on a 60 MHz spectometer) the separation of the methoxy proton peaks into three groups of peaks dispersed onto the field between 2.5 and 4.0 δ . The reason for this dispersion is given in section (4.3). When it is needed to calculate the composition of a copolymer sample with its NMR spectrum given, one only needs to compare the various peaks of individual homopolymers. To find the mole ratio of the monomer units the specific areas must be proportionated with a proper factor which, since peak intensities depend on the number of protons in question, derived from the amount of that particular proton in the monomer. For the copolymer of αMS-MMA the ratio of the peak area of the benzene ring protons and the peak area of methoxy protons with the formula below give the mole fraction of αMS in the copolymer,

$$F_{\alpha MS} = \frac{3(\text{benzene peak area})}{3(\text{benzene peak area}) + 5(\text{methoxy peak area})}$$

since phenyl group contains five protons whereas methoxy group contains three.

Some workers have also used UV spectra to determine copolymer compositions. This was done by the absorbance of one of the benzene peaks at 262 mμ of a solution of the copolymer in $CHCl_3$. This was employed by Izu and O'Driscoll[81] after a calibration curve from elemental analysis and NMR data.

3.5.3 The Dupont Peak Resolver

The resonance peaks of protons in NMR spectra follows the Lorentzian line shape. When these peaks are clustered together it is very difficult to find the areas of the individual peaks. The crudest method

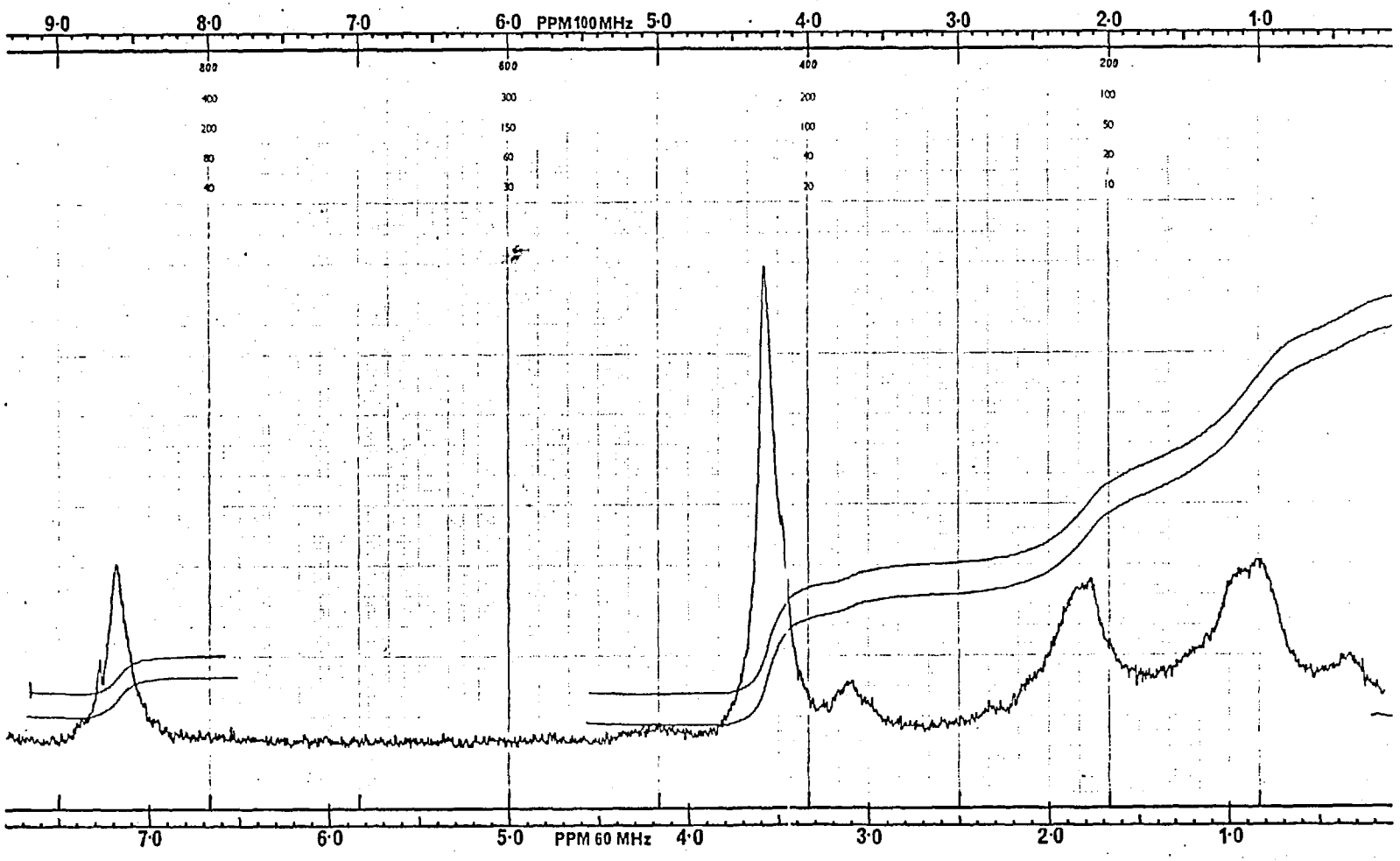

Fig.25a NMR spectrum of MMA-αMS copolymer with 90:10 feed composition prepared at 60°C and 1500 bars. (code-23L)

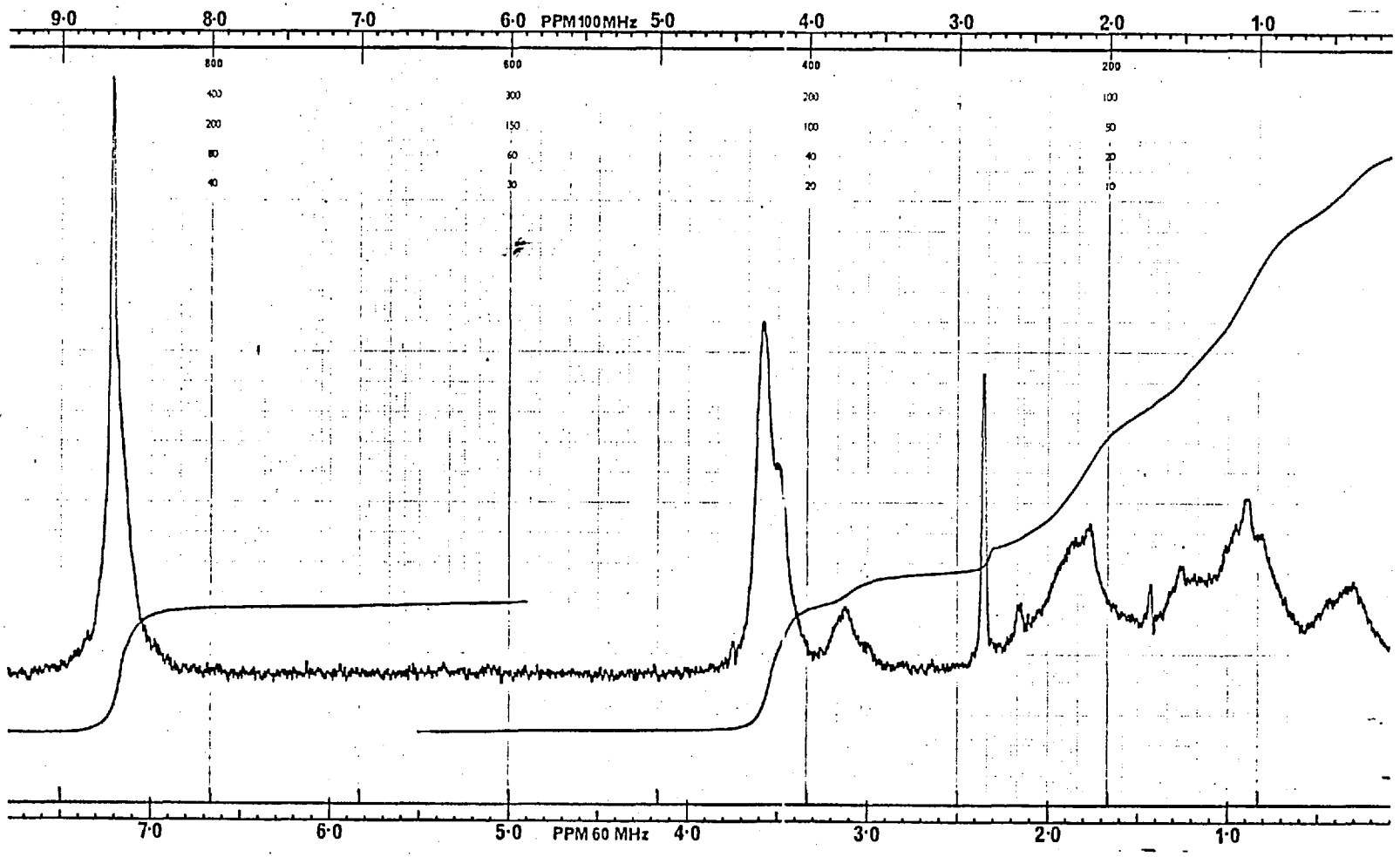

Fig.25b NMR spectrum of MMA-αMS copolymer with 80:20 feed composition prepared at 60°C and 1500 bars. (code-4A)

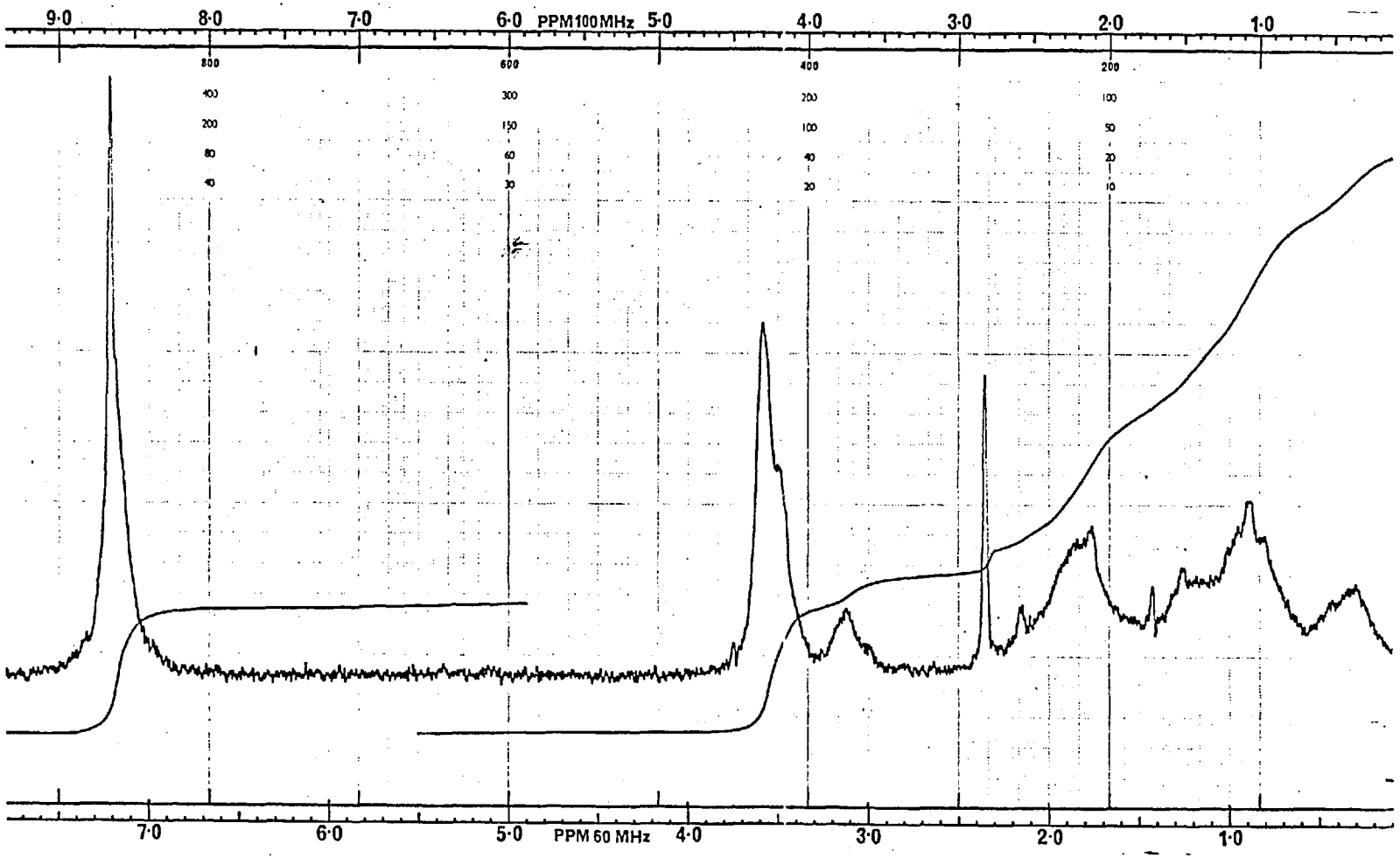

Fig.25b NMR spectrum of MMA-αMS copolymer with 80:20 feed composition prepared at 60°C and 1500 bars. (code-4A)

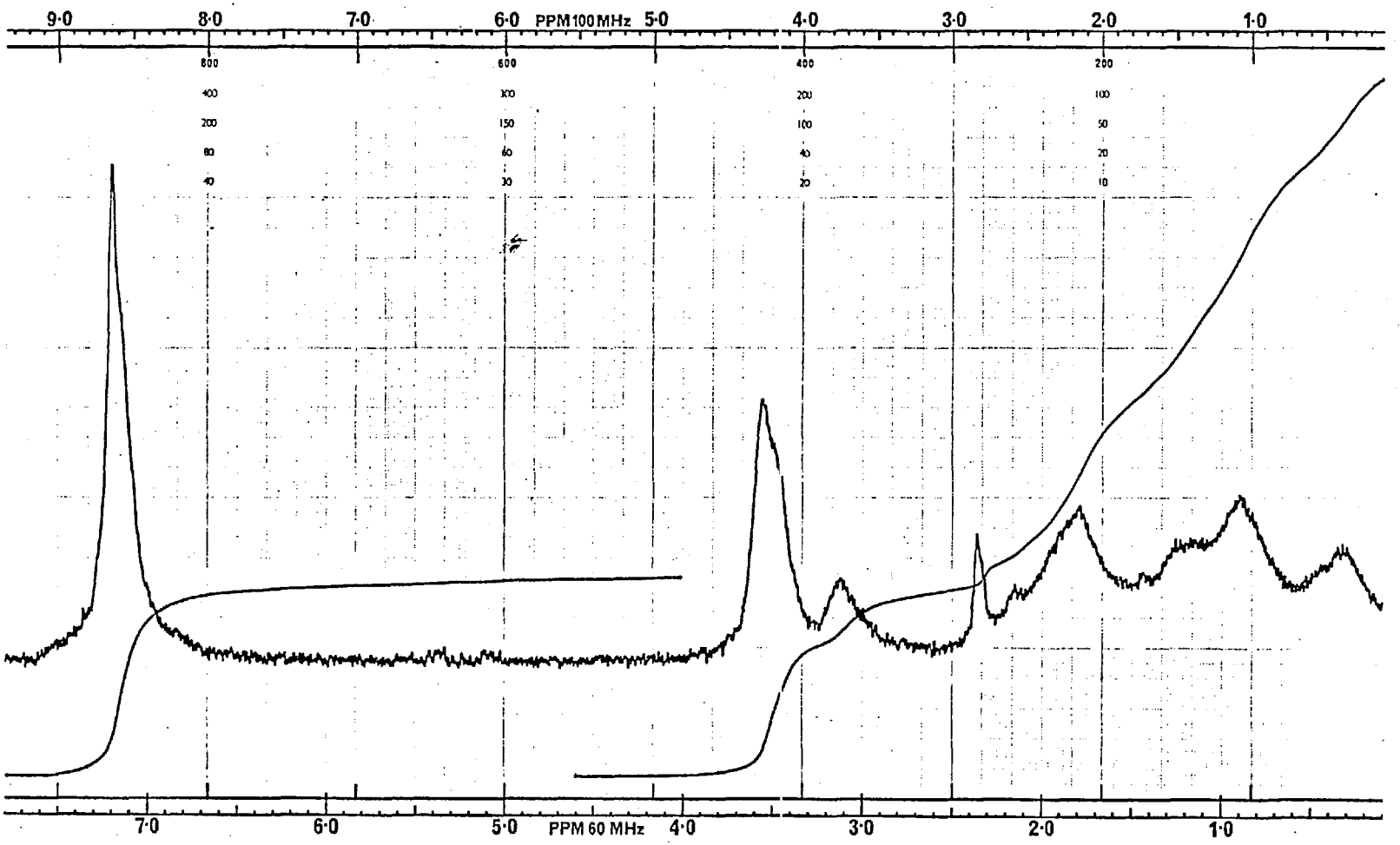

Fig.25c NMR spectrum of MMA-αMS copolymer with 70:30 feed composition prepared at 60°C and 1500 bars. (code-6A)

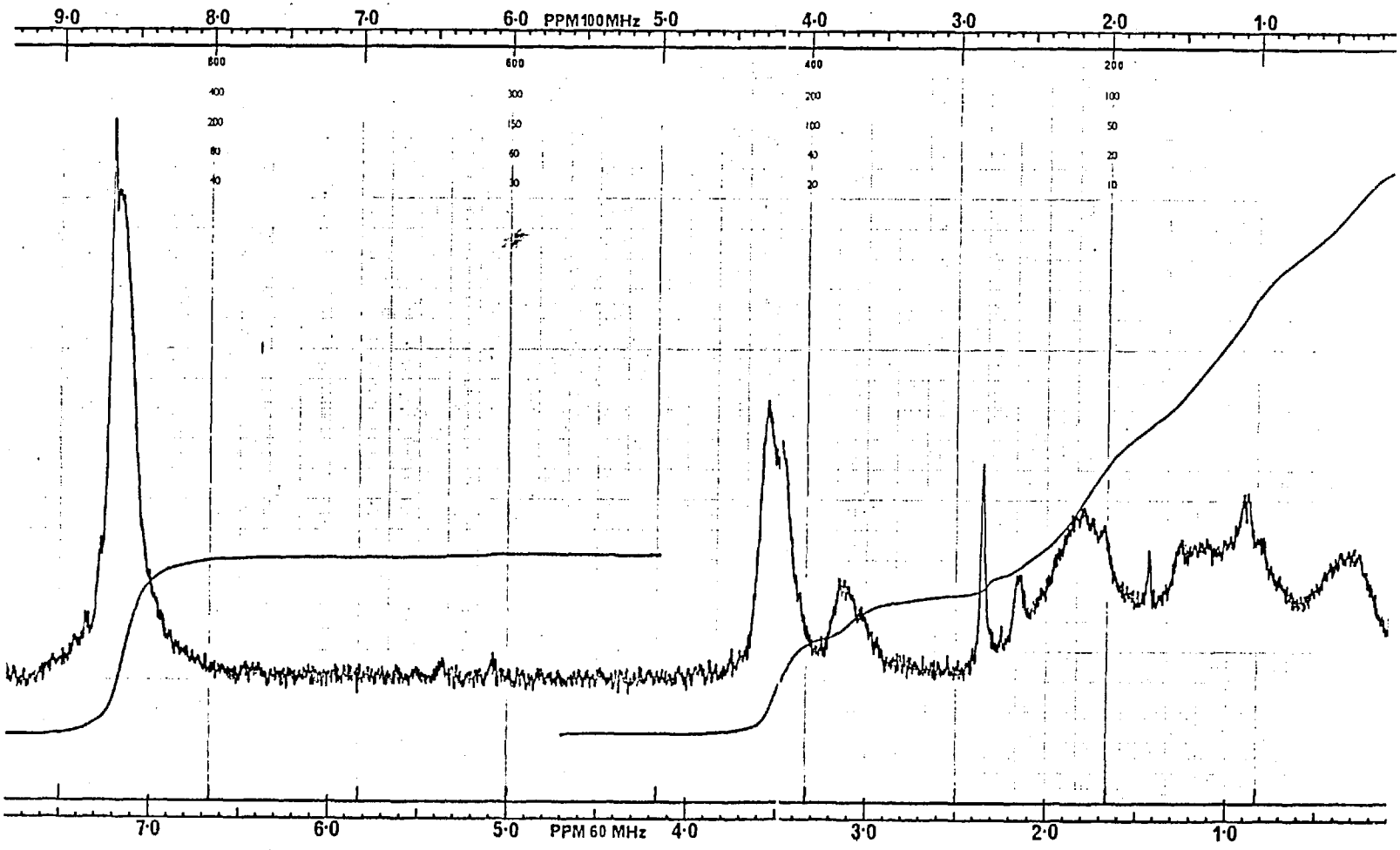

Fig.25d NMR spectrum of MMA-αMS copolymer with 60:40 feed composition prepared at 60°C and 1500 bars. (code-7A)

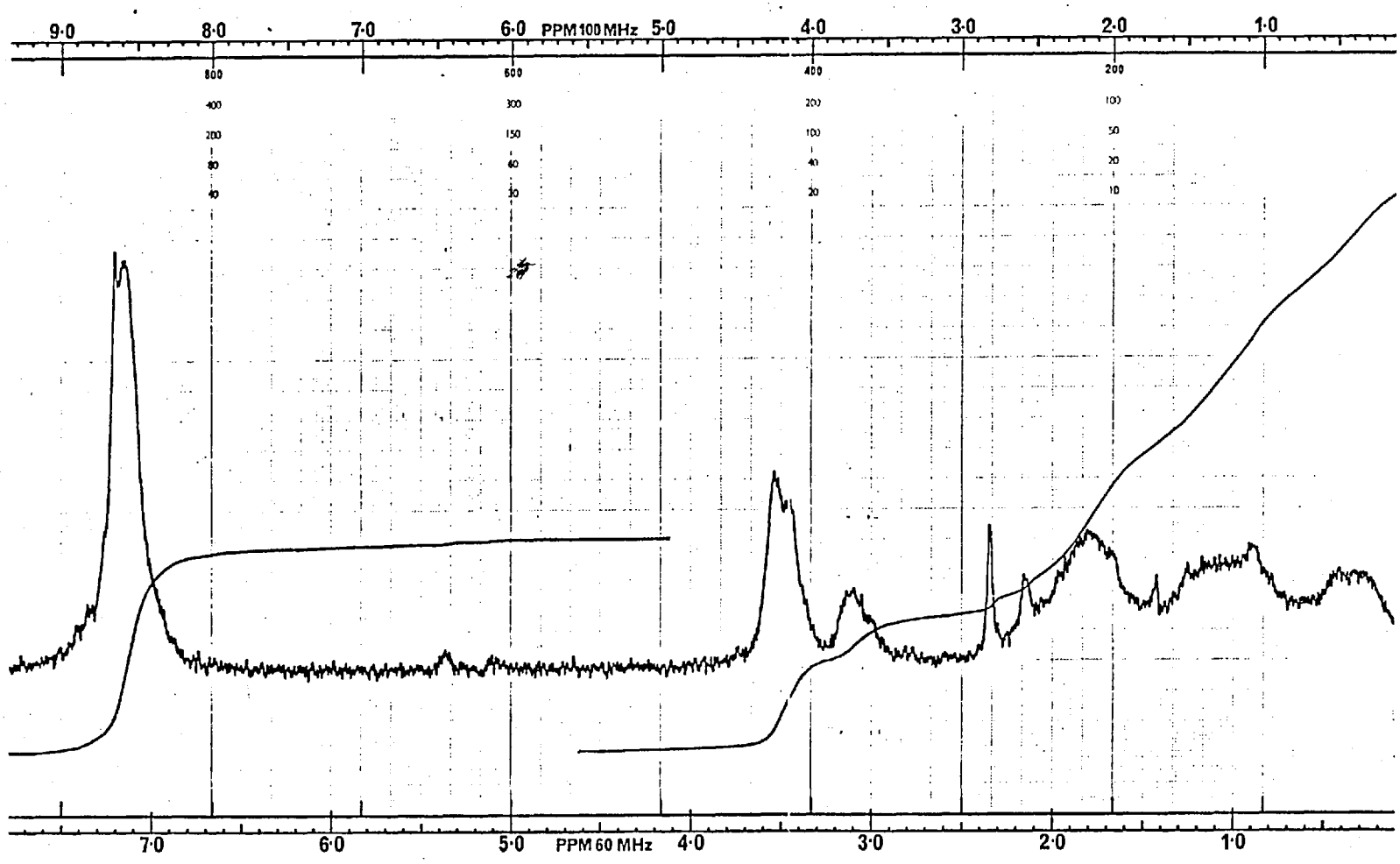

Fig.25e NMR spectrum of MMA-αMS copolymer with 50:50 feed composition prepared at 60°C and 1500 bars. (code-8A)

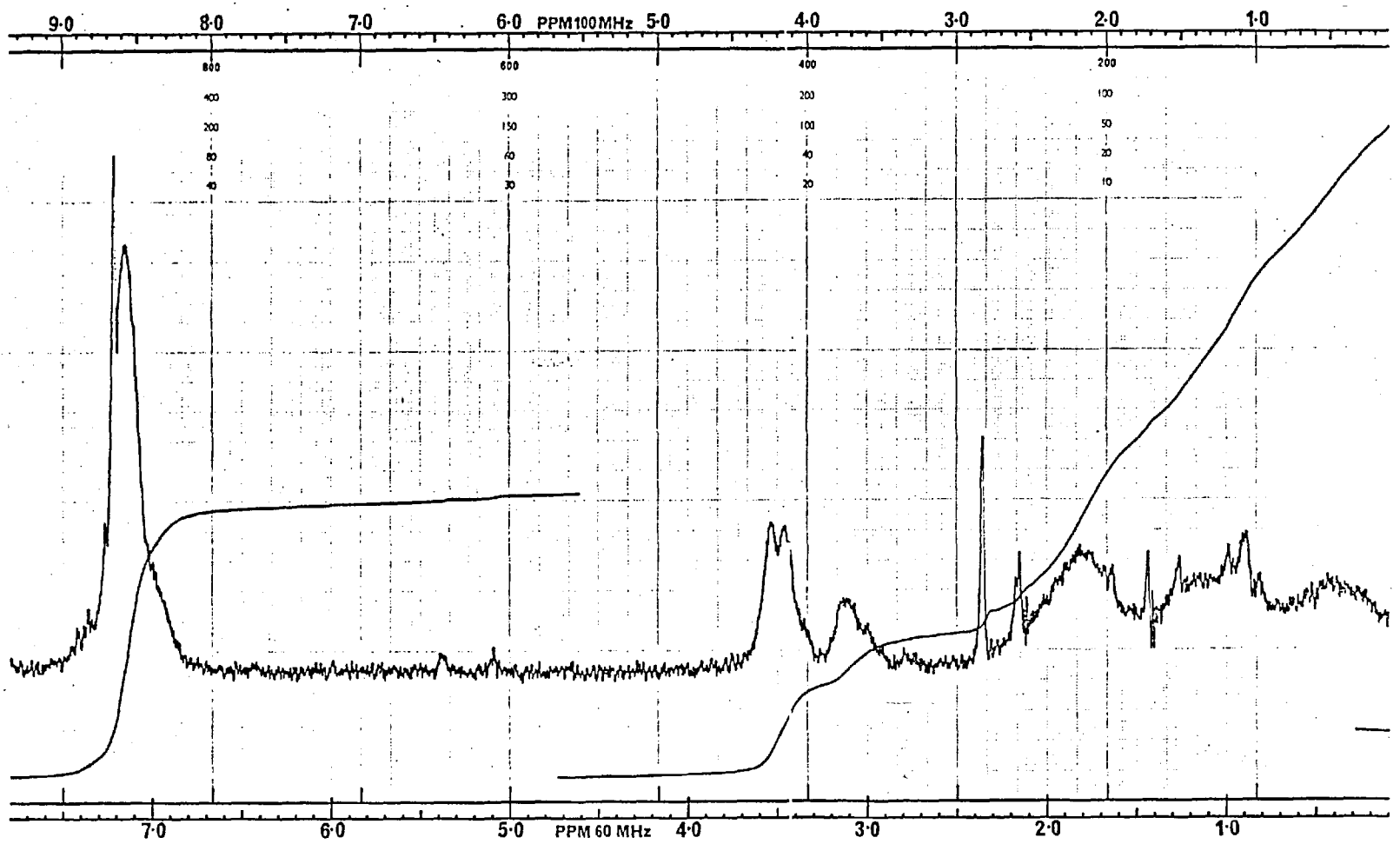

Fig.25f NMR spectrum of MMA-αMS copolymer with 40:60 feed composition prepared at 60°C and 1500 bars. (code-9A)

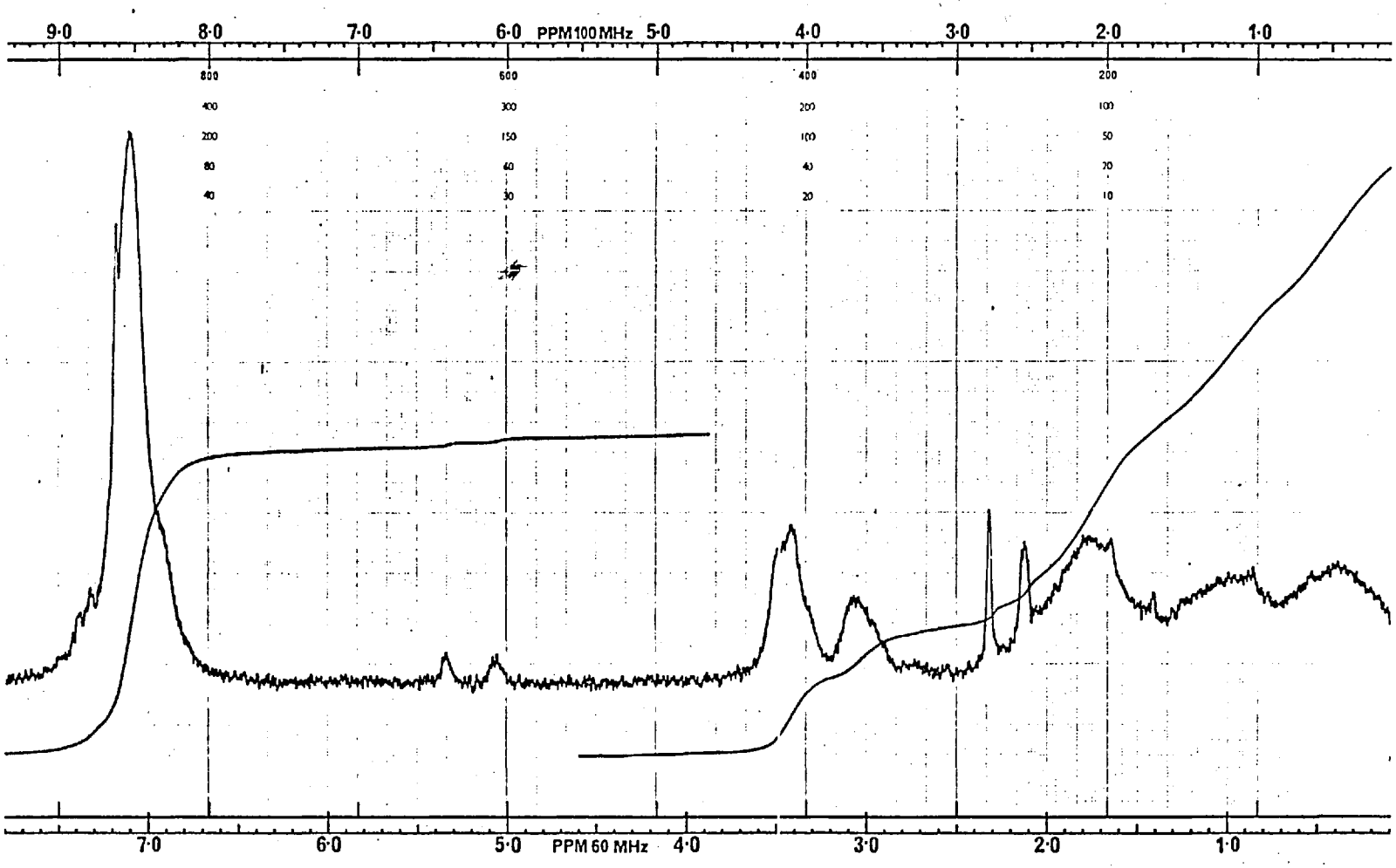

Fig.25g NMR spectrum of MMA-αMS copolymer with 30:70 feed composition prepared at 60°C and 1500 bars. (code-10A)

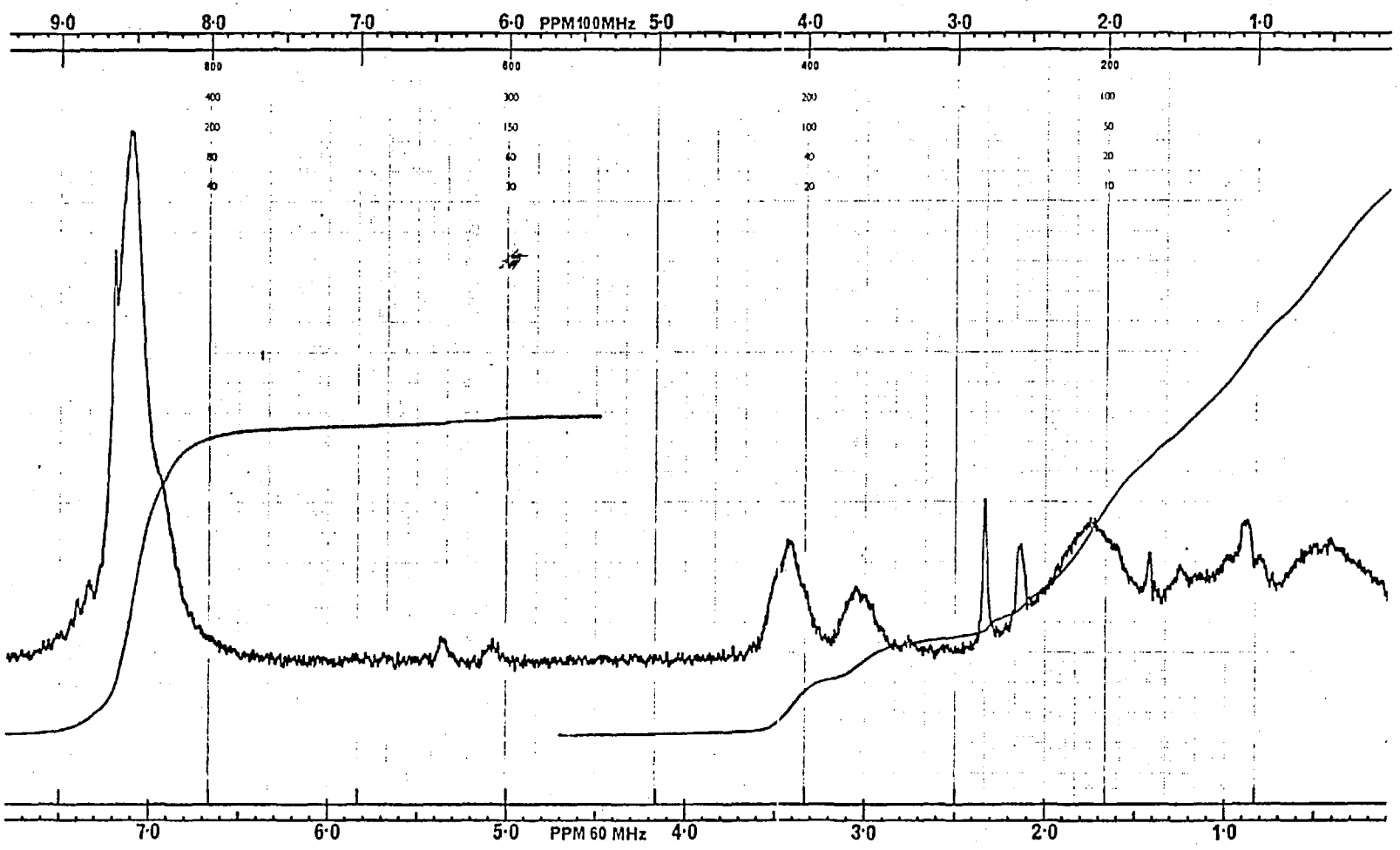

Fig.25h NMR spectrum of MMA-αMS copolymer with 20:80 feed composition prepared at 60°C and 1500 bars. (code-11A)

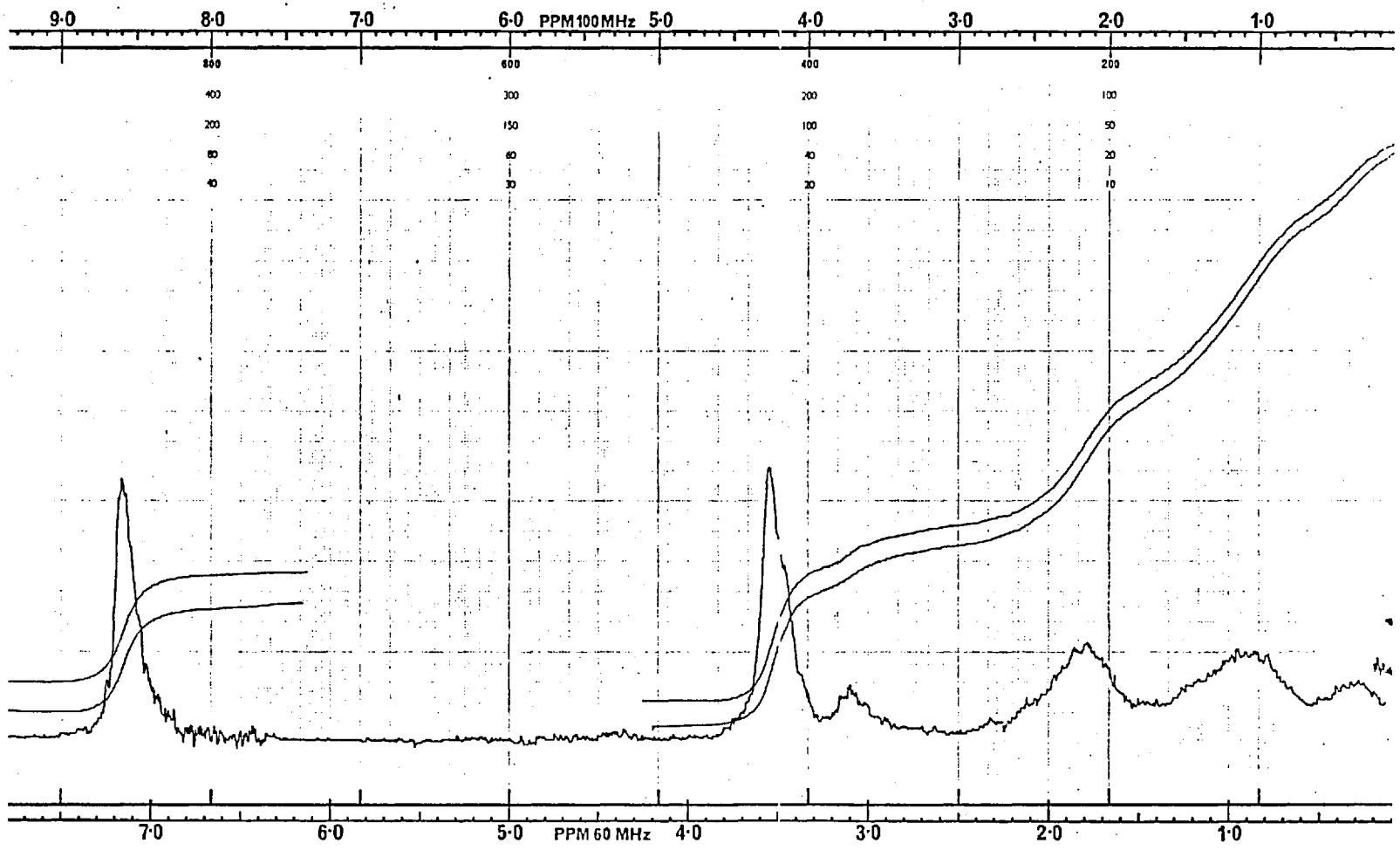

Fig.25i NMR spectrum of MMA-αMS copolymer with 80:20 feed composition prepared at 60°C and 1500 bars. (code-51K) The peaks at 7.20τ (together with copolymer's benzene peak), 2.35τ and 2.15τ in some of the spectra are due to the toluene and αMS monomer impurities in the copolymer sample and were excluded from the actual peak area (benzene) by an elimination process.

involves guesswork, which is far from being reliable. The most recent development in the resolution of such groups of curves is the 'Dupont Peak Resolver'. This equipment takes various statistical distributions and adds up a certain number of their curves on a screen. It consists of a bench to place the spectra on, a vacuum tube where the curves are created, a two way mirror where the two curves are superimposed and a panel of adjustment curves. It can create as many as seven curves on a base line. Initially every individual peak is calibrated with a reference graph for a particular distribution -in this case Lorentzian. These peaks are then adjusted to a certain dispersion which is guessed from the spectra of a particular proton. Finally the spectrum is simulated by moving the peaks into position and adjusting their heights cumulatively.

To achieve a true resolution the exact number of peaks in a peak cluster and their approximate position must be known. The areas of the individual peaks are read off a galvanometre, one at a time.

3.5.4 Elemental Analysis .

The copolymers were analysed for their oxygen content in order to determine their composition. The analytical method used was elemental analysis and was carried out using the Carlo-Erba 'Elemental Analyser Mod.1102'. It is specifically designed for the determination of the carbon, hydrogen, nitrogen and oxygen content of organic materials and was consists of two channels, one of which analyses O and the other C, H and N. For the purpose of this research the determination of oxygen was sufficient since the amount of oxygen was the main difference between the various copolymers. The elemental composition of the two monomer units were,

methyl methacrylate	element	mole%	weight%
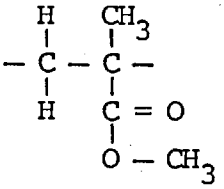	C	33.33	60.00
	H	53.33	8.00
	O	13.33	32.00

α-methyl styrene	element	mole%	weight%
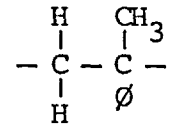	C	47.37	91.53
	H	52.63	8.47
	O	0.00	0.00

Although the copolymers can also be analysed from the differences in their C or H content the fact that the difference in their O content is always larger makes it more accurate.

The weight fraction of oxygen in the copolymer can be given by

$$w_o = W_s\, w_{o,s} + W_m\, w_{o,m} \qquad (3.5.4)$$

where $w_{o,s}$ and $w_{o,m}$ are the oxygen contents in weight fraction in αMS and MMA units respectively and W_s and W_m are the weight fractions of the monomer units in the copolymer sample. Since

$$W_m = 1 - W_s$$

then

$$w_o = W_s\, w_{o,s} + (1-W_s)\, w_{o,m} = (1-W_s)\, w_{o,m} \qquad (3.5.5)$$

Hence W_s can be calculated from the oxygen analysis data. For the mole fraction of αMS in the polymer sample

$$F_s = 1 - \frac{X\, w_o/32}{X/(100F_s + 118(1-F_s))} \qquad (3.5.6)$$

where X is the weight of the sample and 100 and 118 are the molecular weights of MMA and αMS respectively. Rearrenging equation (3.5.6)

$$F_s = 1 - \frac{1.18\, w_o}{32 + 0.18\, w_o} \qquad (3.5.7)$$

w_o can be obtained directly from the peak height and the weight of each sample. For the analysis a standard sample (analysed under the same conditions) is needed for the calibration of peaks. In this case it is 2-4,dinitrophenyl hydrazine:

	w/w %		w/w %
C	51.79	N	20.14
H	5.07	O	23.00

From the oxygen peak height of the standard a factor is calculated.

$$K_o = \frac{23.0(\text{weight of standard})}{(\text{standard peak height})}$$

then for w_o

$$w_o = \frac{K_o(\text{peak height of sample})}{X}$$

The elemental analyser Mod.1102 is fully automatic and can analyse 23 samples at each run consecutively. Each analysis takes approximately 8 minutes and out of 23, 2 or 3 must be allocated to standards and one left as blank to detect any impurity in the gases present. Any blank peak corresponding to the same retention time should be subtracted from all sample peaks, including the standards. The peaks may be measured by area or height (i.e., if the peak is long enough). Samples (including standards) are weighed into silver-foil containers usually approximately in one milligram lots on a micro-balance accurate to the microgram.

The sample to be analysed is dropped from the sample disk automatically into the combustion tube where the organic substance is pyrolized at 1120°C. The combustion tube is filled with activated carbon, thus the reaction products consist of CO, N_2 and traces of CH_4 and H_2 which are carried away by a constant stream of He. The gases are then sent to a chromatographic column where CO and N_2 are separated. Each component is detected by thermal conductivity at its corresponding retention time below

component	retention time
H_2	2 min 15 sec
N_2	3 min
CO	6 min

To check on the reliability of the results the Author calculated the standard deviation of oxygen analysis in a single batch by determining the oxygen amount in standard samples as K_o

no. of standard	K_o	no. of standard	K_o
1	0.1404	4	0.1446
2	0.1374	5	0.1393
3	0.1460	6	0.1381

which gave $\sigma = 0.3358 * 10^{-2}$. The Author also calculated the standard deviation of copolymer composition of one copolymer sample analysed in seven different batches.

no. of batch	F_s	no. of batch	F_s
1	0.4142	5	0.4577
2	0.4114	6	0.4352
3	0.4790	7	0.4660
4	0.4685		

which gives $\sigma = 0.027$ and with 95% confidence limit the confidence interval:

$$\pm 0.0242 \quad \text{or} \quad \pm 5.41\ \%$$

3.5.5 Determination of Molecular Weights

The determination of the molecular weights was done by gel permeation chromatography at the Polymer Supply and Characterisation Centre laboratories of the Rubber and Plastic Research Association of Great Britain. The operating variables of the columns were as follows:

Column:

Set B: 4 columns

(i) 700 - 2000 A

(ii) $1.5 * 10^4 - 5 * 10^4$ A

(iii) $7 * 10^5 - 5 * 10^4$ A

(iv) $5 * 10^6 - 10^7$ A

Flow rate: 1 ml/min.

Solvent: Tetrahydrofuran plus 0.1% 2-6,di-tert-butyl-p-cresol as inhibitor.

Temperature: Ambient.

Calibration: Polystyrene –Mark-Houwink constants used were of polystyrene and due to closeness of these constants to the ones of MMA and αMS no conversion of calibration was made.

The results of this analysis are given in section (6.2) and a sample result sheet chromatogram of one copolymer is shown in fig.(23). For the reliability of the results the Polymer Supply and Characteri-

sation Centre states:"Reproducibility of GPC runs is generally very good in that the original chromatograms will superimpose. The selection of the baseline will sometime affect the interpretation and calculation of molecular weight averages. Generally, calculated molecular weight averages agree for duplicate runs to approximately 1% or better. For comparison of nonduplicate samples accuracy is usually quoted to be 8-10% for $\bar{M}_n$, 3-5% for $\bar{M}_w$ and 5-30% for $\bar{M}_z$."

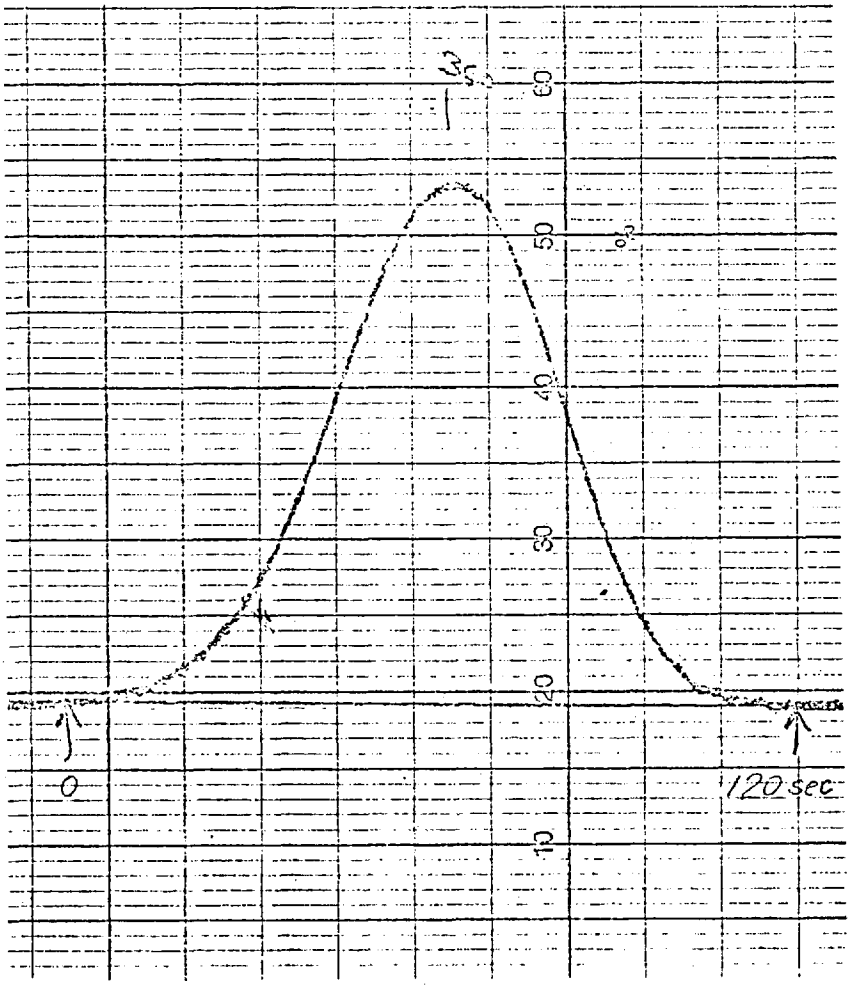

Fig.23 A typical GPC chromatogram of a MMA-αMS copolymer. Sample:B6, solvent:THF, temp.:25°C, concentn.:0.2%, time:120sec.

IV. FURTHER ASPECTS OF COPOLYMERIZATION

4.1 Expansion of Copolymerization Theory

For the derivation of the original copolymerization equation of Mayo and Lewis only four possible propagation steps were taken into account, with the implicit assumption that only the terminal unit of an active radical and the monomer itself decide the course of the reaction. Later Merz, Alfrey and Goldfinger[90] derived an equation for copolymerization which allowed for a possible influence of the penultimate unit of the growing chain on the determination of copolymer composition. This treatment had to take eight possible copolymerization steps into account,i.e.,

$$\begin{aligned}
&\text{-AA}\cdot + \text{A} \longrightarrow \text{-AAA}\cdot \\
&\text{-BA}\cdot + \text{A} \longrightarrow \text{-BAA}\cdot \\
&\text{-AA}\cdot + \text{B} \longrightarrow \text{-AAB}\cdot \\
&\text{-BA}\cdot + \text{B} \longrightarrow \text{-BAB}\cdot \\
&\text{-AB}\cdot + \text{A} \longrightarrow \text{-ABA}\cdot \\
&\text{-BB}\cdot + \text{A} \longrightarrow \text{-BBA}\cdot \\
&\text{-AB}\cdot + \text{B} \longrightarrow \text{-ABB}\cdot \\
&\text{-BB}\cdot + \text{B} \longrightarrow \text{-BBB}\cdot
\end{aligned} \qquad (4.1.1)$$

and yielded the equation

$$\frac{a}{b} = \frac{1 + \frac{A}{\alpha_1 B}\left(\frac{\alpha_1 B + A}{\alpha_2 B + A}\right)}{1 + \frac{\beta_1 B}{A}\left(\frac{\beta_2 B + A}{\beta_1 B + A}\right)} \qquad (4.1.2)$$

where a and b are the mole fractions of the corresponding monomers in the copolymer chain, A and B are similarly of the feed mixture and α and β are the reactivity ratios given by individual propagation rate constants as

$$\alpha_1 = \frac{k_p^{aab}}{k_p^{aaa}} \qquad \alpha_2 = \frac{k_p^{bab}}{k_p^{baa}}$$

$$\beta_1 = \frac{k_p^{abb}}{k_p^{aba}} \qquad \beta_2 = \frac{k_p^{bbb}}{k_p^{bba}}$$

These researchers produced this equation but did not obtain any experimental confirmation. They believed that it would be rather difficult to test an equation of this size, but the main reason for its initial inapplicability was that it contained an error. A corrected version of the same equation, in present-day nomenclature is

$$n \text{ (or } X) = \frac{1 + r_1' x \left(\dfrac{1 + r_1 x}{1 + r_1' x} \right)}{1 + (r_2'/x) \left(\dfrac{1 + r_2/x}{1 + r_2'/x} \right)} \qquad (4.1.3)$$

where $x=A/B$ (of the previous equation), $r_1=1/\alpha_1$, $r_1'=1/\alpha_2$, $r_2=\beta_1$ and $r_2'=\beta_2$.

A detailed study of the styrene-fomaronitrile system by Ham and Fordyce[91] showed evidence of a repulsion between a styrene-ended chain radical with a high fumaronitrile content and the fumaronitrile monomer. To this system the original Mayo-Lewis equation did not apply but instead it was possible for Barb[92] to interpret the data by the penultimate-unit equation. For this he used a simplified version of the equation in which, by assuming $r_2=r_2'=0$,

$$n = 1 + r_1' x \left(\frac{1 + r_1 x}{1 + r_1' x} \right) \qquad (4.1.4)$$

Ham[93] studied the published data on other copolymerization systems using this treatment of Barb's. He found that acrylonitrile also appears to exhibit electrostatic repulsion between the polar monomer and chains rich in that monomer (but with the other terminal unit). The deviation of the composition data from the terminal unit model is similar in shape to the styrene-fumaronitrile system, but much less.

In fact, it was suggested that the ratio r_1'/r_1 can be taken as a measure of relative repelling tendencies of polar monomers, or of the deviation fron the terminal unit model, which gives r_1'/r_1=15 for fumaronitrile, 3-4 for maleic anhydride and 1.5 for acrylonitrile. It is obvious that if a polar monomer contains polar groups on both vinyl carbon atoms the repulsion will be much more pronounced. The ratio r_1'/r_1 becomes ill-conditioned with systems of large r_2 (in the terminal unit model) and the difference between r_1 and r_1' cannot be justified in these systems. The values of r_1 and r_1' calculated in this way were tested by applying them, plus published r_2 values for the penultimate unit model, to a penultimate unit model equation of the type for which $r_2=r_2'$:

$$n = \frac{1 + r_1'x\left(\frac{1 + r_1x}{1 + r_1'x}\right)}{1 + r_2/x} \qquad (4.1.5)$$

The interpretation of the data by this equation were reported to be much better than the terminal unit model equation.

The same treatment was applied by Ham[93] to check on the influence of possible steric hindrances but he failed to obtain a difference between r_1 and r_1'. The system studied was vinyl acetate and crotonic acid. The α-methyl styrene and acrylonitrile system was also studied[80] and a ratio of r_1'/r_1=1.69 was obtained which is not much different from that for styrene and acrylonitrile (r_1'/r_1=1.5).

The 'penultimate unit effect' equation of Merz et al. was derived from the kinetic treatment of copolymerization reactions. It is obvious from the fumaronitrile copolymerization that there is a possible need for the consideration of more remote monomer units in the chain. The derivation of equations,which take into account the penpenultimate or more remote units,from kinetic considerations is extremely complex. To achieve this formidable task researchers tackled the problem differently. Two basic lines of approach were (1)use of probability considerations to derive equations which take into account more remote units, (2)consideration of possible depropagation reactions, leading to derivations of equations to simulate special copolymerization reaction.

The first was pioneered by Ham[78], and by Coleman and Fox[96], whereas the second was pioneered independently by Lowry[97] and by Wittmer[98] using kinetic considerations. The most recent development in this generalization of the copolymerization equation is due to O'Driscoll et al.[107], who combined the 'remote units' effect with depropagation in a probabilistic treatment.

As the terminal unit model is derived from probabilistic considerations in section (1.3.4) the same method can be expanded to derive more remote unit effect equations. It can also be used to develop the equation without the need of steady-state assumptions. The probability of finding a given sequence of 'a' where there is the effect of a penultimate unit in the propagation reaction is

$$N_n = P_{baa} P_{aaa}^{n-2} P_{aab} \qquad \text{for } n>1$$

$$= P_{baa} P_{aaa}^{n-2} (1-P_{aaa}) \qquad (4.1.6)$$

$$N_1 = 1-P_{baa} = P_{bab} \qquad \text{for } n=1$$

where again P_{baa} is the probability of a sequence of 'ba' adding 'a'. For a number average sequence length of 'a'

$$W_a = P_{bab} + 2P_{baa}P_{aab} + 3P_{baa}P_{aaa}P_{aab} + \cdots \qquad (4.1.7)$$

which gives

$$W_a = 1 - \frac{P_{baa}}{P_{aaa}} + \frac{P_{baa}P_{aab}}{P_{aaa}^2} \sum_{n-1} nP_{aaa}^n \qquad (4.1.8)$$

and for 'b' sequences

$$W_b = 1 - \frac{P_{abb}}{P_{bbb}} + \frac{P_{abb}P_{baa}}{P_{bbb}^2} \sum_{n-1} nP_{bbb}^n \qquad (4.1.9)$$

Both of these averages, as shown in section (1.3.4) can be reduced to

$$W_a = 1 + (P_{baa}/P_{aab})$$
$$W_b = 1 + (P_{abb}/P_{bba}) \qquad (4.1.10)$$

so

$$\frac{W_a}{W_b} = \frac{a}{b} = \frac{1 + (P_{baa}/P_{aab})}{1 + (P_{abb}/P_{bba})} \qquad (4.1.11)$$

The individual probabilities can be obtained simply (as in section (1.3.4)) from the competition of appropriate reaction steps, e.g.,

$$P_{baa} = \frac{k_{baa}[BA\cdot][A]}{k_{baa}[BA\cdot][A] + k_{bab}[BA\cdot][B]}$$

$$= r_1'x \,/\, (r_1'x + 1) \qquad (4.1.12a)$$

$$P_{aaa} = r_1x \,/\, (r_1x + 1) \qquad (4.1.12b)$$

$$P_{abb} = (r_2'/x) \,/\, (r_2'/x + 1) \qquad (4.1.12c)$$

$$P_{bba} = 1 \,/\, (r_2/x + 1) \qquad (4.1.12d)$$

When these probabilities are substituted into equation (4.1.11), equation (4.1.3) for the penultimate unit effect is obtained. From equations (1.3.46) and (4.1.11) it can be deduced that

$$P_{ab} = \frac{P_{aab}}{P_{aab} + P_{baa}}$$

$$P_{ba} = \frac{P_{bba}}{P_{bba} + P_{abb}} \qquad (4.1.13)$$

$$P_{aa} = \frac{P_{baa}}{P_{aab} + P_{baa}}$$

$$P_{bb} = \frac{P_{abb}}{P_{bba} + P_{abb}}$$

which is called the 'Progression of Probabilities'; and likewise it is possible to determine the higher probabilities

$$P_{baa} = \frac{P_{bbaa}}{P_{bbaa} + P_{abab}} \qquad (4.1.14)$$

etc.

It is apparent from the equations of both models that the follo-

wing set of relationships between them exists

$$r_1 = r_1' \ (r_1 x + 1) \ / \ (r_1' x + 1) \qquad (4.1.15a)$$

$$r_2 = r_2' \ (r_2/x + 1) \ / \ (r_2'/x + 1) \qquad (4.1.15b)$$

The equation for the model which takes account of the influence of the penultimate unit is derived by the use of equations (4.1.6) and (4.1.14) which yield

$$N_n = \frac{P_{bbaa}}{P_{bbaa} + P_{abab}} \left(\frac{P_{baaa}}{P_{baaa} + P_{aaab}} \right)^{n-2} \left(1 - \frac{P_{baaa}}{P_{baaa} + P_{aaab}} \right) \qquad (4.1.16)$$

$$N_1 = \frac{P_{abab}}{P_{bbaa} + P_{abab}}$$

for 'a' sequences and a similar relationship for 'b' sequences. Finally the equation is obtained as

$$n = \cfrac{1 + r_1' x \left(\dfrac{1 + r_1 x}{1 + r_1' x} \right)}{1 + \cfrac{\dfrac{1}{r_1'' x} \left[1 + \dfrac{r_2''}{x} \left(\dfrac{1 + r_1'' x}{1 + r_1''' x} \right) \right]}{1 + \cfrac{\dfrac{r_2''}{x} \left(\dfrac{r_2''' + x}{r_2'' + x} \right) \left[\dfrac{x}{r_2''} + \dfrac{r_1'''}{r_1''} \left(\dfrac{1 + r_1'' x}{1 + r_1''' x} \right) \right]}{1 + \cfrac{\dfrac{r_2'}{x} \left(\dfrac{r_2 + x}{r_2' + x} \right)}{1 + \cfrac{\dfrac{1}{r_1'' x} \left(\dfrac{1 + r_1'' x}{1 + r_1''' x} \right) \left[r_1''' x + \dfrac{r_2''' + x}{r_2'' + x} \right]}{\dfrac{1}{x} \left[r_2''' + \dfrac{r_2''}{r_1'' x} \left(\dfrac{r_2''' + x}{r_2'' + x} \right) \right]}}}} \qquad (4.1.17)$$

Using this equation Ham[80,99] showed that certain systems follow the equation much more closely than the penultimate unit effect equation, provided some simplifications are made. The system styrene-fumaronitrile

follows

$$n - 1 = \frac{\left[r_1''x\ (r_1'x + 1)\ /\ (r_1''x + 1)\right](r_1x + 1)}{\left[r_1''x\ (r_1'x + 1)\ /\ (r_1''x + 1)\right] + 1} \quad (4.1.18)$$

with $r_1 = 0.8$, $r_1' = 0.3$ and $r_1'' = 4.0$. The system α-methyl styrene -acrylonitrile follows

$$n = \frac{1 + \left[r_1''x\ (2r_1'x + 1)\ /\ (r_1''x + 1)(r_1'x + 1)\right]}{1 + (r_2/x)} \quad (4.1.19)$$

with $r_1 = 0$, $r_1' = 0.04$, $r_1'' = 0.13$ and $r_2 = 0.06$, and the system α-methyl styrene-fumaronitrile obeys

$$n - 1 = \frac{\left[r_1'''x\ (r_1''x + 1)\ /\ (r_1'''x + 1)\right]\left(\frac{r_1'x\ (r_1x + 1)}{r_1' + 1} + 1\right)}{\left[r_1'''x\ (r_1''x + 1)\ /\ (r_1'''x + 1)\right] + 1} \quad (4.1.20)$$

The same set of equations, i.e., composition equations which take into account the influence of the terminal unit, plus some finite number of units further back in the chain, was obtained by Price[100] with the use of transition probabilities of Markoffian statistics; and then by Yamashita et al.[101] by treating the problem with the statistical propositions made by Coleman and Fox[96a]. Both means of derivations yield not only the composition of the copolymer but also its microstrocture. Coleman and Fox in their derivation of the equations for the diastereosequences of a polymer chain proposed the following probability relationships.

The two general definitions to be used in the relationships are (for the sake of adaptation it is more convenient to use Yamashita and coworkers' nomenclature):

(i) $P_n\{X_1X_2\cdots X_n\}$ which is the probability of finding a particular copolymer sequence (a diastereosequence in case of a stereo homopolymer) of type $X_1X_2\cdots X_n$ among all sequences with length n, where X_i can either be monomer A or monomer B.

(ii) $P_{X_1\ X_2\ \cdots\ X_n\ X_{n+1}}$ which is the conditional probability

of a particular monomer X_{n+1} adding to a given chain of a particular sequence $X_1X_2\cdots X_n$

Using these definitions one can intuitively say that,

$$P_1\{A\} + P_1\{B\} = 1 \qquad (4.1.21)$$

or

$$P_2\{AB\} + P_2\{AA\} = P_1\{A\} \qquad (4.1.22a)$$

$$P_2\{BA\} + P_2\{BB\} = P_1\{B\} \qquad (4.1.22b)$$

combining these equations

$$P_2\{AA\} + P_2\{AB\} + P_2\{BA\} + P_2\{BB\} = 1 \qquad (4.1.23)$$

In general

$$P_{n+1}\{X_1X_2\cdots X_nA\} + P_{n+1}\{X_1X_2\cdots X_nB\}$$
$$= P_n\{X_1X_2\cdots X_n\}$$
$$= P_{n+1}\{AX_1X_2\cdots X_n\} + P_{n+1}\{BX_1X_2\cdots X_n\} \qquad (4.1.24)$$

or more generally

$$P_{r|q}\{X_{q+1}X_{q+2}\cdots X_n|X_1X_2\cdots X_q\}*P_q\{X_1X_2\cdots X_q\}$$
$$= P_n\{X_1X_2\cdots X_n\} \qquad q + r = n \qquad (4.1.25)$$

which means the probability of finding a particular sequence $X_1X_2\cdots X_n$ is the conditional probability of finding a sequence $X_{q+1}X_{q+2}\cdots X_n$ given a presequence $X_1X_2\cdots X_q$ times the probability of finding the sequence $X_1X_2\cdots X_q$. The magnitude of q defines the kind of distribution of probability. If q=N, where N is a finite number, the probability distribution is Markoffian and

$$P_{n|N}\{X_{f+N+1}X_{f+N+2}\cdots X_{f+N+n}|X_fX_{f+1}\cdots X_{f+N}\}$$
$$= P_{n|N+m}\{X_{f+N+1}X_{f+N+2}\cdots X_{f+N+n}|X_{f-m}X_{f-m+1}\cdots X_fX_{f+1}\cdots X_{f+N}\}$$
$$f > m \qquad (4.1.26)$$

If N=1 the probability is simple Markoffian and in copolymerization terms it means the only influence on the next addition comes from terminal unit. If N=0 then the probability distribution is Bernouillian and

$$P_{n|m}\{X_{m+1}X_{m+2}\cdots X_{m+n}\ X_1X_2\cdots X_m\}$$
$$= P_n\{X_{m+1}X_{m+2}\cdots X_{m+n}\} \qquad (4.1.27)$$

It is also assumed that

$$P_{n+1}\{A^nB\} = P_{n+1}\{BA^n\} \tag{4.1.28}$$

and for n=1

$$P_1\{AB\} = P_1\{BA\} \tag{4.1.29}$$

(by equation (4.1.22a) and also $P_2\{BA\} + P_2\{AA\} = P_1\{A\}$. See also ref.(102))

Equation (4.1.25) can be put into the form of definition (ii) to be more like the nomenclature used for the composition equation (i.e., P_{xx} instead of $P_{1|1}\{X|X\}$).

$$P_{x_1x_2\cdots x_qx_{q+1}\cdots x_n} * P_q\{X_1X_2\cdots X_q\} = P_n\{X_1X_2\cdots X_qX_{q+1}\cdots X_n\} \tag{4.1.30}$$

and only single additions are considered

$$P_{n+1}\{X_1X_2\cdots X_nX_{n+1}\} = P_n\{X_1X_2\cdots X_n\}P_{x_1x_2\cdots x_nx_{n+1}}$$

$$P_{x_1x_2\cdots x_nx_{n+1}} = P_{n+1}\{X_1X_2\cdots X_nX_{n+1}\}/P_n\{X_1X_2\cdots X_n\}$$

$$P_{ab} = P_2\{AB\}/P_1\{A\} \tag{4.1.31}$$

Equation (4.1.30) can be put in a more general form

$$P_3\{AAB\} = P_2\{AA\}P_{ab} = P_1\{A\}P_{aa}P_{ab} \tag{4.1.32}$$

Equations (4.1.29) and (4.1.31) yield

$$P_1\{A\}P_{ab} = P_1\{B\}P_{ba} \tag{4.1.33}$$

and hence

$$\frac{P_1\{A\}}{P_1\{B\}} = \frac{P_{ba}}{P_{ab}} \tag{4.1.34}$$

Since

$$P_{ab} = 1 \,/\, (1 + r_A x) \tag{1.3.34}$$

$$P_{ba} = 1 \,/\, (1 + r_B/x) \tag{1.3.35}$$

the Mayo-Lewis equation can be derived. The next equation in the series can be derived from equation (4.1.34) and the progression of the probabilities of Ham; but another easy way of deriving the progression of probabilities is by mathematical manipulation of Markoffian probability

relationships. From equations (4.1.30) and (4.1.33)

$$P_1\{A\}P_{aa}P_{aab} = P_2\{BA\}P_{baa} = P_2\{AB\}P_{baa} = P_1\{A\}P_{ab}P_{baa}$$

Since $P_{aa}=1-P_{ab}$ (4.1.35)

$$(1 - P_{ab})P_{aab} = P_{ab}P_{baa} \qquad (4.1.36)$$

so

$$P_{ab} = P_{aab}/(P_{aab} + P_{baa}) \qquad (4.1.37)$$

and likewise the higher probabilities.

The first reliable treatment of copolymerization processes which took depropagation into account was made by Lowry[97]. In his treatment Lowry considered three different cases of copolymerization, as outlined below. He assumed α-methyl styrene to fit the most complex third case but recently O'Driscoll, Gasparro[103] have claimed that case ii corresponds closely to the copolymerization of this monomer. The characteristics for the three cases can be given as follows:

(i) A does not depolymerize;
B may depolymerize only if added to one or more B units.

(ii) A does not depolymerize;
B may depolymerize only if added to two or more B units.

(iii) A and B may depolymerize only if added to two or more B units.

Lowry used kinetic analysis to derive his equations, apart from case (iii) where he combined kinetic analysis and probability analysis. The first two equations are relatively easy to derive, and only the equations will be given here, omitting their derivation. The third is too complex for use by itself, and will not be given here.

With a nomenclature compatible with the rest of this thesis, rather than Lowry's paper, one can write down the two equations as

case (i)

$$n = \frac{B[1/(1 - \alpha)]}{r_A A + B} \qquad (4.1.38)$$

where

$$\alpha = ([1 + KB + (K/r_B)A] - \{[1 + KB + (K/r_B)A]^2 - 4KB\}^{1/2})/2 \qquad (4.1.39)$$

and

$$r_A = k_{aa}/k_{ab} \;,\quad r_B = k_{bb}/k_{ba} \;,\quad K = k_{bb}/k'_{bb}$$

case (ii)

$$n = \frac{\beta\gamma - 1 + \left[1/(1-\beta)\right]^2}{\left[(r_A A/B) + 1\right]\left[\beta\gamma + \left[\beta/(1-\beta)\right]\right]} \qquad (4.1.40)$$

$$\gamma = \{KB + (K/r_B)A - \alpha\}/KB \qquad (4.1.41)$$

and the rest of the parameters are the same as case (i).

Lowry shows that there is an effect of temperature and total monomer concentration on the shapes of the theoretically calculated curves and actually it seems that the difference in the shapes of the curves predicted by the various models is quite small. There is a slight difference between cases (i) and (ii) and very little, if any, between cases (ii) and (iii).

O'Driscoll and Gasparro find that equations (4.1.39) to (4.1.41) can be fitted quite well to their data for the copolymerizations of styrene with α-methyl styrene, acrylonitrile with α-methyl styrene, and styrene with methyl methacrylate. However these researchers, instead of fitting the equation for the estimation of r_A and r_B, calculated r_A by means of an equation derived from the Mayo-Lewis equation for small values of B

$$n - 1 = x / r_A \qquad (4.1.42)$$

The same treatment is not possible for r_B because of the reluctance of B to homopolymerize so an approximate value was obtained from 'molecular orbital theory'. Although K, for most of the monomers, is available from the literature, according to the same authors it is possible to obtain it from a limit equation of equations (4.1.39) to (4.1.41), for large values of B,

$$\lim_{x \to o} b = (2 - KB)/(3 - 2KB) \qquad (4.1.43)$$

Ivin and Spensley[104] also studied the application of Lowry's equation to various depropagating systems and showed that the equation for case (ii) fits the data well, and better than the equation for (i); but, like O'Driscoll and Gasparro, they did not apply the equation for case (iii) due to its compexity.

Later Wittmer[98] studied the influence of depropagation on copolymer composition. His treatment, although it does not lead to

exactly the same equation on outlook, is derived by kinetic analysis using the stationary state assumption, as is Lowry's. Wittmer's treatment was supported by his extensive experiments on the copolymerization of α-methyl styrene with methyl methacrylate (the system studied in this thesis), and α-methyl styrene with acrylonitrile, at various temperatures. From a comparison of the two treatments, although they are based on the same principle, Wittmer's derivation seems to be more explicit and to have more similarities between the various cases. It is surprising that, unlike Lowry's, Wittmer's work is hardly referred to in the English and American literature; but this may be due to the language barrier or to its similarity to Lowry's equation, after rearrangement. Wittmer treats three cases:

(i) Possible depropagation of B when attached to a radical with one or more B units at the end.

(ii) Possible depropagation of A or B when attached to a radical with one or more A or B units, respectively, at the end.

(iii) Possible depropagation of B when attached to a radical with two or more B units at the end.

In the first case the composition equation is derived as

$$n = \frac{1 + r_A \frac{A}{B}}{1 + r_B \frac{B}{A} - r_B \frac{K}{A}(1 - x_1)} \qquad (4.1.44)$$

where $(1-x_1)$ can be thought of basically as the concentration of radical chains ending with B and $(1-K(1-x_1)/B)$ as a factor to give the fraction of the depropagation reaction. $(1-x_1)$ is defined as

$$(1 - x_1) = \frac{\sum_{2}^{\infty} B\cdot_i}{\sum_{1}^{\infty} B\cdot_i} \qquad (4.1.45)$$

and given by

$$\sigma = 1 - x_1 = \frac{1}{2}\frac{r_B(B+K) + A}{r_B K} \pm \sqrt{\frac{1}{4}\left(\frac{r_B(B+K) + A}{r_B K}\right)^2 - \frac{B}{K}} \qquad (4.1.46)$$

With this and the other two relationships the only parameters needed to be estimated are the corresponding reactivity ratios and the

equilibrium constant defined as $K=k_{bbd}/k_{bbp}$. Since the equilibrium constants of the monomers can often be calculated from homopolymerization data there are left only two parameters to be estimated, no matter how complex the case is.

For the other two cases the composition equations are given as follows,

case (ii)

$$n = \frac{1 + r_A \frac{A}{B} - r_A \frac{K_A}{B} \sigma_A}{1 + r_B \frac{B}{A} - r_B \frac{K_B}{A} \sigma_B} \qquad (4.1.47)$$

with $\sigma_B=\sigma$ (of equation (4.1.46)) and $K_B=K$; and

$$\sigma_A = \frac{1}{2} \frac{r_A(A+K_A) + B}{r_A K_A} - \sqrt{\frac{1}{4}\left(\frac{r_A(A+K_A) + A}{r_A K_A}\right)^2 - \frac{A}{K_A}} \qquad (4.1.48)$$

case (iii)

$$n = \frac{1 + r_A \frac{A}{B}}{1 + r_B \frac{B}{A}\left(1 - \frac{r_B \frac{K}{A} \sigma}{1+r_B \frac{B}{A}}\right)} \qquad (4.1.49)$$

with σ as equation (4.1.46).

Recently Wittmer published a general equation which takes account of the reversibility of all four propagation reactions and can be used to derive the above equations as special cases[111]:

$$n = \frac{1 + \frac{r_A \frac{A}{B} - r_A \frac{K_A}{B}(1-x_1)}{1 - q_A \frac{y_1}{B} \frac{B + q_B x_1}{A + q_A y_1}}}{1 + \frac{r_B \frac{B}{A} - r_B \frac{K_B}{A}(1-y_1)}{1 - q_B \frac{x_1}{A} \frac{A + q_A y_1}{B + q_B x_1}}} \qquad (4.1.50)$$

where $K_A=k_{aad}/k_{aap}$, $K_B=k_{bbd}/k_{bbp}$, $q_A=k_{abd}/k_{bap}$, and $q_B=k_{bad}/k_{abp}$; also

$$y_1 = \frac{A}{q_A x_1} \frac{(B + r_A x_1 B)(1 - x_1) - r_A x_1 A}{(q_B - r_A K_A)(1 - x_1) + r_A A} \qquad (4.1.51a)$$

$$x_1 = \frac{B}{q_B y_1} \frac{(A + r_B y_1 A)(1 - y_1) - r_B y_1 B}{(q_A - r_B K_B)(1 - y_1) + r_B B} \qquad (4.1.51b)$$

In all of the above cases $q_A = q_B = 0$.

Wittmer suggests that since the reactivity ratios can be given in Arrhenius form

$$r_A = \frac{A_{aa}}{A_{ab}} \exp\left(-\frac{E_{aa} - E_{ab}}{RT}\right) \qquad (4.1.52)$$

their logarithms should be inversely proportional to temperature. But when ln $r_{\alpha MS}$ of the α-methyl styrene-methyl methacrylate system, obtained from the classical Mayo-Lewis equation, is plotted against 1/T the result is certainly not a sraight line. On the other hand similar plots obtained for α-methyl styrene-methyl methacrylate and α-methyl styrene-acrylonitrile systems with r values derived from equation (4.1.44) show good linearity. The application of equation (4.1.49) to the αMS-MMA system, however, again shows marked linearity in the ln r vs. 1/T relation. This is difficult to explain since although α-methyl styrene copolymerization systems can be approximated by -BB• depolymerizations the more sensible mechanism must be -BBB• depolymerizations probably with a much slower -BB• depolymerization. This can be shown by the substantial amount of dimer formation above the ceiling temperature. But this cannot be a positive proof since the dimer formation is still vague and other theories like transfer reactions and allyl formation exist.

Some special cases have been treated by other researchers in various ways. Hazell and Ivin[105] considered the depropagation of B regardless of the nature of the penultimate unit in the radical. This is not the case for 1,1-disubstituted ethylenes where the depropagation arises because of steric hindrance, but may be the case for copolymerization systems like cyclopentane-isobutane-SO_2 where the depropagation reaction is mainly due to a low heat of reaction which

is not caused by steric hindrance. Hazell and Ivin suggest that the system at low temperatures behaves ideally, i.e.,

$$n = r\frac{B}{A} \qquad (4.1.53)$$

but when the temperature is raised r deviates from a true reactivity ratio, following the relation

$$r_c = \frac{1 + r_o x - r_o x \alpha_c}{1/r_o + x + \gamma r_o x^2 (1 - \alpha_c)} \qquad (4.1.54)$$

r_c being the apparent, and r_o the true reactivity ratios, and also

$$\alpha_c^2 - (2 + 1/r_o x)\alpha_c + 1 = 0 \qquad (4.1.55)$$

$$\gamma = \frac{k_{abd}}{k_{bbd}}$$

when γ=0 the relation corresponds to case (i) of Lowry.

More recently Yamashita and coworkers[106] derived an equation for Hazell and Ivin's case by the Lowry method of treatment and obtained

$$n = (1 - \alpha)\{1 + r_A \frac{A}{B} + (1 - \alpha)\frac{\delta r_B}{\rho B}\} \qquad (4.1.56)$$

where

$$\alpha = \frac{1}{2}\{(\phi B + (\frac{\phi}{r_B})A + 1) - \left[(\phi B + (\frac{\phi}{r_B})A + 1)^2 - 4\phi B\right]^{1/2}\} \qquad (4.1.57)$$

$$\phi = \frac{k_{bbp}}{k_{bbd}}, \quad \rho = \frac{k_{abp}}{k_{abd}}, \quad \delta = \frac{k_{aa}}{k_{bb}}$$

They also investigated the case where the terminal unit depropagates if the penultimate unit is B. By the same method they obtained

$$n = (1 - \alpha)(1 + r_A \frac{A}{B}) \qquad (4.1.58)$$

where

$$\alpha = \frac{1}{2}\{(1 - (\frac{\phi}{r_B})\sigma\beta + (\frac{\phi}{r_B})A + \phi B) - \left[(1 - (\frac{\phi}{r_B})\sigma\beta + (\frac{\phi}{r_B})A + \phi B)^2 - 4\phi B\right]^{1/2}\} \qquad (4.1.59)$$

$$\beta = \frac{r_A A}{r_A + r_A r_B \delta A + r_B \delta B}, \quad \sigma = \frac{k_{bad}}{k_{bap}} \qquad (4.1.60)$$

It is obvious that equations (4.1.56) and (4.1.58) can readily be obtained from Wittmer's general equation (eq.(4.1.50)).

The most recent development in the problem of copolymer composition prediction, by O'Driscoll et al.[107], leads to an equation which is claimed to be 'the most general copolymer equation which has ever been derived'. Two equations were derived, namely, for terminal and penultimate unit models, which contain, without simplifying assumptions, eight and sixteen rate constants respectively. They showed that any equation derived so far concerning penultimate units can be obtained from these equations by appropriate simplifications. Peculiarly, O'Driscoll et al. seem not to have attempted to use these equations to estimate the rate constants by fitting them to experimental data. Instead, in a later paper[81], describing their equation for the copolymerization system α-methyl styrene-methyl methacrylate, they use the literature values of reactivity ratios and adjust them for temperature according to the Arrhenius equation.

In their derivation they use the probability considerations of Bayes (similar to Coleman and Fox's) but incorporate them in a structure similar to kinetic analysis; and without making simplifying assumptions they define transient conditional probabilities as probabilities for radical end groups. The transient probabilities of finding A and B as end group are a and b respectively and

$$a = 1 - b \tag{4.1.61}$$

For diad groups

$$P(A_{n+1}|A_n)_t = \varepsilon = P_{aa}$$

$$P(B_{n+1}|A_n)_t = 1-\varepsilon = P_{ab}$$

$$P(B_{n+1}|B_n)_t = \eta$$

$$P(A_{n+1}|B_n)_t = 1-\eta$$

Then similarly to

$$-\frac{dA}{dt} = [A\cdot]k_1[A] + [B\cdot]k_5[A] - [BA\cdot]k_6 - [AA\cdot]k_2 \tag{4.1.63}$$

$$\frac{P(A_n)}{\tau} = ak_1A + bk_5A - a(1-\varepsilon)k_6 - a\varepsilon k_2 \tag{4.1.64}$$

where τ is the time constant and A and B are the feed concentrations.

Similarly

$$\frac{P(B_n)}{\tau} = bk_7B + ak_3B - b(1-\eta)k_4 + b\eta k_8 \qquad (4.1.65)$$

(A) and (B) are the net addition of corresponding unit to the chain. For diad addition

$$\begin{aligned}
\frac{P(A_nA_{n+1})}{\tau} &= ak_1A - a\varepsilon k_2 \\
\frac{P(A_nB_{n+1})}{\tau} &= ak_3B - b(1-\eta)k_4 \\
\frac{P(B_nA_{n+1})}{\tau} &= bk_5A - a(1-\varepsilon)k_6 \\
\frac{P(B_nB_{n+1})}{\tau} &= bk_7B - b\eta k_8
\end{aligned} \qquad (4.1.66)$$

For triads

$$\frac{P(A_nA_{n+1}A_{n+2})}{\tau} = a\varepsilon k_1A - a\varepsilon^2 k_2 \qquad (4.1.67)$$

and so on. With the use of equation (4.1.24) and these equations the various transient probabilities can be solved in terms of various rate constants and feed concentrations. With the assumption that the transient probabilities are equal to the nontransient probabilities (which needs to be proved) i.e., the probability of finding a radical end group (singlet, diad, triad, etc.) is equal to the probability of finding the same group anywhere in the chain, it is possible to use the above-defined transient probabilities in the derivation of the composition equation. Since

$$\begin{aligned}
P(A_n)P(A_{n+1}|A_n)_t &= P(A_nA_{n+1}) \\
P(B_n)P(B_{n+1}|B_n)_t &= P(B_nB_{n+1})
\end{aligned} \qquad (4.1.68)$$

Therefore

$$\frac{P(A_n)}{P(B_n)} = \frac{P(A_nA_{n+1})_t/P(A_{n+1}\ A_n)}{P(B_nB_{n+1})_t/P(B_{n+1}\ B_n)} \qquad (4.1.69)$$

$$= \frac{a\eta(k_1A - \varepsilon k_2)}{b\varepsilon(k_7B - \eta k_8)} \qquad (4.1.70)$$

This, plus the relationships of a, b etc. in terms of rate constants and feed concentrations, define the composition equation for a termi-

nal unit model.

For a penultimate unit model four more transient probabilities are defined.

$$\begin{aligned} P(A_n|A_{n-1}A_{n-2}) &= \mu \\ P(B_n|B_{n-1}B_{n-2}) &= \nu \\ P(A_n|A_{n-1}B_{n-2}) &= \psi \\ P(B_n|B_{n-1}A_{n-2}) &= \phi \end{aligned} \qquad (4.1.71)$$

The composition equation (given here after the correction of an error in the original presentation) is derived as

$$\frac{(A)}{(B)} = \frac{a\varepsilon\nu\phi(k_1A-\mu k_2)+\mu\nu(b\eta k_{13}A-a(1-\varepsilon)\phi k_{14})}{b\eta\mu\phi(k_{15}B-\nu k_{16})+\mu\nu(b\eta k_{13}A-a(1-\varepsilon)\phi k_{14})} \qquad (4.1.72)$$

and used with the relationships of corresponding probabilities.

O'Driscoll et al. have applied the diad equation to the system αMS-MMA and their results are given in section (6.1) with comment in section (6.3.3).

Probably the ultimate in the prediction of copolymer composition is computer simulation of copolymerization reactions[109,110]. The method is to add or subtract units to or from a growing binary sequence which constitutes the copolymer chain. The transition can be to any degree of Markoffian distribution desired, bearing in mind the increasing size of the program. Any desired assumption and simplification in relation to the rate constants can be incorporated as well.

One point not attempted so far is to use computer simulation for the estimation of the rate constants. This point will be discussed in section (6.5). Also the applicability of various equations mentioned in this section is considered in the last chapter.

4.2 Copolymer Microstructure

The first attempts to study the microstructure of polymers were made to obtain information on the stereoregularities of various α-substituted polyolefins. Early studies on the theory of diastereosequences

were conducted by Coleman and Fox[96] and Bovey[114]. The analysis of diastereosequences by NMR was mainly done by Bovey who later carried this work into the study of copolymerizing systems. Coleman and Fox used Bayesian statistics to study a general chain, which might have propagated according to a Markoffian or non-Markoffian probability, or even, with appropriate assumptions, according to a Bernoullian probability. They considered each addition unit not as a monomer but as an attachment bond. Therefore, if a monomer is attached to a growing radical in the same stereo configuration as the radical end unit this is considered as an isotactic attachment and defined as an I unit. An opposite stereo configuration is a syndiotactic attachment and defined as an S unit. Each of these units were called placements and a couple of them at a time were called pairs. Three kinds of pairs are defined P_i={II} isotactic pairs, P_s={SS} syndiotactic pairs and P_h={ISvSI} (meaning either IS or SI) heterotactic pairs. The placement and pair configurations in terms of molecular structure are shown below for MMA polymer (all additions with a very good approximation are assumed to be head to tail)

{I}

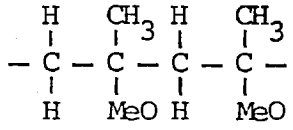

{S}

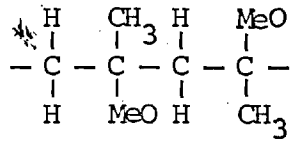

{II}

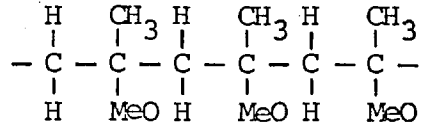

{SS}

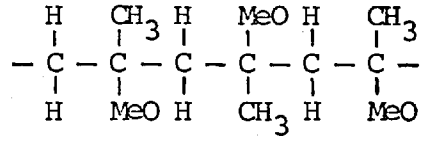

{IS}

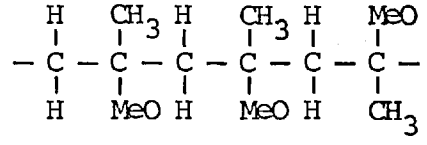

Using Bayesian statistics Coleman and Fox derived the equations given in section (4.1). These equations are presented in the previous section using a copolymer nomenclature in which A replaces I and B replaces S, since copolymerization is also a binary addition process and the same equations may be applied. The only difference is that here for every unit two monomers are involved, whereas in copolymerization every unit stands for one comonomer. This means that, since from NMR (see section (4.3)) information can be gathered only as far as triad concentrations, for stereohomopolymerization one may obtain independent information on doublets, say {II}, and for copolymerization independent information on triplets, say {AAA}. On the other hand if it is necessary to involve stereoregularity in copolymerization that would mean not a binary but a ternary sequence, or otherwise would necessitate the use of the σ propagation of Bovey, as will be seen later in the section. In addition to the equations given in the previous section it will prove useful to state some more general equations given by Coleman and Fox, and proved valid by Kac[112].

The distribution of closed sequences can be given by

$$f_n = P_{n+1}\{SI^{n-1}S\}/P_1\{S\} = P_{n|1}\{SI^{n-1}|S\} \qquad (4.2.1)$$

and by theorem

$$\sum_{n=1} f_n = 1 \qquad (4.2.2)$$

Then the mean recurrence time for S can be defined as

$$\chi\{S\} = \sum_{n=1} nf_n \qquad (4.2.3)$$

which yields

$$\chi\{S\} = \frac{1-q}{P_1\{S\}} \qquad (4.2.4)$$

where $q = \lim_{n \to \infty} P_n\{I^n\}$ and in the case of polymerization reactions it can be taken as being equal to zero, therefore

$$\chi\{S\} = \frac{1}{P_1\{S\}} \qquad (4.2.5)$$

The mean length of closed sequences of the unit I can be defined as

$$\mu\{I\} = \frac{\sum_{n=1} nf_{n+1}}{1-f_1} \qquad (4.2.6)$$

where when $f_1=1$ there are no closed sequences of I. In terms of units

$$\mu\{I\} = \frac{P_1\{I\} - q}{P_1\{S\} - P_2\{SS\}} = \frac{P_1\{I\}}{P_1\{S\} - P_2\{S^2\}} \qquad (4.2.7)$$

Another definition is the persistence ratio which is the ratio of the mean length of closed sequences of certain kinds of units to the mean length of the same kind of unit, which would exist if the distribution had been Bernoullian (q=0 does not apply to Bernoullian distribution). Thus,

$$\rho = \mu\{I\}P_1\{S\} = \mu\{S\}P_1\{I\} \qquad (4.2.8)$$

$\rho-1$ is a measure of departure from Bernoullian statistics or in other words the depth of Markoffian statistics, because in Bernoullian statistics $\mu\{I\}=P_1\{S\}^{-1}$.

The above definitions can be put into various forms by the use of the general equations in the previous section, such as

$$\mu\{I\} = \frac{P_1\{I\}}{P_2\{IS\}} = \frac{2P_1\{I\}}{P_2\{ISvSI\}} \qquad (4.2.9)$$

One equality derived from this new form is

$$\mu\{I\}P_1\{S\} = \frac{P_1\{I\}}{P_2\{IS\}} P_1\{S\} = \frac{P_1\{S\}}{P_2\{SI\}} P_1\{I\} = \mu\{S\}P_1\{I\} \qquad (4.2.10)$$

which gives

$$\frac{\mu\{I\}}{\mu\{S\}} = \frac{P_1\{I\}}{P_1\{S\}} \qquad (4.2.11)$$

Other equations in terms of measurable parameters and, from the equalities of previous section, would be

$$P_2\{ISvSI\} = 2(P_1\{I\} - P_2\{I^2\}) \qquad (4.2.12)$$

$$P_1\{I\} = 1/2\left[1 + P_2\{I^2\} - P_2\{S^2\}\right] \qquad (4.2.13)$$

and so on.

In the case of copolymerization the letters I and S are replaced by A and B and the above equations define the structure of the copolymer. So, by allocating the degrees of freedom in stereoconfiguration to the monomer variation one can get some primary information on the copolymer chain (ignoring any stereoregularity). Therefore,

it is possible to use the following definitions,

$$F_x = \text{mole fraction of } X = P_1\{X\} \quad (X = A \text{ or } B) \tag{4.2.14}$$

$$l_a = \text{no. average length of A sequences} = \mu\{A\} = P_1\{A\}/P_2\{ABvBA\} \tag{4.2.15}$$

$$l_b = \text{no. average length of B sequences} = \mu\{B\} = P_1\{B\}/P_2\{ABvBA\} \tag{4.2.16}$$

$$R = \text{run no., i.e., fraction of all A-B (and B-A) bonds} = 2P_2\{AB\} \tag{4.2.17}$$

In a similar way the persistence ratio is

$$\rho = \mu\{A\}P_1\{B\} = \frac{P_1\{A\}P_1\{B\}}{P_2\{AB\}} \tag{4.2.18}$$

$\eta=1/\rho$ gives a measure of the departure from random (Bernoullian) statistics and

$$R_{random} = 2P_1\{A\}P_1\{B\} \tag{4.2.19}$$

$$F_A = \text{copolymer composition} = P_1\{A\} = 1 - P_1\{B\} \tag{4.2.20}$$

$$F_{AA} = \text{bond or diad fraction} = P_2\{AA\} \tag{4.2.21}$$

These parameters are in terms of experimentally (NMR) obtainable values. To compare the particular copolymerization system with the model assumed it is necessary to define these parameters in terms of the rate constants. To achieve that it is possible to use an approach similar to the statistical derivation of the copolymer composition equation. For this, the above parameters must first be defined in terms of conditional probabilities. Thus[101]

$$R = 2P_1\{A\}P_{ab} = 2P_{ab}P_{ba}/(P_{ab} + P_{ba}) = 2/\ (1/P_{ba}+(1/P_{ab}) \tag{4.2.22}$$

$$\eta = P_2\{AB\}/P_1\{A\}P_1\{B\} = P_{ab}/P_1\{B\} = P_{ab} + P_{ba} \tag{4.2.23}$$

$$l_A = P_1\{A\}/P_2\{AB\} = 1/P_{ab} \tag{4.2.24}$$

$$F_A = P_1\{A\} = P_{ba}/(P_{ab} + P_{ba}) \tag{4.2.25}$$

$$F_{AA} = P_2\{AA\} = P_{ba}(1 - P_{ab})/(P_{ab} + P_{ba}) \tag{4.2.26}$$

The parameters can be calculated by substituting the particular values of the conditional probabilities in terms of the rate constants and feed compositions for particular models. Although for the terminal

unit model P_{ab} (or P_{ba}) can be given in terms of rate constants and feed compositions, for the penultimate unit model it is necessary first to define P_{ab} (or P_{ba}) in terms of progressed probabilities.

Since the copolymerization process involves monomers rather than bonds as statistical units it is possible to get information for triple units of triads. The triad concentration in the chain is given (ignoring the stereoconfiguration) by $P_3\{XXX\}$. Then from general equations,

$$P_3\{AAA\} + P_3\{BAA\} + P_3\{AAB\} + P_3\{BAB\} = P_1\{A\} \qquad (4.2.27)$$

and similarly for monomer B. Then for convenience in using NMR data, triad fractions are given by

$$F_{AAA} = P_3\{AAA\}/P_1\{A\} \qquad (4.2.28a)$$

$$F_{BAB} = P_3\{BAB\}/P_1\{A\} \qquad (4.2.28b)$$

$$F_{BAA} = F_{AAB} = P_3\{AAB\}/P_1\{A\} \qquad (4.2.28c)$$

$$F_{AAA} + F_{BAB} + F_{BAA} + F_{AAB} = 1 \qquad (4.2.29)$$

For comparison with models in terms of conditional probabilities

$$F_{AAA} = P_{aa}P_{aaa} = (1 - P_{ab})(1 - P_{aab}) \qquad (4.2.30a)$$

$$F_{BAB} = P_1\{B\}P_{ba}P_{bab}/P_1\{A\} = P_{ab}(1 - P_{baa}) \qquad (4.2.30b)$$

$$F_{AAB} = P_{aa}P_{aab} = (1 - P_{ab})P_{aab} \qquad (4.2.30c)$$

To study the copolymer microstructure in terms of stereoconfiguration as well as monomer unit sequences one needs to employ the σ propagation suggested by Bovey and Tiers[113]. In stereoconfigurational homopolymerization σ is the probability of the growing radical adding a monomer unit in the stereoconfiguration, or the 'isotacticity factor'. The problem here is that it is assumed that this addition is only affected by the terminal unit. If the penultimate unit is to be taken into consideration it is necessary to allocate two σ values. In simple Markoffian (terminal unit model) stereoconfigurational copolymerization one needs four σ factors for the four types of bonds formed during copolymerization.

If stereoregularity is included there are sixteen possible triad formations in four original groups, thus, d and l denoting right and left configurations,

$$AAA \longrightarrow A_dA_dA_d \ , \ A_dA_dA_1 \ , \ A_1A_1A_d \ , \ A_1A_dA_1$$

and similarly for the other triads. Then defining σ_{xx} the isotactic emchainment between two particular monomers for AAA triad.

$$F_{A_dA_dA_d} = \sigma_{aa}^2 \ (1 - P_{ab})^2 \qquad (4.2.31a)$$

$$F_{A_dA_dA_1} = F_{A_1A_dA_d} = 2\sigma_{aa} \ (1 - \sigma_{aa})(1 - P_{ab})^2 \qquad (4.2.31b)$$

$$F_{A_1A_dA_1} = (1 - \sigma_{aa})^2(1 - P_{ab})^2 \qquad (4.2.31c)$$

$$F_{AAA} = F_{A_dA_dA_d} + F_{A_1A_dA_d} \ (\text{or } F_{A_dA_dA_1}) + F_{A_1A_dA_1} \qquad (4.2.32)$$

Similarly for BAA or AAB triads

$$F_{B_dA_dA_d} = F_{A_dA_dB_d} = 2\sigma_{aa} \ (\sigma_{ba} + \sigma_{ab}) \ P_{ab} \ (1 - P_{ab}) \qquad (4.2.33)$$

etc.

and also for BAB triads.

These equations apply only to simple Markoffian copolymerization. The complexity of considering a more general case can be imagined. But if σ's are obtained experimentally then they become static parameters and it suffices to alter only the conditional probabilities to fit the particular model.

4.3 Copolymer Microstructure by High Resolution NMR

The NMR spectra of monomeric α-methyl styrene and methyl methacrylate are given in figures (24a) and (24b). α-methyl styrene exhibits three groups of peaks namely, for the resonance of phenyl protons at 2.8 τ, α-methyl protons at 8.0 τ and methyne protons at 4.7 and 5.05 τ. The corresponding peaks are further split into their multiplets which does happen in the polymeric state. Methyl methacrylate, too, exhibits three groups of peaks, namely for the resonance of methoxy protons at 6.3 τ, α-methyl protons at 8.1 τ and methyne protons at 3.95 and 4.45 τ, again split into multiplets. The difference between the two monomers is the existence of the phenyl protons in αMS as opposed to the methoxy protons in MMA. This difference is used, as explained in section (3.5.1), for the determination of copolymer

composition. Although the methoxy peak in poly methyl methacrylate presents itself as one single peak when in a copolymer with α-methyl styrene it is shifted up-field (higher H_o) due to the shielding effect of benzene ring as explained in section (3.5.1). The most pronounced effect of shielding comes from the nearest benzene groups to the particular methoxy group. Since the nearest benzene groups to the methoxy group would be on the two neighbouring positions and since any two neighbouring placements can take few configurations due to the comonomer and stereoconfigurational freedoms the shifting will be variable. In fact, depending on the amount of each placement the methoxy peak will experience a split. The benzene rings placed further away than the neighbouring positions have practically no effect or at least no splitting effect. They do have some effect in the sense that the total group of methoxy groups shift up-field as the amount of α-methyl styrene is increased in the polymer. This effect is shown by Bovey[114] and in this research (see section (6.7)). To understand the splitting effect of neighbouring benzene rings it is important to examine the possible configuration and composition of methoxy centered triads can take. The sixteen possible configurations, where M and S denote methoxy and phenyl groups in positions given as below and above a horizontal line to show tacticity, are[114,115]

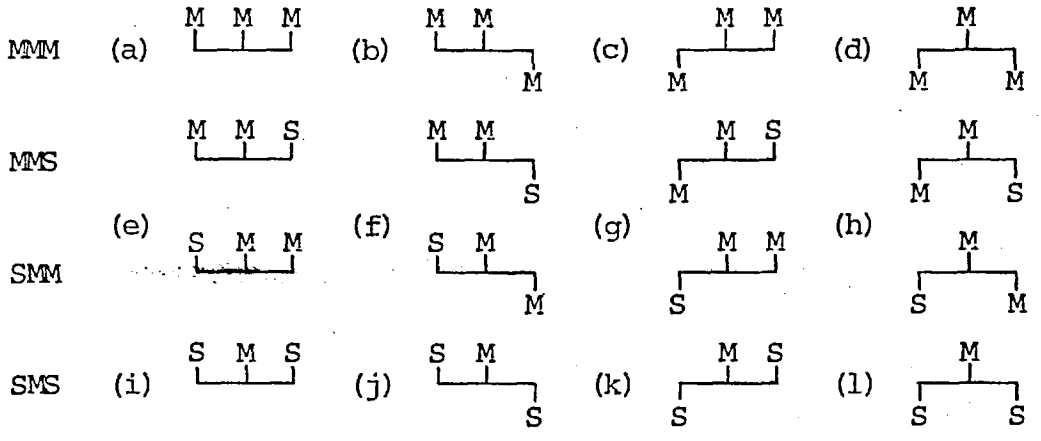

It should be obvious that the most pronounced shifting effect coming from a single neighbouring αMS will be from the one placed isotactically next to the centre MMA unit. This placement is called[114] coisotactic placement and in the structural model is shown as

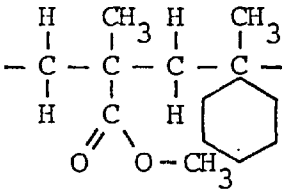

A less pronounced effect will come from a cosyndiotactic placement, i.e.,

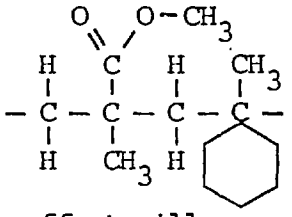

Of course, no shifting effect will come from any MMA group placed in any configuration in the neighbouring position. If one can safely assume that the shifting effect of coisotactic placement is much more pronounced than syndiotactic placement one finds that the determining factor of shifting is the amount of coisotactic placement. There are three possible quanta of coisotactic placements (around one M unit), namely zero, one and two, and the general practice is to find three main splits in the methoxy proton resonance peaks of methyl methacrylate and 'styrene type' copolymers[114,115,116,88]. The NMR spectra of α-methyl styrene-methyl methacrylate copolymers exhibit three peaks in the region of 6.1 τ to 7.4 τ which are attributed to the methoxy proton resonance. These peaks individually are placed at approximately 6.5, 6.9 and 7.2 τ and attributed to configurations with zero, one and two coisotactic placements respectively.

The less pronounced effect of syndiotactic placements would be to split the individual peaks even further according to their possible quanta in every group of triads. Thus first group would be split into three, second group into two and third group would not be split at all. The peak groupings can be shown as below

Methoxy resonance region		Tacticity	Position for 50:50 polymer
1st peak	1st sub-peak	MMM	3.52 δ
	2nd sub-peak	MM_S	3.44
	3rd sub-peak	S^MS	3.36

2nd peak	1st sub-peak	MMS	3.10
	2nd sub-peak	$_S^{MS}$	2.98
3rd peak		SMS	2.78

This second stage of splitting, too, can be seen in the NMR spectra of αMS-MMA copolymers.

Since it is mainly the coisotactic placement that defines the splitting it may be possible to find the amount of each nonconfigurational triad in every peak by suitably defining a coisotacticity factor, σ , and hence obtain information on the tacticity of the copolymer as well as compositional microstructure. This σ is nothing more than $\sigma_{ab} = \sigma_{ba}$ of the previous section. From the above generalizations it follows that

$$\text{peak(I)} \qquad F_x = F_{MMM} + 2(1-\sigma)F_{MMS} + (1-\sigma)^2 F_{SMS} \qquad (4.3.1a)$$

$$\text{peak(II)} \qquad F_y = 2\sigma F_{MMS} + 2(1-\sigma)F_{SMS} \qquad (4.3.1b)$$

$$\text{peak(III)} \qquad F_z = \sigma^2 F_{SMS} \qquad (4.3.1c)$$

where $(1-\sigma)$ is the cosyndiotacticity factor.

The same peak areas can be expressed in terms of conditional probabilities by substituting their conditional probability equivalents instead of their triad fractions. Then necessary simplifications can be made according to the model used to derive the conditional probabilities.

Many researchers have proved the validity of their model by showing the constancy of the coisotacticity factor over a range of feed concentrations. But it is mentioned that [94] the verification of the above peak assignment can be made, by the method given below,

Since for every peak the area is given by

$$P = mF_{SMS} + nF_{SMM} + qF_{MMM} \qquad (4.3.2)$$

and so

$$\begin{aligned} (P_x - F_{MMM})/F_{SMS} &= m + n(F_{SMM}/F_{SMS}) \\ P_y/F_{SMS} &= m' + n'(F_{SMM}/F_{SMS}) \\ P_z/F_{SMS} &= m'' + n''(F_{SMM}/F_{SMS}) \end{aligned} \qquad (4.3.3)$$

these last equations, when plotted as L.H.S. vs. F_{SMM}/F_{SMS} should give straight lines. To achieve this one must first calculate the triad

fractions from some model; and it leaves one with the question whether it is a verification for the Bovey assumptions or for the model used.

By combining this section with the previous section much information can be obtained about the microstructure and hence the mechanism of the copolymerization. Ito et al. attempted to combine equations (4.3.1) with equations (4.2.30) for the terminal unit model to obtain the relations:

$$F_x = (1 - \sigma P_{ab})^2 \qquad (4.3.4a)$$

$$F_y = 2\sigma P_{ab}(1 - \sigma P_{ab}) \qquad (4.3.4b)$$

$$F_z = (\sigma P_{ab})^2 \qquad (4.3.4c)$$

Then by the relation

$$P_{ab} = 1/(1 + r_A/x) \ , \quad x = [B]/[A] \qquad (4.3.5)$$

for the terminal model, produced the linear relation

$$1/(1 - F_x^{1/2}) = 1/\sigma + (r_A/\sigma)(1/x) \qquad (4.3.6)$$

on which the experimental points would lie if they were following the terminal unit model. This straight line then yields the parameters σ and r_A. This approach is debatable since the linearization is not a correct treatment due to the resulting nonlinearization of the experimental errors. The results of this approach will be discussed in the last chapter.

It must be noted that Yamashita et al.[69] found from their experiments that there is no appreciable drift in triad fractions due to conversion, up to a conversion of 5 or even 10%. Therefore the triad fractions obtained from NMR can quite satisfactorily be used as instantaneous triad fractions.

It is suprising that although it is sometime since the beginning of information flow on the microstructure parameters, and of the production of new relationships, no attempt seems to have been made to combine the microstructure relationships with those for composition in order to obtain a better explanation for the mechanism of the process.

V. MATHEMATICAL TREATMENT OF COPOLYMERIZATION DATA

5.1 Theory of Reactivity Ratio Determination

a) Earlier methods

After the establishment of the concept of the reactivity ratios most of the work was concentrated on the determination of reactivity ratios for many different system, rather than on developing methods for obtaining refined statistical estimates of reactivity ratios. It is suprising to find that many reactivity ratio values are presented in the literature with error limits based on no statistical theory. The early method of determining the reactivity ratios can be summed up as follows [73,121]

(i) Approximation

(ii) Curve-fitting

(iii) Mayo-Lewis line intersection

(iv) Linearization method of Fineman and Ross

(i) This is the crudest method of determining reactivity ratios and is based on the assumtion that at very low concentrations of one monomer its reactivity ratio depends on the ratio of concentrations of the other monomer in feed and copolymer, i.e.,

$$r_B = a/A \qquad (5.1.1)$$

where a and A are the mole fractions of monomer A in the feed and in the copolymer. The method has many limitations but sometimes can be useful, especially when the Q and e values of the monomer are not available.

(ii) Curve-fitting is the visual fitting of the experimental points on any one of the curves calculated from the copolymer composition equation using the discrete values of r_A and r_B. This procedure gives a rough but reasonable approximation to the reactivity ratios and its sensitivity can be increased by the method of Alfrey et al. [73]. In this method a few of the better fitting curves are selected and a value of Δ is calculated for each curve which is essentially the sum of the squares of the deviations of each point from the calculated

curve. Plots of r_A and r_B vs. Δ will give minimums at the best-fitting r_A and r_B set. Also the iso-Δ contours of Δ_{min} plotted in the r_A vs. r_B domain will give an ellipse which is a measure of the probable errors. This second method of curve-fitting, if applied by the use of many calculated curves, (and in fact one needs many curves if one wants to make an estimate of the probable errors), is very similar to a least square estimation and was suggested by Alfrey et al. without any probabilistic interpretation. The laborious calculations of this method are probably the reason for its not being used by later researchers.

(iii) The copolymer composition equation of Mayo and Lewis can be rearranged to give a linear parametric equation,

$$r_A = \frac{(X - 1)}{x} + r_B \frac{X}{x^2} \qquad (5.1.2)$$

This, in the r_A vs. r_B domain, will give a sraight line for each set of feed and copolymer composition data. Theoretically these lines must intersect at one single point provided all the experimental points fall on a curve described by the Mayo-Lewis equation. In practice the sraight lines will give $(n^2-n)/2$ intersection points whose gyration centre coordinates are the actual reactivity ratios. One important thing in this method is not to consider intersection points of pair of lines with very acute angles of intersection. These pairs of lines are of experimental points very close to each other, and may give intersection points which are very far from the gyration centre. The other difficulty is the sensitivity of extreme concentrations to analytical errors. These may move a line far from the gyration centre and seriously affect many intersection points. Error estimation in this method is very difficult, and, alhtough the gyration centre is actually a statistical mean of intersection points, the derivation of a variance and standard deviation from the scatter of these points is not in accordance with the statistical theory.

(iv) Fineman and Ross rearranged the Mayo-Lewis equation to give

$$\frac{x(1 - X)}{X} = r_B - \frac{x^2}{X} r_A \qquad (5.1.3)$$

which is linear in the $x(1-X)/X$ vs. $-x^2/X$ domain. A plot of experimental

points according to this is a straight line with slope r_A and intercept r_B. The linear least squares method can be used to obtain the best fit of this line on the experimental points. One difficulty here is that the clustering of the data in the domain may vary due to the choice of one monomer as being A or B and thus giving non-unique (double) sets of reactivity ratios. An example is that if one monomer is chosen as B and one experimental point with a high concentration in B has considerable error, the effect of this error will not be very large since the point will lie close to the ordinate. But if the same monomer is chosen as A, the same point will lie furthest away from the ordinate and will have a considerable influence on the straight line. Another difficulty of this method is that, although a statistical fit of the straight line is obtained by a linear least square procedure, the error estimate of that fit, contrary to many statements in the literature, is not the true error estimate of the reactivity ratios. When transformation of variables is done the error in the composition of the polymer loses its additive property and is statistically wrong to assume otherwise. Besides, in the Fineman-Ross equation the dependent variable becomes a stochastic variable, and since in these estimations it is assumed that the dependent variable is deterministic it is doubtful that the linear least square procedure can be used in this way.

The methods described above, apart from being unsatisfactory, can only be applied to the Mayo-Lewis equation (simple Markoffian). If the equation used, i.e., the mathematical model, is more complicated the application of these methods becomes either impossible or very laborious (curve-fitting only).

b) Estimation of reactivity ratios by non-linear least squares

Least squares estimation of the parameters of the function

$$\eta = f(X_1, X_2, \cdots, X_n; \theta_1, \theta_2, \cdots, \theta_m) \qquad (5.1.4)$$

are the values of $\underset{\sim}{\theta}$ that minimizes

$$\phi = \sum_{k-1}^{N} (y_k - f(\underset{\sim}{x}_k, \underset{\sim}{\theta}))^2 \qquad (5.1.5)$$

where y_k are the actual function values at kth experiment with no error and ϕ is the square of the residuals. The error ε is assumed to be normally distributed with an expected value of zero and a variance σ^2.

$$\eta = y + \varepsilon \tag{5.1.6}$$

The least squares estimates of $\underset{\sim}{\theta}$ can be obtained by the solution of equation

$$\underset{\sim}{X}^T \underset{\sim}{X}\, \underset{\sim}{\theta} = \underset{\sim}{X}^T \underset{\sim}{y} \tag{5.1.7}$$

and were shown to be the best unbiased estimates for the above system by Gauss. When the system is nonlinear, as is the case for copolymer composition equations, the procedure becomes complex and it is necessary to linearize the function and converge it on its best estimations by iterative procedures. For this, the function is first linearized by expanding it in a Taylor's series around the first guesses (supplied by the researcher) of the parameters, and dropping all but linear terms,

$$f(\underset{\sim}{x};\underset{\sim}{\theta}) = f(\underset{\sim}{x};\underset{\sim}{\theta}^o) + \sum_{i=1}^{m} \frac{\partial f(\underset{\sim}{x},\underset{\sim}{\theta})}{\partial \theta_i}\bigg|_{\underset{\sim}{\theta} = \underset{\sim}{\theta}^o} (\theta_i - \theta_i^o) \tag{5.1.8}$$

then for the residuals

$$y_k - f(\underset{\sim}{x}_k;\underset{\sim}{\theta}) = \sum_{i=1}^{m} \frac{\partial f(\underset{\sim}{x}_k;\underset{\sim}{\theta})}{\partial \theta_i}\bigg|_{\underset{\sim}{\theta} = \underset{\sim}{\theta}^o} (\theta_i - \theta_i^o) \tag{5.1.9}$$

which is a set of linear equations with m unknowns and can be treated likewise to obtain the best estimates of the unknowns

$$h_i = (\theta_i - \theta_i^o) \tag{5.1.10}$$

This inturn is used to improve the initial guess for θ

$$\theta_i' = \theta_i^o + h_i \tag{5.1.11}$$

and then used as θ in equation (5.1.9); when the minimum for ϕ is reached $\underset{\sim}{\theta}^r$ is taken as $\hat{\underset{\sim}{\theta}}$, the best estimate for θ.

The method of nonlinear least square estimation has found application in many problems since the development of high speed computers, and has recently been used for the estimation of copolymer reactivity ratios by Tidwell and Mortimer[121,122], and Behnken[123]. The many algorithms written for this estimation can be found in the literature[124-127].

In this research the algorithm used by the Author was one based on Marquard's[124] method and kept updated and in binary form in the NAG library[128] as Subroutine E04FBF, which is substantially the Harwell[129] subroutine VA05A. The convergence of this algorithm was found adequate but does not assure convergence. According to Box[130,122] a simple modification of this method will assure convergence. The modification is as follows: find

$$S_k = \sum (y_k - \hat{y}_k)^2 \qquad (5.1.12)$$

for

$$\theta_i = \theta_i^j + [(K - 1)/2]h_i \qquad (5.1.13)$$

where K=1,2,3 and subscript j denotes the iteration number. Let

$$V = 1/2 + (S_1 - S_3)/[4(S_1 - 2S_2 + S_3)] \qquad (5.1.14)$$

Compute S_4 for $\theta_i = \theta_i^j + Vh_i$; if $S_4 < S_1$ repeat the process using

$$\theta_i^{j+1} = \theta_i^j + Vb_i \qquad (5.1.15)$$

instead of θ_i^j otherwise reevaluate V after first halving h_i's. The method, although not used in this research, was proved succesful by Tidwell and Mortimer, and was claimed to have a faster convergence.

One thing of importance in nonlinear regression is to define the variables so that the error will remain additive, as in the form of equation (5.1.6), with zero expected value and σ^2 variance. If this is not ensured the error may become a function of the dependent variable and be aggrandized, depending on the analytical procedure for composition determination. This was actually observed by Behnken and the Author. For example (by the Author) if the dependent variable is taken as (e.g., see equation (1.3.15))

$$X = a/b$$

for large values of a the error will be incorporated as

$$X = \frac{a \pm \varepsilon}{b \pm \varepsilon} = \begin{cases} \dfrac{a + \varepsilon}{b - \varepsilon} \\ \dfrac{a - \varepsilon}{b + \varepsilon} \end{cases} \qquad (5.1.16)$$

Eventually the error becomes $\varepsilon/(b \pm \varepsilon) \simeq \varepsilon/b$ which depends on b, and

for small values of b it becomes substantial. The dependent variable must also be taken as the actual analytically measured value plus its error (Behneken). For an experiment where the measured variable is the weight fraction of one monomer

$$a = \alpha + \varepsilon$$

the molar ratio X is

$$X = \frac{a/M_a}{(1-a)/M_b} \qquad (5.1.17)$$

where M_a and M_b are the corresponding molecular weights. This yields a variance for the independent variable of

$$V(X_k) = (1 + \frac{M_b}{M_a}\xi)^4\sigma^2 \qquad (5.1.18)$$

where ξ is the actual value of X. As it can be seen the error variance is not constant. Instead the proper way of defining equation (1.3.15) would be

$$a_k = \alpha_k + \varepsilon_k = \frac{r_A + x_k}{(r_A+x_k) + (M_b/M_a)x_k(1+r_B x_k)} + \varepsilon_k \qquad (5.1.19)$$

In this research, although some of the composition values were determined by NMR analysis, for the majority of the copolymer composition values elemental analysis was used. These two analytical procedures do not present the composition values in the same units: the former gives composition values in mole fractions whereas the latter gives weight fractions. The ideal procedure would be to use equation (5.1.19) for the nonlinear least squares treatment of the data and similar equations for higher forms of copolymerization models; and also to treat the two sets of data separately. But since the ratio of molecular weights of αMS and MMA are very close to unity, the elemental analysis data were converted to mole fractions and, assuming there was no change in the properties of the error, equation (5.1.20), which is the same as equation (5.1.19) apart from the use of mole fractions, was used in the terminal unit model treatment of all data.

$$a = \alpha + \varepsilon = \frac{1 + r_B/x}{2 + r_A x + r_B/x} \qquad (5.1.20)$$

Here a is in mole fraction and x=A/B. For higher copolymerization models similar equations were used.

If the conversion is high enough to give a drift in the copolymer composition then the integrated equation (1.3.51) needs to be used. In this research it was found that, due to low conversions, the drift of the most extreme experiment (highest αMS, and highest conversions) was not more than 2%. Therefore a correction on the feed compositions was applied instead [73]:

$$A' = 0.5\left[A_o + (A_o - a)/(1 - c)\right] \qquad (5.1.21)$$

where c is the conversion.

c) Confidence limits

The confidence limits for the estimated parameters (i.e., reactivity ratios in the case of copolymerization) have often been presented quite erroneously in the copolymerization literature. Some have been wrong in the sense of treating the error in the ways described earlier in this section, and a few have given a +/- standard deviation as a measure of the error which needs to be treated further to be meaningful

The most straightforward description of the error limit is by means of the confidence intervals. For a system of 'p' parameters and 'k' experimental points the $100(1-\beta)$ confidence interval on Θ is given by

$$\hat{\theta}_i - \sqrt{\text{var}\,\hat{\theta}_i}\; t_{(\beta/2,k-p)} < \theta_i < \hat{\theta}_i + \sqrt{\text{var}\,\hat{\theta}_i}\; t_{(\beta/2,k-p)} \quad , \; i = 1,2,..,p \qquad (5.1.22)$$

where θ_i is the true solution, with a best estimate of $\hat{\theta}_i$, and $t_{(\beta/2,k-p)}$ is the $100\beta/2$ percentage point of the t-distribution with k-p degrees of freedom. In equation (5.1.23)

$$\text{var}\,\theta_i = \frac{S}{k-p} H_{ii} \qquad (5.1.23)$$

where S is the sum of squares and H_{ii} is the (i,i)th element of the Hessian matrix, defined by the Jacobian matrix as

$$\underset{\sim}{H} = (2\underset{\sim}{J}^T\underset{\sim}{J})^{-1} \qquad (5.1.24)$$

A better way of describing the error, especially if there is a correlation of the estimates, is by the confidence region which is bounded by the ellipse,

$$(\underset{\sim}{\theta} - \hat{\underset{\sim}{\theta}})^T[\underset{\sim}{J}^T\underset{\sim}{J}](\underset{\sim}{\theta} - \hat{\underset{\sim}{\theta}}) = ps^2F_{\beta(p,k-p)} \qquad (5.1.25)$$

where $s^2=s/(k-p)$, and $F_{\beta(p,k-p)}$ is the β percentage point of the tabulated F distribution with p and k-p degrees of freedom.

The correlation of the estimates, which gives an idea on the validity of the model chosen, can be obtained by various correlation formulae in the literature; or the residuals can be plotted as $(\theta_i - \hat{\theta}_i)$ vs. mole fraction in feed to show whether there is a systematic deviation from $(\theta_i - \hat{\theta}_i) = 0$.

d) Design of experiments[122,123,73,130]

As Alfrey et al.[73] have mentioned, the most effective pairs of experimental points are those which are adequately far apart. Since the reactions at composition extremes may contain larger errors the optimum two points are in the region of A = 0.2 and 0.8. It is possible to find a set of exact points for each system which minimizes the confidence region. The two feed concentrations of one monomer, which minimize the confidence region, are the ones[122] which maximize the absolute determinant value of the Jacobian matrix. The parameters used here are the crude estimates determined by some other method. The two optimum concentrations as given by Tidwell and Mortimer[122] for the system of $r_A = 0.40$; $r_B = 0.15$ are

$$M_{b1} = 16.785 \quad ; \quad M_{b2} = 92.968$$

The experiments in this research did not follow this design for various reasons, but mainly because the above pair is for the two parameter terminal model only, and this research was aimed to study many models with varying numbers of parameters.

The complete program listing for NLR is given in fig.(40a); example in subroutine SUMSQ is for Wittmer case(i) equation.

```
      PROGRAM MARPO(INPUT,OUTPUT,TAPE5=INPUT,TAPE6=OUTPUT)                  _0001
      DIMENSION R(30),Y(30),Z(30),THETA(10),W(500),WM(30, 2),TWM( 2,30),    _0002
     1GHAF(2,2),G(2,2),HE(2,2),T(30),U(1),A1(10),VARX(10),CONF(10),         _0003
     2AZ(30),BZ(30)                                                         _0004
      COMMON Y,Z,CK,BZ,AZ                                                   _0005
      EXTERNAL SUMSQ,MONIT                                                  _0006
   11 FORMAT(16F5.2)                                                        _0007
   40 FORMAT(I2)                                                            _0008
   45 FORMAT(I2)                                                            _0009
  911 FORMAT(1X,16F5.2)                                                     _0010
  940 FORMAT(1X,I2)                                                         _0011
  945 FORMAT(1X,I2)                                                         _0012
      READ(5,11)(T(I),I=1,27)                                               _0013
      READ(5,40) KK                                                         _0014
      READ(5,45) N                                                          _0015
      WRITE(6,911)(T(I),I=1,27)                                             _0016
      WRITE(6,940) KK                                                       _0017
      WRITE(6,945) N                                                        _0018
      DO 999 K1=1,KK                                                        _0019
      READ(5,50) M                                                          _0020
   50 FORMAT(I2)                                                            _0021
      WRITE(6,950) M                                                        _0022
  950 FORMAT(1X,I2)                                                         _0023
      READ(5,61) ITEMP                                                      _0024
   61 FORMAT(1X,I5)                                                         _0025
      WRITE(6,61) ITEMP                                                     _0026
      READ(5,60) PRESS                                                      _0027
   60 FORMAT(1X,F6.1)                                                       _0028
      WRITE(6,60) PRESS                                                     _0029
      READ(5,219) REVOL                                                     _0030
  219 FORMAT(1X,F5.3)                                                       _0031
      WRITE(6,219) REVOL                                                    _0032
      TEMP=ITEMP                                                            _0033
      ATMP=TEMP+273.                                                        _0034
      TK=(57.1*ATMP-1.1075*(PRESS-1.)-16026.)/(4.574*ATMP)                  _0035
      CK=EXP(TK)                                                            _0036
      CK=1./CK                                                              _0037
      WRITE(6,166) CK                                                       _0038
  166 FORMAT(1X,F10.5)                                                      _0039
      DTM=0.944/(0.0015*(TEMP-20.)+1.)                                      _0040
      DTA=0.911/(0.00113*(TEMP-20.)+1.)                                     _0041
      IW=2*M*N+2*N*N+2*M+5*N                                                _0042
      DO 10 I=1,M                                                           _0043
      READ(5,100) ZA,YA,CONV                                                _0044
  100 FORMAT(8X,F6.4,4X,F6.4,5X,F6.3)                                       _0045
      ZAA=0.5*(ZA+(ZA-YA*CONV/100.)/(1.-CONV/100.))                         _0046
      BWT=ZAA*118.18                                                        _0047
      AWT=(1.-ZAA)*100.12                                                   _0048
      BVOL=BWT/DTA                                                          _0049
      AVOL=AWT/DTM                                                          _0050
      TVOL=AVOL+BVOL                                                        _0051
      CVOL=TVOL*REVOL                                                       _0052
      AZ(I)=1000.*(1.-ZAA)/CVOL                                             _0053
      BZ(I)=1000.*ZAA/CVOL                                                  _0054
      Y(I)=YA                                                               _0055
      Z(I)=ZAA                                                              _0056
  951 FORMAT(5X,4F8.4)                                                      _0057
   10 CONTINUE                                                              _0058
      U(1)=1                                                                _0059
      IFAIL=1                                                               _0060
      THETA(1)=0.5                                                          _0061
      THETA(2)=0.15                                                         _0062
      DMAX=10.                                                              _0063
      H=1.0E-4                                                              _0064
      ACC=1.0E-8                                                            _0065
      MAX=100                                                               _0066
      CALL E04FBF( M,N,THETA,R,SSQ,ACC,H,DMAX,W,IW,SUMSQ,MONIT,             _0067
     1 0,MAX,IFAIL)                                                         _0068
```

Fig.40a Listing of the NLR program.

```
      I=0                                                               _0069
      DO 101 II=1,M                                                     _0070
      DO 101 JJ=1,N                                                     _0071
      I=I+1                                                             _0072
      WM(II,JJ)=W(I)                                                    _0073
  101 CONTINUE                                                          _0074
      WRITE(6,301)                                                      _0075
  301 FORMAT(1X /* THE JACOBIAN * /)                                    _0076
      WRITE(6,609)((WM(II,JJ),JJ=1,N),II=1,M)                           _0077
  609 FORMAT(1X,10F10.5)                                                _0078
      DO 104 II=1,M                                                     _0079
      DO 104 JJ=1,N                                                     _0080
      TWM(JJ,II)=WM(II,JJ)                                              _0081
  104 CONTINUE                                                          _0082
      WRITE(6,302)                                                      _0083
  302 FORMAT(1X /* THE TRANSPOSED JACOBIAN * /)                         _0084
      WRITE(6,610)((TWM(II,JJ),JJ=1,M),II=1,N)                          _0085
  610 FORMAT(1X,10F10.5)                                                _0086
      DO 12 II=1,N                                                      _0087
      DO 12 JJ=1,N                                                      _0088
      GHAF(II,JJ)=0.0                                                   _0089
      DO 13 IJ=1,M                                                      _0090
      GHAF(II,JJ)=GHAF(II,JJ)+TWM(II,IJ)*WM(IJ,JJ)                      _0091
   13 CONTINUE                                                          _0092
      G(II,JJ)=2.0*GHAF(II,JJ)                                          _0093
   12 CONTINUE                                                          _0094
      CALL F01AAF(G,N,N,HE,N,AI,1)                                      _0095
      WRITE(6,303)                                                      _0096
  303 FORMAT(1X /*(JACOBIAN)T(JACOBIAN)* /)                             _0097
      WRITE(6,611)((GHAF(II,JJ),II=1,N),JJ=1,N)                         _0098
  611 FORMAT(1X,10F10.5)                                                _0099
      WRITE(6,304)                                                      _0100
  304 FORMAT(1X /* THE HESSIAN * /)                                     _0101
      WRITE(6,612)((HE(II,JJ),JJ=1,N),II=1,N)                           _0102
  612 FORMAT(1X,10F10.5)                                                _0103
      WRITE(6,300)                                                      _0104
      DO 102 I=1,N                                                      _0105
      VARX(I)=SSQ*HE(I,I)/(M-N)                                         _0106
      CONF(I)=(VARX(I)**0.5)*T(M-N)                                     _0107
      WRITE(6,103) THETA(I),CONF(I)                                     _0108
  103 FORMAT(10X,E14.6,2X,*+/-*,E12.6/)                                 _0109
  102 CONTINUE                                                          _0110
      WRITE(6,500) SSQ                                                  _0111
      WRITE(6,400) IFAIL                                                _0112
  300 FORMAT(44HOFINAL LEAST SQUARES ESTIMATES OF THETA ARE:,/)         _0113
  400 FORMAT(9H IFAIL = ,I1)                                            _0114
  500 FORMAT(17H SUM OF SQUARES =,E14.6)                                _0115
  999 CONTINUE                                                          _0116
      STOP                                                              _0117
      END                                                               _0118
      SUBROUTINE SUMSQ(M,N,THETA,R)                                     _0119
      DIMENSION THETA(N),R(M),Y(30),Z(30),AZ(30),BZ(30)                 _0120
      COMMON Y,Z,CK,BZ,AZ                                               _0121
      DO 10 I=1,M                                                       _0122
      XS=AZ(I)/BZ(I)                                                    _0123
      AA=(1.+CK*BZ(I)+(CK/THETA(2))*AZ(I))                              _0124
      AL=(AA-(AA*AA-4.*CK*BZ(I))**0.5)/2.                               _0125
      XC=(BZ(I)*(1./(1.-AL)))/(THETA(1)*AZ(I)+BZ(I))                    _0126
   10 R(I)=XC/(1.+XC)-Y(I)                                              _0127
      RETURN                                                            _0128
      END                                                               _0129
      SUBROUTINE MONIT(M,N,V,RESID,S,ICALLS)                            _0130
      DIMENSION V(N),RESID(M)                                           _0131
  100 FORMAT(11HONO. CALLS ,I2)                                         _0132
  200 FORMAT(16H SUM OF SQUARES ,E14.6)                                 _0133
  300 FORMAT(21H VALUES OF THETA ARE ,3E14.6)                           _0134
      WRITE(6,100) ICALLS                                               _0135
      WRITE(6,200) S                                                    _0136
      WRITE(6,300) (V(I),I=1,N)                                         _0137
      RETURN                                                            _0138
      END                                                               _0139
```

Fig.40a Cont'd.

VI. RESULTS AND DISCUSSIONS

6.1 Data of Previous Research Work

a) Copolymer composition

Previous results for the system α-methyl styrene and methyl methacrylate are summarized in this section for reference in the subsequent discussion. Early researchers do not give any composition values but only the calculated reactivity ratios. These are given in section (2.5) with the exception of values obtained by Doak, Deahl and Christmas (terminal unit model) at 99°C, which are

$$r_2 = 0.0$$
$$r_1 = 0.89$$

(αMS=2) and are claimed to indicate an alternating tendency at higher temperatures.

The most extensive set of experimental data on this system at 1 atm is that reported by Wittmer[98,111], and obtained in his study of copolymerization accompanied by depropagation in the case of one of the monomers. The full experimental data is given in Table (XI).

Wittmer calculated the reactivity ratios for 20° to 100°C from the terminal unit model and from two simpler models of the copolymerization-plus-depropagation. The results are given in Table (XIIa) (the results for 60°C were also mentioned in section (4.1)), together with values of K (the monomer-polymer equilibrium constant for α-methyl styrene as k_d/k_p) used in his calculations.

He also calculated reactivity ratios for 100° to 150°C from more complicated models like equations (4.1.47) and (4.1.50). The results are shown in Table (XIIb) together with all four equilibrium constants for all four propagation reactions. The equilibrium constants q_1 and q_2 for the reactions of different monomers are trial values used by Wittmer for the trial and error curve fitting on experimental data.

The system has also been studied by Izu and O'Driscoll and their coworkers. Izu and O'Driscoll[81] present monomer-copolymer compo-

sition data for 60°, 114° and 147° in graph form (data not tabulated). They report that approximate values of the reactivity ratios (terminal unit model) at 60°C are

$$r_2 = 0.15$$
$$r_1 = 0.40$$

(αMS=2) and that the terminal unit model yields negative values of r_1 at the two higher temperatures.

Izu, O'Driscoll et al.[95] tabulate monomer-copolymer composition data at the same three temperatures (presumably the same data, but fewer points are given in the tables than are shown in the graphs in reference (81)). The data of Izu, O'Driscoll et al. are shown in Tables (XIV) to (XVI) together with their microstructure data.

b) Copolymer microstructure

The available data on the microstructure of the α-methyl styrene - methyl methacrylate copolymer are mainly from Izu, O'Driscoll and their coworkers[81]) which are presented besides their composition data. Their microstructure data, as mentioned above, are included in Tables (XIV) to (XVI) which also contain the microstructure parameters calculated therefrom (see section (6.6) for the basis of this calculation).

A similar attempt, on the basis of the terminal unit model, was made by Ito et al.[68] to calculate the microstructure parameters from microstructure data, but the individual analysis values are not reported. The approximate values of Ito et al. are given in Table (XIII) as extracted from their graph.

Table (XVII) gives the coisotacticity parameter calculated by Izu et al. for the copolymerization at various temperatures; with Ito and coworkers' values for σ for comparison. The value of σ at 100°C in the second column was evaluated by using Ito and coworkers' data; but the value of σ at 114°C in the last column was evaluated by using Izu and coworkers' data.

The microstructure data presented by various researchers so far include only the peak fractions (see section(4.3)) F_x, F_y and F_z and there exists no available data on the fractions of individual triads in the copolymer.

Table XI

Copolymerization of αMS and MMA according to Wittmer

αMS mole % in feed	αMS mole % in polymer								
	20°C	50°C	60°C	80°C	100°C	110°C	120°C	130°C	150°C
5	7.79	8.13	9.10	7.79	6.97	7.24	6.16	7.52	1.49
					8.88				
10	17.21	15.47	17.75	14.96	14.68	11.35	11.07	11.07	0.68
20	29.27	26.87	25.38	25.19	21.45	21.45	13.29	13.84	3.68
30	34.41	32.89	33.50	31.33	26.93	25.20	19.46	16.92	4.23
40	41.55	40.59	39.73	37.31	34.00	27.53	24.33	19.18	7.01
50	45.87	45.95	44.68	42.78	37.00	31.94	28.39	23.16	7.01
60	50.57	53.41	52.05	47.42	43.09	36.41	32.52	26.93	6.44
70	57.90	60.49	59.61	51.83	43.40	37.30	33.12	25.48	7.28
			57.75						
80	64.10	64.09	65.99	54.49		40.04	35.00	32.52	7.84
90				68.41			40.03	32.52	15.24
95	81.37								

Table XIIa

Reactivity ratios for αMS-MMA system as calculated by a) equation (4.1.44) and b) equation (4.1.49)

	(a)			(b)	
T(°C)	$r_{\alpha MS}$	r_{MMA}	K(mole/h)	$r_{\alpha MS}$	r_{MMA}
20	0.3	0.5	1.7	0.3	0.5
50	0.4	0.55	5.1	0.51	0.55
60	0.35	0.55	7.1	0.6	0.55
80	0.2	0.6	12.9	0.81	0.65
100	0.05	0.65	22.9	1.0	0.7

Table XIIb

Reactivity ratios for αMS-MMA system as calculated by a) equation (4.1.47) and b) equation (4.1.50).

	(a)						(b)	
T(°C)	$r_{\alpha MS}$	r_{MMA}	$K_{\alpha MS}$	K_{MMA}	q_A	q_B	$r_{\alpha MS}$	r_{MMA}
100	1.0	0.7	22.9	0.119	0.0	1	1.0	0.7
110	1.17	0.72	27.9	0.178	0.0	4	1.17	0.72
120	1.28	0.74	35	0.262	0.0	7	1.28	0.74
130	1.43	0.76	43	0.377	0.0	11	1.43	0.76
150	1.75	0.8	67	0.744	0.0	90	1.75	0.8

Table XIII

Microstructure parameters for αMS-MMA copolymers by Ito et al., prepared at 60°C.

Sample	F_x	F_y	F_z
1	0.59	0.44	-
2	0.65	0.30	0.05
3	0.60	0.35	0.05
4	0.68	0.28	0.04
5	0.73	0.24	0.03
6	0.80	0.18	0.02
7	0.89	0.11	0.00

Table XIV

Microstructure parameters for αMS-MMA copolymers by Izu et al., prepared at 60°C (s=αMS).

Sample	f_s	F_s	F_x	F_y	P_{ab}
1	0.656	0.502	0.649	0.271	0.749
2	0.550	0.471	0.691	0.285	0.673
3	0.449	0.406	0.712	0.240	0.591
4	0.352	0.362	0.775	0.222	0.500
5	0.259	0.287	0.774	0.176	0.399
6	0.169	0.215	0.860	0.114	0.274
7	0.083	0.112	0.896	0.081	0.152

Table XV

Microstructure parameters for αMS-MMA copolymers by Izu et al., prepared at 114°C.

Sample	f_s	F_s	F_x	F_y	P_{ab}
1	0.880	0.390	0.611	0.282	0.516
2	0.765	0.366	0.632	0.261	0.450
3	0.550	0.310	0.771	0.223	0.338
4	0.449	0.274	0.789	0.205	0.285
5	0.352	0.229	0.817	0.169	0.231
6	0.259	0.180	0.825	0.156	0.177

Table XVI

Microstructure parameters for αMS-MMA copolymers by Izu et al., prepared at 147°C.

Sample	f_s	F_s	F_x	F_y
1	0.656	0.096	0.918	0.082
2	0.352	0.089	0.921	0.079
3	0.169	0.080	0.935	0.065

Table XVII

Comparison of coisotacticity parameter (σ).

T°C	Izu et al.	Ito et al.
0	-	0.21 ± 0.03
60	0.26 ± 0.03	0.27 ± 0.03
100	0.31*	0.25 ± 0.03
114	0.40 ± 0.04	0.20*

*See text.

6.2 Analytical Results of This Research

Results on the copolymer-monomer composition relationship and microstructure and kinetic data obtained in this research at 60°C and at pressures from normal to 5000 bar gauge are given in Tables (XVIIIa) and (XVIIIb). Peak area fractions are over a total of methoxy peaks and based on the copolymer MMA mole fractions in Table (XVIIIa) estimated by NMR analysis. Results on the molecular weight analysis for some copolymers prepared in this research are given in Table (XIX).

The nomenclature for the following tables are:

f_s : mole fraction of αMS in feed mixture
F_s : mole fraction of αMS in copolymer, (CHN) by elemental analysis or (NMR) by NMR
In : initiator concentration
conv. : conversion, R_p : rate of reaction
MN : number average molecular weight
MW : weight average molecular weight
MZ : z average molecular weight
MV : viscosity average molecular weight

Table XVIIIa

Code No.	P bar g	t °C	In mg/lt *100	f_s m.fr.	F'_s(CHN) m.fr.	F_s(NMR) m.fr.	conv. % w/w	R_p conv./h
1	0	60	2	0.0			6.722	4.4815
2	0	60	2	0.1933	0.2290	0.2339	3.860	0.1845
3	0	60	2	0.3921	0.3630	0.3784	2.625	0.1105
4	0	60	2	0.4858	0.4296	0.4107	1.841	0.0767
5	0	60	2	0.5837			1.247	0.0520
11	0	60	2	0.0188			5.635	1.1270
12	0	60	2	0.0509	0.0497		2.573	0.5147
13	0	60	2	0.0879	0.2468	0.1437	5.998	0.3076
20	0	60	2	0.1972			4.994	0.1685

Table XVIIIa (cont'd)

Code No.	P bar g	t °C	In mg/lt *100	f_s m.fr.	F'_s(CHN) m.fr.	F_s(NMR) m.fr.	conv. % w/w	R_p conv./h
21	0	60	2	0.3971			4.268	0.0885
C1	0	60	2	0.2906			5.615	0.0981
C2	0	60	2	0.2948			4.751	0.1114
C3	0	60	2	0.2934	0.2963		5.740	0.1003
C4	0	60	2	0.2765			4.717	0.1106
C5	0	60	2	0.2997			3.031	0.1166
C6	0	60	2	0.2927			3.130	0.1204
C7	0	60	2	0.0211			6.204	1.1314
C8	0	60	2	0.0529			3.241	0.5910
D1	0	60	2	0.2093			6.809	0.1586
D2	0	60	2	0.4149			5.094	0.0696
A1	0	60	2	0.0214	0.0032		1.646	1.2348
A2	0	60	2	0.0203			3.084	1.0055
A3	0	60	2	0.0211			2.034	0.5084
A4	0	60	2	0.0494			2.054	0.5135
A5	0	60	2	0.0613			0.850	0.6375
A6	0	60	2	0.0531			1.310	0.4271
A7	0	60	2	0.2072			3.356	0.1891
A8	0	60	2	0.1023			5.497	0.3202
A9	0	60	2	0.1046			8.482	0.3122
A10	0	60	2	0.1936			5.059	0.1862
A11	0	60	2	0.2029			7.005	0.1661
A12	0	60	2	0.2996			2.499	0.1408
A13	0	60	2	0.2945			3.644	0.1341
A14	0	60	2	0.2979	0.3055	0.3060	5.176	0.1228
B1	0	60	2	0.0981			1.669	0.3338
B2	0	60	2	0.0979			3.247	0.3068
B3	0	60	2	0.0958			5.944	0.2957
B4	0	60	2	0.5956			1.346	0.0561
B5	0	60	2	0.6045			2.524	0.0522
B6	0	60	2	0.5839			3.454	0.0480

Table XVIIIa (cont'd)

Code No.	P bar g	t °C	In mg/lt *100	f_s m.fr.	F'_s(CHN) m.fr.	F_s(NMR) m.fr.	conv. % w/w	R_p conv./h
15	0	60	4	0.3915			2.839	0.1175
16	0	60	4	0.4843			3.538	0.1464
NP1	0	60	4	0.1889			5.393	0.2227
NP2	0	60	4	0.2691	0.2855		8.435	0.1771
NP3	0	60	4	0.2169			6.560	0.2066
17	0	60	6	0.1966			5.736	0.3120
18	0	60	6	0.3889			3.685	0.2005
NP4	0	60	6	0.3974	0.3663		4.445	0.1553
C9	0	50	2	0.2005			1.885	0.0713
C10	0	50	2	0.3955			0.985	0.0372
C11	0	50	2	0.2383			3.220	0.0634
C12	0	50	2	0.4157	0.3837		1.728	0.0340
D6	0	70	2	0.1900	0.2126		6.812	0.3161
7	0	70	2	0.3842			5.081	0.2022
NP7	0	70	2	0.1957			6.815	0.3501
NP8	0	70	2	0.4015			3.718	0.1910
NP9	0	70	2	0.2010			7.991	0.2668
NP10	0	70	2	0.3961	0.3455		4.555	0.1521
2G	500	60	2	0.1009	0.1691	0.1696	8.091	0.4624
3G	500	60	2	0.1997	0.2775	0.2759	4.987	0.2850
4G	500	60	2	0.1995	0.2506		6.545	0.2570
5G	500	60	2	0.1996	0.2353		8.634	0.2204
6G	500	60	2	0.2950	0.3384	0.3836	4.957	0.1946
7G	500	60	2	0.3732	0.4008	0.4394	4.847	0.1238
8C	500	60	2	0.5180	0.4590		7.095	0.1001
8G	500	60	2	0.4559	0.4326	0.4397	4.408	0.1125
9C	500	60	2	0.5663	0.5316		5.321	0.0750
9G	500	60	2	0.5948	0.5032	0.4732	5.966	0.0663
10C	500	60	2	0.7155	0.5867		4.405	0.0621
101K	500	60	2	0.7006	0.5172	0.5558	4.566	0.0507
11P	500	60	2	0.7956	0.5857	0.7424	3.421	0.0380

Table XVIIIa (cont'd)

Code No.	P bar g	t °C	In mg/lt *100	f_s m.fr.	F'_s(CHN) m.fr.	F_s(NMR) m.fr.	conv. % w/w	R_p conv./h
2H	1000	60	2	0.1042	0.1711		6.960	0.6736
2F	1000	60	2	0.0992	0.1666	0.1822	9.200	0.7131
3Z	1000	60	2	0.2057	0.2692		2.521	0.4384
3F	1000	60	2	0.2030	0.2595		5.585	0.4330
5Z	1000	60	2	0.1990	0.2489		3.881	0.4281
4H	1000	60	2	0.1997	0.1965		5.655	0.3941
5H	1000	60	2	0.1982	0.2416		6.501	0.4632
3H	1000	60	2	0.2001	0.2634		4.393	0.4252
6Z	1000	60	2	0.2941	0.3404		2.935	0.3237
6F	1000	60	2	0.2902	0.3263		4.009	0.3108
6H	1000	60	2	0.2912	0.3403		4.916	0.3503
7Z	1000	60	2	0.3907	0.3792		2.263	0.2496
7F	1000	60	2	0.3989	0.3960		5.667	0.2227
8H	1000	60	2	0.4998	0.3268		5.466	0.1761
8S	1000	60	2	0.5004	0.4616	0.4654	6.059	0.1579
9H	1000	60	2	0.5991	0.5348		4.195	0.1352
9F	1000	60	2	0.5931	0.5059		3.652	0.1435
9P	1000	60	2	0.6036	0.4529	0.5977	4.085	0.1393
10Z	1000	60	2	0.7298	0.6130		2.562	0.1073
11Z	1000	60	2	0.8206	0.6715	0.6786	1.718	0.0719
2A	1500	60	2	0.1062	0.2399		7.776	1.1296
23L	1500	60	2	0.0975	0.1656	0.1436	7.791	0.9739
3A	1500	60	2	0.1995	0.2598		2.736	0.6620
4A	1500	60	2	0.1991	0.3023	0.2305	8.319	0.6433
51K	1500	60	2	0.2021	0.2973	0.2695	4.867	0.6084
6A	1500	60	2	0.2925	0.3899	0.3504	5.981	0.4977
7A	1500	60	2	0.3965	0.3940	0.4026	4.698	0.3910
8A	1500	60	2	0.4835	0.4877	0.4322	3.892	0.3239
9A	1500	60	2	0.5978	0.5186	0.4814	7.104	0.2279
10A	1500	60	2	0.6965	0.5693	0.5637	5.474	0.1756
11A	1500	60	2	0.7969	0.6391	0.6288	4.063	0.1304

Table XVIIIa (cont'd)

Code No.	P bar g	t °C	In mg/lt *100	f_s m.fr.	F'_s(CHN) m.fr.	F_s(NMR) m.fr.	conv. % w/w	R_p conv./h
24L	2000	60	2	0.0993	0.1723	0.1522	6.609	1.3130
31K	2000	60	2	0.2081	0.2782	0.2495	4.183	0.8311
4B	2000	60	2	0.2034	0.3291	0.3107	5.242	0.8736
52K	2000	60	2	0.1958	0.2741	0.2553	6.529	0.8479
4F	2000	60	2	0.1959	0.2561	0.2670	7.444	0.8623
6B	2000	60	2	0.2987	0.3369	0.3552	7.972	0.6962
7K	2000	60	2	0.4009	0.4119	0.4015	5.725	0.4706
8B	2000	60	2	0.4952	0.4594		5.213	0.4553
9B	2000	60	2	0.5890	0.5139		7.476	0.3563
10B	2000	60	2	0.6861	0.6032		5.854	0.2790
11B	2000	60	2	0.7930	0.6389	0.6693	4.010	0.1911
2D	2500	60	2	0.1020	0.2143		8.070	2.1330
21O	2500	60	2	0.1010	0.0899	0.0539	5.700	1.8587
3L	2500	60	2	0.2010	0.2721		3.730	1.2162
4D	2500	60	2	0.2037	0.3145		8.081	1.2793
5D	2500	60	2	0.2022	0.2712	0.2530	5.261	1.3152
6D	2500	60	2	0.2903	0.3447	0.3505	4.081	1.0203
7D	2500	60	2	0.3980	0.3891	0.4246	4.583	0.7255
8D	2500	60	2	0.4967	0.4901	0.4855	4.037	0.6391
9D	2500	60	2	0.5805	0.5482	0.5091	8.868	0.4284
10D	2500	60	2	0.6949	0.6159	0.6109	-	-
11D	2500	60	2	0.8306	0.6701	0.6687	5.298	0.2560
2E	3000	60	2	0.1011	0.1760	0.3000	8.723	2.5285
3E	3000	60	2	0.1963	0.2821	0.3248	5.346	1.5494
4E	3000	60	2	0.1974	0.2745		3.413	1.7063
5E	3000	60	2	0.1950	0.2500		8.968	1.4741
6O	3000	60	2	0.2835	0.2690	0.3718	7.968	1.1119
7E	3000	60	2	0.4058	0.5475	0.4843	5.509	0.9056
8E	3000	60	2	0.4918	0.4513	0.5010	4.632	0.7614
9E	3000	60	2	0.6064	0.5275	0.5685	7.028	0.5637
102K	3000	60	2	0.6744	0.5620	0.6314	3.709	0.5176

Table XVIIIa (cont'd)

Code No.	P bar g	t °C	In mg/lt *100	f_s m.fr.	F'_s(CHN) m.fr.	F_s(NMR) m.fr.	conv. % w/w	R_p conv./h
11E	3000	60	2	0.7893	0.6457	0.7796	4.588	0.3680
22O	3500	60	2	0.1028	0.1870	0.1630	6.235	3.1174
3J	3500	60	2	0.2130	0.2230		3.961	1.9807
4L	3500	60	2	0.1988	0.2736	0.2862	5.585	1.9370
5M	3500	60	2	0.1937	0.2839		8.279	1.8399
6J	3500	60	2	0.2920	0.3546	0.3545	4.355	1.5104
72O	3500	60	2	0.3899	0.3494	0.4025	5.104	1.1962
8J	3500	60	2	0.4852	0.3998	0.5069	4.281	1.0033
9J	3500	60	2	0.5872	0.5251	0.5366	7.611	0.7714
10J	3500	60	2	0.7171	0.6216	0.6773	6.037	0.6119
111T	3500	60	2	0.8056	0.6999	0.7909	7.277	0.4428
11M	3500	60	2	0.7880	0.6601		4.842	0.4908
2M	4000	60	2	0.0999	0.0888	0.2000	8.911	4.6093
32O	4000	60	2	0.2041	0.2069		5.369	2.7773
4M	4000	60	2	0.2030	0.2912		7.808	2.6028
5T	4000	60	2	0.1981	0.2749		10.976	2.1952
6M	4000	60	2	0.2968	0.3434	0.3641	5.807	1.9358
7H	4000	60	2	0.3883	0.4209	0.4706	6.195	1.5487
8M	4000	60	2	0.4912	0.4734	0.5624	5.146	1.2864
92S	4000	60	2	0.6100	0.4853	0.5334	7.777	0.6419
9M	4000	60	2	0.6001	0.5346		7.165	0.9883
10S	4000	60	2	0.6919	0.6393		6.500	0.5365
10F	4000	60	2	0.7302	0.6207		5.704	0.7868
112S	4000	60	2	0.8163	0.6842	0.6677	4.796	0.3958
23O	5000	60	2	0.0964	0.1245		26.308	13.1540
3T	5000	60	2	0.1982	0.2489		9.822	4.9109
6S	5000	60	2	0.3022	0.3580	0.4040	13.599	3.3034
7S	5000	60	2	0.3929	0.3725		10.988	2.6692
8T	5000	60	2	0.4937	0.4474	0.5055	8.431	2.0480
91S	5000	60	2	0.5845	0.4777	0.5261	11.625	1.6848
10P	5000	60	2	0.6948	0.5408	0.6069	9.241	1.3392
112T	5000	60	2	0.7921	0.6970	0.6673	7.121	1.0321

Table XVIIIb

Code	F_x	F_{MMM}	δ	F_{SMM}	δ	F_{SMS}	δ	F_y	F_{SMM}	δ	F_{SMS}	δ	F_z	δ
2	0.8625	0.6250	3.54	0.2037	3.48	0.0388	3.41	0.1425	0.1130	3.10	0.0300	2.98	0.0010	2.79
3	0.7570	0.3570	3.54	0.3286	3.45	0.0588	3.37	0.2210	0.1440	3.11	0.0800	2.99	0.0240	2.80
4	0.7140	0.3240	3.52	0.3286	3.43	0.0586	3.31	0.2570	0.1750	3.09	0.0810	2.95	0.0386	2.73
12	0.9720	0.9660	3.57	0.0060	3.46	0.00	-	0.0260	-	3.10	-	-	0.0120	2.90
13	0.9250	0.7500	3.58	0.1750	3.50	0.00	3.42	0.0780	0.0850	-	0.00	-	0.00	-
A14	0.7450	0.3088	3.54	0.3625	3.45	0.0700	3.35	0.2075	0.1590	3.11	0.0450	2.97	0.0387	2.75
2G	0.8600	0.5900	3.57	0.1600	3.49	0.1120	3.41	0.1000	0.0770	3.07	0.0230	2.93	0.0350	2.79
3G	0.7890	0.4330	3.52	0.2330	3.44	0.1267	3.35	0.1640	0.1230	3.05	0.0400	2.92	0.0410	2.50
6G	0.6700	0.2840	3.55	0.2600	3.46	0.1180	3.37	0.2600	0.1670	3.11	0.0940	3.02	0.0700	2.79
7G	0.5950	0.2060	3.53	0.2725	3.45	0.1190	3.33	0.2875	0.2240	3.10	0.1150	2.97	0.1125	2.75
8G	0.5875	0.2460	3.50	0.2440	3.41	0.1000	3.30	0.2750	0.1590	3.09	0.1200	2.96	0.1375	2.72
9G	0.5830	0.2267	3.50	0.2667	3.41	0.0917	3.30	0.3330	0.2330	3.08	0.1110	2.97	0.0880	2.73
10lK	0.6330	0.3330	3.49	0.1730	3.42	0.1267	3.32	0.2930	0.1830	3.07	0.1100	2.98	0.1000	2.74
11P	0.6670	0.0470	3.45	0.4870	3.40	0.1530	3.31	0.2470	0.1330	3.07	0.0870	2.97	0.1130	2.73
2F	0.8430	0.6330	3.56	0.1930	3.46	0.0330	3.34	0.0867	0.0770	3.10	0.0070	3.03	0.0667	2.84
8S	0.6460	0.2790	3.50	0.2860	3.43	0.0680	3.32	0.2220	0.1430	3.08	0.0890	2.94	0.0870	2.91
9P	0.7370	0.2330	3.49	0.4700	3.41	0.0430	3.29	0.2470	0.1500	3.07	0.0870	2.96	0.0160	2.68
11Z	0.6360	0.2730	3.45	0.2270	3.38	0.1590	3.29	0.2726	0.1420	3.02	0.1410	2.93	0.1045	2.70
23L	0.8500	0.6560	3.57	0.1750	3.45	0.0175	3.33	0.1190	0.0900	3.08	0.0280	2.99	0.0375	2.78
4A	0.8200	0.5800	3.57	0.2150	3.47	0.0230	3.39	0.1630	0.1420	3.11	0.0260	2.99	0.0100	2.77
51K	0.8200	0.5800	3.53	0.2120	3.44	0.0380	3.34	0.1520	0.1180	3.09	0.0340	2.99	0.0300	2.71

Table XVIIIb (cont'd)

Code	F_x	F_{MMM}	δ	F_{SMM}	δ	F_{SMS}	δ	F_y	F_{SMM}	δ	F_{SMS}	δ	F_z	δ
6A	0.7220	0.4500	3.54	0.2000	3.47	0.0840	3.38	0.2220	0.1500	3.11	0.0720	2.99	0.0550	2.77
7A	0.7110	0.3170	3.54	0.3030	3.45	0.0856	3.36	0.2510	0.1470	3.13	0.0550	3.02	0.0330	2.79
8A	0.7050	0.3666	3.52	0.2617	3.44	0.0867	3.36	0.2600	0.1950	3.10	0.0670	2.98	0.0280	2.78
9A	0.7040	0.2800	3.53	0.3840	3.45	0.0400	3.33	0.3000	0.2340	3.10	0.0740	2.98	0.0140	2.76
10A	0.6300	0.2060	3.49	0.3580	3.40	0.0800	3.29	0.3200	0.2600	3.05	0.0740	2.95	0.0440	2.72
11A	0.6125	0.1625	3.47	0.3400	3.40	0.1125	3.30	0.3500	0.2750	3.04	0.0700	2.94	0.0325	2.73
24L	0.8140	0.5610	3.55	0.2140	3.45	0.0430	3.32	0.1430	0.1140	3.10	0.0340	2.94	0.0470	2.80
31K	0.7200	0.4800	3.54	0.2480	3.44	0.0450	3.31	0.1620	0.1130	3.07	0.0500	2.97	0.0510	2.77
4B	0.8000	0.5280	3.55	0.2240	3.47	0.0480	3.37	0.1440	0.1080	3.10	0.0400	2.97	0.0600	2.83
52K	0.7920	0.5955	3.58	0.1580	3.48	0.0420	3.39	0.1600	0.1250	3.08	0.0360	2.98	0.0355	2.84
4F	0.8130	0.5167	3.56	0.2730	3.45	0.0430	3.35	0.1730	0.1530	3.11	0.0330	2.99	0.0330	2.73
6B	0.8050	0.5500	3.53	0.2650	3.45	0.0100	3.32	0.1950	0.1600	3.10	0.0400	2.97	0.0300	2.83
7K	0.7290	0.3750	3.53	0.2810	3.43	0.0660	3.32	0.2190	0.1620	3.10	0.0660	2.97	0.0625	2.76
11B	0.5500	0.1650	3.49	0.2750	3.41	0.1200	3.33	0.3300	0.2100	3.08	0.1200	3.00	0.1350	2.75
21O	0.8200	0.2040	3.54	0.5300	3.50	0.0800	3.37	0.1300	0.1060	3.11	0.0350	2.93	0.0500	2.70
5D	0.7717	0.5217	3.56	0.2167	3.46	0.0330		0.1830	0.1500	3.12	0.0380	2.97	0.0550	2.78
6D	0.7300	0.4660	3.51	0.1760	3.43	0.0880	3.36	0.2200	0.1540	3.07	0.0600	2.94	0.0600	2.77
7D	0.6925	0.4250	3.50	0.2375	3.41	0.0375	3.30	0.2500	0.1880	3.09	0.0600	2.95	0.0500	2.77
8D	0.6540	0.3540	3.49	0.2275	3.40	0.0825	3.30	0.2875	0.2170	3.09	0.0730	2.95	0.0540	2.75
9D	0.5900	0.3000	3.49	0.2160	3.41	0.0810	3.30	0.3010	0.2240	3.08	0.0800	2.98	0.1090	2.73
10D	0.6075	0.2500	3.48	0.2650	3.40	0.1125	3.30	0.3075	0.2300	3.04	0.0900	2.94	0.0925	2.75

Table XVIIIb (cont'd)

Code	F_x	F_{MMM}	δ	F_{SMM}	δ	F_{SMS}	δ	F_y	F_{SMM}	δ	F_{SMS}	δ	F_z	δ
11D	0.5375	0.1575	3.45	0.2500	3.39	0.1250	3.30	0.3600	0.1750	3.07	0.2050	2.96	0.1075	2.71
2E	0.8900	0.2767	3.55	0.2400	3.46	0.0500	3.38	0.1167	0.0930	3.10	0.0300	2.96	0.1667	2.80
3E	0.7500	0.4250	3.53	0.2417	3.45	0.0867	3.33	0.1880	0.1130	3.08	0.0750	2.94	0.0667	2.80
6O	0.8300	0.3575	3.53	0.3875	3.46	0.0575	3.34	0.1375	0.0950	3.11	0.0500	3.00	0.0500	2.78
7E	0.6417	0.3250	3.50	0.2567	3.41	0.0617	3.30	0.2717	0.1930	3.09	0.0820	2.96	0.0817	2.74
8E	0.6080	0.2717	3.49	0.2400	3.41	0.1000	3.30	0.3000	0.2130	3.08	0.0920	2.96	0.0900	2.71
9E	0.6000	0.2675	3.47	0.2750	3.39	0.0600	3.28	0.3075	0.2270	3.06	0.0880	2.96	0.1050	2.74
102K	0.6380	0.0692	3.46	0.4935	3.40	0.0753	3.31	0.3100	0.2500	3.04	0.0500	2.95	0.0520	2.81
11E	0.5500	0.4000	3.45	0.1000	3.37	0.0650	3.30	0.3350	0.2450	3.06	0.1000	2.96	0.1100	2.71
22O	0.8400	0.6160	3.57	0.2240	3.48	0.0260	3.34	0.1040	0.0720	3.12	0.0260	3.01	0.0600	2.76
4L	0.7540	0.5120	3.57	0.1900	3.47	0.0480	3.37	0.1980	0.1600	3.13	0.0380	3.00	0.0500	2.77
6J	0.6825	0.3925	3.52	0.2325	3.42	0.0675	3.31	0.2000	0.1630	3.08	0.0500	2.95	0.1125	2.80
72O	0.7000	0.3500	3.50	0.3300	3.40	0.0340	3.26	0.2260	0.1940	3.07	0.0600	2.93	0.0680	2.72
8J	0.6200	0.2550	3.49	0.2375	3.40	0.1250	3.30	0.2875	0.1850	3.07	0.1150	2.95	0.1000	2.76
9J	0.5800	0.2340	3.48	0.2340	3.40	0.1140	3.30	0.3000	0.2040	3.05	0.1100	2.95	0.1140	2.72
10J	0.6000	0.2000	3.48	0.2550	3.40	0.1450	3.30	0.3500	0.2680	3.03	0.1000	2.91	0.0500	2.73
111T	0.6300	0.1450	3.47	0.4000	3.39	0.1100	3.29	0.3400	0.2500	3.03	0.1000	2.95	0.0300	2.73
2M	0.8000	0.5000	3.57	0.1875	3.50	0.1200	3.42	0.1200	0.1230	3.09	0.1000	2.95	0.0825	2.85
6M	0.6950	0.3500	3.53	0.2550	3.43	0.0875	3.33	0.2400	0.1680	3.10	0.0800	2.97	0.0750	2.76
7H	0.6850	0.3625	3.50	0.2675	3.42	0.0675	3.31	0.2450	0.1530	3.09	0.1000	2.97	0.0700	2.77
8M	0.6800	0.3500	3.51	0.3250	3.42	0.0550	3.30	0.2350	0.1850	3.08	0.0600	2.93	0.0650	2.76

Table XVIIb (cont'd)

Code	F_x	F_{MMM}	δ	F_{SMM}	δ	F_{SMS}	δ	F_y	F_{SMM}	δ	F_{SMS}	δ	F_z	δ
92S	0.6000	0.2800	3.50	0.2230	3.41	0.1000	3.31	0.2970	0.1870	3.07	0.1000	2.94	0.1130	2.74
10S	0.8625	0.1625	3.48	0.5250	3.40	0.1750	3.32	0.1375					0.00	2.75
112S	0.5250	0.1250	3.45	0.1850	3.37	0.2100	3.32	0.3350	0.1450	3.02	0.2000	2.92	0.1500	2.65
6S	0.8830	0.4000	3.53	0.4830	3.45	0.00	3.30	0.0670	0.0470	3.10	0.0300	3.02	0.0550	2.80
8T	0.6670	0.3200	3.48	0.3170	3.38	0.0430	3.30	0.3000	0.2000	3.09	0.0960	2.95	0.0270	2.68
91S	0.5960	0.1800	3.50	0.3400	3.42	0.0800	3.30	0.3000	0.1980	3.08	0.1120	2.95	0.1040	2.70
10P	0.6200	0.2520	3.45	0.3480	3.40	0.0560	3.30	0.3240	0.2080	3.05	0.1200	2.95	0.0540	2.72
112T	0.6000	0.1330	3.45	0.4200	3.36	0.0600	3.27	0.3500	0.3330	3.05	0.0600	2.95	0.0670	2.72

Table XIX

Code	P	f_s	F_s(CHN)	$MN*10^{-5}$	$MW*10^{-5}$	$MZ*10^{-5}$	$MV*10^{-5}$	MW/MN	MZ/MN
A1	0	0.0214	0.0032	1.7465	3.5537	7.0375	3.2247	2.03	4.03
12	0	0.0509	0.0497	1.1460	2.0619	3.3848	1.9118	1.80	2.95
13	0	0.0879	0.2468	1.0338	1.8385	2.8720	1.7138	1.78	2.78
2	0	0.1933	0.2290	0.5393	0.9324	1.4176	0.8733	1.73	2.63
C3	0	0.2934	0.2963	0.4454	0.8536	1.3470	0.7918	1.92	3.02
A14	0	0.2979	0.3055	0.3405	0.6179	0.9205	0.5782	1.81	2.70
3	0	0.3921	0.3630	0.3436	0.6075	0.9040	0.5691	1.77	2.63
4	0	0.4858	0.4296	0.1922	0.3972	0.6200	0.3678	2.07	3.23
B6	0	0.5839		0.3019	0.5812	0.9251	0.5384	1.93	3.06
24L	2000	0.0993	0.1723	4.8223	10.475	21.959	9.3662	2.17	4.55
52K	2000	0.1958	0.2741	2.5509	4.884	9.2372	4.4580	1.91	3.62
4F	2000	0.1959	0.2561	3.0088	6.1364	12.886	5.5313	2.04	4.28
6B	2000	0.2987	0.3369	2.2846	4.2722	7.5801	3.9209	1.87	3.32
7K	2000	0.4009	0.4119	1.7099	3.2020	5.5253	2.9496	1.87	3.23
8B	2000	0.4952	0.4594	1.5421	2.9231	5.1099	2.6924	1.90	3.31
9B	2000	0.5890	0.5139	1.1632	2.1392	3.4870	1.9829	1.84	3.00
10B	2000	0.6861	0.6032	1.1068	1.9629	3.1350	1.8253	1.77	2.83
11B	2000	0.7930	0.6389	0.8575	1.5730	2.5804	1.4602	1.83	3.01
4G	500	0.1995	0.2506	0.9573	1.6816	2.7130	1.5654	1.76	2.83
5H	1000	0.1982	0.2416	1.4134	2.4875	4.1109	2.3069	1.76	2.91
3A	1500	0.1995	0.2598	2.0575	3.8593	6.7971	3.5458	1.88	3.30
3L	2500	0.2010	0.2721	3.4796	7.2653	14.629	6.5501	2.09	4.20
3E	3000	0.1963	0.2821	4.6804	10.679	23.586	9.4912	2.28	5.04
4L	3500	0.1988	0.2736	5.3840	14.462	31.778	12.725	2.69	5.90
5T	4000	0.1981	0.2749	6.5195	17.707	41.810	15.451	2.72	6.41
3T	5000	0.1982	0.2489	8 6656	24.594	60.640	21.275	2.84	7.00

6.3 Comparison of Composition Data with Results of Previous Work

A general inspection of the data of previous workers and this research reveals, qualitatively, a change in copolymer composition due to pressure and temperature. With increasing temperature there seems to be a tendency of the formation of αMS in the copolymer to decrease, although this is not obvious in the case of Wittmer's data between 20° and 60°C (fig.(27a)).

The only direct comparison of copolymer composition results between this research and previous ones which is possible is at 1 atm and 60°C. As seen from fig.(26) all three sets of data compare satisfactorily and the reactivity ratios calculated for the terminal model by the Author and as given by the researchers are shown in Table (XX).

Increase in polymerization pressure seems to have the effect of increasing the αMS content of the copolymer up to 3000 bars. At pressures above 3000 bars there is a less-pronounced reverse effect, and the αMs content of the copolymer decreases with pressure (fig.(27b)).

Table XX

	This research	Wittmer		Izu et al.	
		Calctd. by A.	given	Calctd. by A.	given
$r_{\alpha MS}$	0.148	0.297	0.30	0.192	0.15
r_{MMA}	0.567	0.512	0.55	0.564	0.40

6.4 Treatment of the Data by means of Various Copolymerization Models

6.4.1 Copolymerization Models without any Depropagation Reaction

a) Terminal unit model

The composition data obtained by the two analytical methods, namely CHN and NMR, were used to attempt to identify the best copolymerization model which fits to the particular system, and then to analyse the effect of pressure on the copolymerization parameters (usually the

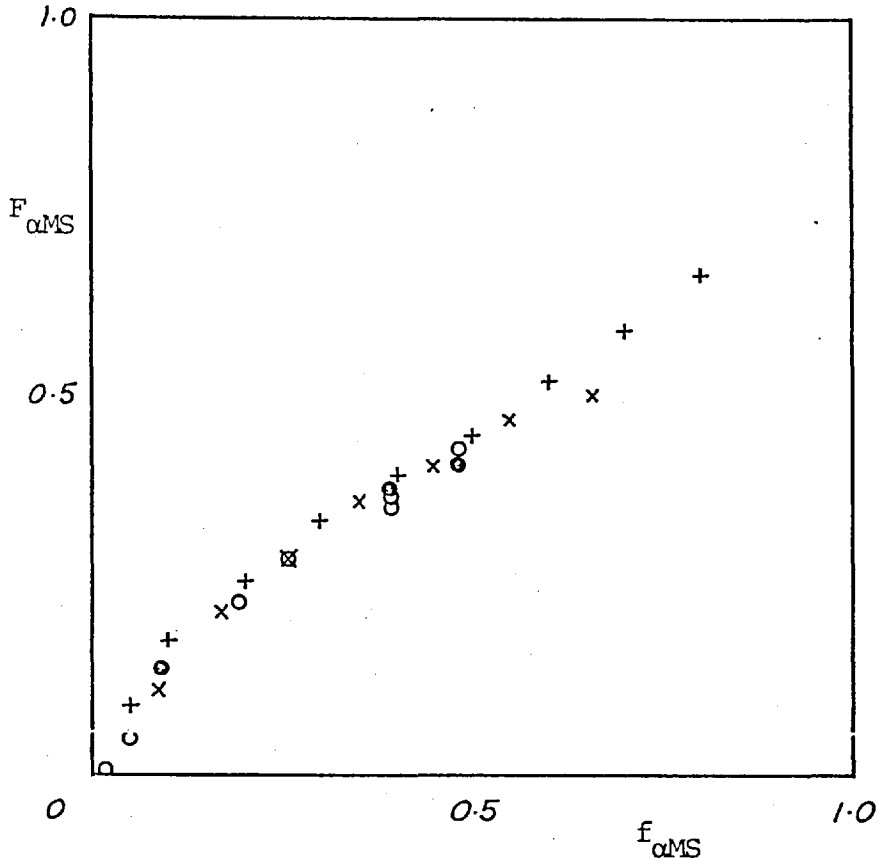

Fig.26 Comparison of 1 atm., 60°C copolymerization data for αMS-MMA system from various researchers.
o) this research CHN, ⊙) this research NMR,
+) Wittmer, x) Izu et al.

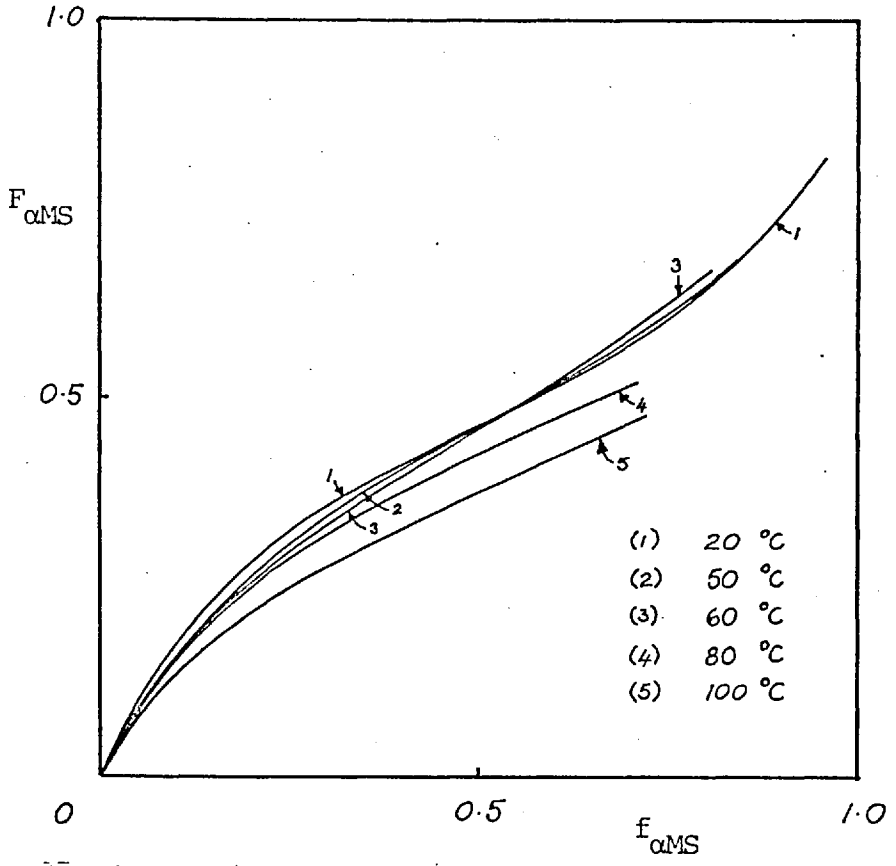

Fig.27 General temperature (at 1 atm.) and pressure (at 60°C) dependence of αMS-MMA system. Above: temperature dependence from Wittmer; below: pressure dependence from the Author.

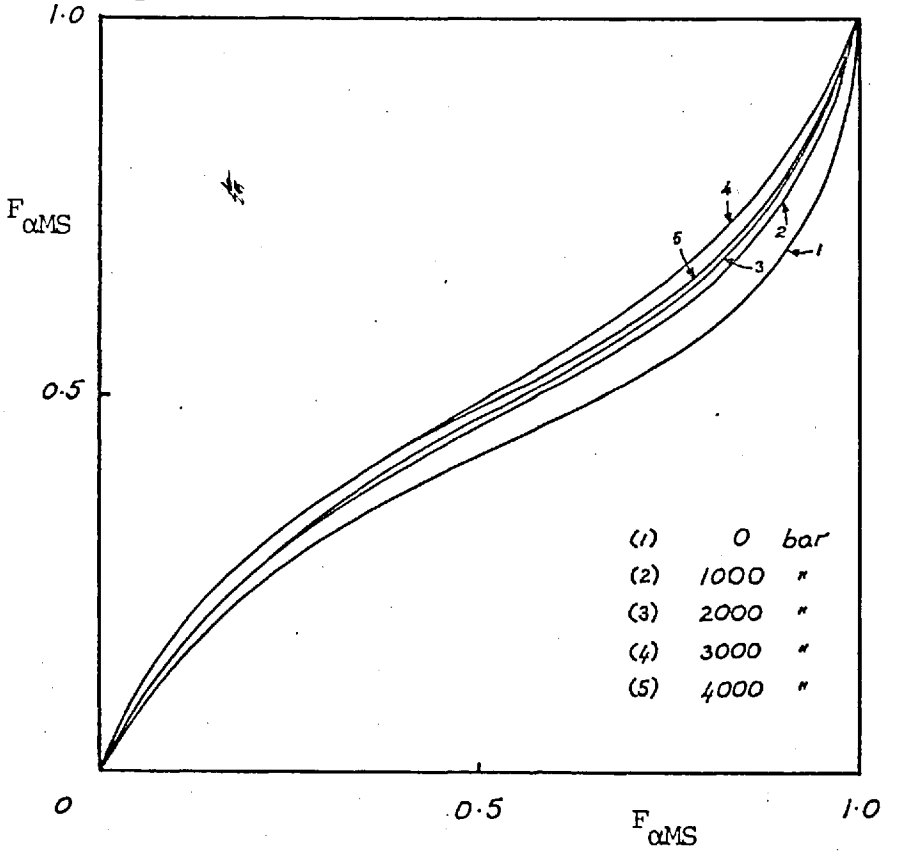

reactivity ratios). The first model tested was the simple Markoffian process of Mayo-Lewis, known also as the terminal unit model, in which only the ultimate unit of a radical chain has an influence on the copolymerization reaction. There are several methods (section (5.1)) of fitting the equation of this model to the data in order to obtain the reactivity ratios. Beside the widely used nonlinear regression (NLR) in this research, two other methods were used (which apply only to the terminal unit model), for comparison. These were the Mayo-Lewis line intersection method and the Fineman-Ross linearization method. Obviously only the NLR method can give true error values. The results of the NLR method were assessed by two kinds of error analysis (plus the sum of squares of the residuals): 1) The ± error as calculated by equation (5.1.22) and 2) the Jacobian matrix given for the calculation of error ellipses according to equation (5.1.25). Two ellipses calculated in this way are given in fig.(29). The other two methods were assessed approximately by a special procedure on a high speed computer: 1) the Mayo-Lewis method was used to produce a large number of intersection points. Then, after discarding a number of outliers, their gyration centre was calculated. The standard deviation given, as mentioned in section (5.1), is only a measure of the scatter of these points. 2) The coordinates of the Fineman-Ross plots were calculated and a line was fitted by linear least-squares. Again, the standard deviation given is only a measure of the residuals of linear least-squares.

The f_s-F_s curves from the NLR reactivity ratios are given in figures (28a) to (28j). The results of the three methods are given in Tables (XXIa-e) and figures (30a) to (30c). As seen in figures (30a-c) of the three methods the worst scatter along the pressure coordinate was from the Fineman-Ross linearization method. The Mayo-Lewis line intersection method gave slightly less scatter than NLR, but since the NLR method is a better and general method, priority was given to these results in the interpretation. The NLR method was used to treat the data of Wittmer and Izu et al. for most of the copolymerization models examined in this research. The terminal unit model reactivity ratios from the data obtained in this research at 60°C and normal pressure were closer to those estimated from Izu et al.'s data

than Wittmer's.

As seen in fig.(30c) there is quite noticeable change of the terminal unit model (apparent) reactivity ratios along the pressure coordinate. The change is an increase in r_B and a decrease in r_A with pressure. The rate of change of r_B with pressure levels off after 3000 atm which becomes a slight maximum due to a subsequent decrease at higher pressures. The mode of change of r_A is similar since a plot of $1/r_A$ shows a very similar change to that of r_B, in a larger scale.

The effect of pressure on reactivity ratios is expressed as a combined effect on both the rate constants involved, therefore in terms of activation volumes

$$\partial \ln \frac{k_{bb}}{k_{ba}} = \partial \ln r_B = - RT(V^{\neq}_{bb} - V^{\neq}_{ba}) \partial P \qquad (6.4.1)$$

and if

$$|\Delta V^{\neq}_{bb}| < |\Delta V^{\neq}_{ba}| \qquad (6.4.2)$$

one expects an increase in r_B with pressure. Although the increase in r_B in fig.(30c) may show that equation (6.4.2) is true, the nature of equation (6.4.1) which predicts an exponential increase of r_B with pressure may throw doubt on the validity of the terminal unit model as applied to this system. An explanation of the maximum is considered in a later section.

A similar mode of change in the 'terminal unit model' r's, but with respect to temperature, can be seen from analysis of the data of Wittmer and of Izu et al. In this case the change is in the direction of the inverse temperature axis (fig.(30d)). In fact the shape of the curves are very similar to those of the P curves, which may reopen the possibility that the decrease of r_B at the highest pressure may not be due entirely to experimental error.

The data of Wittmer and Izu et al. also demonstrates the invalidity of the terminal unit model for this system, at normal pressure. This is shown by the negative reactivity ratios which are obtained from the terminal unit model at higher temperatures, and have no physical meaning.

The usual way to check the goodness of fit of the model would be

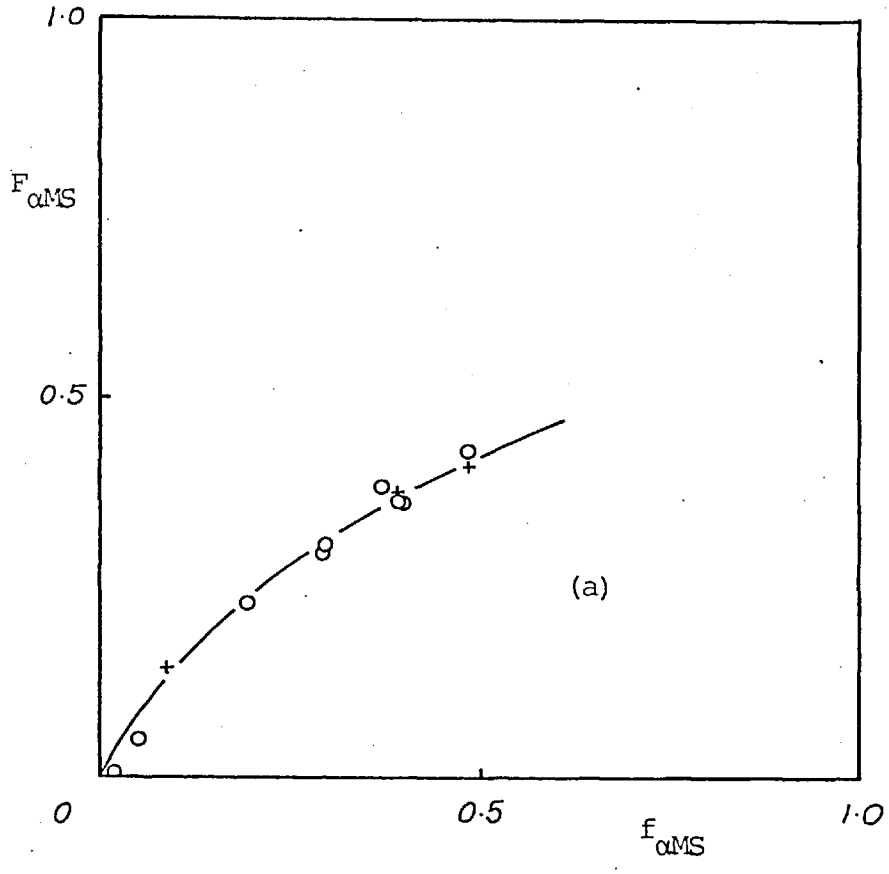

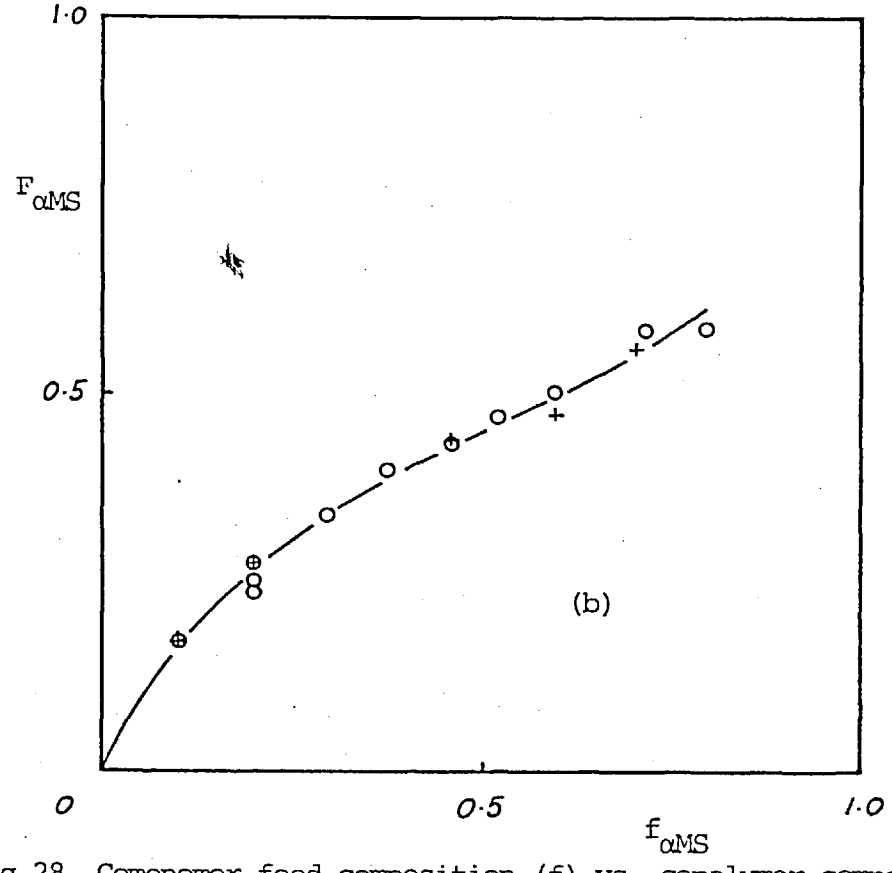

Fig.28 Comonomer feed composition (f) vs. copolymer composition (F) as obtained in this research for the constant temp. copolymerization of αMS and MMA, (cont'd)

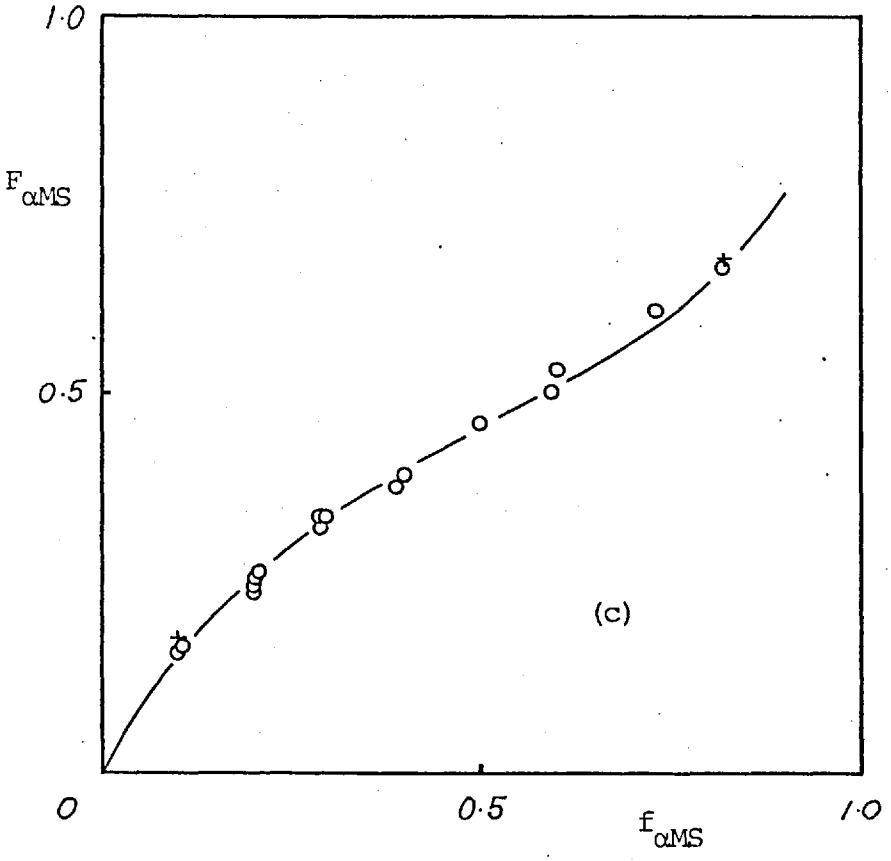

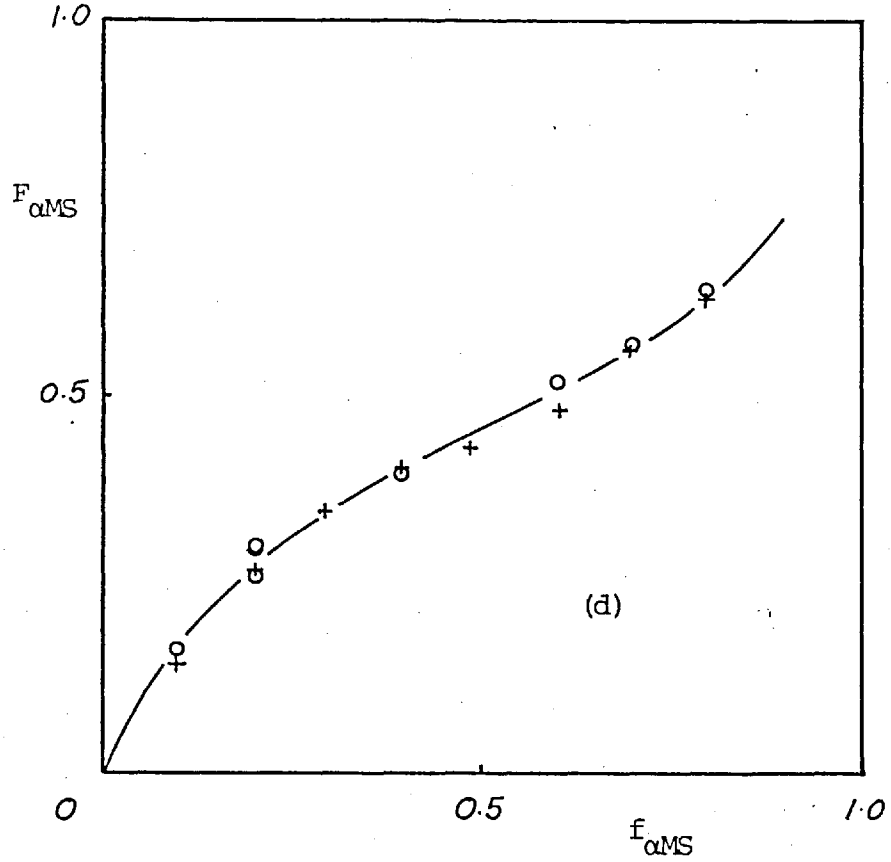

Fig.28 (Cont'd) o) copolymer composition from elemental analysis, x) from NMR; curves give the theoretical values for the terminal unit model as obtained by NMR; (cont'd)

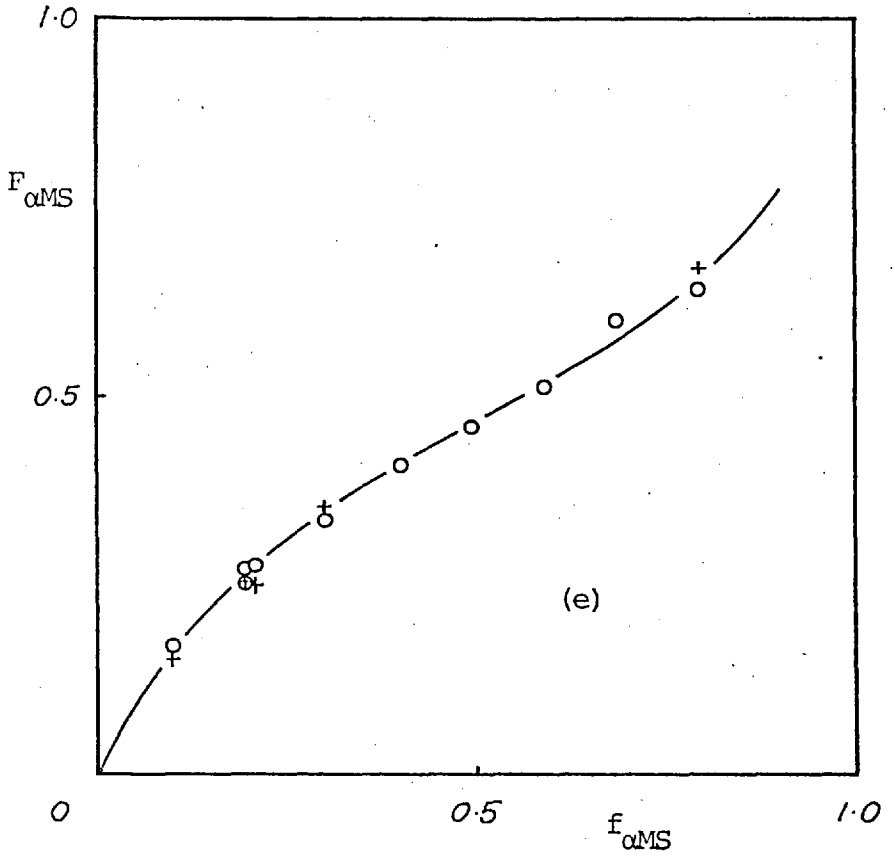

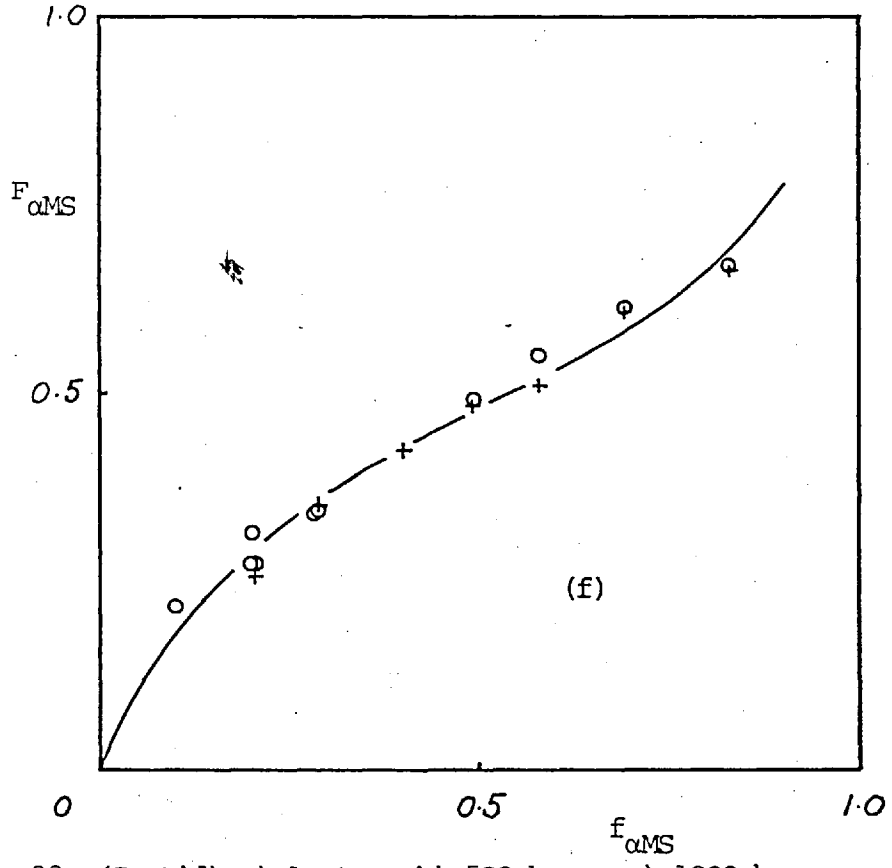

Fig.28 (Cont'd) a) 1 atm., b) 500 bars, c) 1000 bars, d) 1500 bars, e) 2000 bars, f) 2500 bars, (cont'd)

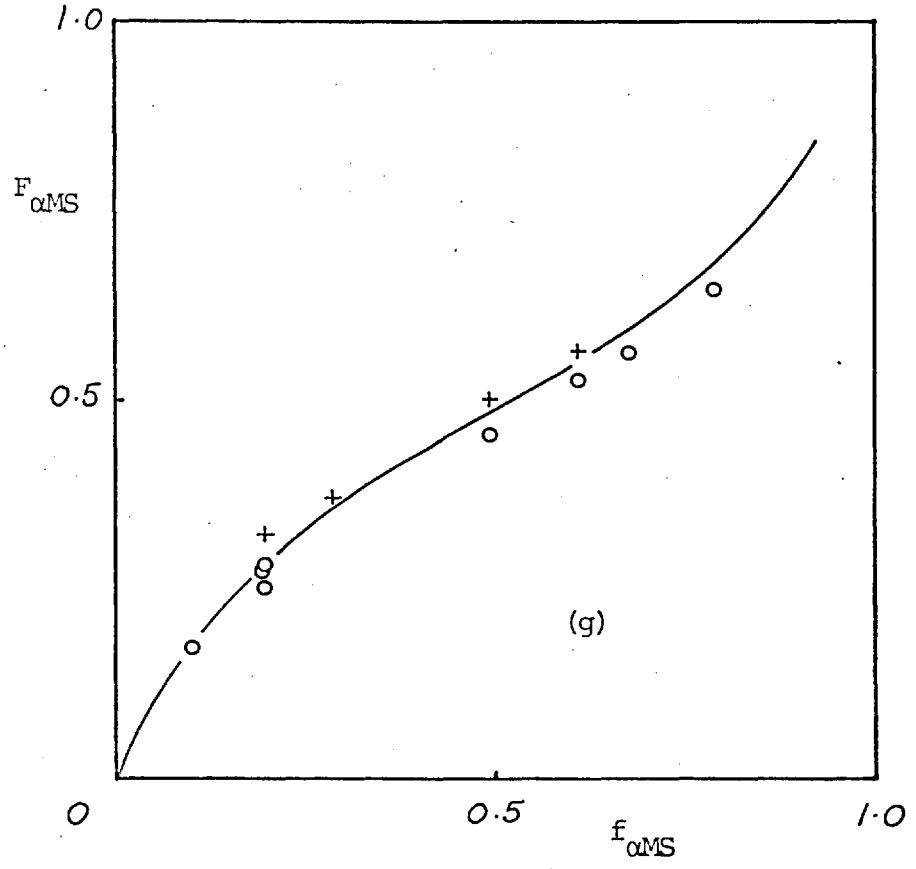

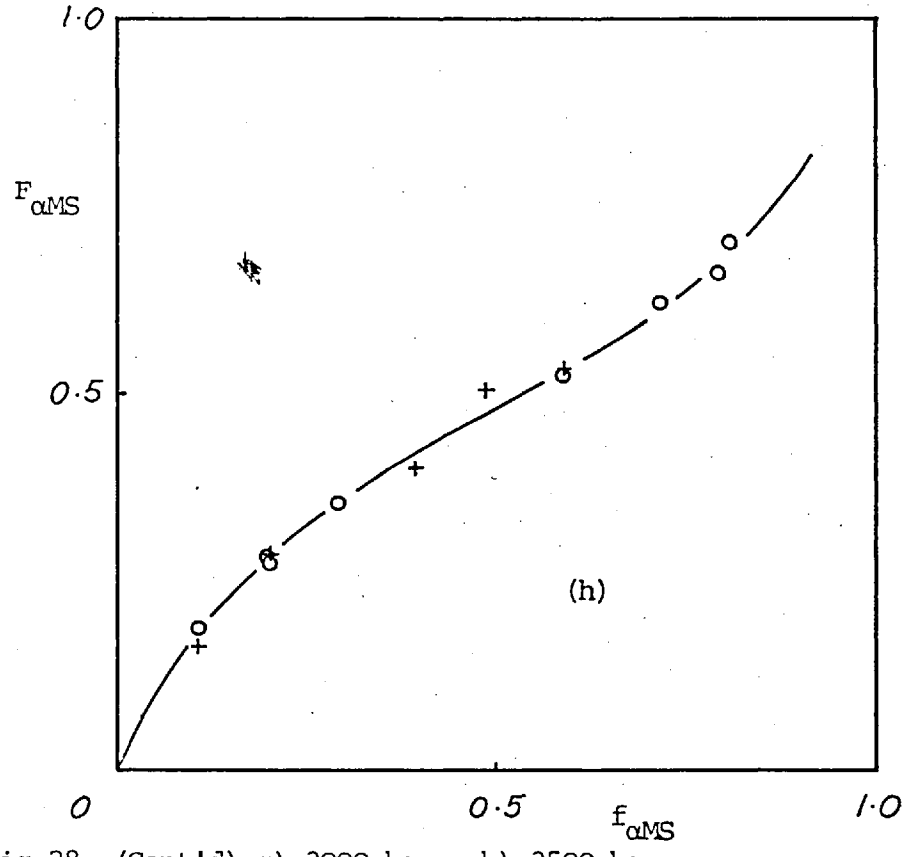

Fig.28 (Cont'd) g) 3000 bars, h) 3500 bars, (cont'd)

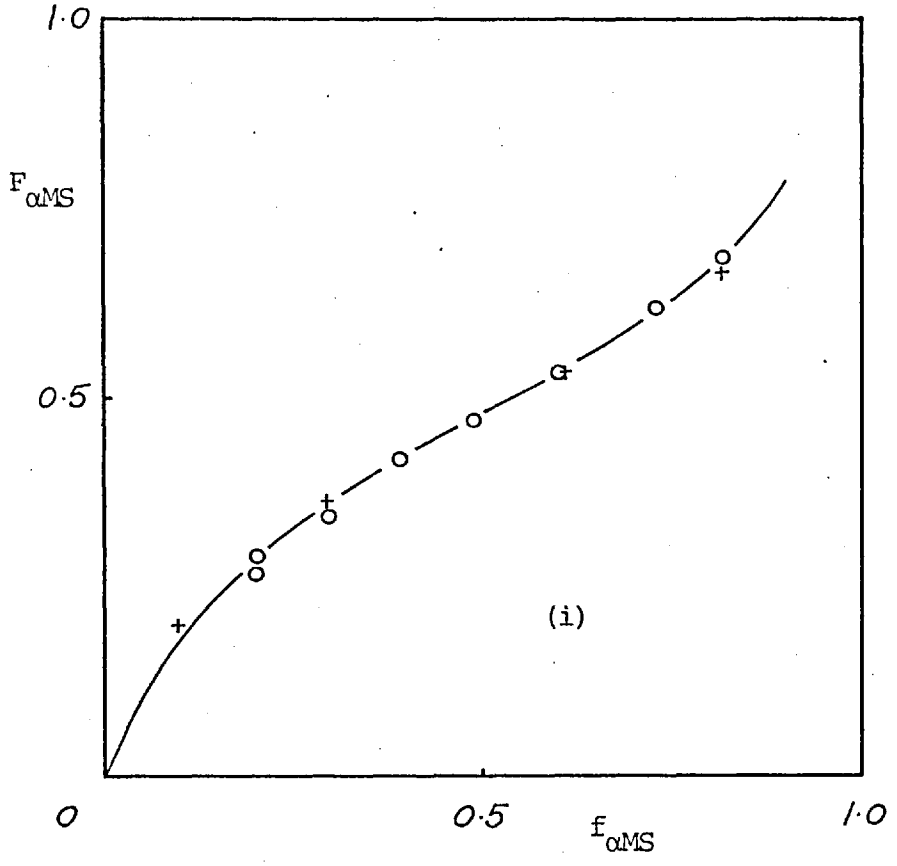

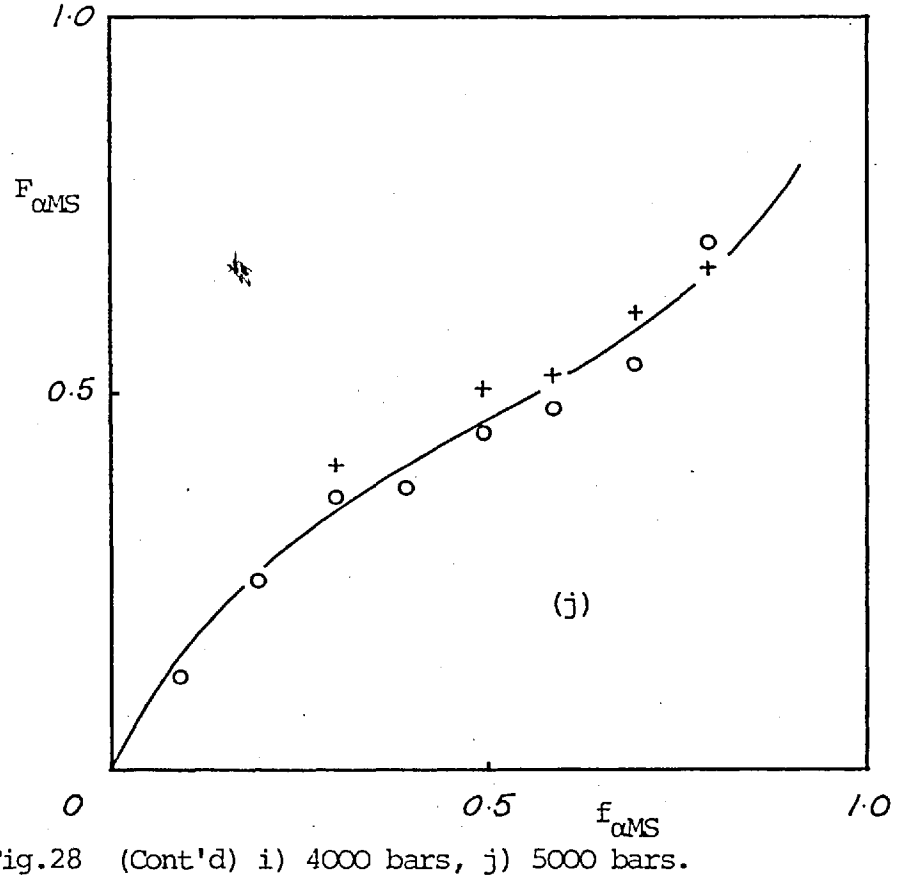

Fig.28 (Cont'd) i) 4000 bars, j) 5000 bars.

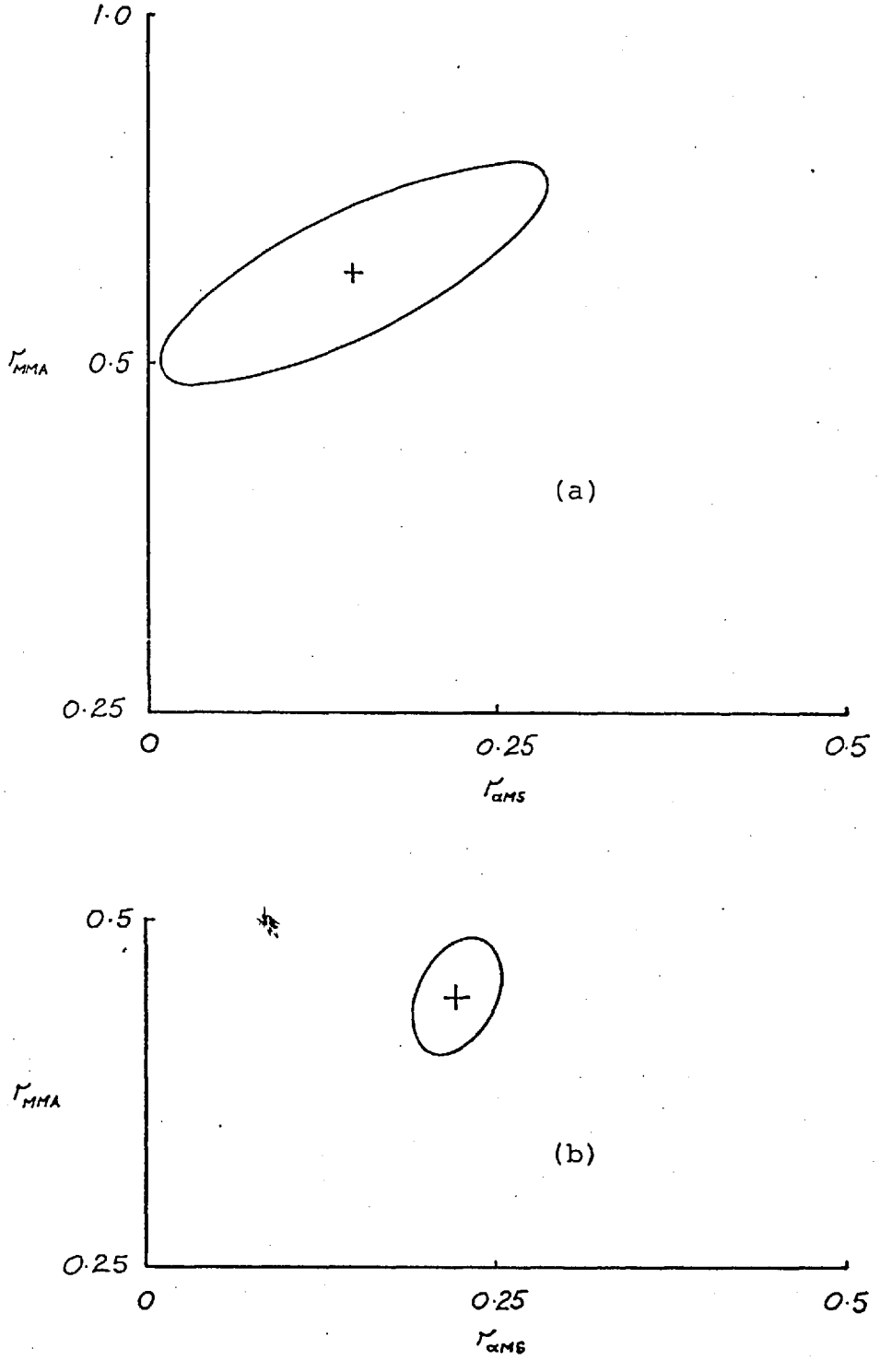

Fig.29 Terminal unit model confidence ellipses for two sets of data of this research, a) 60°C and 1 atm., b) 60°C and 1500 bars.

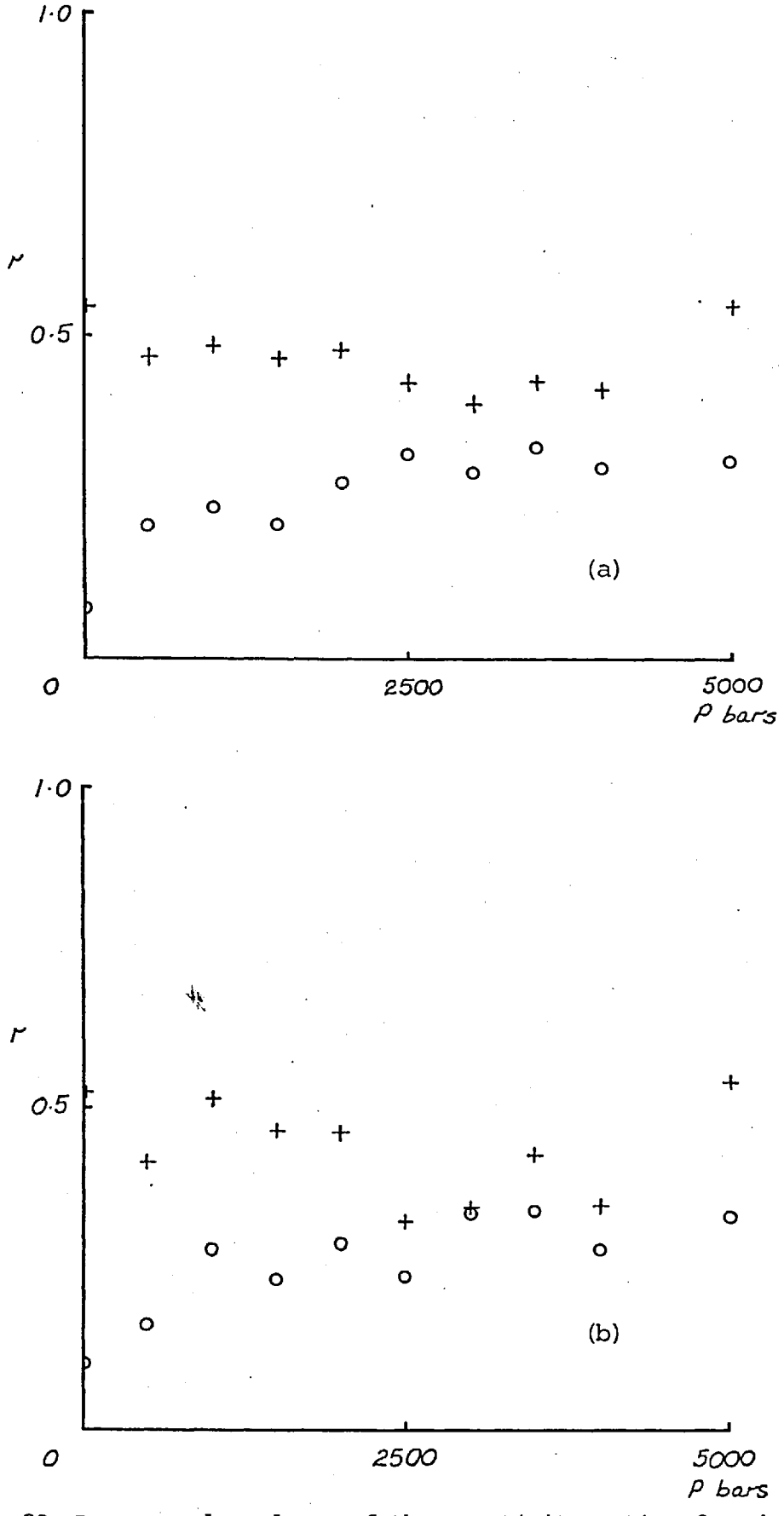

Fig.30 Pressure dependence of the reactivity ratios for the terminal unit model from the data of this research by a) Mayo-Lewis line intersection, b) Fineman-Ross linearization, (cont'd)

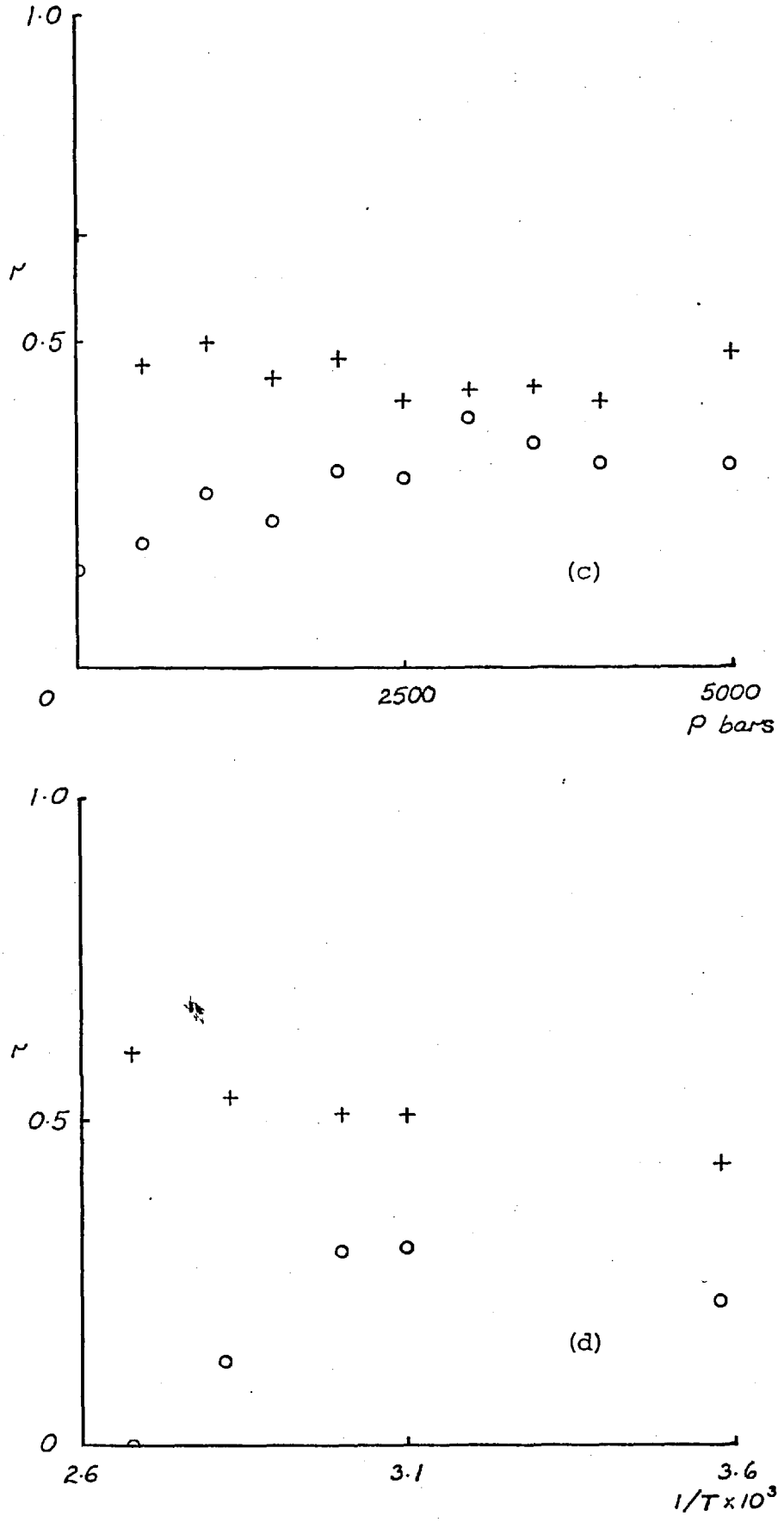

Fig.30 (Cont'd) c) NLR; temperature dependence of the reactivity ratios for the terminal unit model from the data of Wittmer by NLR. (o) $r_{\alpha MS}$, +) r_{MMA})

the existance of a correlation in the results but it is believed that the data are too scattered to make any systematic correlation obvious.

b) Penultimate unit model

The penultimate unit model was first tried without any simplifying assumptions, i.e., employing all four of the parameters, as in equation (4.1.3). This gave an abnormally scattered set of estimated parameters, which was attributed to trying to fit an equation of too many parameters to an insufficiently accurate set of data. Hence, another attempt was made using the simplifying assumption that $k_{bbb} = 0$. So,

$$X = \frac{1 + r'_A x \dfrac{1 + r_A x}{1 + r'_A x}}{1 + \dfrac{r_B/x}{1 + r_B/x}} \qquad (6.4.3)$$

This was a necessary assumption as seen from the results of this estimation, and also a justifiable assumption as indicated below. As seen in fig.(31) (from Table (XXIIa)) the three parameters now follow a rather consistent set of curves and the behaviour of the points at the end the curves seems too smooth to be attributed simply to experimental errors. Although the shoulder at 1000 atm in curves (ii) and (iii) may be due to experimental error the maxima in curves (ii) and (iv) (for $1/r'_A$) are far too prominent. The locations of the maxima, too, are similar to those from the terminal unit model at 3000 atm.

In general it can be said that:

1) k_{bbb} can be assumed to be zero or very close to it.

2) The rates of change of k_{aaa} and k_{aab} with pressure are of similar magnitude.

3) k_{abb} is largely increased by pressure but the curve of $r'_B = k_{abb}/k_{aba}$ has an abnormality similar to $r_B = k_{bb}/k_{ba}$ (terminal unit model) and gives a maximum at 3000 atm.

4) Similar behaviour to that of k_{abb} is seen in k_{bab} (especially when r'_A plotted as $1/r'_A$), possibly indicating that an A unit between two B units does not reduce their mutual repulsions.

Fig.(32) (Table (XXIIb)) shows the penultimate unit model reactivity ratios for the data of Wittmer.

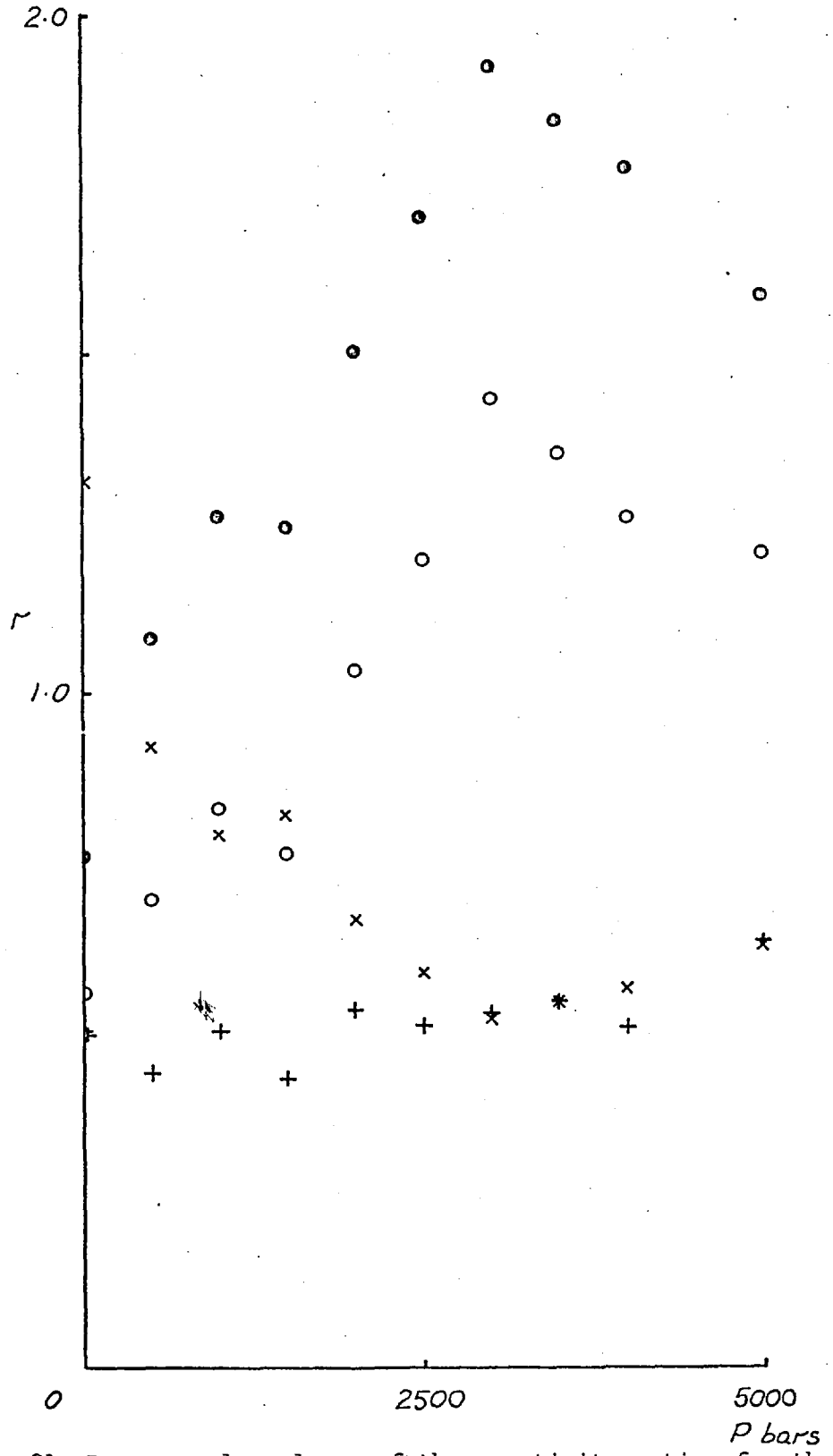

Fig.31 Pressure dependence of the reactivity ratios for the simplified penultimate unit model (eq.(6.4.3)) from the data of this research. (o) r_B, +) r_A, x) r_A', ⊙) $1/r_{A'}$)

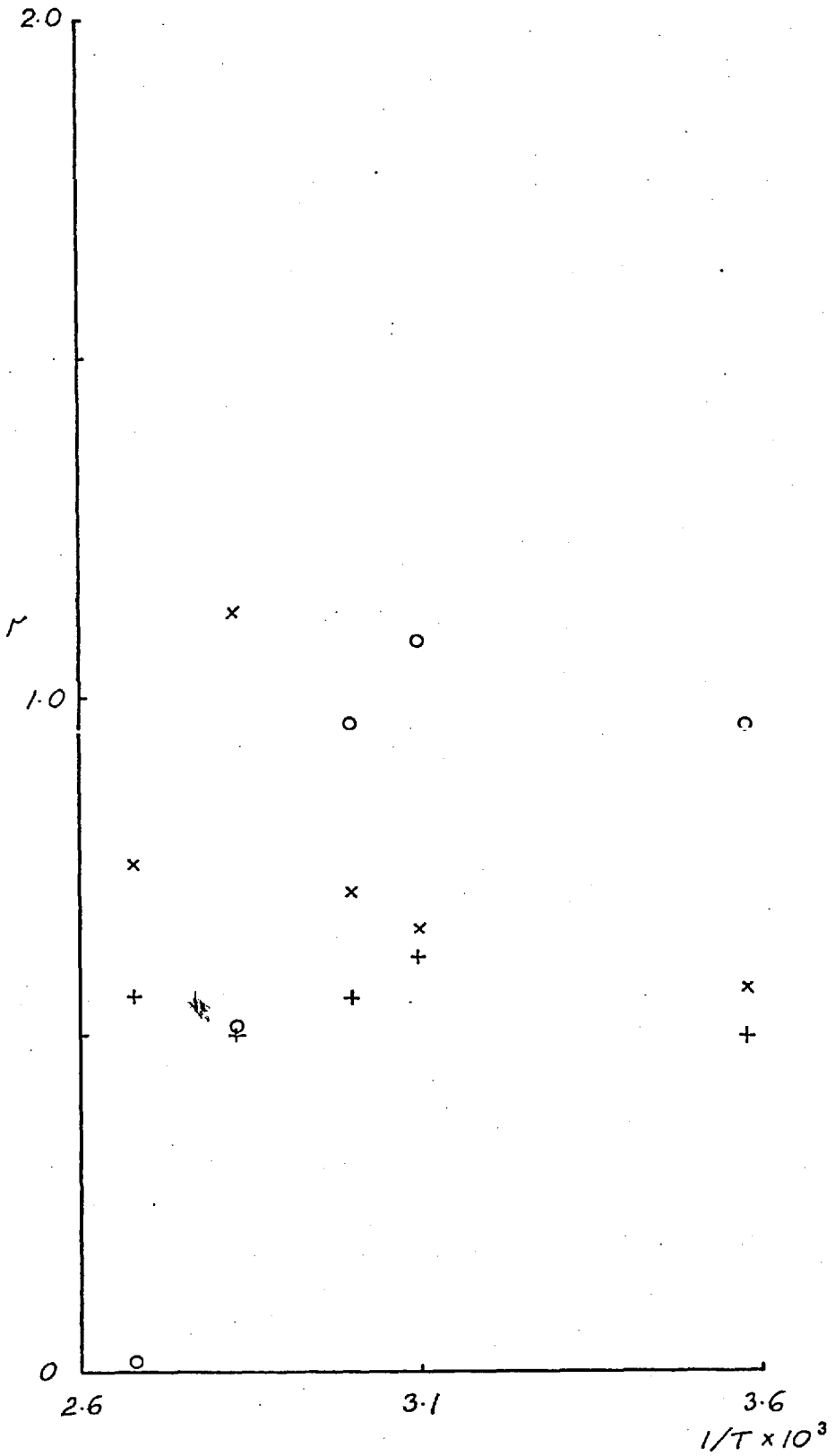

Fig.32 Temperature dependence of the reactivity ratios for the simplified penultimate unit model (eq.(6.4.3)) from the data of Wittmer. (legend same as fig.(31))

c) The penpenultimate unit model

As mentioned above it seems that the insufficient accuracy of the data makes an attempt to fit an equation with more than three parameters futile. But, as will be explained in later sections, there appears to be an indication of a penpenultimate effect of the form

$$BAA\cdot + B \longrightarrow BAAB\cdot$$

B being the sterically-hindered monomer (see section (1.3.2)). To show this effect by means of an equation the penpenultimate unit equation was used with simplifying assumptions, which make it equivalent to equations (4.1.3) with $k_{bbb} = 0$ and with k_{aaa} split into two components, k_{baaa} and k_{aaaa}. Both approaches yield the equation

$$X = \frac{1 + r'_A x \dfrac{1 + r_A x}{1 + r'_A x}}{1 + \dfrac{1 + 1/r''_A x}{1 + \dfrac{r_B}{r_B + x}}} \qquad (6.4.4)$$

Although containing four parameters, equation (6.4.4), supposedly a better equation, was expected to give a better fit. As seen in fig.(33) (from Table (XXIIIa)) the scatter of points in the r vs. P domain is low enough to reveal some information.

In another attempt the same equation was tried with r_B values as estimated from equation (6.4.3) thus reducing it to a three parameter equation. This did not improve the estimation much.

The effect of pressure on the reactivity ratios, as obtained from equation (6.4.4), can be summarized as follow:

1) Rate of change of k_{aaaa} and k_{aaab} are of similar magnitude

2) There is a sharp increase in k_{baab} though it is difficult to discern a logarithmic decrease of r'_A ($=k_{baaa}/k_{baab}$).

For the rest of the rate constants the same considerations apply as for the equation (6.4.3).

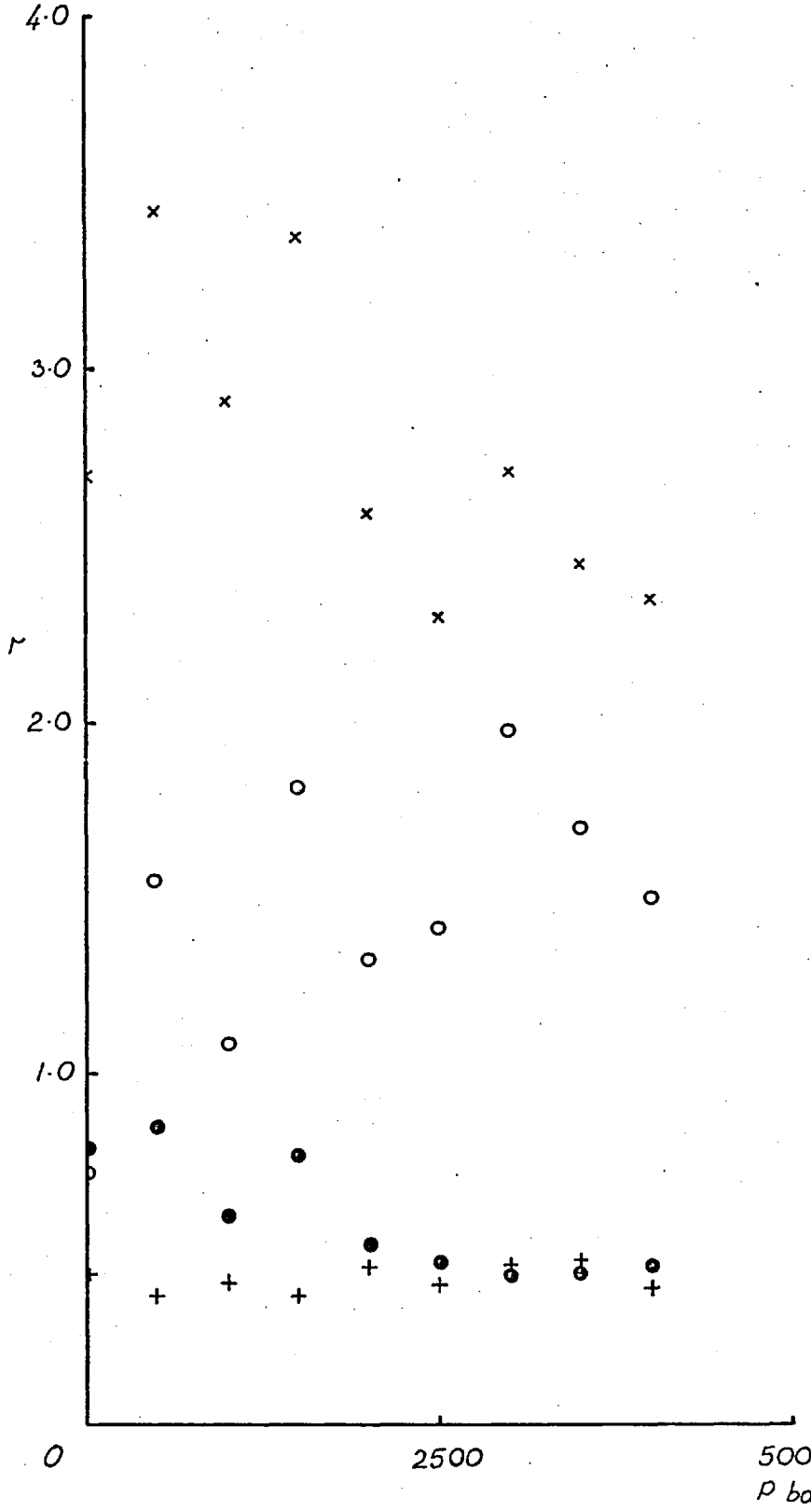

Fig.33 Pressure dependence of the reactivity ratios for the simplified penpenultimate unit model (eq.(6.4.4)) from the data of this research. (+) r_A, x) r_A', ●) r_A'', o) r_B)

Table XXIa

Reactivity ratios of αMS-MMA system at various pressures (this research) calculated by computerized Mayo-Lewis line intersection. T = 60°C.

P, bar g	r_{MMA}	$\sigma_{r_{MMA}}$	$r_{\alpha MS}$	$\sigma_{r_{\alpha MS}}$
0	0.5427	0.1019	0.0768	0.2260
500	0.4661	0.0982	0.2040	0.0928
1000	0.4846	0.1011	0.2319	0.1633
1500	0.4638	0.1316	0.2047	0.1349
2000	0.4775	0.0932	0.2709	0.1611
2500	0.4267	0.1385	0.3135	0.1770
3000	0.3931	0.1170	0.2894	0.1419
3500	0.4270	0.0870	0.3252	0.1508
4000	0.4156	0.0797	0.2924	0.1607
5000	0.5044	0.2068	0.3062	0.1713

Table XXIb

Reactivity ratios of αMS-MMA system at various pressures (this research) calculated by Fineman-Ross method. T = 60°C.

P, bar g	r_{MMA}	$\sigma_{r_{MMA}}$	$r_{\alpha MS}$	$\sigma_{r_{\alpha MS}}$
0	0.5237	0.0306	0.0991	0.0491
500	0.4167	0.0503	0.1610	0.0144
1000	0.5157	0.0417	0.2810	0.0120
1500	0.4653	0.0296	0.2318	0.0080
2000	0.4627	0.0380	0.2882	0.0133
2500	0.3218	0.0538	0.2359	0.0115
3000	0.3445	0.2005	0.3355	0.0715
3500	0.4277	0.0377	0.3406	0.0119
4000	0.3482	0.0679	0.2813	0.0159
5000	0.5419	0.1214	0.3341	0.0359

Table XXId

Reactivity ratios of αMS-MMA system at various temperatures (a) Wittmer, b) Izu et al.) calculated by Fineman-Ross method. P = 1 atm.

T, °C	r_{MMA}	$\sigma_{r_{MMA}}$	$r_{\alpha MS}$	$\sigma_{r_{\alpha MS}}$
a) 20	0.3339	0.0738	0.1820	0.0028
50	0.4568	0.0629	0.2637	0.0190
60	0.5084	0.0323	0.2996	0.0100
80	0.5927	0.0854	0.1399	0.0067
100	0.5864	0.0411	0.0129	0.0146
b) 60	0.5545	0.0365	0.1740	0.0233
114	1.3646	0.1074	0.0339	0.0031

Table XXIc

Reactivity ratios of αMS-MMA system at various pressures (this research) calculated by NLR, equation (1.3.15). T = 60°C.

P = 0 bar g

Reac. ratio	value	95% conf. limits	Jacobian^2	
r_{MMA}	0.5668	±0.0443	0.4516	-0.2124
$r_{\alpha MA}$	0.1475	±0.0762	-0.2124	0.1529

Sum of squares = $0.1236*10^{-2}$

P = 500 bar g

r_{MMA}	0.4647	±0.0377	1.0248	0.3834
$r_{\alpha MS}$	0.1905	±0.0300	0.3834	0.6491

Sum of squares = $0.3865*10^{-2}$

P = 1000 bar g

r_{MMA}	0.5003	±0.0349	0.8753	-0.4135
$r_{\alpha MS}$	0.2675	±0.0341	-0.4135	0.9182

Sum of squares = $0.7291*10^{-2}$

Table XXIc (cont'd)

P = 1000 bar g

Reac. ratio	value	95% conf. limits	Jacobian^2	
r_{MMA}	0.5003	±0.0349	0.8753	-0.4135
$r_{\alpha MS}$	0.2675	±0.0341	-0.4135	0.9182

Sum of squares = $0.7291*10^{*-2}$

P = 1500 bar g

r_{MMA}	0.4455	±0.0327	0.6761	-0.3363
$r_{\alpha MA}$	0.2228	±0.0259	-0.3363	1.0789

Sum of squares = $0.3745*10^{-2}$

P = 2000 bar g

r_{MMA}	0.4739	±0.0293	0.9198	-0.3546
$r_{\alpha MS}$	0.2997	±0.0358	-0.3546	0.6160

Sum of squares = $0.4385*10^{-2}$

P = 2500 bar g

r_{MMA}	0.4095	±0.0463	0.8010	-0.3744
$r_{\alpha MS}$	0.2904	±0.0451	-0.3744	0.8446

Sum of squares = $0.8317*10^{-2}$

P = 3000 bar g

r_{MMA}	0.4278	±0.0900	0.6269	-0.2651
$r_{\alpha MS}$	0.3828	±0.1014	-0.2651	0.4929

Sum of squares = $0.1782*10^{-1}$

P = 3500 bar g

r_{MMA}	0.4317	±0.0319	0.5282	-0.2351
$r_{\alpha MS}$	0.3452	±0.0311	-0.2351	0.5540

Sum of squares = $0.2200*10^{-2}$

P = 4000 bar g

r_{MMA}	0.4085	±0.0450	0.5959	-0.3569
$r_{\alpha MS}$	0.3112	±0.0374	-0.3569	0.8641

Sum of squares = $0.4135*10^{-2}$

Table XXIc (cont'd)

P = 5000 bar g

Reac. ratio	value	95% conf. limits	Jacobian^2	
r_{MMA}	0.4863	±0.1057	0.3976	-0.3082
$r_{\alpha MS}$	0.3126	±0.0767	-0.3082	0.7545

Sum of squares = $0.1381*10^{-2}$

Table XXIe

Reactivity ratios of αMS-MMA system at various temperatures (a) Wittmer, b) Izu et al.) calculated by NLR, equation (1.3.15). P = 1 atm.

a) T = 20°C

Reac. ratio	value	95% conf. limits	Jacobian^2	
r_{MMA}	0.4324	±0.0423	0.3681	-0.2106
$r_{\alpha MS}$	0.2221	±0.0288	-0.2106	0.7936

Sum of squares = $0.1672*10^{-2}$

T = 50°C

r_{MMA}	0.5110	±0.0510	0.2799	-0.1741
$r_{\alpha MS}$	0.3051	±0.0426	-0.1741	0.4015

Sum of squares = $0.1335*10^{-2}$

T = 60°C

r_{MMA}	0.5116	±0.0406	0.3145	-0.2260
$r_{\alpha MS}$	0.2969	±0.0316	-0.226	0.5210

Sum of squares = $0.1071*10^{-2}$

T = 80°C

r_{MMA}	0.5369	±0.0406	0.2498	-0.2279
$r_{\alpha MS}$	0.1282	±0.0161	-0.2279	1.5891

Sum of squares = $0.1071*10^{-2}$

Table XXIe (cont'd)

$T = 100^{\circ}C$

Reac. ratio	value	95% conf. limits	Jacobian^2	
r_{MMA}	0.6042	±0.0658	0.1819	-0.2064
$r_{\alpha MS}$	-0.0068	±0.0349	-0.2064	0.6477

Sum of squares = $0.1005*10^{-2}$

b) $T = 60^{\circ}C$

r_{MMA}	0.5639	±0.0513	0.2426	-0.1594
$r_{\alpha MS}$	0.1922	±0.0514	-0.1594	0.2412

Sum of squares = $0.5467*10^{-3}$

$T = 114^{\circ}C$

r_{MMA}	1.3030	±0.1325	0.0362	-0.1835
$r_{\alpha MS}$	-0.0368	±0.0093	-0.1835	7.2920

Sum of squares = $0.5743*10^{-3}$

Table XXIIa

Reactivity ratios of αMS-MMA system at various pressures (this research) calculated from equation (6.4.3).

$T = 60^{\circ}C$. (A=MMA, B=αMS).

$P = 0$ bar g

Reac. ratio	value	95% conf. limits	Jacobian^2		
r_A	0.4971	±0.0968	0.2121	0.0300	-0.0603
r'_A	1.3141	±35.89	0.0300	0.0070	-0.0141
r_B	0.5532	±17.54	-0.0603	-0.0141	0.0285

Sum of squares = $0.8278*10^{-3}$

$P = 500$ bar g

r_A	0.4405	±0.2427	0.2797	0.0560	-0.0573
r'_A	0.9224	±22.35	0.0560	0.0277	-0.0293
r_B	0.6945	±20.70	-0.0573	-0.0293	0.0310

Sum of squares = $0.3396*10^{-2}$

Table XXIIa (cont'd)

P = 1000 bar g

Reac. ratio	value	95% conf. limits	Jacobian^2		
r_A	0.5047	±0.4648	0.3507	0.1021	-0.0719
r'_A	0.7922	±40.19	0.1021	0.0558	-0.0401
r_B	0.8332	±54.87	-0.0719	-0.0401	0.0288

Sum of squares = $0.1866*10^{-1}$

P = 1500 bar g

r_A	0.4298	±0.2867	0.3004	0.0729	-0.0571
r'_A	0.8023	±14.57	0.0729	0.0392	-0.0321
r_B	0.7646	±17.17	-0.0571	-0.0321	0.0263

Sum of squares = $0.7556*10^{-2}$

P = 2000 bar g

r_A	0.5312	±0.5618	0.3356	0.1246	-0.0573
r'_A	0.6645	±87.59	0.1246	0.0711	-0.0329
r_B	1.0356	±187.2	-0.0573	-0.0329	0.0152

Sum of squares = $0.1098*10^{-1}$

P = 2500 bar g

r_A	0.5077	±1.089	0.2274	0.1135	-0.0394
r'_A	0.5863	±725.3	0.1135	0.0925	-0.0321
r_B	1.1980	±2081	-0.0394	-0.0321	0.0112

Sum of squares = $0.1292*10^{-1}$

P = 3000 bar g

r_A	0.5283	±1.7519	0.1926	0.1042	-0.0261
r'_A	0.5191	±81.57	0.1042	0.0926	-0.0229
r_B	1.4369	±338.2	-0.0261	-0.0229	0.0057

Sum of squares = $0.3467*10^{-1}$

Table XXIIa (cont'd)

P = 3500 bar g

Reac. ratio	value	95% conf. limits	Jacobian^2		
r_A	0.5445	±0.8573	0.2065	0.1083	-0.0300
r'_A	0.5417	±63.37	0.1083	0.0925	-0.0254
r_B	1.3556	±234.5	-0.0300	-0.0254	0.0070

Sum of squares = $0.1222*10^{-1}$

P = 4000 bar g

r_A	0.5070	±0.8675	0.1564	0.0853	-0.0268
r'_A	0.5624	±514.2	0.0853	0.0788	-0.0247
r_B	1.2624	±1642	-0.0268	-0.0247	0.0078

Sum of squares = $0.1373*10^{-1}$

P = 5000 bar g

r_A	0.6334	±1.152	0.0955	0.0645	-0.0231
r'_A	0.6286	±40.09	0.0645	0.0732	-0.0258
r_B	1.2090	±116.3	-0.0231	-0.0258	0.0091

Sum of squares = $0.2348*10^{-1}$

Table XXIIb

Reactivity ratios of MS-MMA system at various temperatures (a) Wittmer, b) Izu et al.) calculated from equation (6.4.3). P = 1 atm. (A=MMA, B=αMS).

a) T = 20°C

Reac. ratio	value	95% conf. limits	Jacobian^2		
r_A	0.4973	±1.050	0.1201	0.0423	-0.0221
r'_A	0.6898	±86.79	0.0423	0.0327	-0.0174
r_B	0.9605	±160.7	-0.0221	-0.0174	0.0093

Sum of squares = $0.2907*10^{-1}$

T = 50°C

r_A	0.6171	±0.5821	0.0853	0.0414	-0.0177
r'_A	0.6603	±157.4	0.0414	0.0386	-0.0164
r_B	1.0841	±371.7	-0.0177	-0.0164	0.0070

Sum of squares = $0.3314*10^{-2}$

Table XXIIb (cont'd)

T = 60°C

Reac. ratio	value	95% conf. limits	Jacobian^2		
r_A	0.5544	±0.6541	0.1013	0.0399	-0.0215
r'_A	0.7150	±115.1	0.0399	0.0345	-0.0187
r_B	0.9605	±211.6	-0.0215	-0.0187	0.0102

Sum of squares = $0.6147*10^{-2}$

T = 80°C

r_A	0.5014	±0.3162	0.1156	0.0211	-0.0352
r'_A	1.1278	±16.60	0.0211	0.0107	-0.0188
r_B	0.5135	±9.079	-0.0352	-0.0188	0.0334

Sum of squares = $0.5089*10^{-2}$

T = 100°C

r_A	0.5591	±0.1215	0.0839	0.0244	-0.0591
r'_A	0.7537	±0.4541	0.0244	0.0192	-0.0778
r_B	0.0153	±0.0795	-0.0591	-0.0778	0.4384

Sum of squares = $0.9036*10^{-3}$

b) T = 60°C

r_A	0.6770	±0.1507	0.0612	0.0963	-0.0742
r'_A	0.4077	±0.1499	0.0963	0.1869	-0.1566
r_B	0.1928	±0.113	-0.0742	-0.1566	0.1518

Sum of squares = $0.2206*10^{-3}$

T = 114°C

r_A	0.9959	±0.1536	0.0218	0.0034	-0.0787
r'_A	0.2463	±0.9153	0.0034	0.0012	-0.0742
r_B	-0.0211	±0.0074	-0.0787	-0.0742	9.8911

Sum of squares = $0.1109*10^{-3}$

Table XXIIIa

Reactivity ratios of αMS-MMA system at various pressures (this research) calculated from equation (6.4.4). T = 60°C. (A=MMA, B=αMS)

P, bar g	r_A	r'_A	r''_A	r'_B	ss*10^3
0	0.4292	2.6963	0.7857	0.7175	0.5230
500	0.3714	3.4513	0.8481	1.5517	3.1916
1000	0.4055	2.9102	0.5945	1.0853	15.824
1500	0.3709	3.3749	0.7701	1.8188	6.8204
2000	0.4486	2.5896	0.5128	1.3275	9.3562
2500	0.3967	2.3039	0.4604	1.4170	10.824
3000	0.4571	2.7088	0.4258	1.9784	33.218
3500	0.4705	2.4521	0.4290	1.7031	10.669
4000	0.3912	2.3512	0.4487	1.5050	11.547

ss = sum of squares

Table XXIIIb

Reactivity ratios of αMS-MMA system at various temperatures (a) Wittmer, b) Izu et al.) calculated from equation (6.4.4). P = 1 atm. (A=MMA, B=αMS).

T, °C	r_A	r'_A	r''_A	r_B	ss*10^3
a)					
20	0.4410	4.4788	0.5733	1.7902	27.699
50	0.5463	2.5302	0.5116	1.3349	2.5262
60	0.4622	2.5791	0.5494	1.1770	4.7116
80	0.4937	0.5302	1.1147	0.5179	5.0876
100	0.5305	1.6995	0.4835	-0.0009	0.8126
b)					
60	0.6754	1.5221	0.3012	0.1718	0.2177
114	1.5106	0.4088	3.9952	-0.0147	0.0047

ss = sum of squares

6.4.2 Equilibrium Constants for Depropagating Monomers

Before discussing copolymerization models which include polymer-monomer equilibria it is useful to consider available data on equilibria for the monomers.

Since for models with depropagating reaction steps the reversible reaction is assumed to follow the rules of equilibrium homopolymerization it is important to establish the equilibrium constant accurately. Wittmer[98] calculated the equilibrium conatant for αMS from the equilibrium monomer concentration data of McCormick[64] which yield

Table XXIV

T^oC	K(mole/lt)
20	1.7
40	3.6
50	5.1
60	7.1
80	12.9
100	22.9
150	67

where $K=k_d/k_p=[M]_e$ unlike the usual equilibrium constant of $K=k_p/k_d=1/[M]_e$. This set of data has been found (present work) to be expressed by the empirical equation (6.4.5).

$$K_t = \exp(3487/(273 + t) - 12.4309) \qquad (6.4.5)$$

where $K=k_p/k_d$. Equation (6.4.5) was used during the analysis of data by the models described by Wittmer and Lowry.

Worsfold and Bywater[65] obtained results for equilibrium monomer concentrations of αMS slightly different from those of McCormick but close to those of other researchers (see section (2.4)). Their results were also used by O'Driscoll and Gasparro[103]. The $1/[M]_e$ data of Worsfold and Bywater against temperature are found (present work) to fit the following empirical equation.

$$K_t = \exp(4025/(273 + t) - 14.4498) \qquad (6.4.6)$$

where $K=k_p/k_d$. Equation (6.4.6) was favoured in this research for the analysis of data but equation (6.4.5) was also used alongside, especially to analyse the data of Wittmer.

The dependence of K upon pressure was calculated from the molar volume difference of reactants and products plus the assumption that this molar volume difference remains constant over the whole pressure range. Then from

$$RT\left(\frac{\partial \ln K}{\partial P}\right)_T = -\Delta V^o \qquad (1.4.10)$$

at 60°C one obtains

$$K_p = \exp(0.005312P + \ln K_{1\ atm}) \qquad (6.4.8)$$

where P is in bar and ΔV^o is the value of Kilroe and Weale[59], and $K=k_p/k_d$.

Stein, Wittmer and Tölle, in their paper on the ceiling temperatures of αMS[66] (see section (2.4)), give an extensive set of results on the monomer-polymer equilibrium constant at various temperatures and pressures. The complete set of results is given in Table(XXV). Again McCormick's values for ΔH and ΔS^o were used in the calculations.

Table XXV

$\underline{K}$ (mole/lt) (= $M_e = k_d/k_p$)

P(atü)	40°C	50°C	60°C	80°C	100°C
0	3.63	5.14	7.10	12.9	22.9
500	2.46	3.53	4.96	9.15	15.9
1000	1.67	2.42	3.43	6.49	11.4
1500	1.13	1.66	2.38	4.60	8.27
2000	0.766	1.14	1.65	3.25	5.97
2500	0.519	0.780	1.14	2.30	4.31
3000	0.325	0.536	0.794	1.63	3.11
3500	0.239	0.367	0.551	1.16	2.24
4000	0.161	0.252	0.382	0.819	1.41
4500	0.109	0.173	0.265	0.580	1.17
5000	0.074	0.119	0.174	0.410	0.841
M_{max}	7.56	7.48	7.40	7.25	7.08

The last row shows the monomer concentration of the undiluted monomer.

The above workers produced the general equation for K by integrating equations (6.4.9) and (6.4.10)

$$\left(\frac{\partial \Delta H}{\partial P}\right)_T = \Delta V - T \left(\frac{\partial \Delta V}{\partial T}\right)_P \qquad (6.4.9)$$

$$\left(\frac{\partial \Delta S^o}{\partial P}\right)_T = \left(\frac{\partial \Delta V}{\partial T}\right)_P \qquad (6.4.10)$$

combining into equation (6.4.11)

$$0 = \Delta H_1 - T\Delta S_1^o + \Delta V(P - 1) - RT \ln[M]_e \qquad (6.4.11)$$

and treating the data of Table (XXV) , as

$$\ln [M]_e = \frac{-6960 + 24.8\ T - 0.481\ (P - 1)}{1.968\ T} \qquad (6.4.12)$$

The depropagation of methyl methacrylate at 60°C is almost negligible with an equilibrium constant of

$$K = k_p/k_d = 93.46 \text{ lt/mole}$$

Therefore it was assumed to be nondepropagating for all models except the Monte-Carlo simulation model in section (6.5). For this model the equilibrium monomer concentration of Bywater[108] was used to obtain the empirical equation

$$K_t = \exp(6450/(273 + t) - 14.83) \qquad (6.4.13)$$

where $K=k_p/k_d$. Since an increase in pressure will only increase K even more, the effect of pressure on K (MMA) was ignored altogether.

6.4.3 Copolymerization Model with Depropagating Reaction Steps

The simplest model of copolymerization combined with depropagation is one which considers the depropagation of only one monomer whenever it is attached to its own kind. Therefore of the four terminal unit reactions only one is reversible, i.e.,

$$\sim\sim B\cdot + B \rightleftharpoons \sim\sim BB\cdot$$

To a close approximation (according to Wittmer) the system of αMS and MMA follows this mechanism with equation (4.1.44). The data obtained in this research were analysed by the case (i) equation of Wittmer and by the case (i) equation of Lowry, which are derived from the same reaction scheme and give exactly the same results.

Surprisingly it was found impossible to duplicate Wittmer's results from his data using his case (i) equation. The reactivity ratios obtained from Wittmer's data by the case (i) equation using equation (6.4.6) and (6.4.12) for the calculation of K values are given in Tables (XXVIb) and (XXVId) and shown in figures (36b) and (34b) respectively. They also include one set of r's obtained from Izu et al.'s data. The reactivity ratios obtained from the data of this research similarly using equations (6.4.8) and (6.4.12) for the calculation of K values are given in Tables (XXVIa) and (XXVIc) and shown in figures (36a) and (34a) respectively.

The reactivity ratios obtained from Wittmer's data using equation (6.4.5) (as used by Wittmer) and his case (i) equation do not seem to be similar to those calculated by Wittmer. Apart from the values, the trend of change also does not seem to be similar, as, instead of being logarithmic, they pass through a maximum with increase of T. The reason for this discrepancy has not been found but it may be useful, although not conclusive, to mention that NLR was used for the present estimation whereas Wittmer used trial-and-error visual curve fitting. (at 1 atm. eq.(6.4.12)= eq.(6.4.5))

When equation (6.4.6) is used to produce K values the reactivity ratios obtained from Wittmer's data by the case (i) equation become anomalous. The maximum appears at r_B=513.24. This is due to the ill-conditioning of the equation and its physical meaning is further considered in section (6.9).

The reactivity ratios obtained from the data of this research by the case (i) equation using both sets of K values do not show any anomalies and are much smoother; but both sets of r's pass through a maximum. The physical meaning of this maximum, too, is considered in section (6.4.6).

As far as known to the Author the case (i) equation of Lowry (which is similar to Wittmer's case (i)) was used only by Ivin and

Spensley[104] for the system of styrene-methyl methacrylate at 132°C (ceiling temperature of MMA = 160°C). For some unknown reason only composition high in MMA were treated by the equation.

The case (iii) equation of Wittmer (which is similar to Lowry's case (ii) equation) was also used to treat the data of this research and the other workers. This model, as in equations (4.1.40) and (4.1.49) considers only the reversibility of one monomer when attached to two or more of its own kind

$$\sim\sim BB\cdot + B \rightleftharpoons \sim\sim BBB\cdot$$

With this equation, as seen in Tables (XXVIIa) to (XXVIId) and figures (35) and (37) it was possible to produce reactivity ratio values, from the data of Wittmer, close to the reactivity ratios presented by this worker. The difference between the K producing equations did not make much difference in the estimated values.

The estimated reactivity ratios from the data of this research are given in Tables (XXVIIa) and (XXVIIc) and shown in figures (35a) and (37a). Although the estimated reactivity ratios are fairly smooth the maximum in r_B at around 3000 bars is prominent; whereas r_A follows a steady decrease.

Wittmer's paper does not compare the goodness of fit of the different models and it is difficult to judge the best fit, but from the curves it seems there is not much difference. The argument put forward by Wittmer is that since

$$k = A\, e^{-E/RT} \qquad (6.4.14)$$

and

$$r_{bb} = \frac{A_{bb}}{A_{ba}} \exp\left(-\frac{E_{bb} - E_{ba}}{RT}\right) \qquad (6.4.15)$$

ln r should be a linear function of 1/T and on this basis it seems that case (i) defines (according to Wittmer) the best model.

Wittmer fits his higher temperature data on the αMS-MMA system (100° - 150°C) to equation (4.1.50) but since the conditions of polymerization are different from those of this research they have not been treated by the Author.

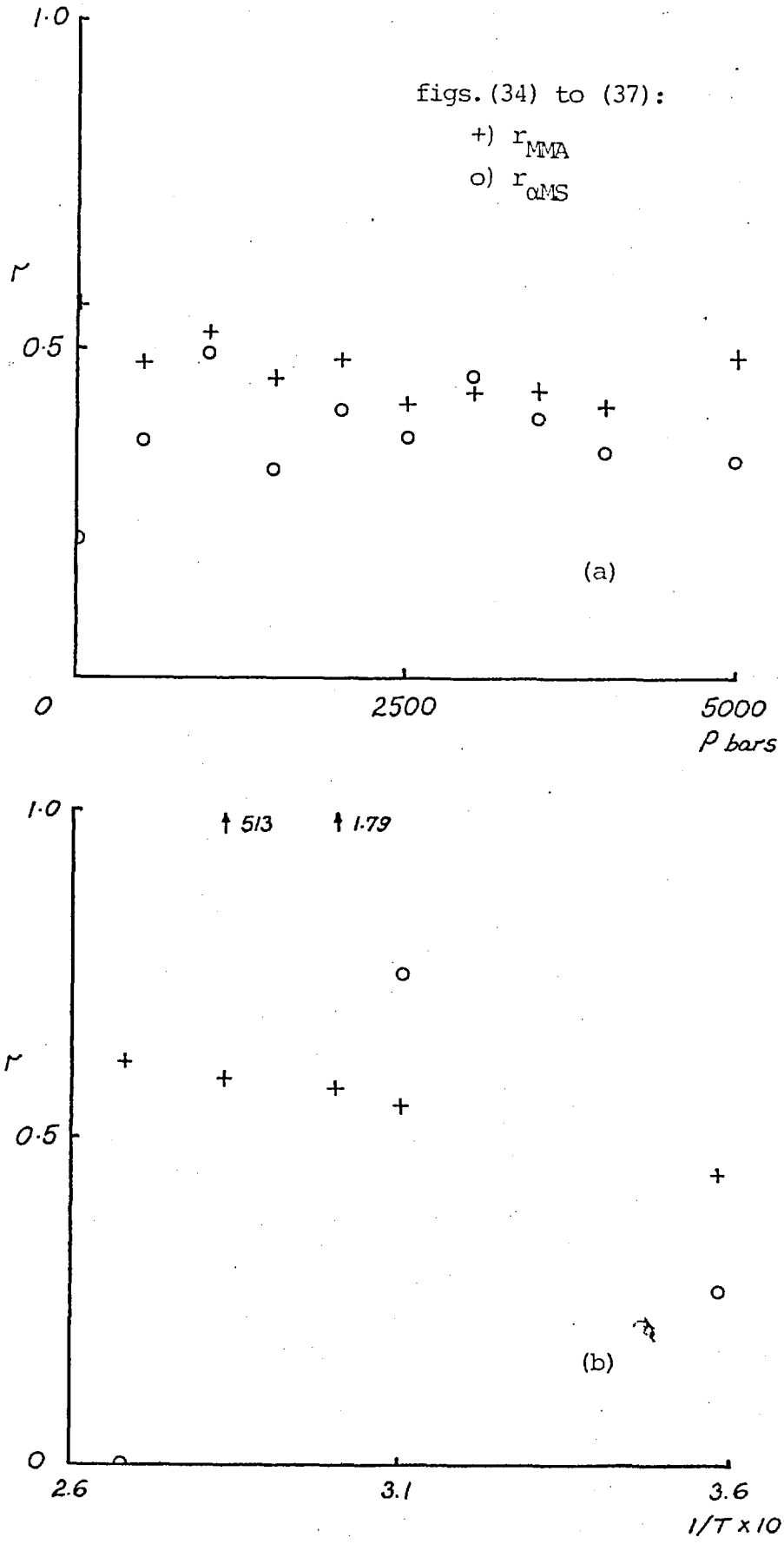

Fig. 34 Pressure and temperature dependence of the reactivity ratios for case (i) eq. (4.1.44) of Wittmer; a) data of this research with eq. (6.4.12), b) data of Wittmer with eq. (6.4.12).

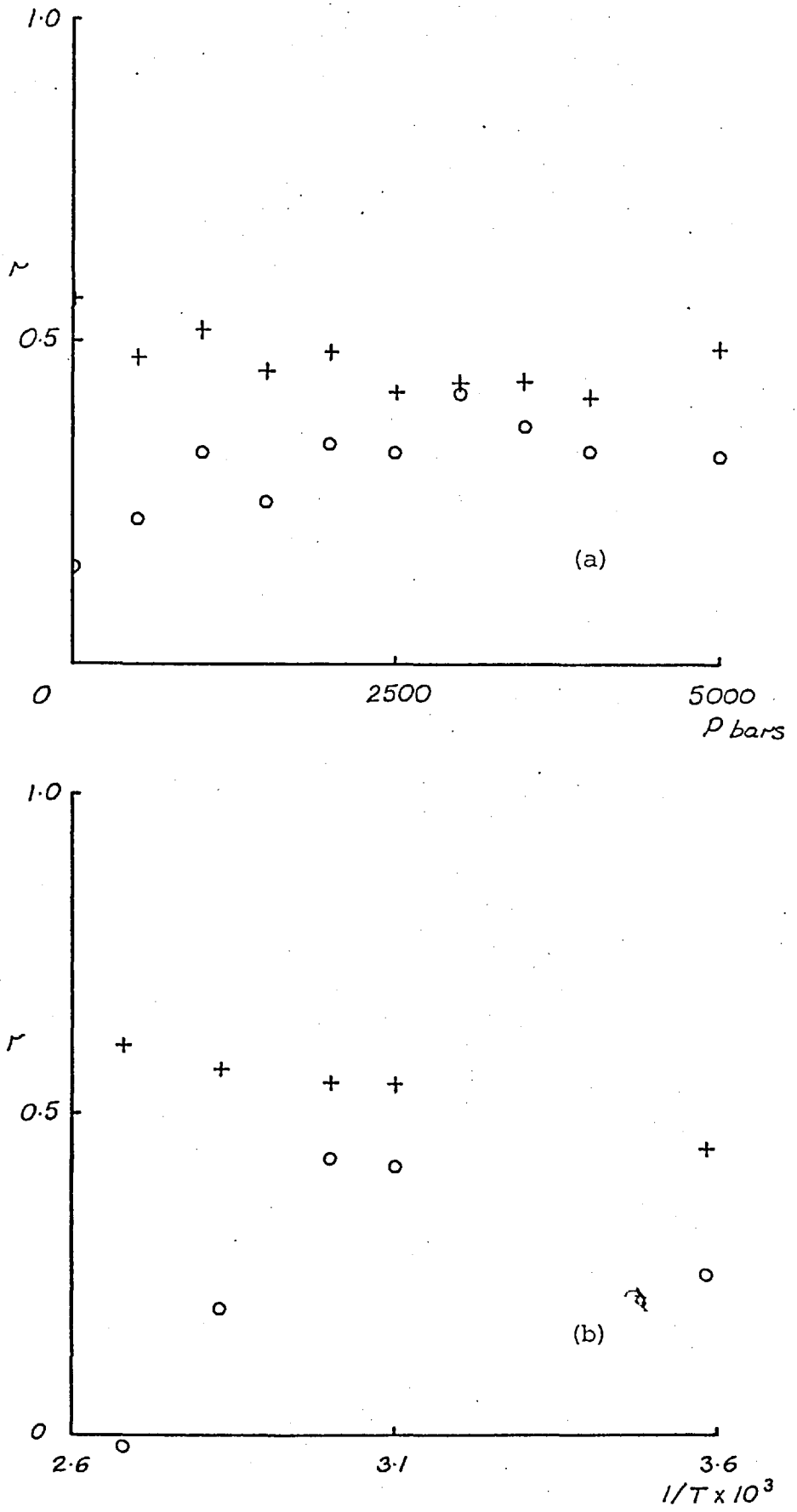

Fig.35 Pressure and temperature dependence of the reactivity ratios for case(iii) eq.(4.1.49) of Wittmer; a) data of this research with eq.(6.4.8), b) data of Wittmer with eq.(6.4.6).

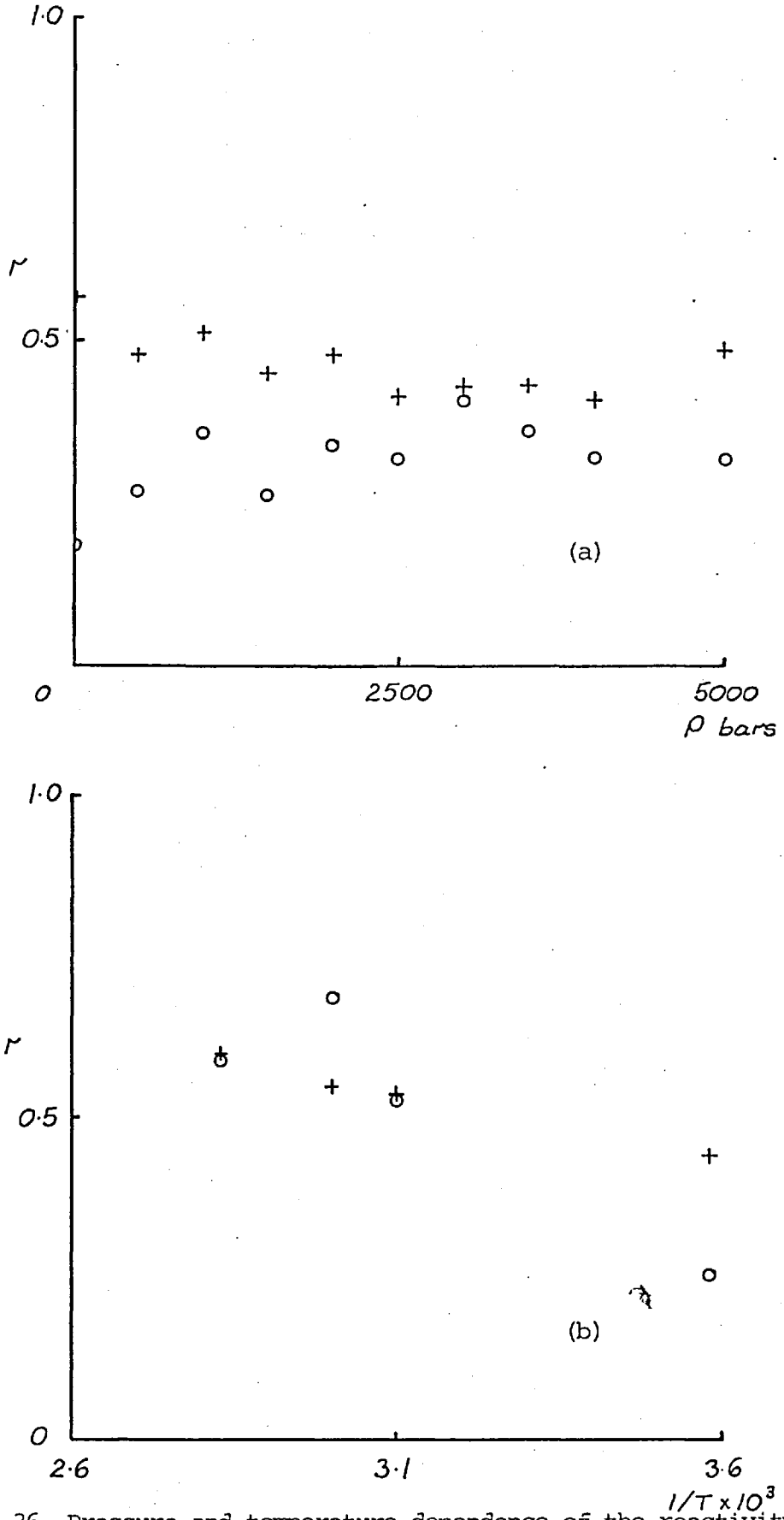

Fig.36 Pressure and temperature dependence of the reactivity ratios for case(i) eq.(4.1.44) of Wittmer; a) data of this research with eq.(6.4.8), b) data of Wittmer with eq.(6.4.6).

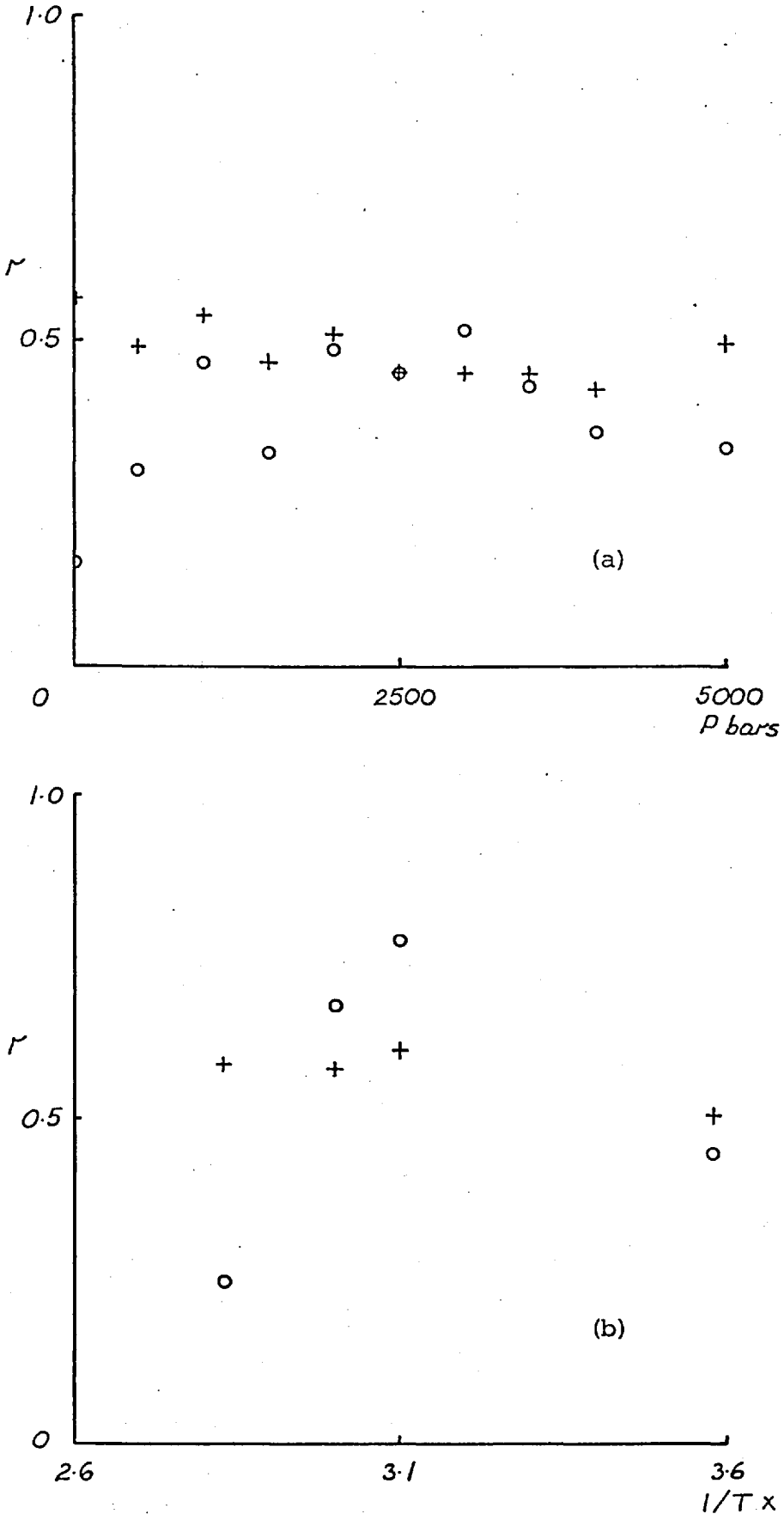

Fig.37 Pressure and temperature dependence of the reactivity ratios for case(iii) eq.(4.1.49) of Wittmer; a) data of this research with eq.(6.4.12), b) data of Wittmer with eq.(6.4.12).

Table XXVIa

Reactivity ratios of αMS-MMA system at various pressures (this research) calculated from equation (4.1.44) and equation (6.4.6). T = 60°C.

P = 0 bar g

Reac. ratio	value	95% conf. limits	Jacobian^2	
r_{MMA}	0.5685	±0.0491	0.4106	-0.1010
$r_{\alpha MS}$	0.2107	±0.1643	-0.1010	0.0367

Sum of squares = $0.1285*10^{-2}$

P = 500 bar g

r_{MMA}	0.4831	±0.0387	0.6361	-0.1621
$r_{\alpha MS}$	0.3611	±0.0875	-0.1621	0.1241

Sum of squares = $0.3534*10^{-2}$

P = 1000 bar g

r_{MMA}	0.5251	±0.0429	0.7943	-0.1826
$r_{\alpha MS}$	0.493	±0.1013	-0.1826	0.1426

Sum of squares = $0.8977*10^{-2}$

P = 1500

r_{MMA}	0.4560	±0.0362	0.6817	-0.2316
$r_{\alpha MS}$	0.3156	±0.0510	-0.2316	0.3431

Sum of squares = $0.4204*10^{-2}$

P = 2000 bar g

r_{MMA}	0.4844	±0.0302	0.9376	-0.2516
$r_{\alpha MS}$	0.4076	±0.0580	-0.2516	0.2542

Sum of squares = $0.4473*10^{-2}$

P = 2500

r_{MMA}	0.4189	±0.0456	0.7776	-0.2775
$r_{\alpha MS}$	0.3647	±0.0609	-0.2775	0.4360

Sum of squares = $0.7641*10^{-2}$

Table XXVIa (cont'd)

P = 3000 bar g

Reac. ratio	value	95% conf. limits	Jacobian^2	
r_{MMA}	0.4341	±0.0929	0.6081	-0.2040
$r_{\alpha MS}$	0.459	±0.1342	-0.2040	0.2912

Sum of squares = $0.1823*10^{-1}$

P = 3500 bar g

r_{MMA}	0.4367	±0.0287	0.6509	-0.2211
$r_{\alpha MS}$	0.3935	±0.0370	-0.2211	0.3908

Sum of squares = $0.2183*10^{-2}$

P = 4000 bar g

r_{MMA}	0.4124	±0.0454	0.5777	-0.2919
$r_{\alpha MS}$	0.3423	±0.0445	-0.2919	0.6003

Sum of squares = $0.4082*10^{-2}$

P = 5000 bar g

r_{MMA}	0.4891	±0.1065	0.3955	-0.2848
$r_{\alpha MS}$	0.3294	±0.0835	-0.2848	0.6424

Sum of squares = $0.1387*10^{-1}$

Table XXVIb

Reactivity ratios of αMS-MMA system at various temperatures (a) Wittmer, b) Izu et al.) calculated from equations (4.1.44) and (6.4.6). P = 1 atm.

a) T = 20°C

Reac. ratio	value	95% conf. limits	Jacobian^2	
r_{MMA}	0.4431	±0.0381	0.3929	-0.2699
$r_{\alpha MS}$	0.2648	±0.0283	-0.2699	0.7115

Sum of squares = $0.1267*10^{-2}$

Table XXVIb (cont'd)

T = 50°C

Reac. ratio	value	95% conf. limits	Jacobian^2	
r_{MMA}	0.5502	±0.0448	0.3330	-0.0660
$r\alpha_{MS}$	0.7516	±0.1528	-0.0660	0.0287

Sum of squares = $0.9159*10^{-3}$

T = 60°C

r_{MMA}	0.5756	±0.0850	0.2451	-0.0116
$r_{\alpha MS}$	1.7942	±1.1972	-0.0116	0.0012

Sum of squares = $0.2938*10^{-2}$

T = 80°C

r_{MMA}	0.5913	±0.2193	0.2204	0.0
$r_{\alpha MS}$	513.2	$\pm 0.9067*10^{6}$	0.0	0.0

Sum of squares = $0.1181*10^{-1}$

T = 100°C

r_{MMA}	0.6165	±0.1820	$973*10^{7}$	$243*10^{8}$
$r_{\alpha MS}$	0.00001	±0.0728	$243*10^{8}$	$608*10^{8}$

Sum of squares = $0.1028*10^{-2}$

b) T = 60°C

r_{MMA}	0.5870	±0.0429	0.2842	-0.0499
$r_{\alpha MS}$	0.4382	±0.1788	-0.0499	0.0163

Sum of squares = $0.3673*10^{-3}$

T = 114°C

Equation ill-conditioned.

Table XXVIIa

Reactivity ratios of αMS-MMA system at various pressures (this research) calculated from equations (4.1.49) and (6.4.8). T = 60°C.

P = 0 bar g

Reac. ratio	value	95% conf. limits	Jacobian^2	
r_{MMA}	0.5667	±0.0454	0.4544	-0.2019
$r_{\alpha MS}$	0.1504	±0.0837	-0.2019	0.1341

Sum of squares = $0.1248*10^{-2}$

P = 500 bar g

r_{MMA}	0.4749	±0.0387	0.6108	-0.3085
$r_{\alpha MS}$	0.2251	±0.0424	-0.3085	0.5092

Sum of squares = $0.3540*10^{-2}$

P = 1000 bar g

r_{MMA}	0.5173	±0.0430	0.8079	-0.3308
$r_{\alpha MS}$	0.3288	±0.0594	-0.3308	0.4219

Sum of squares = $0.8803*10^{-2}$

P = 1500 bar g

r_{MMA}	0.452	±0.0357	0.6749	-0.3076
$r_{\alpha MS}$	0.2498	±0.0368	-0.3076	0.6358

Sum of squares = $0.4104*10^{-2}$

P = 2000 bar g

r_{MMA}	0.4831	±0.0309	0.9215	-0.3246
$r_{\alpha MS}$	0.3420	±0.0470	-0.3246	0.3973

Sum of squares = $0.4453*10^{-2}$

P = 2500 bar g

r_{MMA}	0.4196	±0.0457	0.7711	-0.3281
$r_{\alpha MS}$	0.3259	±0.0530	-0.3281	0.5752

Sum of squares = $0.7467*10^{-2}$

Table XXVIIa (cont'd)

P = 3000 bar g

Reac. ratio	value	95% conf. limits	Jacobian^2	
r_{MMA}	0.4343	±0.0941	0.6120	-0.2369
$r_{\alpha MS}$	0.4165	±0.1221	-0.2369	0.3637

Sum of squares = $0.1843*10^{-1}$

P = 3500 bar g

r_{MMA}	0.4371	±0.0290	0.6325	-0.2276
$r_{\alpha MS}$	0.3686	±0.0348	-0.2276	0.4395

Sum of squares = $0.2184*10^{-2}$

P = 4000 bar g

r_{MMA}	0.4128	±0.0453	0.6158	-0.3607
$r_{\alpha MS}$	0.3266	±0.0421	-0.3607	0.7126

Sum of squares = $0.4044*10^{-2}$

P = 5000 bar g

r_{MMA}	0.4891	±0.1069	0.3956	-0.2963
$r_{\alpha MS}$	0.3204	±0.0811	-0.2963	0.6864

Sum of squares = $0.1390*10^{-1}$

Table XXVIIb

Reactivity ratios of αMS-MMA system at various temperatures (a) Wittmer, b) Izu et al.) calculated from equations (4.1.49) and (6.4.6). P = 1 atm.

a) T = 20°C

Reac. ratio	value	95% conf. limits	Jacobian^2	
r_{MMA}	0.4427	±0.0361	0.3549	-0.1920
$r_{\alpha MS}$	0.2479	±0.0279	-0.1920	0.5943

Sum of squares = $0.1144*10^{-2}$

Table XXVIIb (cont'd)

$T = 50^{o}C$

Reac. ratio	value	95% conf. limits	Jacobian^2	
r_{MMA}	0.5438	±0.0463	0.3331	-0.1619
$r_{\alpha MS}$	0.4176	±0.0687	-0.1619	0.1513

Sum of squares = $0.8603*10^{-3}$

$T = 60^{o}C$

r_{MMA}	0.5473	±0.0713	0.2632	-0.1208
$r_{\alpha MS}$	0.4308	±0.1047	-0.1208	0.1222

Sum of squares = $0.2195*10^{-2}$

$T = 80^{o}C$

r_{MMA}	0.5690	±0.0863	0.2289	-0.1466
$r_{\alpha MS}$	0.1960	±0.0760	-0.1466	0.2945

Sum of squares = $0.3478*10^{-2}$

$T = 100^{o}C$

r_{MMA}	0.6066	±0.0521	0.2358	-0.1295
$r_{\alpha MS}$	-0.0198	±0.0442	-0.1295	0.3288

Sum of squares = $0.1004*10^{-2}$

b) $T = 60^{o}C$

r_{MMA}	0.5729	±0.0496	0.2622	-0.1501
$r_{\alpha MS}$	0.2197	±0.0630	-0.1501	0.1626

Sum of squares = $0.4612*10^{-3}$

$T = 114^{o}C$

Equation ill-conditioned.

Table XXVIc

Reactivity ratios of αMS-MMA system at various pressures (this research) calculated from equations (4.1.44) and (6.4.12). T = 60°C.

P, bar g	r_{MMA}	$r_{\alpha MS}$	$ss*10^2$
0	0.5675 ±0.0462	0.1844 ±0.1237	0.1268
500	0.4792 ±0.0379	0.2682 ±0.0528	0.3611
1000	0.5126 ±0.0388	0.3585 ±0.0564	0.7988
1500	0.4503 ±0.0343	0.2613 ±0.0356	0.3931
2000	0.4782 ±0.0295	0.3403 ±0.0437	0.4404
2500	0.4139 ±0.0458	0.3157 ±0.0483	0.8041
3000	0.4300 ±0.0908	0.4081 ±0.1117	1.7957
3500	0.4335 ±0.0294	0.3601 ±0.0332	0.2191
4000	0.4096 ±0.0451	0.3202 ±0.0393	0.4118
5000	0.4870 ±0.1060	0.3167 ±0.0784	1.3822

Table XXVId

Reactivity ratios of αMS-MMA system at various temperatures (a) Wittmer, b) Izu et al.) calculated from equations (4.1.44) and (6.4.5). P = 1 atm.

T, °C	r_{MMA}	$r_{\alpha MS}$	$ss*10^2$
a)			
20	0.4410 ±0.0389	0.2554 ±0.0273	0.1332
50	0.5357 ±0.0450	0.5243 ±0.0867	0.0988
60	0.5487 ±0.0604	0.6868 ±0.1604	0.1835
80	0.5984 ±0.1085	0.5881 ±0.5227	
100	Equation ill-conditioned		
b)			
60	0.5784 ±0.0450	0.3094 ±0.1038	0.0427
114	Equation ill-conditioned		

Table XXVIIc

Reactivity ratios of αMS-MMA system at various pressures (this research) calculated from equations (4.1.49) and (6.4.12). T = 60°C.

P, bar g	r_{MMA}	$r_{\alpha MS}$	$ss*10^2$
0	0.5671 ±0.0471	0.1575 ±0.0962	0.1267
500	0.4897 ±0.0426	0.2989 ±0.0801	0.3565
1000	0.5402 ±0.0696	0.4636 ±0.1823	1.4602
1500	0.4664 ±0.0466	0.3254 ±0.0830	0.5627
2000	0.5100 ±0.0432	0.4869 ±0.1224	0.5733
2500	0.4503 ±0.0489	0.4514 ±0.093	0.6322
3000	0.4499 ±0.1090	0.5139 ±0.2067	2.0407
3500	0.4491 ±0.0321	0.4272 ±0.0490	0.2320
4000	0.4207 ±0.0463	0.3578 ±0.0494	0.3958
5000	0.4929 ±0.1092	0.3316 ±0.0878	1.4029

Table XXVIId

Reactivity ratios of αMS-MMA system at various temperatures (a) Wittmer, b) Izu et al.) calculated from equations (4.1.49) and (6.4.5). P = 1 atm.

T, °C	r_{MMA}	$r_{\alpha MS}$	$ss*10^2$
a)			
20	0.5043 ±0.1343	0.4472 ±0.2553	0.8893
50	0.6038 ±0.1140	0.7776 ±0.4183	0.2115
60	0.5792 ±0.1424	0.6765 ±0.4478	0.5044
80	0.5840 ±0.1156	0.2489 ±0.1465	0.5119
100	Equation ill-conditioned		
b)			
60	0.5862 ±0.0479	0.2721 ±0.0850	0.0366
114	Equation ill-conditioned		

6.4.4 More Advanced Copolymerization Equations

In the ceiling temperature concept of αMS it is assumed that the equilibrium constant K is equal for every reaction of chain growth, including dimerization. Due to the influence of steric hindrance on the magnitude of the equilibrium constant the above assumption may not be entirely valid which in turn gives a slightly different physical outlook to the ceiling temperature concept. Although the concentration of polymer chains drops sharply towards the ceiling temperature the concentration of dimers may not drop so sharply (see section (2.4)) and may reach a higher ceiling temperature than the one obtained by extrapolating the overall drop. Therefore, on this basis, it is possible to assume that all propagation steps have the same K except the dimerization. This would explain the existance of dimers at the ceiling temperature. Even the trimerization equilibrium constant may be different, although much less, from the overall equilibrium constant but the concentration of trimers and higher-mers will be undetectably low at the overall ceiling temperature. Nevertheless the variation in K would influence the copolymer composition and a more elaborate model would be necessary provided the varying values for K were known.

At present the only composition equation that takes into account both penultimate effects and depropagation is O'Driscoll's triad depropagation equation (equation (4.1.72)). This equation contains sixteen parameters (as the rate constants) and for the estimation of these parameters by NLR a set of nonlinear equations with eight unknowns has to be solved at each iteration. Apart from long computer time the estimation of sixteen parameters needs data of high accuracy which may be impossible to obtain.

Similar difficulties still exist even if the number of parameters are reduced to ten by simplifying assumptions.

The diad depropagation equation of O'Driscoll (equation (4.1.71)), with eight parameters and four nonlinear equations, was tried by the Author but it failed to give any estimates since the Harwell NS01A subroutine for the solution of nonlinear equations did not work succesfully in the entire parameter space. The diad equation was solved

Table XXVIIIa

Solution of O'Driscoll and co-workers' nonlinear equations[*] (107,95) using k's[**] calculated from their parameter values.

Feed αMS	Cop. αMS	F_{AAA}	a	b	ε	η
0.1000	0.0725	0.4734	0.5175	0.2461	0.9228	0.0129
0.2000	0.1328	0.4173	0.4942	0.4920	0.8511	0.0276
0.3000	0.1844	0.3659	0.4701	0.7378	0.7840	0.0448
0.4000	0.2300	0.3185	0.4449	0.9835	0.7207	0.0651
0.5000	0.2717	0.2745	0.4182	1.2292	0.6604	0.0896
0.6000	0.3113	0.2331	0.3893	1.4747	0.6022	0.1199
0.7000	0.3510	0.1938	0.3574	1.7203	0.5451	0.1587
0.8000	0.3942	0.1553	0.3204	1.9659	0.4870	0.2118
0.9000	0.4774	0.1162	0.2737	2.2115	0.4264	0.2914

[*] $b = k_3 S + k_6(1-\varepsilon)$ S=feed αMS concn.

$a = k_5 M + k_4(1-\eta)$ M=feed MMA concn.

$k_4\varepsilon(1-\eta)(k_3 S+k_6(1-\varepsilon) = (k_5 M+k_4(1-\eta)(\varepsilon(k_1 M+k_2+k_3 S)-(k_1 M+\varepsilon^3 k_2))$

$k_6\eta(1-\varepsilon)(k_5 M+k_4(1-\eta) = (k_3 S+k_6(1-\varepsilon)(\eta(k_5 M+k_8+k_7 S)-(k_7 S+\eta^2 k_8))$

[**] k_1=1.0, k_2=0.0094, k_3=2.44, k_4=0.361, k_5=0.179, k_6=0.027, k_7=0.029, k_8=0.067.

Table XXVIIIb

Monte-Carlo simulation results using the k's of Table XXVIIIa

Feed αMS	Cop. αMS	F_{AAA}
0.1	0.0712	0.7976
0.2	0.1285	0.6406
0.3	0.1776	0.5202
0.4	0.2231	0.4127
0.5	0.2733	0.3132
0.6	0.3063	0.2568
0.7	0.3551	0.1872
0.8	0.3883	0.1518
0.9	0.4657	0.0874

Table XXIX

Parameter values of O'Driscoll et al.

	60°C	114°C	147°C
ΔG_1^o, kcal/mole	-3.08	-1.48	-0.51
ΔG_2^o, kcal/mole	-1.26	0.31	1.27
ΔG_3^o, kcal/mole	-1.26	0.31	1.27
ΔG_4^o, kcal/mole	0.55	2.11	3.06
r_1	0.41	0.41	0.41
r_2	0.16	0.16	0.16
s_1	5.6	5.6	5.6

for copolymer compositions with the parameter values given by O'Driscoll et al.[81] The results did not match the experimental curve, contrary to O'Driscoll, and this was also supported by Monte-Carlo simulation. The results are given in Table (XXVIII).

The parameter values of O'Driscoll are given in Table (XXIX). K_4, as calculated from ΔS and ΔH with ΔH adjusted to 100°C, is larger than the values of other workers as calculated from $1/[M]_e$. When smaller K_4 values of section (6.4.2) are used for composition calculations there seems to be little improvement. Also the assumption that

$$\Delta G_2 = \Delta G_3 = 1/2\ (\Delta G_1 + \Delta G_3) \qquad (6.4.16)$$

is by no means justifiable[117].

6.4.5 Progression of Wittmer's Equation

Although some of the equations of Wittmer consider the depropagation of one unit after being attached to two of the same units it is not in the true sense a penultimate effect: it considers both forward reactions.

$$\sim\!\!\sim B\cdot + B \xrightarrow{k_{bb}} \sim\!\!\sim BB\cdot$$

$$\sim\!\!\sim BB\cdot + B \underset{\leftarrow - - -}{\xrightarrow{k_{bb}}} \sim\!\!\sim BBB\cdot$$

to have the same reaction rates and not even a slight reversibility for the first reaction. The possibility of deriving an equation for a model, which would consider the penultimate unit effects and treat both of the above reactions as reversible, was considered. The results are presented in this section.

The consideration was made for the full eight penultimate-unit-effect reactions with one monomer depropagating whenever it is attached to its own kind but with different reverse rates for different forward rates. Therefore the eight reactions were

$$AA\cdot + A \longrightarrow AAA\cdot$$

$$BA\cdot + A \longrightarrow BAA\cdot$$

$$AB\cdot + A \longrightarrow ABA\cdot$$

for copolymer compositions with the parameter values given by O'Driscoll et al.[81] The results did not match the experimental curve, contrary to O'Driscoll, and this was also supported by Monte-Carlo simulation. The results are given in Table (XXVIII).

The parameter values of O'Driscoll are given in Table (XXIX). K_4, as calculated from ΔS and ΔH with ΔH adjusted to 100°C, is larger than the values of other workers as calculated from $1/[M]_e$. When smaller K_4 values of section (6.4.2) are used for composition calculations there seems to be little improvement. Also the assumption that

$$\Delta G_2 = \Delta G_3 = 1/2\ (\Delta G_1 + \Delta G_4) \qquad (6.4.16)$$

is by no means justifiable[117].

6.4.5 Progression of Wittmer's Equation

Although some of the equations of Wittmer consider the depropagation of one unit after being attached to two of the same units it is not in the true sense a penultimate effect: it considers both forward reactions.

$$\sim\!\!\sim B\cdot + B \xrightarrow{k_{bb}} \sim\!\!\sim BB\cdot$$

$$\sim\!\!\sim BB\cdot + B \underset{\leftarrow - - -}{\xrightarrow{k_{bb}}} \sim\!\!\sim BBB\cdot$$

to have the same reaction rates and not even a slight reversibility for the first reaction. The possibility of deriving an equation for a model, which would consider the penultimate unit effects and treat both of the above reactions as reversible, was considered. The results are presented in this section.

The consideration was made for the full eight penultimate-unit-effect reactions with one monomer depropagating whenever it is attached to its own kind but with different reverse rates for different forward rates. Therefore the eight reactions were

$$AA\cdot + A \longrightarrow AAA\cdot$$

$$BA\cdot + A \longrightarrow BAA\cdot$$

$$AB\cdot + A \longrightarrow ABA\cdot$$

$$BB\cdot + A \longrightarrow BBA\cdot$$
$$AA\cdot + B \longrightarrow AAB\cdot$$
$$BA\cdot + B \longrightarrow BAB\cdot$$
$$AB\cdot + B \rightleftharpoons ABB\cdot$$
$$BB\cdot + B \rightleftharpoons BBB\cdot$$

For the rate of disappearance of the individual monomers one has

$$-\frac{d[A]}{dt} = k_{aaa}[A]\sum_2[A\cdot]_i + k_{baa}[A][A\cdot]_1 + k_{aba}[A][B\cdot]_1 + k_{bba}A\sum_2 B\cdot_i \qquad (6.4.17)$$

$$-\frac{d[B]}{dt} = k_{bbb}[B]\sum_2[B\cdot]_i + k_{abb}[B][B\cdot]_1 + k_{bab}[B][A\cdot]_1 + k_{aab}[B]\sum_2[A\cdot]_i - k'_{bbb}\sum_2[B\cdot]_i - k'_{abb}[B\cdot]_2 \qquad (6.4.18)$$

also

$$k_{ba}[A]\sum_1[B\cdot]_i = k_{ab}[B]\sum_1[A\cdot]_i \qquad (6.4.19)$$

$$= k_{bba}[A]\sum_2[B\cdot]_i + k_{aba}[A][B\cdot]_i = k_{aab}[B]\sum_2[A\cdot]_i + k_{bab}[A\cdot]_1[B] \qquad (6.4.20)$$

and

$$\sum_2^{\infty}[A\cdot]_i = \sum_1[A\cdot]_i - [A\cdot]_1 \qquad (6.4.21)$$

For simplicity treat each monomer separately. For A, dividing equation (6.4.17) by an appropriate factor

$$\frac{d[A]}{dt} \Big/ (k_{aba}[B\cdot]_1[A] + k_{bba}[A]\sum_2[B\cdot]_i)$$

$$= \frac{k_{aba}[A][B\cdot]_1 + k_{bba}[A]\sum_2[B\cdot]_i + k_{aaa}[A]\sum_2[A\cdot]_i + k_{baa}[A][A\cdot]_1}{k_{aba}[B\cdot]_1[A] + k_{bba}[A]\sum_2[B\cdot]_i}$$

$$= 1 + \frac{k_{aaa}[A]\sum_2[A\cdot]_i + k_{baa}[A][A\cdot]_1}{k_{bab}[A\cdot]_1[B] + k_{aab}[B]\sum_2[A\cdot]_i} \qquad (6.4.22)$$

define

$$\frac{[A\cdot]_1}{\sum_1 [A\cdot]_i} = x_1 \quad , \quad \frac{\sum_2 [A\cdot]_i}{\sum_1 [A\cdot]_1} = \frac{\sum_1 [A\cdot]_i - [A\cdot]_1}{\sum_1 [A\cdot]_i} = 1 - x_1 \tag{6.4.23}$$

Therefore

$$\frac{d[A]}{dt} \Big/ (k_{aba}[B\cdot]_1[A] + k_{bba}[A]\sum_2 [B\cdot]_i)$$

$$= 1 + \frac{k_{aaa}[A](1 - x_1) + k_{baa}[A]x_1}{k_{aab}[A](1 - x_1) + k_{bab}[B]x_1} \tag{6.4.24}$$

To find x_1 it is necessary to find the concentration of the radicals from their rate of formation

$$\frac{d[A\cdot]}{dt} = k_{bba}[A]\sum_2 [B\cdot]_i + k_{aba}[A][B\cdot]_1 - k_{bab}[A\cdot]_1[B] - k_{baa}[A\cdot]_1[A] \tag{6.4.24}$$

Therefore from the stationary state assumption and equations (6.4.20) and (6.4.21)

$$k_{aab}[B]\sum_1 [A\cdot]_i = k_{aab}[A\cdot]_1[B] + k_{baa}[A\cdot]_1[A] \tag{6.4.26}$$

$$1 = x_1 \frac{k_{aab}[B]}{k_{aab}[B]} + \frac{k_{baa}[A]}{k_{aab}[B]}$$

$$1 = x_1 \left(1 + \frac{k_{baa}}{k_{aab}} \frac{[A]}{[B]}\right) \tag{6.4.27}$$

then

$$x_1 = \frac{k_{aab}[B]}{k_{aab}[B] + k_{baa}[A]} \tag{6.4.28}$$

$$1 - x_1 = \frac{k_{baa}[A]}{k_{aab}[B] + k_{baa}[A]} \tag{6.4.29}$$

When substituted in equation (6.4.24)

$$R.H.S = 1 + \frac{r_{baa}(r_{aaa}x + 1)}{r_{baa}x + 1}, \quad x = \frac{[A]}{[B]} \qquad (6.4.30)$$

which is nothing than the numerator of the penultimate unit equation.

For monomer B, again dividing by appropriate factor

$$-\frac{d[B]}{dt} \Big/ (k_{aba}[B^\bullet]_1[A] + k_{bba}[A]\sum_2[B^\bullet]_i)$$

$$= 1 + \frac{k_{bbb}[B](1 - x_1) + k_{abb}[B]x_1}{k_{bba}[A](1 - x_1) + k_{aba}[A]x_1} + \frac{k'_{bbb}(1 - x_1 - x_2) + k'_{abb}x_2}{k_{bba}[A](1 - x_1) + k_{aba}[A]x_1} \qquad (6.4.31)$$

where

$$x_1 = \frac{[B^\bullet]_1}{\sum_1[B^\bullet]_i}, \quad x_2 = \frac{[B^\bullet]_2}{\sum_1[B^\bullet]_i}$$

For x_1 and x_2 from the rates of radical formation

$$\frac{d[B^\bullet]_1}{dt} = k_{aab}[B]\sum_2[A^\bullet]_i + k_{bab}[B][A^\bullet]_1 - k_{aba}[B^\bullet]_1[A] - k_{abb}[B^\bullet]_1[B] + k'_{abb}[B^\bullet]_2$$

$$\frac{d[B^\bullet]_2}{dt} = k_{abb}[B^\bullet]_1[B] - k_{bba}[B^\bullet]_2[A] + k'_{bbb}[B^\bullet]_3 - k_{bbb}[B^\bullet]_2[B] - k'_{abb}[B^\bullet]_2$$

$$\frac{d[B^\bullet]_3}{dt} = k_{bbb}[B^\bullet]_2[B] + k'_{bbb}[B^\bullet]_4 - k'_{bbb}[B^\bullet]_3 - k_{bbb}[B^\bullet]_3[B] - k_{bba}[B^\bullet]_3[A]$$

$$\frac{d[B^\bullet]_n}{dt} = k_{bbb}[B^\bullet]_{n-1}[B] + k'_{bbb}[B^\bullet]_{n+1} - k'_{bbb}[B^\bullet]_n - k_{bbb}[B^\bullet]_n[B] - k_{bba}[B^\bullet]_n[A] \qquad (6.4.32)$$

Dividing by

$$k_{bba}[A]\sum_1[B^\bullet]_i$$

(using also equations (6.4.20) and (6.4.21) and applying the stationary state assumption)

$$1 = x_1 \left(1 + \frac{k_{abb}}{k_{bba}} \frac{[B]}{[A]}\right) - x_2 \frac{k_{abb}}{k_{bba}} \frac{K}{[A]}$$

$$x_1 \frac{k_{abb}}{k_{bba}} \frac{[B]}{[A]} = x_2 \left(1 + \frac{k_{bbb}}{k_{bba}} \frac{[B]}{[A]} + \frac{k_{abb}}{k_{bba}} \frac{K}{[A]}\right) - x_3 \frac{k_{bbb}}{k_{bba}} \frac{K'}{[A]}$$

$$x_2 \frac{k_{bbb}}{k_{bba}} \frac{[B]}{[A]} = x_3 \left(1 + \frac{k_{bbb}}{k_{bba}} \frac{[B]}{[A]} + \frac{k_{bbb}}{k_{bba}} \frac{K}{[A]}\right) - x_4 \frac{k_{bbb}}{k_{aab}} \frac{K'}{[B]}$$

$$x_n \frac{k_{bbb}}{k_{bba}} \frac{[B]}{[A]} = x_{n+1} \left(1 + \frac{k_{bbb}}{k_{bba}} \frac{[B]}{[A]} + \frac{k_{bbb}}{k_{bba}} \frac{K'}{[A]}\right) - x_{n+1} \frac{k_{bbb}}{k_{aab}} \frac{K'}{[B]} \qquad (6.4.33)$$

where $K=k_{abb}/k_{aba}$ and $K'=k_{bbb}/k_{bba}$. Using equation (6.4.33) with equation (6.4.34)

$$\sum_{1} x_i = 1 \qquad (6.4.34)$$

one obtains

$$x_1 = \frac{1 + x_2 r_R \frac{K}{[A]}}{1 + r_R \frac{[B]}{[A]}} \qquad (6.4.35)$$

$$x_2 = \frac{r_B \frac{[B]}{[A]} + \left(1 + r_R \frac{[B]}{[A]}\right)^2}{2 + 2r_B \frac{[B]}{[A]} + (r_B + r_R)\frac{K'}{[A]} + r_B \frac{K[B]}{[A]^2}} \qquad (6.4.36)$$

where $r_B=k_{bbb}/k_{bba}$, $r_R=k_{abb}/k_{bba}$. When equations (6.4.30) and (6.4.31) are combined they yield

$$\frac{d[A]}{d[B]} = \frac{1 + \frac{r'_A\left(r_A \frac{[A]}{[B]} + 1\right)}{r'_A \frac{[A]}{[B]} + 1}}{1 + \frac{r'_B\left(r_B \frac{[B]}{[A]} + 1\right)}{r'_B \frac{[B]}{[A]} + 1} - \frac{r_B K'(1 - x_1 - x_2) + r_R K x_2}{[A](1 - x_1) + \frac{r_R}{r'_B}[A]x_1}} \qquad (6.4.37)$$

where $r'_A=k_{baa}/k_{bab}$ and $r_A=k_{aaa}/k_{aab}$.

Since the application of a six-parameter equation needs fairly

accurate data no attempt was made for estimation with the data obtained in this research. A special feature in Wittmer's equations is that the denominator and the nomerator can be treated separately. A simple version was derived which considers the penultimate unit effects for radicals ending with A and depropagation for radicals ending with BBB where $r_B=r'_B$.

$$\frac{A}{B} = \frac{1 + r'_A\ (1 + r_A[A]/[B])/(1 + r'_A[A]/[B])}{1 + r_B[B]/[A] - r_B K(1 - x_1)/[A]} \qquad (6.4.38)$$

where x_1 is as in equation (4.1.44). The application of this equation, contrary to expectations, gave a constant r_B over pressure (fig.(38)). Since the results are quite scattered it is difficult to ascertain and interpret this.

Although the Wittmer type equations derived from kinetic scheme do not give any information on microstructure (as advocated by O'Driscoll) it is possible to overcome this disadvantage by using the estimated parameters in a Monte-Carlo simulation to obtain the diad or triad functions.

6.4.6 Behaviour of r_B over Pressure

As mentioned in earlier sections although the direction of change (increase or decrease) of the reactivity ratios over pressure depends on the difference between the activation volume ($\Delta V^{\neq}$) of the constituent rate constants the mode of change should always be exponential. This is also true for the dependence of reactivity ratios on temperature where the activation energy replaces activation volume. Therefore any deviation from the exponential change could be attributed to the incompetence of the model and the reactivity ratios obtained would be only apparent reactivity ratios[98]. It would be interesting to investigate the functional relationship between the actual and apparent reactivity ratios.

The relation between an actual reactivity ratio in a penultimate unit model equation and the apparent reactivity ratio in the simplified equation of terminal unit model is

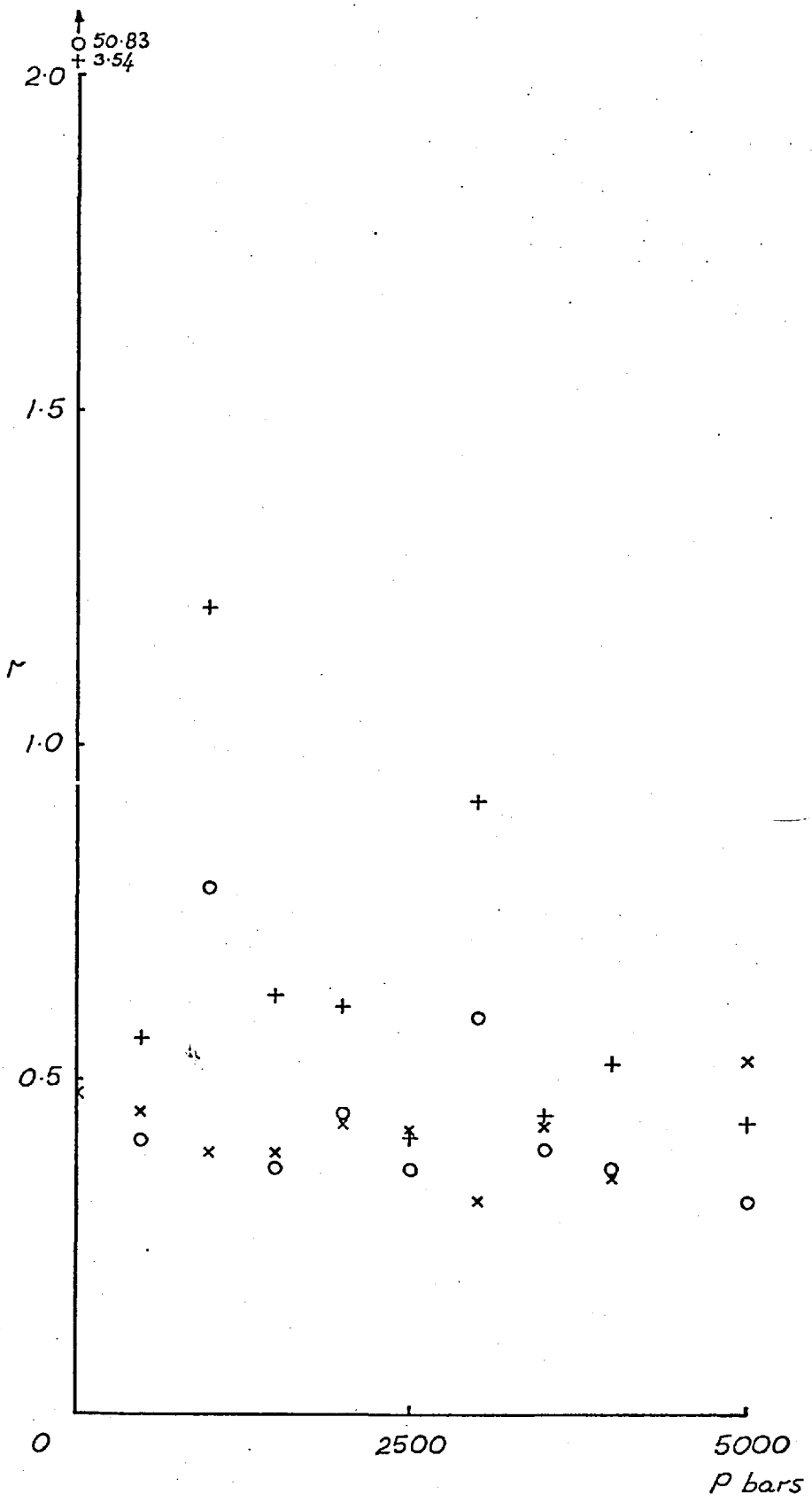

Fig.38 Pressure dependence of the reactivity ratios for copolymerization model with depropagation assumptions according to the progressed Wittmer equation (6.4.38).(+) r'_A, x) r_A, o) r_B).

$$r_{aa} = r_{baa}(1 + r_{aaa}\frac{[A]}{[B]})/(1 + r_{baa}\frac{[A]}{[B]}) \quad (6.4.39)$$

as derived by probabilistic as well as kinetic means.

In the case of an actual reactivity ratio in a depropagating model and the apparent reactivity ratio in a model simplified by ignoring depropagation it can be derived as follows. For the case where BB depropagate but not BA or AB, for the consumption of monomer B

$$-\frac{d[B]}{dt} = k_{ab}[A\cdot][B] + k_{bb}[B\cdot][B] - k'_{bb}[B\cdot] \quad (6.4.40)$$

whereas for a non-depropagating model

$$-\frac{d[B]}{dt} = k_{ab}[A\cdot][B] + k_{bb(app)}[B\cdot][B] \quad (6.4.41)$$

Hence from equations (6.4.40) and (6.4.41)

$$k_{bb(app)}[B] = k_{bb}[B] - k'_{bb}$$

and since $K=k'/k$

$$k_{bb(app)}[B] = k_{bb}[B] - k_{bb}K \quad (6.4.42)$$

Dividing both sides by k_{ba} B yields the relationship

$$r_{bb(app)} = r_{bb} - r_{bb}\frac{K}{[B]} \quad (6.4.43)$$

Since the rate constants and equilibrium constant can be shown as

$$k = \Xi' e^{-\frac{\Delta V^{\neq}}{RT}P} \qquad (\Xi' = \text{constant})$$

and

$$K = \Psi\, e^{\frac{\Delta V^{O}}{RT}P} \qquad (K=k'/k),\ (\Psi = \text{constant})$$

respectively, one can define equation (6.4.39) as

$$r_{aa} = \Xi_2 e^{-\frac{\Delta P}{RT}(\Delta V^{\neq}_{baa} - \Delta V^{\neq}_{bab})} \frac{(1 + \Xi_1 e^{-\frac{\Delta P}{RT}(\Delta V^{\neq}_{aaa} - \Delta V^{\neq}_{baa})}\frac{[A]}{[B]})}{(1 + \Xi_2 e^{-\frac{\Delta P}{RT}(\Delta V^{\neq}_{baa} - \Delta V^{\neq}_{bab})}\frac{[A]}{[B]})} \quad (6.4.44)$$

and equation (6.4.43) as

$$r_{bb(app)} = \Xi\, e^{-\frac{\Delta P}{RT}(\Delta V^{\neq}_{bb} - \Delta V^{\neq}_{ba})} \left(1 - \frac{e^{\Delta V^{o}\frac{\Delta P}{RT}}}{[B]}\right) \quad (6.4.45)$$

Equation (6.4.44) shows exponential change with pressure apart from when $\Delta V^{\neq}$ differences are equal and opposite in sign then r_{ca} becomes unity at all pressures. Equation (6.4.45) shows three different changes depending on V differences:

(i) $\Delta V^{\neq}_{bb} = \Delta V^{\neq}_{ba}$ - change of the type $(1-e^{-x})$

(ii) $\Delta V^{\neq}_{bb} > \Delta V^{\neq}_{ba}$ - change of the type e^{x}

(iii) $\Delta V^{\neq}_{bb} < \Delta V^{\neq}_{ba}$ - change with a maximum

The observation of this functional maximum may also explain the experimental maximum. If the experimentally observed maximum can be truly explained by the above relation the implication is that neither case (i) nor case (iii) equations of Wittmer can explain the copolymerization system system MS-MMA and a more complicated relation is necessary to define $d[B]/dt$. The similar maximum observed in $1/r_{baa}$ in fig.(31) may also mean that there is a certain depropagation in

$$BA\cdot + B \longrightarrow BAB\cdot$$

in which case there needs to be a depropagative relation to define $d[A]/dt$. This would be more complex than equation (6.4.37).

6.5 Monte-Carlo Simulation of General Copolymerization Process

A Monte-Carlo process was developed to simulate the chain formation of a binary copolymerization reaction. The aims of this were
1) to have a better understanding of the copolymerization process,
2) to check on the validity of various copolymerization models,
3) to obtain information on the microstructure of copolymers and
4) to use the simulation in the estimation of the reaction parameters.
The last aim was not achieved because, although the simulation needed less time than the solution of equations like those of O'Driscoll, the model which would find simulation as the best solution would still

involve too many parameters to make estimation possible with the accuracy of the present data. But in any case a simulation model would involve less parameters than a complex equation for the same mechanism due to the better possibility of parameter grouping (k's as r's).

The simulation takes into account the eight propagation reactions to consider the penultimate unit effects together with their eight depropagation reactions. The computer program is flexible and by incorporating various assumptions can be transformed into any model from simple terminal unit model to fully depropagative penultimate unit model. In one case, with certain modifications it was transformed into a partly penpenultimate unit model.

The program time and core storage characteristics are as follows:

1.3 seconds compilation time
+ 0.6 seconds per thousand units of copolymer
+ 1.2 seconds auxillary calculations
51000 core storage (2000 units of copolymer)

Computer time refers to CDC 6400.

The simulation program propagate the chain according to the transition probabilities of the monomers reacting with the radical end. Therefore for a radical of BAA• the transition probabilities are:

possible reaction	transition probability
⋀⋀AA• + A	$P_{aaa} = \frac{k_{aaa}[A]}{k_{aaa}[A] + k_{aab}[B] + k'_{baa}}$
⋀⋀AA• + B	$P_{aab} = \frac{k_{aab}[B]}{k_{aaa}[A] + k_{aab}[B] + k'_{baa}}$
⋀⋀BAA• - A	$\bar{P}_{baa} = \frac{k'_{baa}}{k_{aaa}[A] + k_{aab}[B] + k'_{baa}}$

with the condition

$$P_{aaa} + P_{aab} + \bar{P}_{baa} = 1$$

One of the reactions can be picked up by a random number x_r where

$0 \leq x_r \leq 1$. The block representation of the program is shown in fig.(39) and the actual program is given in fig.(40b).

The storage of the chain in the computer is in binary numbers: 1 denoting A units and 0 denoting monomer B. On the output the whole chain can be short-listed if needed, as seen in fig.(41), and the total amount of depropagating units are shown as x's to give an idea about the depropagativity of the particular copolymerization reaction.

The oscillation of the Monte-Carlo process damps after about 1500 chain units and after 2000 units there is an oscillation of ± 0.005 in composition mole fraction output which is reduced down to ± 0.00025 after 3500 units. In this research the chain growth was carried out up to 2000 units.

The program listing for case (iii) Wittmer equation is given in fig.(40b). The composition and microstructure results are given in figures (42a) to (42e) as computer outputs. The results are also shown for triad fractions ($[AAA]/[A]$) in fig.(43) (curves) with the experimental points for copolymerization at 1500 bars. It seems the penultimate unit model approximates to the experimental points but a split of r_{aaa} into r_{aaaa} and r_{baaa} of penpenultimate unit model seems to result in overall higher AAA fractions than the experimental results.

6.6 Microstructure of αMS-MMA Copolymer and its Pressure Dependence

It is possible to fit a variety of copolymer composition equations, derived from various models, to the experimental data with a good accuracy. From the curves of various equations and the experimental points in fig.(43a) it is not possible to decide which model is strictly superior to the others. The dependence on pressure and temperature of the reactivity ratios calculated from various models can throw some light on the problem (see section (6.4)) but certain ambiguities prevents it from being a good and absolute test.

A more enlightening source of information on the mechanism is the microstructure of the copolymer. As seen in fig.(43a) and (43b) similar composition curves of different models may produce various triad curves. Although all models fit to the experimental composition

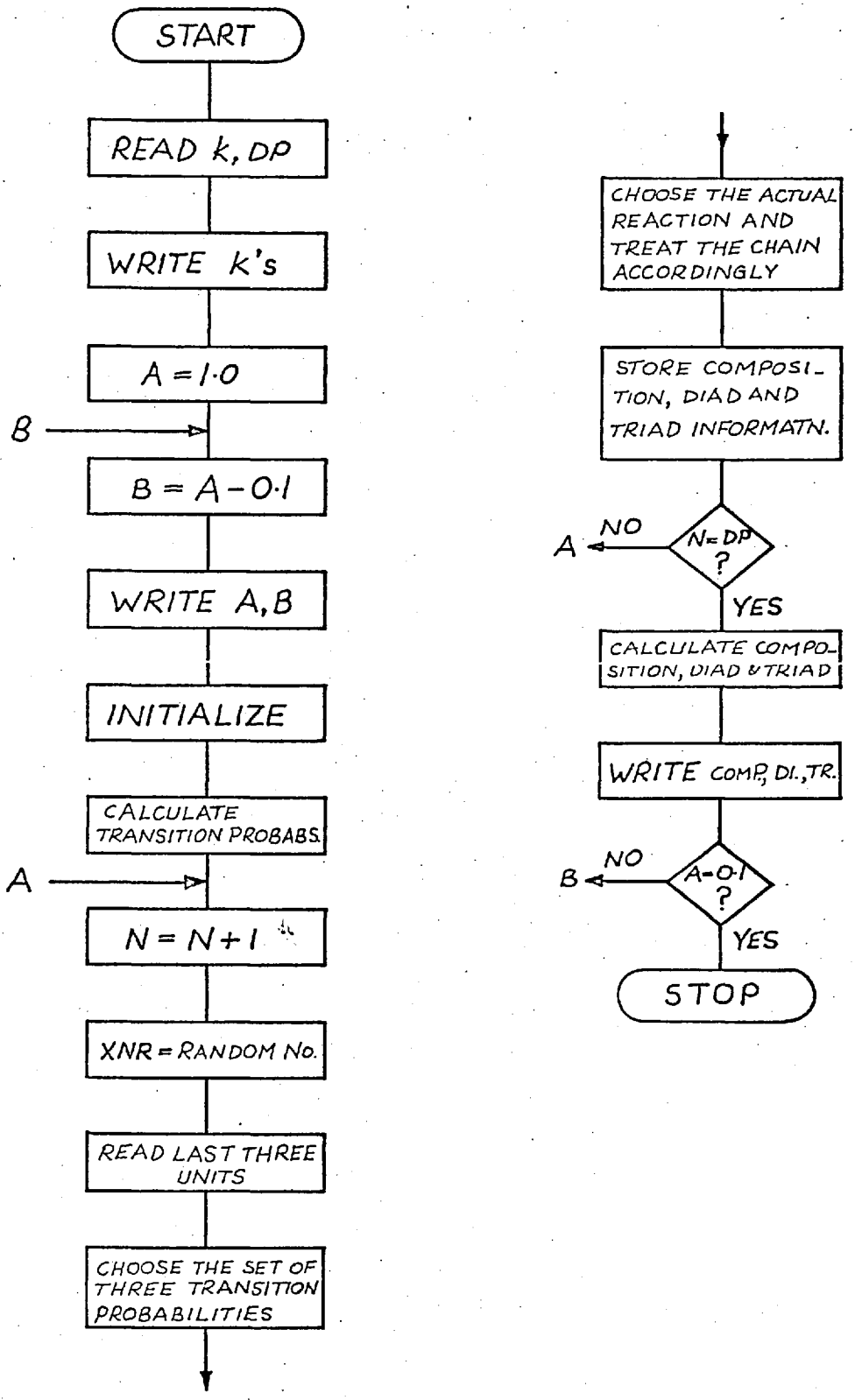

Fig.39 Block representation of the computer program for the Monte-Carlo simulation of the copolymerization reaction.

```
      PROGRAM MC(INPUT,OUTPUT,TAPE5=INPUT,TAPE6=OUTPUT)                    _0001
      DIMENSION THETA(16),NUMIT(2000),YE(30),Z(30)                         _0002
      NDP=2000                                                             _0003
      CONV=0.0                                                             _0004
      CK=.31248                                                            _0005
      THETA(1)=0.75                                                        _0006
      THETA(2)=0.42                                                        _0007
      THETA(3)=0.37                                                        _0008
      XK1=1.                                                               _0009
      XK2=0.0                                                              _0010
      XK3=XK1/THETA(1)                                                     _0011
      XK4=0.0                                                              _0012
      WRITE(6,1000) XK1,XK2,XK3,XK4,XK5,XK6,XK7,XK8,XK9,XK10,XK11,         _0013
     1XK12,XK13,XK14,XK15,XK16                                             _0014
 1000 FORMAT(//1X,16F8.4//)                                                _0015
      DO 2000 NNN=1,9                                                      _0016
      A=0.0                                                                _0017
      B=0.0                                                                _0018
      XNNN=NNN                                                             _0019
      EXN=XNNN*0.1                                                         _0020
      B=B+EXN                                                              _0021
      A=1.-B                                                               _0022
  726 FORMAT(3F6.5,I6)                                                     _0023
      WRITE(6,726) A ,B ,CONV,NCP                                          _0024
      XDR=RANF(5.0)                                                        _0025
    1 NAAA=3                                                               _0026
      NAAB=0                                                               _0027
      NABA=0                                                               _0028
      NBAA=0                                                               _0029
      NABB=0                                                               _0030
      NBAB=0                                                               _0031
      NBBA=0                                                               _0032
      NBBB=0                                                               _0033
      NRUN=0                                                               _0034
      NA=5                                                                 _0035
      NB=0                                                                 _0036
      DO 5 I=1,5                                                           _0037
      NUMIT(I)=1                                                           _0038
    5 CONTINUE                                                             _0039
      I=5                                                                  _0040
      DAAA=XK1*A+XK3*B+XK2                                                 _0041
      PAAA1X=XK1*A/DAAA                                                    _0042
      PAAB1X=XK3*B/DAAA                                                    _0043
      PAAA2X=XK2/DAAA                                                      _0044
      DBAA=XK1*A+XK3*B+XK10                                                _0045
      PAAA1Y=XK1*A/DBAA                                                    _0046
      PAAB1Y=XK3*B/DBAA                                                    _0047
      PBAA2Y=XK10/DBAA                                                     _0048
      DAAB=XK5*A+XK7*B+XK4                                                 _0049
      PABA1X=XK5*A/DAAB                                                    _0050
      PABB1X=XK7*B/DAAB                                                    _0051
      PAAB2X=XK4/DAAB                                                      _0052
      DBAB=XK5*A+XK7*B+XK12                                                _0053
      PABB1Y=XK7*B/DBAB                                                    _0054
      PABA1Y=XK5*A/DBAB                                                    _0055
      PBAB2Y=XK12/DBAB                                                     _0056
      DABB=XK13*A+XK15*B+XK8                                               _0057
      PBBA1X=XK13*A/DABB                                                   _0058
      PBBB1X=XK15*B/DABB                                                   _0059
      PABB2X=XK8/DABB                                                      _0060
      DBBB=XK13*A+XK15*B+XK16                                              _0061
      PBBA1Y=XK13*A/DBBB                                                   _0062
      PBBB1Y=XK15*B/DBBB                                                   _0063
      PBBB2Y=XK16/DBBB                                                     _0064
      DABA=XK9*A+XK11*B+XK6                                                _0065
      PBAA1X=XK9*A/DABA                                                    _0066
      PBAB1X=XK11*B/DABA                                                   _0067
      PABA2X=XK6/DABA                                                      _0068
```

Fig.40b Listing of the Monte-Carlo simulation program.

```
      DBBA=XK9*A+XK11*B+XK14                                          _0069
      PBAA1Y=XK9*A/DBBA                                               _0070
      PBAB1Y=XK11*B/DBBA                                              _0071
      PBBA2Y=XK14/DBBA                                                _0072
      DO 909 L=6,NDP                                                  _0073
      XNR=RANF(0.0)                                                   _0074
      IF(NUNIT(I).EQ.1) GO TO 55                                      _0075
      IF(NUNIT(I).EQ.0) GO TO 56                                      _0076
   55 IF(NUNIT(I-1).EQ.1) GO TO 57                                    _0077
      IF(NUNIT(I-1).EQ.0) GO TO 58                                    _0078
   57 IF(NUNIT(I-2).EQ.1) GO TO 59                                    _0079
      IF(NUNIT(I-2).EQ.0) GO TO 60                                    _0080
   58 IF(NUNIT(I-2).EQ.1) GO TO 61                                    _0081
      IF(NUNIT(I-2).EQ.0) GO TO 62                                    _0082
   56 IF(NUNIT(I-1).EQ.1) GO TO 63                                    _0083
      IF(NUNIT(I-1).EQ.0) GO TO 64                                    _0084
   63 IF(NUNIT(I-2).EQ.1) GO TO 65                                    _0085
      IF(NUNIT(I-2).EQ.0) GO TO 66                                    _0086
   64 IF(NUNIT(I-2).EQ.1) GO TO 67                                    _0087
      IF(NUNIT(I-2).EQ.0) GO TO 68                                    _0088
   59 IF(XNR.GT.PAAA1X) GO TO 100                                     _0089
      I=I+1                                                           _0090
      NUNIT(I)=1                                                      _0091
      NAAA=NAAA+1                                                     _0092
      NA=NA+1                                                         _0093
      GO TO 909                                                       _0094
  101 IF(XNR.GT.(PAAA1X+PAAB1X)) GO TO 101                            _0095
      I=I+1                                                           _0096
      NUNIT(I)=0                                                      _0097
      NAAB=NAAB+1                                                     _0098
      NRUN=NRUN+1                                                     _0099
      NB=NB+1                                                         _0100
      GO TO 909                                                       _0101
  101 I=I-1                                                           _0102
      NAAA=NAAA-1                                                     _0103
      NA=NA-1                                                         _0104
      GO TO 909                                                       _0105
   60 IF(XNR.GT.PAAA1Y) GO TO 200                                     _0106
      I=I+1                                                           _0107
      NUNIT(I)=1                                                      _0108
      NAAA=NAAA+1                                                     _0109
      NA=NA+1                                                         _0110
      GO TO 909                                                       _0111
  200 IF(XNR.GT.(PAAA1Y+PAAB1Y)) GO TO 201                            _0112
      I=I+1                                                           _0113
      NUNIT(I)=0                                                      _0114
      NAAB=NAAB+1                                                     _0115
      NRUN=NRUN+1                                                     _0116
      NB=NB+1                                                         _0117
      GO TO 909                                                       _0118
  201 I=I-1                                                           _0119
      NBAA=NBAA-1                                                     _0120
      NA=NA-1                                                         _0121
      GO TO 909                                                       _0122
   61 IF(XNR.GT.PBAA1X) GO TO 300                                     _0123
      I=I+1                                                           _0124
      NUNIT(I)=1                                                      _0125
      NBAA=NBAA+1                                                     _0126
      NA=NA+1                                                         _0127
      GO TO 909                                                       _0128
  300 IF(XNR.GT.(PBAA1X+PBAB1X)) GO TO 301                            _0129
      I=I+1                                                           _0130
      NUNIT(I)=0                                                      _0131
      NBAB=NBAB+1                                                     _0132
      NRUN=NRUN+1                                                     _0133
      NB=NB+1                                                         _0134
      GO TO 909                                                       _0135
  301 I=I-1                                                           _0136
```

Fig.40b Cont'd.

```
      NABA=NABA-1                                                    _0137
      NRUN=NRUN-1                                                    _0138
      NA=NA-1                                                        _0139
      GO TO 909                                                      _0140
   62 IF(XNR.GT.PBAA1Y) GO TO 400                                    _0141
      I=I+1                                                          _0142
      NUNIT(I)=1                                                     _0143
      NBAA=NBAA+1                                                    _0144
      NA=NA+1                                                        _0145
      GO TO 909                                                      _0146
  400 IF(XNR.GT.(PBAA1Y+PBAB1Y)) GO TO 401                           _0147
      I=I+1                                                          _0148
      NUNIT(I)=0                                                     _0149
      NBAB=NBAB+1                                                    _0150
      NRUN=NRUN+1                                                    _0151
      NB=NB+1                                                        _0152
      GO TO 909                                                      _0153
  401 I=I-1                                                          _0154
      NBBA=NBBA-1                                                    _0155
      NRUN=NRUN-1                                                    _0156
      NA=NA-1                                                        _0157
      GO TO 909                                                      _0158
   65 IF(XNR.GT.PABA1X) GO TO 500                                    _0159
      I=I+1                                                          _0160
      NUNIT(I)=1                                                     _0161
      NABA=NABA+1                                                    _0162
      NRUN=NRUN+1                                                    _0163
      NA=NA+1                                                        _0164
      GO TO 909                                                      _0165
  500 IF(XNR.GT.(PABA1X+PABB1X)) GO TO 501                           _0166
      I=I+1                                                          _0167
      NUNIT(I)=0                                                     _0168
      NABB=NABB+1                                                    _0169
      NB=NB+1                                                        _0170
      GO TO 909                                                      _0171
  501 I=I-1                                                          _0172
      NAAB=NAAB-1                                                    _0173
      NRUN=NRUN-1                                                    _0174
      NB=NB-1                                                        _0175
      GO TO 909                                                      _0176
   66 IF(XNR.GT.PABA1Y) GO TO 600                                    _0177
      I=I+1                                                          _0178
      NUNIT(I)=1                                                     _0179
      NABA=NABA+1                                                    _0180
      NRUN=NRUN+1                                                    _0181
      NA=NA+1                                                        _0182
      GO TO 909                                                      _0183
  600 IF(XNR.GT.(PABA1Y+PABB1Y)) GO TO 601                           _0184
      I=I+1                                                          _0185
      NUNIT(I)=0                                                     _0186
      NABB=NABB+1                                                    _0187
      NB=NB+1                                                        _0188
      GO TO 909                                                      _0189
  601 I=I-1                                                          _0190
      NBAB=NBAB-1                                                    _0191
      NRUN=NRUN-1                                                    _0192
      NB=NB-1                                                        _0193
      GO TO 909                                                      _0194
   67 IF(XNR.GT.PBBA1X) GO TO 700                                    _0195
      I=I+1                                                          _0196
      NUNIT(I)=1                                                     _0197
      NBBA=NBBA+1                                                    _0198
      NA=NA+1                                                        _0199
      NRUN=NRUN+1                                                    _0200
      GO TO 909                                                      _0201
  700 IF(XNR.GT.(PBBA1X+PBBB1X)) GO TO 701                           _0202
      I=I+1                                                          _0203
      NUNIT(I)=0                                                     _0204
```

Fig.40b Cont'd.

```
      NBBB=NBBB+1                                                       _0205
      NB=NB+1                                                           _0206
      GO TO 909                                                         _0207
  701 I=I-1                                                             _0208
      NABB=NABB-1                                                       _0209
      NB=NB-1                                                           _0210
      GO TO 909                                                         _0211
   68 IF(XNR.GT.PBBA1Y) GO TO 800                                       _0212
      I=I+1                                                             _0213
      NUNIT(I)=1                                                        _0214
      NBBA=NBBA+1                                                       _0215
      NA=NA+1                                                           _0216
      NRUN=NRUN+1                                                       _0217
      GO TO 909                                                         _0218
  800 IF(XNR.GT.(PBBA1Y+PBBB1Y)) GO TO 801                              _0219
      I=I+1                                                             _0220
      NUNIT(I)=0                                                        _0221
      NBBB=NBBB+1                                                       _0222
      NB=NB+1                                                           _0223
      GO TO 909                                                         _0224
  801 I=I-1                                                             _0225
      NBBB=NBBB-1                                                       _0226
      NB=NB-1                                                           _0227
  909 CONTINUE                                                          _0228
      NNOP=I                                                            _0229
      XNAAA=NAAA                                                        _0230
      XNAAB=NAAB                                                        _0231
      XNABA=NABA                                                        _0232
      XNBAA=NBAA                                                        _0233
      XNABB=NABB                                                        _0234
      XNBAB=NBAB                                                        _0235
      XNBBA=NBBA                                                        _0236
      XNBBB=NBBB                                                        _0237
      XNA=NA                                                            _0238
      XNB=NB                                                            _0239
      XNRUN=NRUN                                                        _0240
      MOLW=NA*100+NB*118                                                _0241
      COMPA=XNA/(XNA+XNB)                                               _0242
      COMPB=XNB/(XNA+XNB)                                               _0243
      RUNNUM=XNRUN/(XNA+XNB)                                            _0244
      AAAFR=XNAAA/(XNA+XNB)                                             _0245
      AABFR=XNAAB/(XNA+XNB)                                             _0246
      ABAFR=XNABA/(XNA+XNB)                                             _0247
      BAAFR=XNBAA/(XNA+XNB)                                             _0248
      ABBFR=XNABB/(XNA+XNB)                                             _0249
      BABFR=XNBAB/(XNA+XNB)                                             _0250
      BBAFR=XNBBA/(XNA+XNB)                                             _0251
      BBBFR=XNBBB/(XNA+XNB)                                             _0252
      WRITE(6,827) NNOP,COMPA,COMPB,RUNNUM                              _0253
  827 FORMAT(/1X,I7,3(5X,F6.5))                                         _0254
      WRITE(6,828) AAAFR,AABFR,ABAFR,BAAFR,ABBFR,BABFR,BBAFR,BBBFR      _0255
  828 FORMAT(1X,8(2X,F10.9)/)                                           _0256
 2000 CONTINUE                                                          _0257
      STOP                                                              _0258
      END                                                               _0259
```

Fig.40b Cont'd.

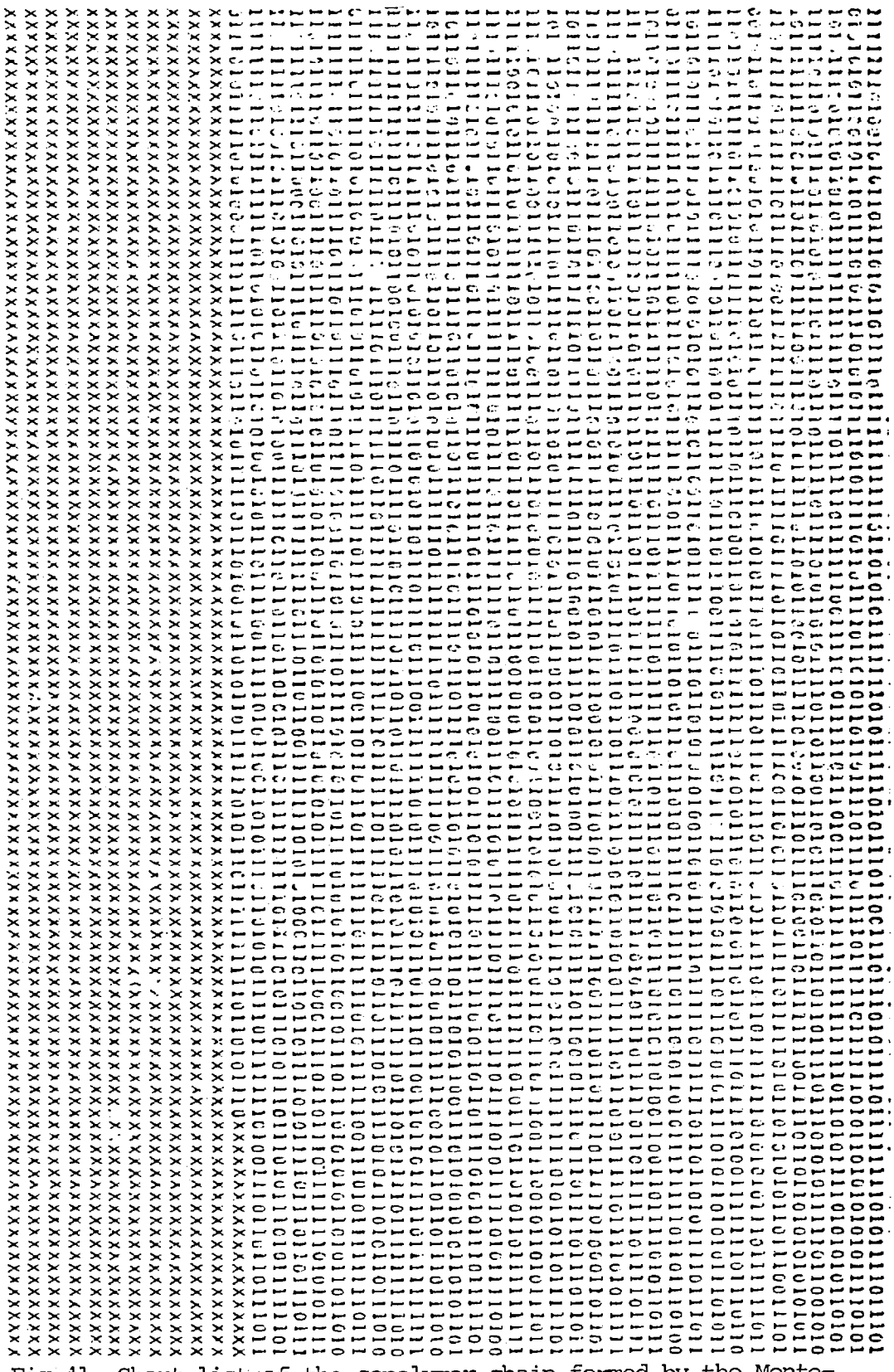

Fig.41 Short-list of the copolymer chain formed by the Monte-Carlo simulation.

```
.90000.10000      1  2000

    2000      .82350      .17650      .34700
 .512000000  .139000000  .170500000  .139010000  .003000000  .034500000  .003000000           0

.80000.20000      1  2000

    2000      .72950      .27050      .52100
 .301500000  .167000000  .250500000  .166500000  .010000000  .093500000  .010000000           0

.70000.30000      1  2000

    2000      .65700      .34300      .61800
 .196000000  .181500000  .276500000  .161000000  .032500000  .147500000  .032500000  .001500000

.60000.40000      1  2000

    2000      .59350      .40650      .70750
 .089000000  .181500000  .308000000  .151000000  .045500000  .202500000  .045500000  .007000000

.50000.50000      1  2000

    2000      .54150      .45850      .75850
 .047500000  .114500000  .313500000  .114000000  .065500000  .265000000  .065500000  .013500000

.40000.60000      1  2000

    2000      .49500      .50500      .76750
 .027500000  .083500000  .292500000  .083000000  .091500000  .300500000  .091000000  .029500000

.30000.70000      1  2000

    2000      .44250      .55750      .74200
 .013000000  .059000000  .251000000  .057500000  .120000000  .313000000  .120000000  .066500000

.20000.80000      1  2000

    2000      .37750      .62250      .67800
 .004500000  .023500000  .184500000  .033000000  .154500000  .305500000  .154500000  .129000000

.10000.90000      1  2000

    2000      .26300      .73200      .49550
 .003000000  .017000000  .087000000  .016500000  .160500000  .231000000  .160500000  .323500000
```

Fig.42 Composition and Microstructure results of Monte-Carlo simulation for various copolymerization models.
Row 1 : feed MMA mole fractn.; feed αMS mole fractn.; conversion(if not instantns.); no. of additions
Row 2 : copolym. chain length; copolym. MMA mole fractn.; copolym. αMS mole fractn.; run number
Row 3 : AAA, AAB, ABA, BAA, ABB, BAB, BBA, BBB fractions in copolymer.(rows throughout figs.42a to e)
(a) Terminal unit model, k_{aa},k_{ba}=1.0; k_{ab}=2.2422; k_{bb}=0.22 (this page). (cont'd.)

```
.90000.10000      0  2000
    2000      .82000      .17950      .33000
 .510500000  .144000000  .150500000  .144000000  .014500000  .021000000  .014500000          0
.80000.20000      0  2000
    2000      .73100      .26900      .46300
 .322000000  .177000000  .194000000  .176500000  .037500000  .054500000  .037500000          0
.70000.30000      0  2000
    2000      .64100      .35150      .55200
 .196500000  .175500000  .200500000  .175000000  .075500000  .100500000  .075500000          0
.60000.40000      0  2000
    2000      .58300      .41700      .63250
 .100500000  .136000000  .215500000  .165500000  .100500000  .150500000  .100500000          0
.50000.50000      0  2000
    2000      .53000      .46200      .65300
 .063500000  .147500000  .191000000  .147000000  .135500000  .179000000  .135500000          0
.40000.60000      0  2000
    2000      .48300      .51700      .66850
 .037500000  .111000000  .151500000  .110500000  .182500000  .223500000  .182500000          0
.30000.70000      0  2000
    2000      .44400      .55600      .68300
 .017500000  .094500000  .127000000  .084000000  .214500000  .257000000  .214500000          0
.20000.80000      0  2000
    2000      .40100      .59200      .68650
 .008500000  .056000000  .095000000  .055500000  .248500000  .287500000  .248000000          0
.10000.90000      0  2000
    2000      .37300      .62700      .66800
 .002500000  .035500000  .041000000  .035500000  .293000000  .298500000  .293000000          0
```

Fig.42 (Cont'd.) (b) Penultimate unit model, k_{aaa},k_{aba},k_{baa},k_{bba}=1.0; k_{bbb}=0.0 (by simplifying assumption); k_{aab}=2.3256; k_{abb}=0.76; k_{bab}=1.25.

(cont'd.)

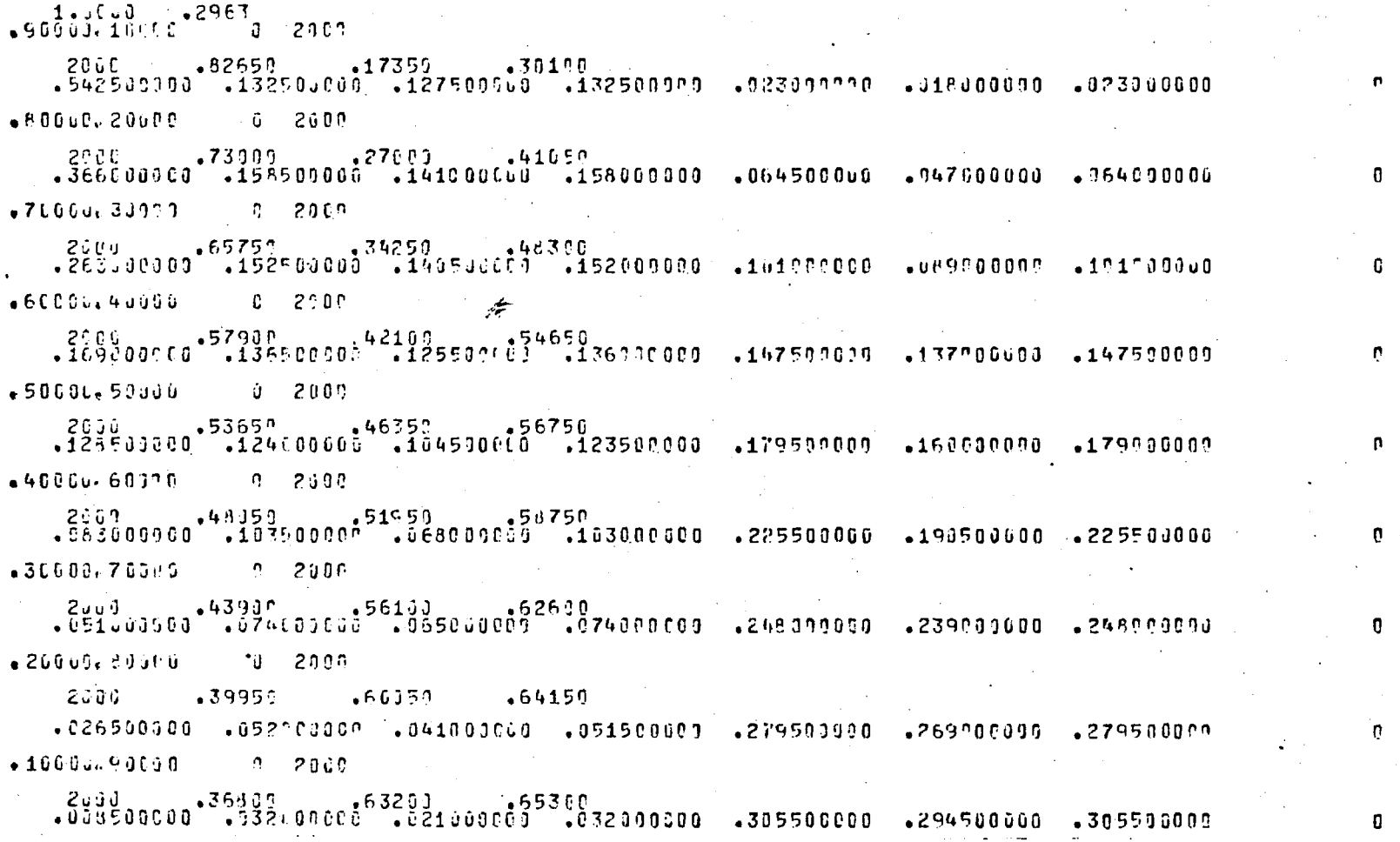

Fig.42 (Cont'd.) (c) Penpenultimate unit model (with simplifying assumptions), k_{aaaa},k_{aba},k_{baa},k_{bba},k_{baaa}=1.0; k_{bbb}=0.0; k_{aaab}=2.6954; k_{abb}=1.819, k_{bab}=1.2987; k_{baab}=0.2963.

(cont'd.)

```
.90000.10000      ) 2000
    1984      .82611      .17389      .34476
 .514112903  .138608871  .170866935  .138608871  .001512097  .033770161  .001512097            0
.80000.20000      ) 2000
    1944      .73817      .26183      .51440
 .313786008  .139666667  .252572016  .166152263  .004629630  .090534979  .004629630            0
.70000.30000      ) 2000
    1890      .66807      .33193      .62381
 .193361433  .162276080  .292413066  .161749210  .019494204  .149631191  .019494204  .000526870
.60000.40000      ) 2000
    1832      .60639      .39301      .72216
 .087336245  .138296943  .334061135  .157751092  .026746725  .203056769  .026746725  .004912664
.50000.50000      ) 2000
    1714      .57235      .42765      .78705
 .059425904  .127103851  .359976663  .122520420  .033255543  .270711785  .033255543  .000583431
.40000.60000      ) 2000
    1572      .54262      .45738      .83015
 .034351145  .092875318  .374601934  .092239186  .040712468  .322519084  .040076336  .001272265
.30000.70000      ) 2000
    1326      .50130      .49170      .85219
 .017345400  .064102564  .370286576  .063348416  .055806938  .361990950  .055806938  .009803922
.20000.80000      ) 2000
    1054      .48577      .51423      .86717
 .004743833  .046489564  .365275142  .045540797  .068311195  .387096774  .068311195  .012333966
.10000.90000      ) 2000
     640      .47344      .52656      .86719
 .007812500  .031250000  .354687500  .029687500  .078125000  .403125000  .078125000  .014062500
```

Fig.42 (Cont'd.) (d) Wittmer's case(i) model, k_{aa},k_{ba}=1.0; k'_{aa},k'_{ab},k'_{ba}=0.0; k_{ab}=2.193; k_{bb}=0.316; k'_{bb}=1.5127.

(cont'd.)

```
.90000.10000      0  2000
    2000      .86430      .13550      .26400
 .629000000  .103500000  .128500000  .103510000  .003500000  .028500000  .003500000          0
.80000.20000      0  2000
    2000      .77250      .22750      .41800
 .428500000  .134500000  .190500000  .134000000  .018500000  .074500000  .018500000          0
.70000.30000      0  2000
    2000      .67800      .32200      .57000
 .294000000  .139500000  .248000000  .138010000  .037000000  .146500000  .037000000          0
.60000.40000      0  2000
    2000      .59000      .40200      .67950
 .126500000  .131500000  .277500000  .131000000  .062000000  .208500000  .062000000          0
.50000.50000      0  2000
    2000      .54150      .45150      .72800
 .079000000  .089000000  .269500000  .098510000  .094500000  .265000000  .094500000          0
.40000.60000      1  2000
    2000      .49200      .50800      .74450
 .037000000  .032500000  .236500000  .082010000  .135500000  .290000000  .135500000          0
.30000.70000      0  2000
    2000      .45150      .54850      .75100
 .019000000  .036500000  .202500000  .056000000  .173000000  .319000000  .173000000          0
.20000.80000      0  2000
    2000      .41550      .58450      .74900
 .007000000  .033500000  .164500000  .033000000  .210000000  .341000000  .210000000          0
.10000.90000      0  2000
    2000      .38100      .62000      .70650
 .003000000  .023500000  .096500000  .023000000  .266500000  .330000000  .266500000          0
```

Fig.42 (Cont'd.) (e) Wittmer's case(ii) model, k_{aa},k_{ba}=1.0; k'_{aa},k'_{ab},k'_{ba},k'_{bb}=0.0; k_{ab}=2.2222; k_{bb},k_{bbb}=0.25; k'_{bbb}=1.1967.

(cont'd.)

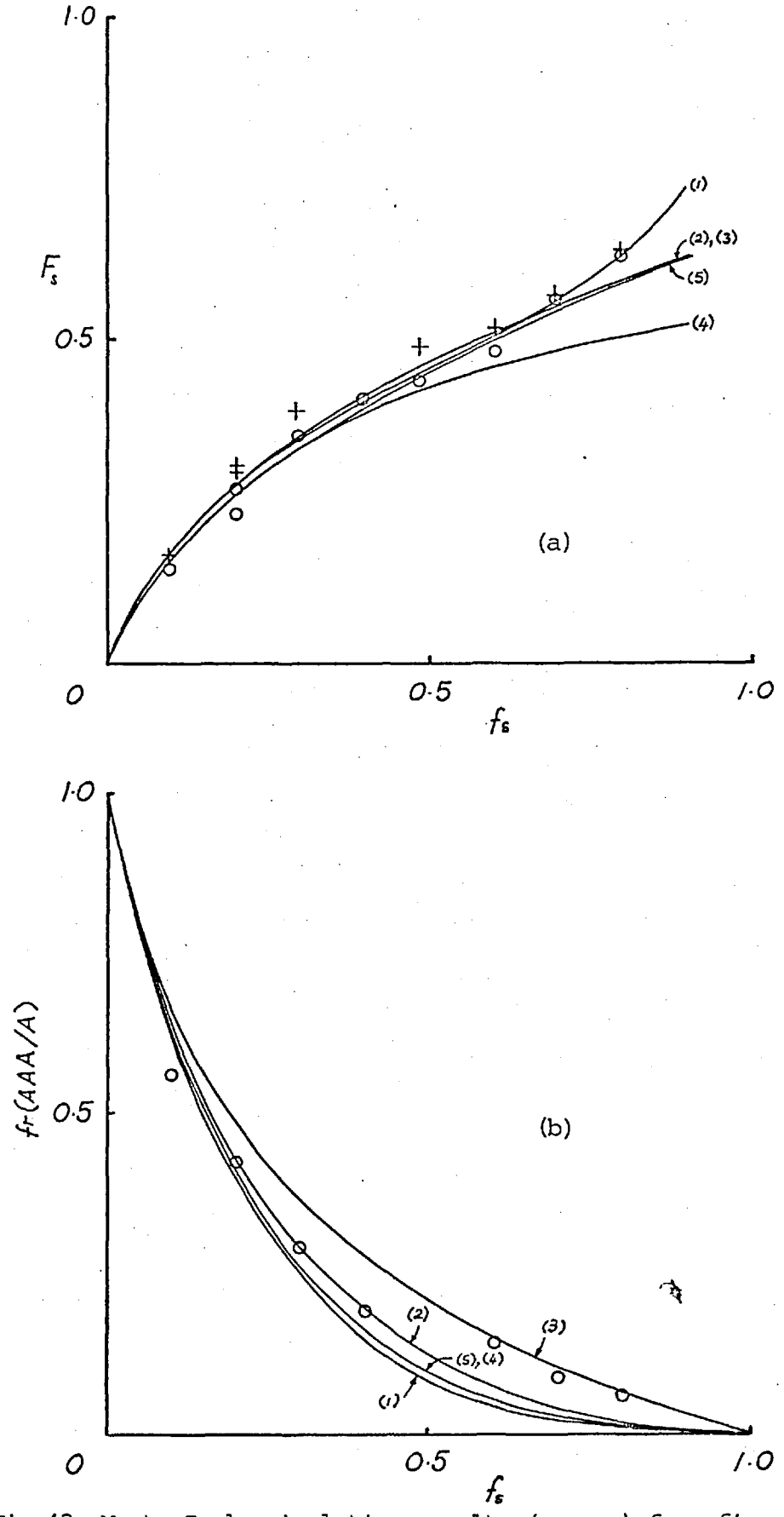

Fig.43 Monte-Carlo simulation results (curves) from figs.(42) and their relation to the actual experimental data (data of this research -1500bars, 60°C); a) copolymer comp. vs. feed comp., b) AAA/A triad frac. vs. feed comp. (curves: (1)terminal, (2)penult., (3)penpenult., (4)Wittmer(i), (5)Wittmer(iii))

data only some are close enough to the experimental triad concentration data.

It seems from figure.(43b) that the best fit on triad fraction points is obtainable by the penultimate unit model for low αMS copolymer and by the penpenultimate unit model for high αMS copolymers. It could probably be said that the mechanism involves certain depropagation of AB links to give the block character at high αMS copolymers. This was also supported in section(6.4.6). Terminal unit and simple depropagation models certainly do not conform with microstructure data.

It is possible to define the microstructure in numerical values of parameters as described in section(4.2). The main parameters which define the microstructure were,

ρ = the persistance ratio of Coleman and Fox;

$\eta = 1/\rho$, departure from random statistics of Ito et al.;

$\mu[A]$ = average sequence length for A sequences,

where

$$\mu[A] = \frac{P_1[A]}{P_2[AB]} \quad , \quad \rho = \mu[A]P_1[B] = 1/\eta \qquad (6.6.1)$$

From NMR data

$$\frac{2P_2[AB]}{P_1[A]} = 2F_{SMS} + 2F_{MMS} \qquad (6.6.2)$$

where

$$F_{MMM} + 2F_{MMS} + F_{SMS} = 1$$

On the other hand for comparison same parameters for terminal and penultimate unit models can be calculated by:

Terminal

$$\mu[A] = P_{ab} \sum_{n=1} nP_{aa}^{n-1} \qquad (6.6.3)$$

Penultimate

$$\mu[A] = P_{bab} + P_{baa}P_{aab} \sum_{n=1} (n+1)P_{aaa}^{n-1} \qquad (6.6.4)$$

or simply by Ito's formulae,

$$\eta = 1/(\mu[A]P_1[B]) \tag{6.6.5}$$

where for the terminal unit model

$$P_1[B] = \frac{1 + r_B/x}{r_A x + 2 + r_B/x} \tag{6.6.6}$$

$$\mu[A] = 1 + r_A x \tag{6.6.7}$$

and for the penultimate unit model

$$P_1[B] = \frac{1 + \frac{r'_B}{x}\left(\frac{r_B + x}{r'_B + x}\right)}{r'_A x\left(\frac{1 + r_A x}{1 + r'_A x}\right) + 2 + \frac{r'_B}{x}\left(\frac{r_B + x}{r'_B + x}\right)} \tag{6.6.8}$$

$$\mu[A] = 1 + r'_A\left(\frac{1 + r_A x}{1 + r'_A x}\right) x \tag{6.6.9}$$

The results of the comparison are shown in Table(XXX) below, and NMR results utilised were those of 1500 atm because of their better accuracy over the rest.

Table XXX

	NMR analyses			Obs.		Term.		Penult.	
Code	$P_1[B]$	$P_1[A]$	$2/\mu[A]$	$\mu[A]$	η	$\mu[A]$	η	$\mu[A]$	η
23L	0.144	0.856	0.433	4.62	1.51	5.13	1.36	5.39	1.29
4A	0.230	0.770	0.475	4.21	1.03	2.79	1.55	3.08	1.41
6A	0.350	0.650	0.772	2.59	1.10	2.08	1.37	2.35	1.22
7A	0.403	0.597	0.798	2.51	0.99	1.68	1.48	1.91	1.30
8A	0.432	0.568	0.821	2.44	0.95	1.48	1.58	1.67	1.38
9A	0.481	0.519	0.874	2.89	0.91	1.30	1.60	1.45	1.43
10A	0.564	0.436	1.014	1.97	0.90	1.19	1.49	1.31	1.36
11A	0.629	0.371	1.047	1.91	0.83	1.11	1.43	1.19	1.34

From the results it can clearly be seen that the copolymer has a more block character than that of penultimate unit model and even more from terminal unit model. Since $\eta=1$ denotes a random copolymer it seems that the copolymer is closer to a random distribution than the other models, which means a more block character since decreasing η is due to increasing block character.

For other pressures these calculations were carried out but due to less accurate data the results are given in fig.(50) (together with the coisotacticity parameters of the preceding paragraphs) without further analysis. They may still reveal some information on the pressure dependence of the above parameters. Nevertheless a plot of F_{AAA} (fig.(44)) on four different concentrations against pressure shows a convergence towards high pressures, indicating increased block character.

Another microstructure parameter is the coisotacticity parameter of Bovey, as described in section (4.2). This was calculated by other researchers in various ways for the results given in section (6.1). Izu and coworkers[95] calculate P_{ab} $(=1-\varepsilon)$ for σ from the depropagating model by equations (4.1.66) and (4.1.67). Ito et al. calculated σ from equation (4.3.6) and its linear plot. An attempt was made in this research in the latter method with 1500 atm data. The parameters were calculated as

$$\sigma = 0.23 \ , \quad r_{MMA} = 0.54$$

but the plot was far from being satisfactory. The parameter was also calculated from equation (4.3.1a) and believed to be more satisfactory since it was calculated from individual triad fractions instead of F_x, F_y and F_z peaks. The value of σ for 1500 atm was found to be 0.38. The results for other pressures are given in Table (XXXI). A slight increase in this parameter is observed with pressure. Izu et al. claim that there should be an increase in this parameter with temperature since there will be an increase in randomness. On the other hand, one can say that there should be an increase in this parameter with pressure since there should be a more random attachment less inhibited by steric hindrance which causes stereospecificity.

Another attempt was made on the definition of the microstructure by a calculation of the codiastereosequence distribution of the copolymer. This is the calculation of the same parameters of average length

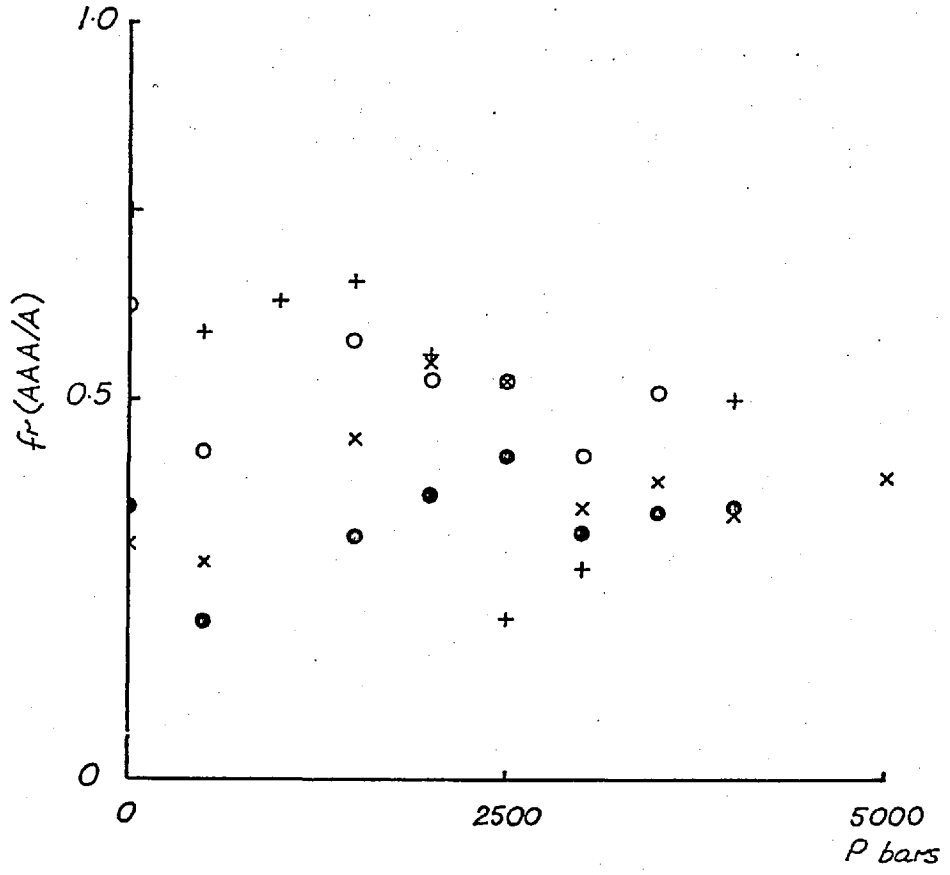

Fig.44 Pressure dependence of the (AAA) triad concentrations for various monomer feed compositions: +) 0.1, o) 0.2, x) 0.3, ⊙) 0.4 αMS.

and persistance ratio as earlier in the section but for I (=coisotactic enthainment) and S (=cosyndiotactic enchainment) instead of A and B, and IS instead of AB. The NMR data yield information as

$$P_1[I] = (F_{x,SMS} + F_{y,SMS}/2)/F_{SMS} \qquad (6.6.10a)$$

$$P_2[IS] = F_{y,SMS}/F_{SMS} \qquad (6.6.10b)$$

$$P_1[S] = (F_{z,SMS} + F_{y,SMS}/2)/F_{SMS} \qquad (6.6.10c)$$

where $F_{x,SMS}$ is the amount of SMS triads in F_x peak etc. The calculations are similar to monomer unit calculations. The results for 1500 atm data are given in Table (XXXII). The average value for ρ is

$$\rho = 0.66 \quad \text{or} \quad \eta = 1.52$$

indicating a block character for the codiastereosequences.

Table XXXI

Coisotacticity parameter for MS-MMA copolymers prepared at various pressures. T = 60°C.

Pressure	σ
0	0.337
500	0.369
1000	0.349
1500	0.383
2000	0.389
2500	0.443*
3000	0.418
3500	0.407
4000	0.404
5000	0.420*

* after rejecting one outlier.

The pressure dependence of σ, when plotted, will show the same trend of change as the pressure dependence of $r_{\alpha MS}$, i.e., a steady increase up to around 3000 bars followed by a levelling off.

NP= 5 P= 0

RA= 0.567 RB= 0.148 RPA1= 0.497 RPA2= 1.314 RPB1= 0.553

CODE	FEED-AMS	COP.-AMS	FX1	FX2	FX3	FY1	FY2	F7
13	0.0879	0.1437	75.0	17.5	0.0	8.5	0.0	0.0
2	0.1900	0.2339	62.5	20.4	3.9	11.3	3.0	0.1
3	0.3921	0.3744	35.7	32.9	5.9	14.4	8.0	2.4
4	0.4858	0.4107	32.4	32.9	5.9	17.5	8.1	3.9
A14	0.2979	0.3060	30.9	36.3	7.0	15.9	4.5	3.9

P= 0

CODE	SIGMA	P(A)	P(B)	2P(AB)/P(A)	M(A)OB	HOB	M(A)TER	HTER	M(A)PEN	HPEN	(I)	(IS)	(S)	RO
13	-.000	0.856	0.144	0.260	7.692	0.905	6.861	1.314	6.729	1.034	0.0	0.0	0.0	0.0
2	0.332	0.766	0.234	0.457	4.376	0.977	3.417	1.351	3.646	1.172	0.771	0.429	0.229	0.411
3	0.333	0.622	0.378	0.799	2.503	1.056	1.879	1.306	2.188	1.208	0.607	0.491	0.393	0.484
4	0.371	0.589	0.411	0.862	2.320	1.049	1.600	1.322	1.888	1.290	0.556	0.453	0.444	0.546
A14	0.311	0.694	0.306	0.830	2.410	1.356	2.336	1.399	2.641	1.237	0.601	0.292	0.399	0.821

NP= 8 P= 500

RA= 0.465 RB= 0.191 RPA1= 0.441 RPA2= 0.922 RPB1= 0.695

CODE	FEED-AMS	COP.-AMS	FX1	FX2	FX3	FY1	FY2	F7
2G	0.1009	0.1696	59.0	16.0	11.2	7.7	2.3	3.5
3G	0.1997	0.2759	43.3	23.3	12.7	12.3	4.0	4.1
6G	0.2950	0.3935	28.4	26.0	11.8	16.7	9.4	7.0
7G	0.4008	0.4334	20.6	27.3	11.9	22.4	11.5	11.3
8G	0.4559	0.4397	24.6	24.4	10.0	15.9	12.0	13.8
9G	0.5948	0.4732	22.7	26.7	9.2	23.3	11.1	8.8
101K	0.7006	0.5558	33.3	17.3	12.7	18.3	11.0	10.0
11P	0.7956	0.7424	4.7	48.7	15.3	13.3	8.7	11.3

P= 500

CODE	SIGMA	P(A)	P(B)	2P(AB)/P(A)	M(A)OB	HOB	M(A)TER	HTER	M(A)PEN	HPEN	(I)	(IS)	(S)	RO
2G	0.253	0.830	0.170	0.577	3.466	1.701	5.142	1.147	5.394	1.093	0.726	0.135	0.274	1.459
3G	0.285	0.724	0.276	0.772	2.591	1.349	2.863	1.266	3.178	1.141	0.707	0.192	0.293	1.074
6G	0.374	0.616	0.384	0.991	2.018	1.292	2.111	1.235	2.413	1.080	0.585	0.337	0.415	0.724
7G	0.435	0.561	0.439	1.191	1.679	1.355	1.695	1.343	1.962	1.160	0.509	0.331	0.491	0.554
8G	0.432	0.560	0.440	1.119	1.787	1.272	1.555	1.353	1.800	1.264	0.447	0.335	0.553	0.737
9G	0.455	0.527	0.473	1.082	1.848	1.145	1.317	1.405	1.502	1.407	0.507	0.381	0.493	0.655
101K	0.447	0.444	0.556	1.030	1.942	0.927	1.199	1.301	1.336	1.347	0.540	0.326	0.460	0.761
11P	0.271	0.258	0.742	1.326	1.508	0.693	1.119	1.203	1.213	1.110	0.557	0.244	0.443	1.001

Fig.50 Computer output for the calculation of the microstructure parameters of the copolymers. NP=number of points, P=pressure, RA=r_{MMA}, RB=$r_{\alpha MS}$ (terminal), RPA1=r_A, RPA2=$r_{A'}$, RPB1=r_B (penultimate), F=peak area %, M=μ, H=η, TER=terminal, PEN=penultimate, RO=ρ. (cont'd)

NO= 4 P= 1000

RA= 0.500 RB= 0.268 RRA1= 0.505 RRA2= 0.792 RRB1= 0.833

CODE	FEED-AMS	COP.-AMS	FX1	FX2	FX3	FY1	FY2	FZ
2F	0.0992	0.1822	43.3	19.3	3.3	7.7	0.7	6.7
8S	0.5004	0.4654	27.9	28.6	6.8	14.3	8.9	8.7
9D	0.6036	0.5977	23.3	47.0	4.3	15.0	8.7	1.6
11Z	0.8206	0.6786	27.3	22.7	15.9	14.2	14.1	10.5

P= 1000

CODE	SIGMA	P(A)	P(B)	2P(AB)/P(A)	M(A)OB	HOB	M(A)TER	HTER	M(A)PEN	HPEN	(I)	(IS)	(S)	PO
2F	0.337	0.818	0.182	0.484	4.132	1.328	5.538	0.991	5.901	0.930	0.341	0.065	0.659	3.436
8S	0.388	0.535	0.465	0.917	2.181	0.985	1.499	1.433	1.664	1.201	0.461	0.365	0.539	0.451
9D	0.291	0.402	0.598	0.912	2.193	0.763	1.328	1.250	1.496	1.149	0.592	0.595	0.408	0.405
11Z	0.378	0.321	0.679	1.179	1.696	0.869	1.109	1.328	1.164	1.266	0.567	0.348	0.433	0.705

NO= 9 P= 1500

RA= 0.446 RB= 0.223 RRA1= 0.430 RRA2= 0.802 RRB1= 0.765

CODE	FEED-AMS	COP.-AMS	FX1	FX2	FX3	FY1	FY2	FZ
23L	0.0975	0.1436	65.6	17.5	1.8	9.0	2.8	3.8
4A	0.1991	0.2305	58.0	21.5	2.3	14.2	2.6	1.0
51K	0.2021	0.2635	58.0	21.2	3.6	11.8	3.4	3.0
6A	0.2925	0.3504	46.0	20.0	8.4	15.0	7.2	5.5
7A	0.3965	0.4035	31.7	33.3	8.6	14.7	5.5	3.3
8A	0.4835	0.4332	36.7	25.2	8.7	19.5	5.7	2.8
9A	0.5978	0.4814	28.0	39.4	4.0	23.4	7.4	1.4
10A	0.6965	0.5637	20.6	35.8	8.0	26.0	7.4	4.4
11A	0.7969	0.6288	16.3	34.0	11.3	27.5	7.0	3.3

P= 1500

CODE	SIGMA	P(A)	P(B)	2P(AB)/P(A)	M(A)OB	HOB	M(A)TER	HTER	M(A)PEN	HPEN	(I)	(IS)	(S)	PO
23L	0.390	0.856	0.144	0.433	4.619	1.508	5.127	1.358	5.388	1.292	0.391	0.333	0.619	0.707
4A	0.394	0.770	0.230	0.475	4.211	1.030	2.794	1.553	3.084	1.407	0.610	0.441	0.390	0.540
51K	0.366	0.731	0.269	0.534	3.745	0.991	2.761	1.344	3.050	1.217	0.539	0.333	0.451	0.745
6A	0.403	0.650	0.350	0.772	2.591	1.102	2.079	1.373	2.346	1.216	0.569	0.341	0.431	0.719
7A	0.316	0.597	0.403	0.798	2.506	0.991	1.679	1.483	1.909	1.301	0.652	0.316	0.348	0.718
8A	0.386	0.568	0.432	0.821	2.436	0.950	1.476	1.557	1.673	1.383	0.662	0.358	0.338	0.608
9A	0.391	0.519	0.481	0.874	2.288	0.908	1.300	1.593	1.552	1.431	0.602	0.578	0.398	0.415
10A	0.405	0.436	0.564	1.014	1.972	0.899	1.194	1.585	1.307	1.357	0.591	0.374	0.409	0.447
11A	0.393	0.371	0.629	1.047	1.910	0.833	1.114	1.423	1.188	1.338	0.685	0.324	0.315	0.656

Fig.50 (Cont'd).

NP= 8 P= 2000

PA= 0.474 PB= 0.300 PPA1= 0.531 PPA2= 0.665 PPB1= 1.036

CODE	FEED-AMS	COP.-AMS	FX1	FX2	FX3	FY1	FY2	FZ
24L	0.0993	0.1522	56.1	21.4	4.3	11.4	3.4	4.7
31K	0.2081	0.2495	48.0	24.8	4.5	11.3	5.0	5.1
44	0.2034	0.3107	52.8	22.4	4.8	10.9	4.0	5.0
52K	0.1958	0.2553	59.6	15.8	4.2	12.5	3.5	3.6
4F	0.1959	0.2670	51.7	27.3	4.3	15.3	3.3	3.3
64	0.2987	0.3552	55.0	26.5	1.0	16.0	6.0	3.0
7K	0.4009	0.4015	37.5	28.1	6.6	18.2	6.6	6.3
118	0.7930	0.6693	16.5	27.5	12.0	21.0	12.0	13.5

P= 2000

CODE	SIGMA	P(A)	P(B)	2P(AB)/P(A)	M(A)OB	HOB	M(A)TEP	HTEP	M(A)PEN	HPEN	(I)	(IS)	(S)	PO
24L	0.368	0.848	0.152	0.576	3.472	1.892	5.298	1.240	5.985	1.098	0.484	0.274	0.516	0.911
31K	0.355	0.751	0.249	0.653	3.063	1.309	2.804	1.430	3.165	1.266	0.479	0.342	0.721	0.725
44	0.362	0.689	0.311	0.628	3.185	1.011	2.856	1.127	3.225	0.998	0.459	0.270	0.541	0.919
52K	0.426	0.745	0.255	0.511	3.914	1.001	2.947	1.325	3.328	1.177	0.525	0.316	0.474	0.789
4F	0.362	0.733	0.267	0.644	3.106	1.206	2.946	1.271	3.327	1.126	0.546	0.303	0.454	0.819
64	0.417	0.645	0.355	0.585	3.419	0.823	2.113	1.332	2.370	1.186	0.375	0.500	0.625	0.459
7K	0.384	0.599	0.401	0.833	2.401	1.037	1.708	1.458	1.894	1.315	0.508	0.338	0.662	0.738
118	0.434	0.331	0.669	1.235	1.619	0.923	1.124	1.330	1.168	1.279	0.480	0.320	0.520	0.790

NP= 8 P= 2500

PA= 0.410 PB= 0.290 PPA1= 0.508 PPA2= 0.586 PPB1= 1.198

CODE	FEED-AMS	COP.-AMS	FX1	FX2	FX3	FY1	FY2	FZ
210	0.1010	0.0539	20.4	53.0	8.0	10.6	3.5	5.0
50	0.2022	0.2530	52.3	21.7	3.3	15.0	3.9	5.5
6C-D	0.2903	0.3505	46.6	17.6	8.8	15.4	6.0	6.0
70	0.3980	0.4245	42.5	23.8	3.8	18.8	6.0	5.0
80	0.4967	0.4855	35.4	22.8	8.3	21.7	7.3	5.4
90	0.5805	0.5091	30.0	21.6	8.1	22.4	8.0	10.9
10D	0.6949	0.6109	25.0	26.5	11.3	23.0	9.0	9.3
11D	0.8306	0.6687	15.8	25.0	12.5	17.5	20.5	10.8

P= 2500

CODE	SIGMA	P(A)	P(B)	2P(AB)/P(A)	M(A)OB	HOB	M(A)TEP	HTEP	M(A)PEN	HPEN	(I)	(IS)	(S)	PO
210	0.205	0.946	0.054	0.966	2.070	8.961	4.649	3.991	5.631	3.295	0.591	0.212	0.[illegible]	1.140
50	0.430	0.747	0.253	0.619	3.231	1.223	2.618	1.510	3.097	1.276	0.419	0.302	0.557	0.[illegible]
6C-D	0.415	0.650	0.350	0.746	2.681	1.064	2.002	1.425	2.320	1.230	0.547	0.268	0.437	0.551
70	0.455	0.575	0.425	0.722	2.770	0.850	1.620	1.454	1.831	1.286	0.459	0.405	0.541	0.[illegible]
80	0.446	0.515	0.485	0.865	2.312	0.891	1.415	1.455	1.564	1.317	0.569	0.348	0.631	0.705
90	0.487	0.491	0.509	0.980	2.041	0.962	1.296	1.515	1.407	1.396	0.648	0.296	0.552	0.835
10D	0.430	0.389	0.611	1.087	1.840	0.890	1.180	1.387	1.250	1.309	0.534	0.304	0.466	0.[illegible]
11D	0.440	0.331	0.669	1.301	1.537	0.973	1.084	1.380	1.118	1.338	0.519	0.488	0.481	0.533

Fig.50 (Cont'd).

NP= 8 P= 3000

RA= 0.428 RB= 0.383 RPA1= 0.528 RPA2= 0.519 RPB1= 1.437

CODE	FEED-AMS	COP.-AMS	FX1	FX2	FX3	FY1	FY2	F7
2E	0.1011	0.3000	60.0	24.0	5.0	9.3	3.0	16.7
3E	0.1963	0.3248	42.5	24.2	8.7	11.3	7.5	6.7
6E	0.2835	0.3718	35.4	39.8	5.8	9.5	5.0	5.0
7E	0.4058	0.4843	32.5	25.7	6.2	19.3	8.2	8.2
8E	0.4918	0.5010	27.2	24.0	10.0	21.3	9.2	9.0
9E	0.6064	0.5645	26.8	27.5	6.0	22.7	8.8	10.5
102K	0.6744	0.6314	6.7	47.7	7.3	25.0	5.0	5.0
11E	0.7893	0.7796	40.0	10.0	6.5	24.5	10.0	11.0

P= 3000

CODE	SIGMA	P(A)	P(B)	2P(AB)/P(A)	M(A)OB	HOB	M(A)TER	HTER	M(A)PEN	HPEN	(I)	(IS)	(S)	RO
2E	0.398	0.700	0.300	0.827	2.418	1.378	4.805	0.694	5.677	0.587	0.243	0.121	0.737	1.595
3E	0.348	0.675	0.325	0.813	2.460	1.252	2.752	1.119	3.150	0.977	0.544	0.328	0.456	0.758
6E	0.257	0.628	0.372	0.799	2.503	1.075	2.082	1.292	2.325	1.157	0.525	0.316	0.475	0.788
7E	0.446	0.516	0.484	0.902	2.217	0.931	1.627	1.266	1.766	1.169	0.456	0.363	0.544	0.694
8E	0.443	0.499	0.501	1.017	1.967	1.015	1.442	1.384	1.540	1.296	0.518	0.326	0.492	0.755
9E	0.473	0.432	0.568	1.008	1.984	0.887	1.278	1.377	1.338	1.314	0.411	0.348	0.589	0.696
102K	0.345	0.369	0.631	1.073	1.864	0.850	1.207	1.313	1.251	1.266	0.566	0.289	0.434	0.850
11E	0.631	0.220	0.780	0.895	2.235	0.574	1.114	1.151	1.139	1.126	0.418	0.364	0.582	0.669

NP= 8 P= 3500

RA= 0.432 RB= 0.345 RPA1= 0.545 RPA2= 0.542 RPB1= 1.356

CODE	FEED-AMS	COP.-AMS	FX1	FX2	FX3	FY1	FY2	F7
220	0.1028	0.1630	61.6	22.4	2.6	7.2	2.6	6.0
4J	0.1488	0.2862	51.2	15.0	4.8	16.0	3.9	5.0
6J	0.2920	0.3545	39.3	23.3	6.8	16.3	5.0	11.3
720	0.3899	0.4025	35.0	33.0	3.4	19.6	6.0	5.8
8J	0.4452	0.5059	25.5	23.8	12.5	18.5	11.5	10.0
9J	0.5872	0.5356	23.4	23.4	11.4	20.4	11.0	11.4
10J	0.7171	0.6773	20.0	25.5	14.5	26.8	10.0	5.0
111T	0.8056	0.7909	14.5	40.0	11.0	25.0	10.0	5.0

P= 3500

CODE	SIGMA	P(A)	P(B)	2P(AB)/P(A)	M(A)OB	HOB	M(A)TER	HTER	M(A)PEN	HPEN	(I)	(IS)	(S)	RO
220	0.327	0.837	0.163	0.520	3.846	1.595	4.770	1.296	5.749	1.067	0.348	0.232	0.652	0.978
4J	0.441	0.714	0.286	0.622	3.215	1.047	2.741	1.275	3.193	1.094	0.493	0.279	0.507	0.895
6J	0.430	0.646	0.354	0.858	2.331	1.210	2.047	1.378	2.318	1.217	0.403	0.216	0.597	1.111
720	0.412	0.598	0.402	0.848	2.358	1.053	1.676	1.482	1.850	1.343	0.395	0.370	0.605	0.645
8J	0.416	0.493	0.507	1.103	1.813	1.088	1.458	1.353	1.576	1.252	0.537	0.338	0.463	0.735
9J	0.444	0.463	0.537	1.114	1.795	1.038	1.304	1.425	1.382	1.349	0.500	0.325	0.500	0.768
10J	0.423	0.323	0.677	1.113	1.797	0.822	1.170	1.261	1.214	1.216	0.661	0.339	0.339	0.661
111T	0.365	0.209	0.791	1.130	1.770	0.714	1.104	1.145	1.131	1.118	0.667	0.417	0.333	0.533

Fig.50 (Cont'd).

NP= 6 P= 4000

PA= 0.409 PB= 0.311 PPA1= 0.507 PPA2= 0.562 PPB1= 1.262

CODE	FEED-AMS	COP.-AMS	FX1	FX2	FX3	FY1	FY2	FZ
2M	0.0799	0.2000	50.0	19.8	12.0	12.3	10.0	8.3
6M	0.2468	0.3641	35.0	25.5	8.8	16.8	8.0	7.5
7M	0.3883	0.4706	36.3	26.8	6.8	15.3	10.0	7.0
8M	0.4912	0.5624	35.0	32.5	5.5	18.5	6.0	5.5
92S	0.6100	0.5334	28.0	22.3	10.0	18.7	10.0	11.3
112S	0.8163	0.6677	12.5	18.5	21.0	14.5	20.0	15.0

P= 4000

CODE	SIGMA	P(A)	P(B)	2P(AB)/P(A)	M(A)OB	HOB	M(A)TER	HTER	M(A)PEN	HPEN	(I)	(IS)	(S)	RO
2M	0.382	0.800	0.200	0.917	2.181	2.292	4.685	1.067	5.647	0.885	0.561	0.330	0.439	0.744
6M	0.398	0.636	0.364	0.909	2.200	1.248	1.969	1.395	2.257	1.217	0.527	0.329	0.473	0.757
7M	0.403	0.529	0.471	0.897	2.230	0.953	1.644	1.292	1.845	1.152	0.496	0.420	0.504	0.595
8M	0.387	0.438	0.562	0.870	2.299	0.777	1.424	1.249	1.561	1.139	0.472	0.333	0.528	0.748
92S	0.446	0.467	0.533	1.036	1.931	0.971	1.261	1.486	1.350	1.389	0.479	0.319	0.521	0.781
112S	0.405	0.332	0.668	1.450	1.379	1.086	1.092	1.375	1.125	1.331	0.554	0.357	0.446	0.692

NP= 5 P= 5000

PA= 0.486 PB= 0.313 PPA1= 0.633 PPA2= 0.629 PPB1= 1.209

CODE	FEED-AMS	COP.-AMS	FX1	FX2	FX3	FY1	FY2	FZ
6S	0.3022	0.4040	40.0	48.3	0.0	4.7	3.0	5.7
8T	0.4937	0.5055	32.0	31.7	4.3	20.0	9.5	2.7
91S	0.5845	0.5251	18.0	34.0	8.0	19.8	11.2	10.4
10P	0.6948	0.6059	25.2	34.8	5.6	20.8	12.0	5.4
112T	0.7921	0.6673	13.3	42.0	6.0	33.3	6.0	5.7

P= 5000

CODE	SIGMA	P(A)	P(B)	2P(AB)/P(A)	M(A)OB	HOB	M(A)TER	HTER	M(A)PEN	HPEN	(I)	(IS)	(S)	RO
6S	0.195	0.596	0.404	0.704	2.841	0.871	2.122	1.156	2.458	1.007	0.172	0.345	0.828	0.414
8T	0.414	0.495	0.505	0.849	2.356	0.848	1.498	1.320	1.647	1.201	0.548	0.574	0.452	0.428
91S	0.411	0.474	0.526	1.130	1.770	1.074	1.345	1.413	1.448	1.313	0.459	0.378	0.541	0.656
10P	0.415	0.393	0.607	1.016	1.969	0.837	1.213	1.358	1.277	1.291	0.504	0.522	0.496	0.479
112T	0.440	0.333	0.667	1.127	1.775	0.844	1.128	1.329	1.165	1.286	0.481	0.321	0.519	0.778

Fig.50 (Cont'd).

Table XXXII

Microstructure data of αMS-MMA copolymers, prepared at 1500 bars, for the calculation of ρ for entanglements.

Copolymer	[B]	[A]	2[AB]/[A]	[I]	[IS]	[S]	ρ
23L	0.1436	0.8564	0.433	0.381	0.333	0.619	0.707
4A	0.2305	0.7695	0.475	0.610	0.441	0.390	0.540
6A	0.3504	0.6496	0.772	0.569	0.341	0.431	0.719
7A	0.4026	0.5974	0.798	0.652	0.316	0.348	0.718

6.7 Effect of Pressure and Composition on the Rate of Polymerization and on Polymer Molecular Weight.

The dependence of reaction rates on pressure and also on the monomer feed composition was also investigated by assessing the rates of polymerization gravimetrically. For accuracy the conversions were generally kept below 5% so that as well as avoiding composition drift an overall copolymerization rate close to initial rate and a molecular weight close to zero conversion molecular weight was ensured.

a) Reaction rate

The addition of the comonomer αMS into the MMA-AZBN solutions seems to reduce the rate of the reaction drastically (fig.(45) and Table (XVIII)). It is beyond the scope of this research to analyse the implications of this reduction to obtain the exact mechanism of the of the αMS effect on the copolymerization rate therefore only the experimental results will be presented.

Curve (i) of fig.(45) shows a sudden drop in the rate where 0.02 mole fraction of αMS in the monomer mixture causes the rate to fall to 25% of that for pure MMA, although the composition of the copolymer is high in MMA (app. 97 mole %). With a comonomer mixture of 1:1 mole fraction the rate is only 0.01675 of that of pure MMA. The drastic fall of the rate without any doubt is assisted by the depropagation of αMS units but it seems toohigh to be attributed solely to that. There seem to be other kinetic reasons possibly transfer or early

termination (see subsection (b)) which increase the effect.

The effect of pressure on the rate of copolymerization is to increase it exponentially up to 3000 atm, from where on the rate of increase slows down. This form of pressure dependence is in line with other polymerizations under pressure as mentioned in section (1.6). The magnitude of the increase depends on the initial composition of the comonomer mixture. The rate increases 10 fold between 1 atm and 3000 bars for an equimolar feed mixture, whereas it increases 8.63 fold for a 20:80 αMS-MMA mixture, and app. 11 fold for an 80:20 αMS-MMA mixture. This is still low compared with the 14.36 fold increase for pure MMA, but high compared with the 6.44 fold increase for pure styrene. This mode of dependence of the pressure effect on initial composition shows that the higher the αMS in the feed mixture the more the effect of pressure on the rate. This may be due to the increase of K, the equilibrium constant (=k/k') due to pressure.

The initial linear rate of copolymerization expectedly curves down after some conversion and there will be a natural dispersion in conversion rate vs. feed composition curves since the rate results were taken at varying low conversions. The curve points for conversion rate vs. pressure curves in fig.(46) were derived from fig.(45).

b) Molecular weight

The change in molecular weight with pressure and feed composition shows a parallelism with the change in reaction rate. The dependence of molecular weight on pressure and feed composition is shown in fig.(47) at two concentrations and one pressure separately. Again there is an exponential increase of molecular weight with increasing pressure up to 3000 bars, after which the rate of increase drops. The effect of αMS on molecular weight is a drastic decrease. Although the molecular weight of poly-MMA prepared in this work was not measured the theoretically calculated (fig.(12)) molecular weight indicates a sudden drop with the addition of αMS. The Monte-Carlo simulation, which gives also the relative molecular weights after depropagation, shows a less drop in the degree of molecular weight with increased αMS in monomer feed mixture (fig.(42b)). This indicates that the molecular weight decrease cannot be merely due to depropagation. Kang and O'Driscoll[132] att-

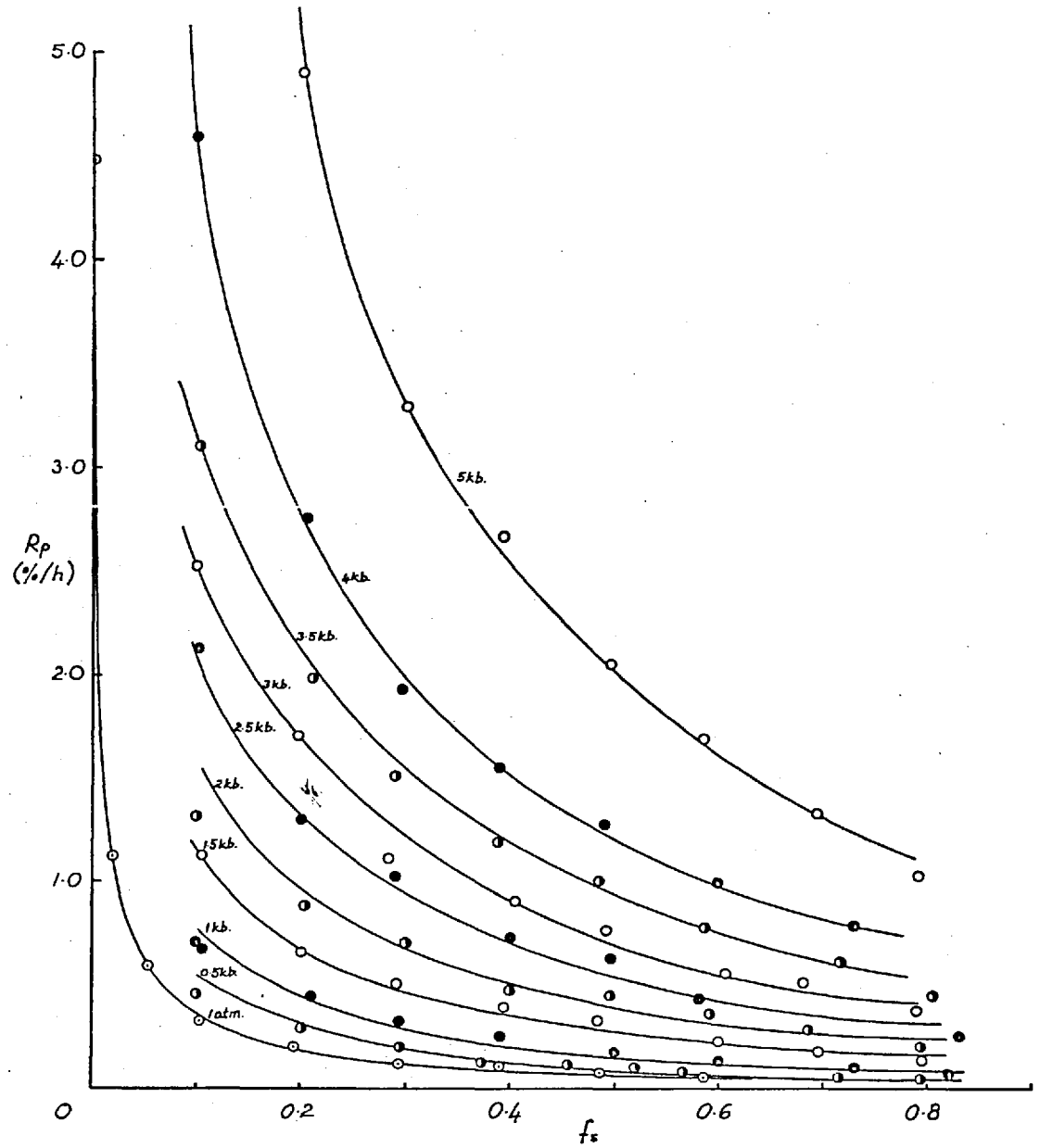

Fig.45 Pressure dependence of the rate of copolymerization on the intial feed monomer composition at various pressures.

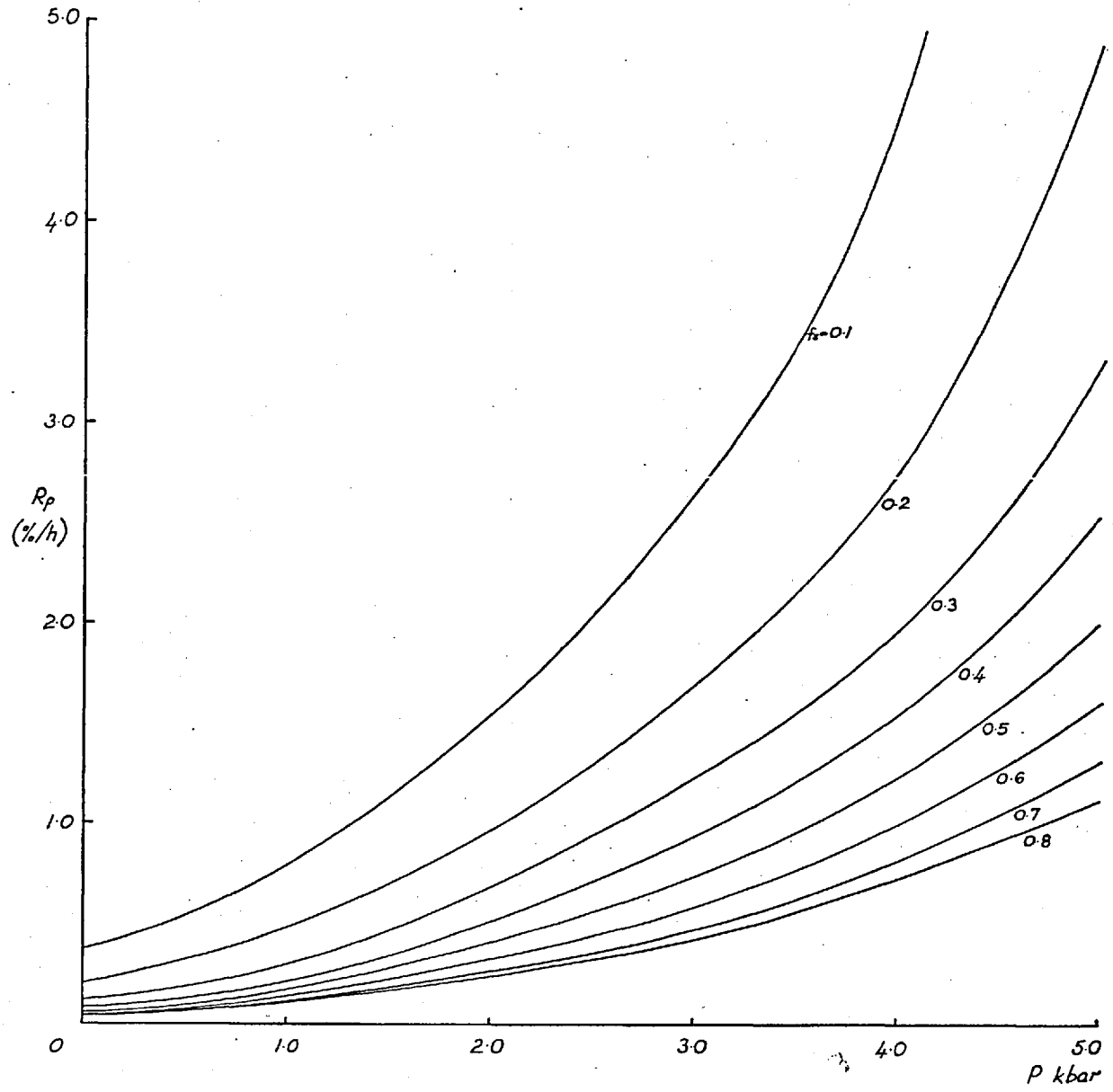

Fig.46 Pressure dependence of the rate of copolymerization on pressure at various initial feed monomer compositions.

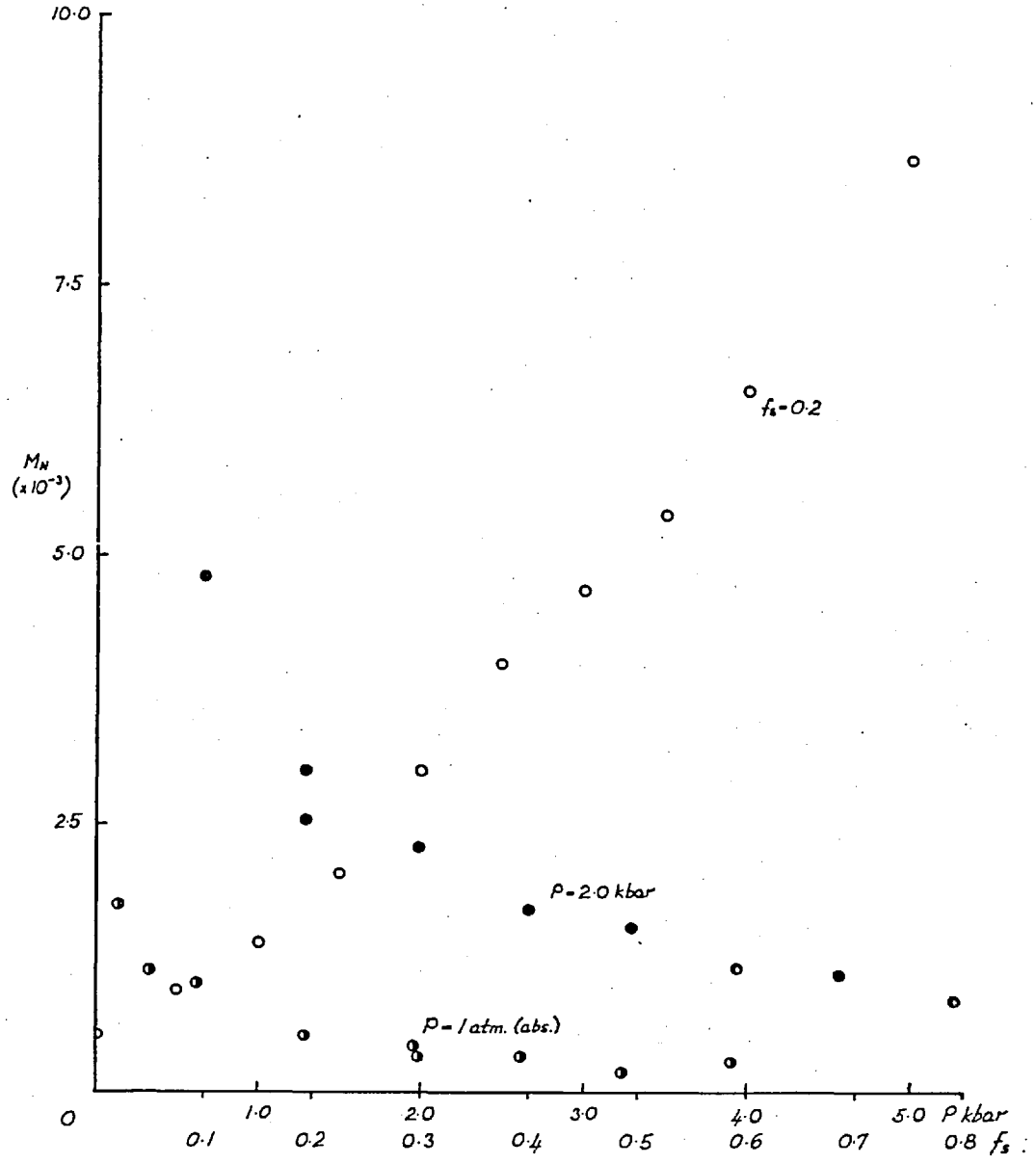

Fig.47 Pressure and initial monomer feed composition dependence of the molecular weight.

ributed the sudden drop of molecular weight with composition mainly to the premature termination of chains by a high number of highly mobile small αMS radicals formed by depropagation.

The full molecular weight data with M_w, M_n, M_v and M_z are given in Table (XIX). As for the dispersion of molecular weights an increase in M_w/M_n was observed with increasing pressure. There is also a decrease in M_w/M_n with increasing αMS in the feed composition, but this is very small and only apparent in the O bar copolymers.

6.8 The Effect of Feed Compositions on the Positions of the NMR Peaks

The peak positions and their respective areas are given in section (6.2). The peaks and sub-peaks are scattered between 2.60δ and 3.60δ as seen in fig.(25). The peak positions for 1500 bar data are shown in fig.(48a) as sub-peak positions vs. feed composition and there seems to be a shift in peak positions downfield with increasing αMS in the feed mixture, as shown by Bovey[114].

The triad areas were plotted against feed compositions in the view of obtaining similar curves to those of Bovey and Tiers[113]. The curves in fig.(48b) are slightly different and this may be due to the fact that the curves of Bovey and Tiers preassume a terminal model.

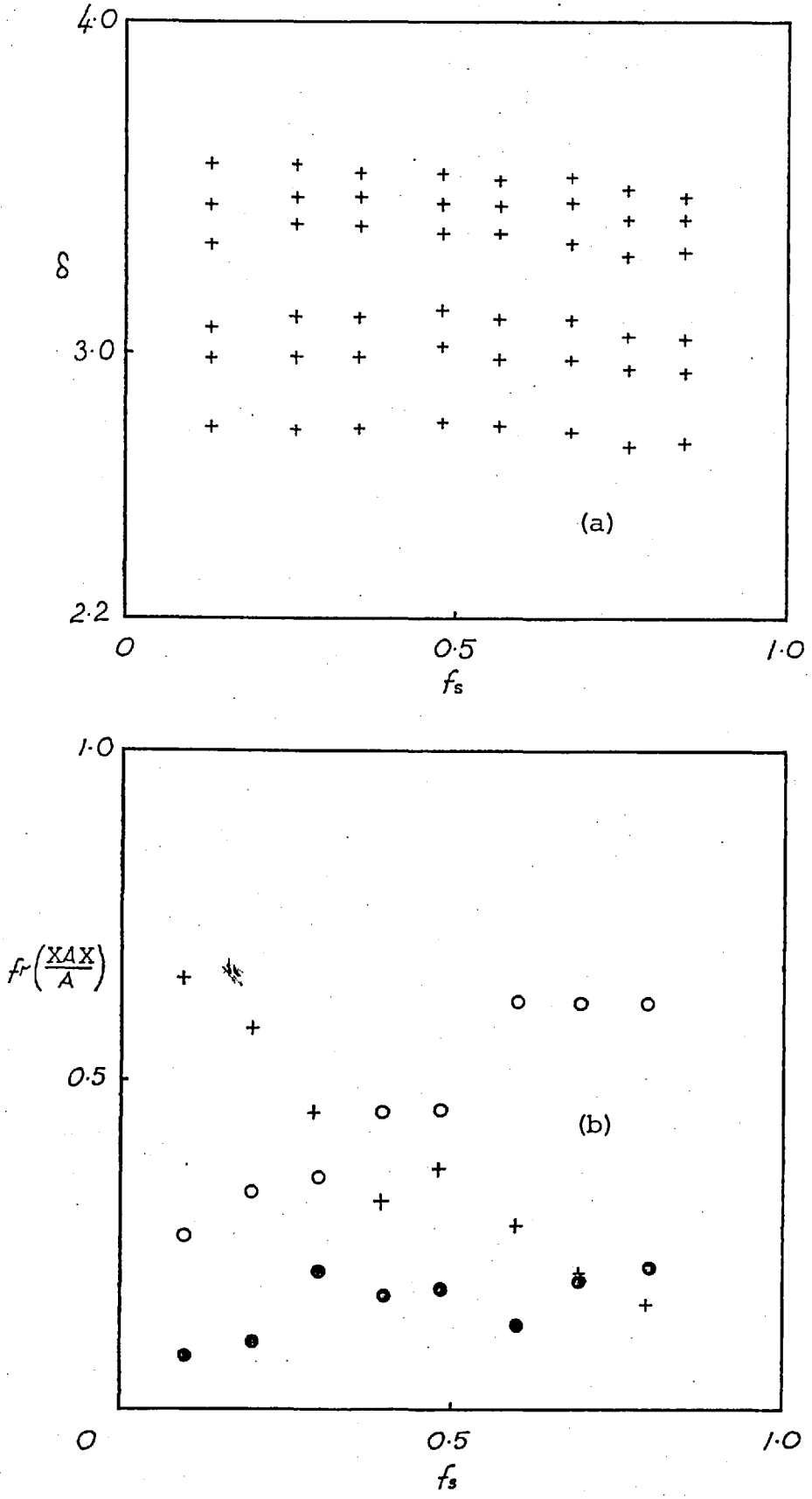

Fig.48 The change in a) NMR peak positions and b) triad areas according to the initial monomer feed compositions. (+) AAA, o) BAA or AAB, o) BAB)

VII GENERAL CONCLUSIONS

Research work on copolymerizations which are more complex than those which follow the simple Mayo-Lewis scheme has usually concentrated on the monomer-copolymer composition relationship. There has been relatively little systematic study of the effect of other parameters such as temperature. The usual treatment has been to make a visual fit of some preferred equation to the composition data, and to compare this with the fit of other 'inferior' equations. This allowed only a semi-empirical explanation of the copolymerization processes but not a detailed explanation of the reaction sequences.

The first researchers to study such copolymerizations by systematic variation of temperature, as well as composition, was Paul Wittmer. He attempted to assess which one of several theoretical copolymerization equations, based on different models, best fitted the data. This was done not only by fitting curves visually to the composition data but also by using the criterion that the reactivity ratios so obtained must vary with temperature in accordance with the Arrhenius relationship.

The aim of this research was to extend the study of one of Wittmer's systems by investigating the effect of varying another reaction parameter, the pressure. This could be expected not only to provide a further test of the model adopted for the particular system but also to give results of general interest in copolymerization theory.

It is evident from the findings discussed in the preceding sections that copolymerization in the system αMS-MMA is, in detail, a complex process. This has been further revealed by the analysis of its pressure dependence and by evaluation of the microstructure data obtained from the NMR analysis. It was this complexity which enforced the Author to study the system in relation to a wider range of mathematical models and although a single satisfactory model was not found the new information obtained has shed further light on the copolymerization processes.

Initially the Author tried to confirm Wittmer's conclusions by an independent mathematical treatment of Wittmer's data. Some of the

results were reproduced satisfactorily but the set of results which, according to Wittmer, prove the validity of his case (i) equation by giving a straight line plot for ln r vs. 1/T did not produce a linear relation. When the K values of Bywater and Worsfold were used in calculations (instead of those of McCormick, as used by Wittmer) the results were more diverse; in fact one reactivity ratio was found to be app. 500. The discrepancy between the results of the Author and of Wittmer can only be attributed to the different methods of curve-fitting. Since nonlinear regression analysis is much superior to visual trial and error, and in the absence of any special factors, it is assumed that the Author's results are more reliable.

Another point against the application of the case (i) equation to the MS-MMA system is that it produces very diverse results from the two experimental sets of K values mentioned above. The curves obtained from the case (i) equation by using the two K sets are shown, with the data points, in figures (49a) and (49b). Since neither of the K sets can be claimed to be the positively correct one it is not possible to discriminate between the results produced from them. In fact the reactivity ratio results were not expected to be so sensitive to small changes (probably within the experimental error) in K. When the equation is studied the reason for the sensitivity is found to be the high value of K ($=k_d/k_p$). Therefore it may be wrong to assume that at this high rate of depropagation the -BB chain ends depropagate as fast as the -BBB chain ends; otherwise increase in r_B would not have much effect on the composition of the copolymer (since increasing k_{bb} will increase k'_{bb} as well) and hence the equation will become K sensitive.

Because of the failure to reproduce Wittmer's results a considerable number of more complex equations was tried by a two-stage fit method; namely a composition fit, followed by a linear lnrvs. P curve. A good fit was not achieved with any of the equations, indicating that the system is more complex than these equations can define. A one-stage fit using a modified equation on parameters[133], in which

$$F = f(f, r_1, r_2, \ldots, r_n)$$

is replaced by

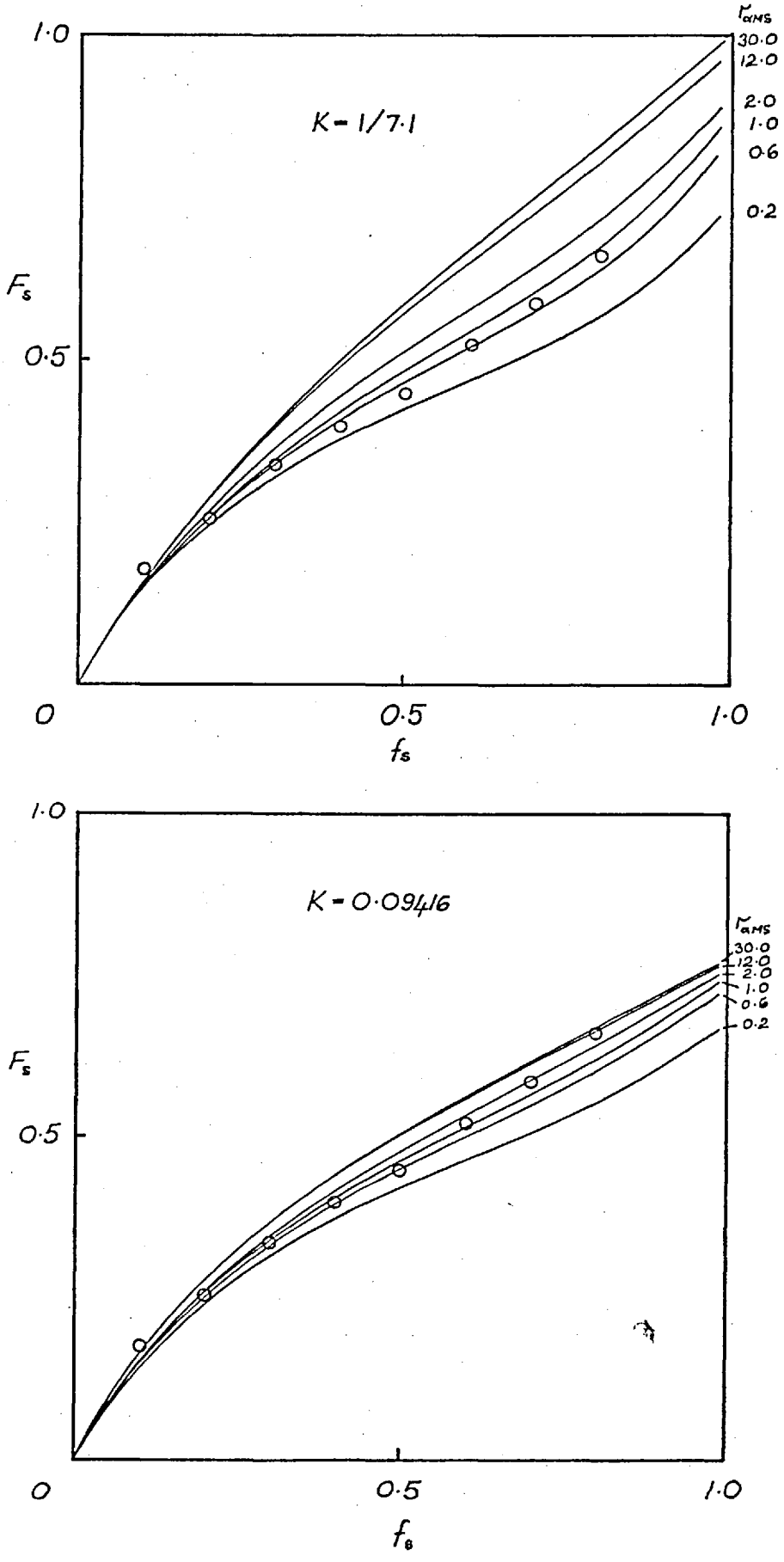

Fig.49 The effect of the two K's of αMS depropagation on $r_{\alpha MS}$.

$$F = f(f,T',e^{\theta_1},e^{\theta_2},\ldots,e^{\theta_n},e^{\phi_1},e^{\phi_2},\ldots,e^{\phi_n})$$

where

$$k_i = A_i e^{\left(-\frac{\Delta E}{RT_o}\right)} e^{\left(-\frac{\Delta E}{R}\left(\frac{1}{T}-\frac{1}{T_o}\right)\right)}$$

$$= A_i^* e^{-\frac{\Delta E}{R}\left(\frac{1}{T}-\frac{1}{T_o}\right)}$$

$$= e^{\theta_i}{}_e - e^{\phi_i}{}_{T'}$$

was tried (as recently applied also by Pritchard and Bacon[133] to homogeneous catalysis) but this failed not only because of the increased number of parameters but the obvious absence of a proportional ln r vs. P relation in the equations used. Ultimately it was found best to base conclusions and inferences on the imperfect results obtained from the two-stage method and the microstructure data.

As far as possible all the available equations were used to fit the data for this system. A limitation on the number of the reactivity ratios which could be estimated simultaneously was imposed by the accuracy of the composition data. Some of the most complex theoretical equations could therefore not be used.

As far as the composition data is concerned all of the equations gave fairly satisfactory visual fits. The terminal model equation gave a good fit by all three methods of fitting (Fineman-Ross, Mayo-Lewis and NLR). The confidence intervals obtained from NLR were quite satisfactory. The other two-parameter equations, namely Wittmer's case (i) and case (iii) depropagation equations gave the same satisfactory fits and confidence intervals. As the number of parameters were increased although the visual fits or the sum of squares were still satisfactory the confidence region enlarges abnormally. The three-parameter penultimate and four-parameter penpenultimate unit equations gave quite satisfactory sums of squares, but the confidence region was large due to a shallow minimum. Any equations other than these failed because they did not yield satisfactory smooth r vs. P curves

The abnormality of the effect of pressure is shown mainly by the existence of a maximum in some r vs. P curves. The persistence of the

maximum in various models suggests that the depropagation process is not a simple one and may involve equilibrium constants and forward rates which depend on the nature of the penultimate unit (section (6.4.6)). Also a maximum in $1/r_{bab}$ (fig.(31)) suggests a possible depropagation of the -BAB· radical. This possibility is also supported by the microstructure evidence; and the presence of a large number of 'AAA' triads in high-αMS copolymers may even imply a penpenultimate unit effect of 'XAA·' on the forward reaction, if not on the depropagation as well.

The best fit on the microstructure parameters was obtained from the four-parameter penpenultimate unit effect from the αMS unit in the -BAA· end group (B=αMS).

In conclusion it can be said that the results obtained in this research by the analysis of the various models show that the copolymerizing system αMS-MMA follows a complicated mechanism and although it has proved impossible to calculate the parameters of an equation which would be fully satisfactory for this system (due to lack of sufficiently accurate data) the mechanism and the effect of pressure on it can be established qualitatively or semi-quantitatively. It can also be said that the general effect of pressure is to reduce the depropagation and penultimate unit effects, and to move the system closer to ideal systems.

REFERENCES

1. Talat-Erben, M. and Bywater, S. J.A.C.S. 77, 3710 (1955). Talat-Erben, M. and Isfendiyaroglu, A. N. Canad.J.Chem. 36, 1156 (1958); 37, 1165 (1959).
2. Smith, P. and Rosenberg, A. M. J.A.C.S. 81, 2037 (1959).
3. Hammond, G. S., Trapp, O. B., Keys, R. T. and Neff, D. L. J.A.C.S. 81, 4878 (1959).
4. Thiele, J. and Heuser, K. Ann. 290, 1 (1896)
5. Bickel, A. F. and Waters, W. A. Rec.Trav.Chim. 69, 149 (1950).
6. Talat-Erben, M. and Onol, N. Canad.J.Chem. 38, 1154 (1960).
7. van Hook, J. P. and Tobolsky, A. V. J.A.C.S. 80, 779 (1958).
8. Burnett, G. M. and Melville, H. W. Proc.Roy.Soc. A 189, 456, 481, 494 (1947).
9. Kwart, H., Broadbent, H. S. and Bartlett, P. D. J.A.C.S. 72, 1060 (1950).
10. Mayo, F. R. J.A.C.S. 70, 3689 (1948).
11. Gee, G. and Melville, H. W. T.F.S. 40, 240 (1944).
12. Sawada, H. Chem.High Polymers(Tokyo) 20, 261 (1963).
13. Sawada, H. Chem.High Polymers(Tokyo) 21, 251 (1964).
14. Bursian, V. and Sorokin, V. Z.phys.Chem. B, 12, 247 (1931).
15. Schulz, G. V. Z.phys.Chem. B, 30, 379 (1935); 43, 25 (1939).
16. Herington, E. T. G. and Robertson, A. T.F.S. 38, 490 (1942).
17. Simha, R. and Branson, H. J.Chem.Phys. 12, 253 (1944).
18. Stockmayer, W. H. J.Chem.Phys. 13, 199 (1945).
19. Melville, H. W., Noble, B. and Watson, W. F. J.P.S. 2, 229 (1947); 4, 629 (1949).
20. Dostal, H. Monatsh 69, 424 (1936).
21. Norrish, R. W. G. and Brookman, E. F. Proc.Roy.Soc.(London) A 171, 147 (1939).
22. Wall, F. T. J.A.C.S. 63, 1862 (1941).
23. Mayo, F. R. and Lewis, F. M. J.A.C.S. 66, 1594 (1944).
24. Alfrey, Jr., T. and Goldfinger, G. J.Chem.Phys. 12, 205 (1944).
25. Alfrey, Jr., T. and Price, C. C. J.P.S. 2, 101 (1947).

26. Bevington, J. C. 'Radical Polymerisation', Academic Press, London, 1961.
27. Evans, M. G., Gergely, J. and Seamom, E. C. J.P.S. 3, 866 (1948).
28. Goldfinger, G. and Kane, T. J.P.S. 3, 462 (1948).
29. Skeist, I. J.A.C.S. 68, 1781 (1946).
30. Walling, C. J.A.C.S. 71, 1930 (1949).
31. Eyring H. J.Chem.Phys. 3, 107 (1935).
32. Evans, M. G. and Polanyi, M. T.F.S. 31, 875 (1935).
33. Glasstone, S. 'Textbook of Physical Chemistry' 2nd Ed., p.1087-1111, Van Nostrand Co. Inc., New York, 1946.
34. Benson, S. W. and Berson, J. A. J.A.C.S. 86, 259 (1964).
35. Hamann, S. D. 'High Pressure Physics and Chemistry' (Ed. Bradley, R. S.) Vol.2, p.181, Academic Press, New York, 1963.
36. Asai, H. Nippon Kagaku Zasshi 85, 347 (1964).
37. Nozaki, K. and Bartlett, P. D. J.A.C.S. 68, 1686 (1946).
38. Perrin, M. W. T.F.S. 34, 144 (1938).
39. Ewald, A. H. D.F.S. 22, 138 (1956).
40. Nicholson, A. E. and Norrish, R. G. W. D.F.S. 22, 104 (1956).
41. Nicholson, A. E. and Norrish, R. G. W. D.F.S. 22, 97 (1956).
42. Merret, F. M. and Norrish, R. G. W. Proc.Roy.Soc. A 206, 309 (1951).
43. Walling, C. and Pellon, J. J.A.C.S. 79, 4776 (1957).
44. Salahuddin, K. and Weale, K. E. unpublished work.
45. Maulik, B. S. and Weale, K. E. unpublished work.
46. Kobeko, P. P., Kuvshinskii, E. V. and Semenova, A. S. Zhur.Fiz.Khim. 24, 345 (1950); 24, 415 (1950).
47. Lamb, J. A. and Weale, K. E. Symp.Phys. and Chem. of High Pressures, 1963 (Soc.Chem.Ind.,London) p.229.
48. Ogo, Y. and Imoto, T. The Rev. of Phys.Chem. of Japan 42, No.1, 36 (1972).
49. Baysal, B. and Tobolsky, A. V. J.P.S. No.5, 8, 529 (1952).
50. Arnett, L. M. J.A.C.S. 74, 2027 (1952).
51. O'Brien, J. L. and Gornick, F. J.A.C.S. 77, 4757 (1955).
52. Bonsall, E. P., Valentine, L. and Melville, H. W. T.F.S. 48, 763 (1952).
53. Schuele, E. M., Kinsinger, J. and Fox, T. G. (see ref. 51).
54. Overberger, C. G., O'Shaugnessy, M. J. and Shalit, H. J.A.C.S. 71, 2661 (1949).

55. Lewis, F. M. and Matheson, M. S. J.A.C.S. 71, 747 (1949).
56. Dainton, F. S. and Ivin, K. J. Nature 162, 705 (1948).
57. Bywater, S. T.F.S. 51, 1267 (1955).
58. Tobolsky, A. V. 'Properties and Structure of Polymers' p.266, Wiley, New York, 1960.
59. Kilroe, J. G. and Weale, K. E. J.Chem.Soc. 3849 (1960).
60. Mintani, T., Ogo, Y. and Imoto, T. The Rev. of Phys.Chem. of Japan 42, No.1, 25 (1972).
61. Eisenberg, A. Macromol.Chem. 65, 122 (1963).
62. Tobolsky, A. V. and Eisenberg, A. J.Colloid Sci. 17, 49 (1962).
63. Shultz, A. R. and Flory, P. J. J.P.S. 15, 231 (1955).
64. McCormick, H. W. J.P.S. 25, 488 (1957).
65. Worsfold, D. J. and Bywater, S. J.P.S. 26, 299 (1957).
66. Stein, D. J., Wittmer, P. and Tolle, J. Die Angewandte Makromolekulare Chemie 8, N.97, 61 (1969).
67. Walling, C., Briggs, E. R. and Wolfstirn, K. B. J.A.C.S. 70, 1543 (1948).
68. Ito, K., Iwase, S., Umehara, K. and Yamashita, Y. J.Macromol.Sci. (Chem.) A1(5), 891 (1967).
69. Yamashita, Y. and Ito, K. Polymer Letters 6, 219 (1968); Ito, K. and Yamashita, Y. Polymer Letters 6, 233 (1968).
70. Schulz, G. V. and Huseman, E. Z. Phys.Chem. B 39, 246 (1938).
71. Matheson, M. S. J.Chem.Phys. 13, 584 (1945).
72. Spinner, I. H., Benjamin, C., Lu, Y. and Graydon, W. F. J.A.C.S. 77, 2198 (1955).
73. Alfrey, Jr., T., Bohrer, J. J. and Mark, H. 'Copolymerization', page 14, Interscience Pub. Inc., New York, 1952.
74. Guarise, G. B. Polymer 7, 497 (1966).
75. Doak, K. W., Deahl, M. A. and Christmas, I. H. 'Abstracts of Papers' 137th Meeting, ACS, April 1960, p.151.
76. Tobolsky, A. V., Rembaum, A. and Eisenberg, A. J.P.S. 45, 347 (1960).
77. 'Encyclopedia of Polymer Science and Technology', Ed. Mark, H. F. et al., Interscience, 1964-72.
78. Ham, G. E. J.P.S. 45, 169 (1960).
79. Ham, G. E. J.P.S. 45, 177 (1960).

80. Ham, G. E. J.P.S. 45, 183 (1960).
81. Izu, M. and O'Driscoll, K. F. J.P.S. A-1, 8, 1687 (1970).
82. Rowlinson, J. S., Saville, G. and Bett, K. E. 'Thermodynamics for Chemical Engineers', chapter 8, to be published.
83. Hopff, H. and Lussi, H. Makromol.Chem. 62, 31 (1963).
84. Sapiro, R. H., Linstead, R. P. and Newitt, D. M. J.Chem.Soc. 1784 (1937).
85. Elroy, I. Ph.D. Thesis, London University, 1961.
86. Brown, C. P. and Mathieson, A. R. J.Chem.Soc. 3445 (1958); 3507 (1958).
87. Lowry, G. G. J.P.S. 31, 187 (1958).
88. Ito, K., Iwase, S., Umehara, K. and Yamashita, Y. J.Macromol.Sci. (Chem.) A1(5), 891-908 (1967).
89. Perrin, D. D. 'Purification of Laboratory Chemicals', Pergamon Press, London, 1966.
90. Merz, E., Alfrey, T. and Goldfinger, G. J.P.S. 1, 75 (1946).
91. Ham, G. E. and Fordyce, R. G. J.A.C.S. 73, 1186 (1951).
92. Barb, W. G. J.P.S. 11, 117 (1953).
93. Ham, G. E. J.P.S. 14, 87 (1954).
94. Johnston, N. W. and Kopf, P. W. Macromolecules 5, N.1, 87 (1972).
95. Izu, M., O'Driscoll, K. F., Hill, R. J., Quinn, M. J. and Harwood, H. J. Macromolecules 5, N.1, 90 (1972).
96. a) Coleman, B. D. and Fox, T. G. J.P.S. A1, 3183 (1963).
b) Coleman, B. D. and Fox, T. G. J.Chem.Phys. 38, N.5, 1065 (1963).
97. Lowry, G. G. J.P.S. 42, 463 (1960).
98. Wittmer, P. Macromol.Chem. 103, 188 (1967).
99. Ham, G. E. J.P.S. 54, 1 (1961).
100. Price, F. P. J.Chem.Phys. 36, N.1, 209 (1962).
101. Ito, K. and Yamashita, Y. J.P.S. A3, 2165 (1965).
102. Ham, G. E. J.P.S. A3, 103 (1965).
103. O'Driscoll, K. F. and Gasparro, F. P. J.Macromol.Sci.(Chem.) A1(4), 643 (1967).
104. Ivin, K. J. and Spensley, R. H. J.Macromol.Sci.(Chem.) A1(4), 653 (1967).
105. Hazell, J. E. and Ivin, K. J. T.F.S. 58, 176 (1962).
106. Yamashita, Y., Kasahara, H., Suyama, K. and Okada, M. Makromol. Chem. 117, 242 (1968).
107. Howell, J. A., Izu, M. and O'Driscoll, K. F. J.P.S. A-1, 8, 699 (1970).
108. Bywater, S. T.F.S. 51, 1267 (1955).

109. Izu, M. and O'Driscoll, K. F. J.P.S. A-1, 8, 1675 (1970).
110. Marconi, P. F., Tartarelli, R. and Capovani, M. Quad.Ing. Chim.Ital. 7, N.2, 27 (1971); 7, N.1, 1 (1971).
111. Wittmer, P. Adv. in Chem.Ser. 99, 141 (1971).
112. Kac, M. 'Probability and Related Topics in Physical Sciences', Interscience, New York-London, 1959; Kac, M. Bull.Am.Math.Soc. 53, 1012 (1947).
113. Bovey, F. A. and Tiers, G. V. D. J.P.S. 44, 173 (1960).
114. Bovey, F. A. J.P.S. 62, 197 (1962).
115. Ito, K. and Yamashita, Y. Polym.Letters 3, 625 (1965).
116. Kato, Y., Ashikari, N. and Nishioka, A. Bull.Chem.Soc.Jap. 37, N.11, 1630 (1964).
117. Saville, G. Private communications.
118. Toohey, A. C. and Weale, K. E. T.F.S. 58, 2439, 2446 (1962).
119. Okumara, S., Higashiyama, T. and Imanishi, Y. J.P.S. 33, 491 (1958).
120. Ref. 73, pages 12-24.
121. Tidwell, P. W. and Mortimer, G. A. J.Macromol.Sci.,Rev.Macromol.Chem. 4(2), 281 (1970).
122. Tidwell, P. W. and Mortimer, G. A. J.P.S. A3, 369 (1965).
123. Behneken, D. W. J.P.S. A2, 645 (1964).
124. Marquard, D. W. J.Soc.Ind.App.Math. 11, 431 (1963).
125. Fletcher, R. Comp.Phys.Comm. 3, 159 (1972).
126. Powell, M. J. D. Harwell Report AERE-R5947, H.M.S.O. (1968).
127. Peckham, G. Computer J. 13, 418 (1970).
128. National Algorithms (NAG) software library.
129. Harwell software library.
130. Box, G. E. P. Bull.Inst.Intern.Statistique 36, 215 (1958).
131. Box, G. E. P. and Lucas, H. L. Biometrika 46, 77 (1959).
132. Kang, B. K. and O'Driscoll, K. F. Macromolecules 7, N.6, 886 (1974).
133. Pritchard, D. J. and Bacon, D. W. Chem.Eng.Sci. 30, 567 (1975).

J.A.C.S. = J.Amer.Chem.Soc.

J.P.S. = J.Polym.Sci.

T.F.S. = Trans.Farad.Soc.